CHARACTERIZATION STUDIES OF Ni-P-TiO_2 NANOCOMPOSITE COATING ON MILD STEEL DEPOSITED BY ELECTROLESS COATING METHOD

Ph.D. Thesis

VIBHA UTTAM
I.D.: 2015RMT9057

DEPARTMENT OF METALLURGICAL AND MATERIALS ENGINEERING
MALAVIYA NATIONAL INSTITUTE OF TECHNOLOGY JAIPUR

May 2019

Characterization Studies of Ni-P-TiO_2 Nanocomposite Coating on Mild Steel Deposited by Electroless Coating Method

A THESIS

Submitted in partial fulfillment of the

requirements for the award of degree

of

Doctor of Philosophy

by

VIBHA UTTAM
I.D.: 2015RMT9057

Under the supervision of

Dr. Rajendra Kumar Duchaniya

DEPARTMENT OF METALLURGICAL AND MATERIALS ENGINEERING
MALAVIYA NATIONAL INSTITUTE OF TECHNOLOGY JAIPUR

May 2019

This thesis is dedicated to

Our Professors

My Supervisor

My Grand Parents

My Parents

My Husband

DECLARATION

I, **Vibha Uttam**, declare that this thesis titled, **"Characterization Studies of Ni-P-TiO_2 Nanocomposite Coating on Mild Steel Deposited by Electroless Coating Method"** and the work presented in it, are my own. I confirm that:

- This work was done wholly or mainly while in candidature for a research degree at this university.

- Where any part of this thesis has previously been submitted for a degree or any other qualification at this university or any other institution, this has been clearly stated.

- Where I have consulted the published work of others, this is always clearly attributed.

- Where I have quoted from the work of others, the source is always given. With the exception of such quotations, this thesis is entirely my own work.

- I have acknowledged all main sources of help.

- Where the thesis is based on work done by myself, jointly with others, I have made clear exactly what was done by others and what I have contributed myself.

Date:

Place:

Vibha Uttam

(2015RMT9057)

CERTIFICATE

This is to certify that the thesis entitled **"Characterization Studies of Ni-P-TiO_2 Nanocomposite Coating on Mild Steel Deposited by Electroless Coating Method**" being submitted by **Vibha Uttam (2015RMT9057)** is a bonafide research work carried out under my supervision and guidance in fulfillment of the requirement for the award of the degree of Doctor of Philosophy in the **Department of Metallurgical and Materials Engineering**, Malaviya National Institute of Technology, Jaipur, India. The matter embodied in this thesis is original and has not been submitted to any other University or Institute for the award of any other degree.

Dr. Rajendra Kumar Duchaniya
Associate Professor
Department of Metallurgical and Materials Engineering
MNIT Jaipur

Place: Jaipur
Date:

ACKNOWLEDGEMENT

While bringing out this thesis to its final form, I came across a number of people whose contributions in various ways helped my field of research and they deserve special thanks. It is a pleasure to convey my gratitude to all of them.

First and foremost, I would like to express my deep sense of gratitude and indebtedness to my supervisor **Dr. Rajendra Kumar Duchaniya** for his invaluable encouragement, suggestions and support from an early stage of this research and providing me extraordinary experiences throughout the work. Above all, his priceless and meticulous supervision at each and every phase of work inspired me in innumerable ways.

I specially acknowledge him for his advice, supervision, and the vital contribution as and when required during this research. His involvement with originality has triggered and nourished my intellectual maturity that will help me for a long time to come. I am proud to record that I had the opportunity to work with an exceptionally experienced Professor like him.

I wish to express my sincere gratitude to Dr. Vishnu Kumar Sharma, Head of Department of Metallurgical and Materials Engineering, MNIT Jaipur for his kind support and for providing good research environment.

I wish to express my sincere gratitude to Dr. Rajendra Kumar Duchaniya, DPGC Convenor of Department of Metallurgical and Materials Engineering for his kind support and help.

I am thankful to Prof. Upender Pandel, Dr. Sushil Kumar Gupta, Dr. Ajaya Kumar Pradhan, and Dr. Vijay Navaratna Nadakuduru as DREC members for providing their valuable support and guidance whenever needed during my research work and thankful to all the faculty members of the Department of Metallurgical and Materials Engineering, MNIT Jaipur for their motivation and positive presence.

I would like to acknowledge our technical and administrative staff of the department Mr. Lalchand Kumawat, Mr. Vidhyasagar, Mr. R.M. Vairagi, Mr. Nathu Singh, Mr. Mahesh, for their help at various stages of the work.

I would like to thank to all team members, Dr. Shrikant Verma, Mrs. Vandana Kaler, Mr. Vijay Kumar Pandey, Mr. Sunil Kumar Jatav, Ms. Nitika Kundan, Ms. Akanksha Shukla Ms. Premlata, Ms. Neelam, Mr. Nikunj and others.

I also express my thanks to Materials Research Centre and Advance Research Lab for Tribology, MNIT Jaipur and Advance Centre for Material Science, IIT Kanpur to provide me facilities of characterization and wear test.

I express my deep sense of gratitude to my parents and family for their wishes and continuous support. Last but not the least I am grateful to all known and unknown persons who helped me directly or indirectly during my dissertation work.

(VIBHA UTTAM)

ABSTRACT

Electroless nanocomposite coating on various substrate (metals, metal alloys, ceramics, composite etc) has used for the enhanced the surface properties of substrates. Surface enhancement of materials through the deposition of electroless nanocomposite coating is a new process. Nano-sized second phase particles are co-deposited with Ni-P matrix on the surface of substrate by the use of electroless coating process. Lots of outstanding characteristics of electroless nanocomposite coatings have generated great interest in numerous industries including construction, automotive, chemical processing, manufacturing and materials handling, mining, gas and oil production, and electronic industries. Some of outstanding properties of electroless nanocomposite coatings are self-lubricating property, high hardness, superior wear and corrosion resistance in different environments, uniform coating thickness and superb erosion resistance properties.

Electroless coating deposition is an autocatalytic process in which reduction of the metallic ions in the deposition can be done through the oxidation of a chemical compound present in the deposition bath itself i.e. reducing agent, which supplies an internal current. In this process, external current source is not required.

The objectives of this research work were to synthesis of electroless Ni-P and Ni-P-TiO_2 nanocomposite coatings on mild steel and to evaluate various characteristics of both type of coatings. In the first phase of this research work, Ni-P coating and Ni-P-TiO_2 nanocomposite coatings with various of concentration of nickel sulphate as a nickel source, concentration of sodium hypophosphite as a reducing agent and concentration of nano TiO_2 particles as second phase material were deposited on mild steel. In the second phase of this research work, various characterisation methods were implemented to evaluate properties of these coatings. Also, effects of various deposition parameters including nickel and phosphorous contents on the properties of electroless Ni-P-TiO_2 nanocomposite coatings on mild steel were broadly investigated. Furthermore, the effect of inclusion of different concentration of nano TiO_2 on various properties of these coating was studied. Concentration of TiO_2 in the deposition bath was vary from 0.4 g/l to 2 g/l.

The results of this research work showed that the various properties of mild steel i.e. corrosion resistance, wear resistance, microhardness and surface finishing are enhanced by the deposition of the electroless Ni-P and Ni-P-TiO_2 nanocomposite coatings on mild steel.

The results of this research work showed that various characteristics of electroless Ni-P-TiO_2 nanocomposite coatings are directly related to the nickel, phosphorous, TiO_2 contents of the coatings. FESEM and EDS analysis carried out on all Ni-P-TiO_2 composite coatings samples revealed the co-deposition of nano TiO_2 particles into Ni-P matrix and formation of a uniformly distributed homogeneous coating layer on mild steel substrate. X-ray diffraction results also revealed that co-deposited second phase particles (TiO_2) did not influence the structure and phase transformation behavior. Microhardness of the electroless Ni-P-TiO_2 nanocomposite coating is 343 HV_{10} (for 0.4 g/l TiO_2 concentration) and 517 HV_{10} (for 2 g/l TiO_2 concentration). Nanocomposite coating with high TiO_2 concentration (2 g/l) shows decreased corrosion resistance compared to nanocomposite coating with low TiO_2 concentration (0.4 g/l). Wear during the pin-on-disc tests of coatings under 5 N load and 500 m sliding distance are calculated by weight loss methods. Wear loss is decreased with increased concentration of nano TiO_2 particles in the deposition bath. Wear resistance property of the material is inversely propositional to the wear loss. Wear resistance of the nanocomposite coatings are increased when the concentration of nano TiO_2 particles is increased.

The study showed that incorporation of TiO_2 in coating causes increasing of corrosion resistance, microhardness, wear resistance and improved surface morphology. The improvement in surface properties offered by such composite coatings will have a significant impact on numerous industrial applications as aerospace, marine, automotive, military, oil and gas production etc., and in the future, they will secure a more prominent place in the surface engineering of metals and alloys.

Contents

LIST OF FIGURES

LIST OF TABLES

ABBREVIATIONS

EN	Electroless Nickel
CVD	Chemical Vapour Deposition
PVD	Physical Vapour Deposition
EIS	Electrochemical Impedance Spectroscopy
FRA	Frequency Response Analyser
PAR	Princeton Applied Research
OCP	Open Circuit Potential
SEM	Scanning Electron Microscopy
FESEM	Field Emission Scanning Electron Microscopy
AFM	Atomic Force Microscopy
TBCs	Thermal Barrier Coatings
SOFCs	Solid Oxide Fuel Cell
YSZ	Yttria Stabilized Zirconia
pH	Power of Hydrogen
PCTFE	Polychlorotrifluoroethylene
PTFE	Polytetrafluoroethylene
WC	Tungsten Carbide
HV	Vickers Hardness
HVN	Vickers Hardness Number
GO	Graphene Oxide
EDS	Energy Dispersive X-ray Spectroscopy
FWHM	Full Width Half Maxima
SE	Secondary Electron
I_{corr}	Corrosion Current
E_{corr}	Corrosion Potential

R_a	Average Roughness
R_q	Root Mean Square Roughness
β_a	Anodic Polarizer Slop
β_c	Cathodic Polarization Slop
PM	Powder Metallurgy
mpy	Miles per year
FCC	Face Centered cubic
BCT	Body Centered cubic
W	Tungsten
DTAB	Dodecyl Trimethyl Ammonium Bromide
SDS	Sodium Dodecyl Sulphate

Chapter 1

INTRODUCTION

1.1. Background

Mild steel has extensive use in construction, automotive, machining, marine, military, chemical processing industry, oil and gas production, mining and material handling application due to the mechanical, physical, electrical and magnetic properties. Due to it's versatility, cost-effective and easy to manufacture quality, mild steel is a commonly used material by the various industries. Mild steel has some adverse characterization such as wear, corrosion, erosion-corrosion, and finishing at the surface on different working conditions with some advantages. For the advancement of the surface of mild steel to increase its engineering application, surface modification of mild steel is needed.

Surface coatings have been used for hundreds of years and electroplating started in 1800's. Subsequently, last 50 years, continuous progress has been taken place to increase the types and performance of coatings. In recent years, various researches have done widespread research on electroless nickel deposition particularly on electroless cermet/ nanocomposite coating as well as the co-deposition of silicon nitride, diamond, silicon carbide titanium oxide, and aluminum particles.

Electroless deposition is a category of the process in which plating is deposited with the use of a reducing agent chemical in solution and without the use of any external current source. Autocatalytic plating, a synonym of electroless deposition, is well-defined as the film formation of a metallic plating through a precise chemical reduction that is catalyzed by the metal or metal-alloy being deposited. In addition, electroless plating as compared to traditional electroplating processes can be used on numerous substrates (electrically conductive and nonconductive), since no external electric power is supplied to the element.

The co-deposition of composite materials with electroless plating is called as electroless composite plating. Electroless composite coating becomes electroless nanocomposite coating, if the thickness of the obtained coating or embedded particles that are dispersed

into the Ni-P coating in the nano size (less than 100 nanometers). The clue of co-depositing several nanosized second phase materials in the electroless nickel plating bath, to take advantage of their uniformity in coating thickness, hardness, corrosion resistance, chemical resistance, thermal resistance and wear resistance and is led to the generation of electroless nanocomposite plating.

Electroless nanocomposite coatings have been broadly applied in mechanical, automobile, electronic, chemical and oil production industries because of their hardenability, wear resistance and corrosion resistance. Co-deposition of nano TiO_2 into Ni-P coating improves the properties such as thermal resistance, wear resistance or corrosion resistance and improve the performance of the coating. In 2008, A. Abdel Aal et.al. reported electroless Ni-P-TiO_2 composite coating through variation in concentration of nano TiO_2 particles on commercial carbon rod. In 2010, Weiwei Chen et.al. worked on the electroless deposition of novel Ni-P-TiO_2 nanocomposite coating on commercial AZ31 Mg alloy. In 2013 and 2014, Preeti Makkar et. al. worked on the preparation of nanosized TiO_2 powder and synthesis of Ni-P-TiO_2 nanocomposite plating on mild steel discs. As T.R. Tamilarasan and his team (2015) mentioned in their work, Ni-P and Ni-P-TiO_2 coatings on low carbon steel were developed by the electroless coating process and they studied effects of two surfactants (SDS and DTAB) on the properties of the coatings. In 2015, Xiaoyan Wu et. al. synthesized electroless Ni-P-TiO_2 nanocomposite coating on 211Z Al alloy and they investigated the properties of 211Z Al alloy with electroless Ni-P alloy and Ni-P-TiO_2 nanocomposite coating. Electroless Ni-P-TiO_2 nanocomposite plating on various substrates have shown excellent properties such as good corrosion resistance, superior wear resistance, superior mechanical properties, solderability, and uniform coating thickness.

As research work recorded in literature, synthesis of electroless Ni-P-TiO_2 nanocomposite plating was done on magnets, carbon rod, stainless steel, Al alloy, and AZ31 Mg alloy. Work on the deposition of electroless Ni-P-TiO_2 nanocomposite coating on mild steel is limited till date. Characterization studies of electroless Ni-P-TiO_2 nanocomposite coated mild steel such tribological study and mechanical properties evaluation are also limited.

1.2. Objectives

On the basis of research gaps, the primary aim of this research work was to improve the wear resistance and corrosion resistance properties of mild steel by the deposition of Ni-P-TiO_2 nanocomposite coating on the mild steel by an electroless deposition method. To achieve the primary objective of this research work, the following specific objectives were carried out:

- Synthesis the electroless Ni-P coating and Ni-P-TiO_2 nanocomposite coatings with a variation on the concentration of TiO_2 on the mild steel substrates.
- Effect of phases presented in the electroless Ni-P and Ni-P-TiO_2 nanocomposite coatings.
- Effect of the surface texture of these coatings on their properties.
- To evaluate and compare the corrosion behavior of the uncoated mild steel, Ni-P coated mild steel and Ni-P-TiO_2 nanocomposite coated mild steels with various concentration of nano TiO_2 particles.
- To evaluate and compare the microhardness of the uncoated mild steel, Ni-P coated mild steel and Ni-P-TiO_2 nanocomposite coated (with various concentration of nano TiO_2 particles) mild steels.
- To evaluate and compare the wear resistance property of the uncoated mild steel, Ni-P coated mild steel and Ni-P-TiO_2 nanocomposite coated mild steels with various concentration of nano TiO_2 particles.

1.3. Thesis outline

The matter of this thesis is constituted of six chapters. Chapter 1 consists of the introduction of this thesis and chapter 2 consists of a literature review on electroless nanocomposite coatings on different substrates. Parameters optimization for the synthesis of the electroless Ni-P coating and Ni-P-TiO_2 nanocomposite coating on mild steel specimen are discussed in chapter 3. Experimental procedure for this research work is given in chapter 4. Chapter 5 assigned to show the obtained results and discussion. Chapter 6 presents conclusions obtained from this study and probable future research work. The research work in this study is schematically shown in Figure 1.1. In

the first phase, including the first stage of this study, electroless Ni-P and electroless Ni-P-TiO_2 nanocomposite coatings on the mild steel were developed. In the next phase of this study, several microstructural, mechanical (wear-resistance and microhardness), physical and electrochemical properties of both type electroless coatings were investigated.

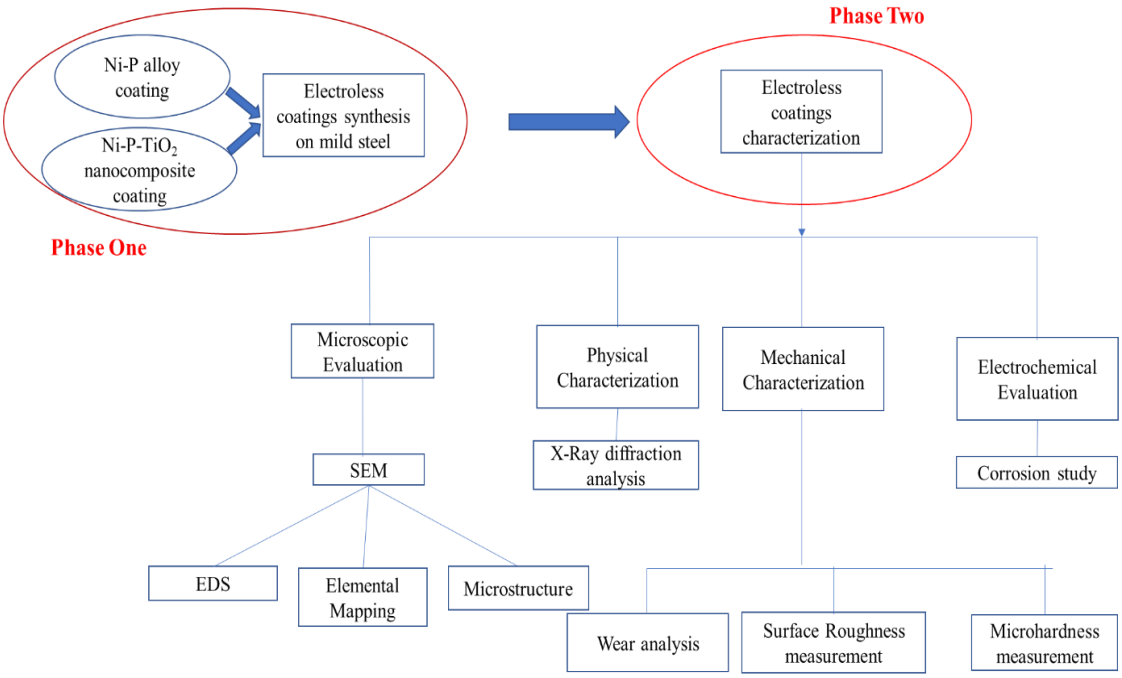

Figure 1.1: Outline of the research work

Chapter 1 presents an introduction to the necessary background of this research work including the objectives of this research work followed by the thesis outline.

Chapter 2 provides a critical review of the surface engineering of the engineering components as well as fundamental of the electroless nanocomposite coating and its types, mechanism, properties, and applications. Bath chemistry during the electroless Ni-P and Ni-P-TiO_2 nanocomposite coatings and properties of these coatings have also thoroughly been reviewed. Surface structure, phase analysis, physical properties, wear analysis corrosion analysis and other characteristics of the electroless coatings on different substrates have been also reviewed in this chapter. Research gaps between previous work done in this field and the present study are mentioned in the same chapter.

Chapter 3 deals with the optimization of the parameters for the synthesis of Ni-P coating and Ni-P-TiO_2 nanocomposite coatings on mild steel. Parameters optimization

included the selection of suitable parameters for the coatings such as bath loading, the temperature of the chemical bath, pH of the bath and the time period for deposition.

Chapter 4 contains the materials and experimental procedure used to complete this research work. Chapter four has four sections. Compositional analysis of mild steel is given in the first section. The second section of this chapter focuses on the procedure of substrate preparation. The deposition method of electroless Ni-P-TiO_2 nanocomposite coatings on the mild steel is given in the third section of this chapter. The obtained coatings were characterized in term of microstructure, chemical composition, phases present, coating roughness, microhardness, corrosion resistance and wear resistance. Details of these characterizations are mentioned in section four.

Chapter 5 presents the results obtained from the experiments and their discussion. Firstly, the electroless Ni-P coating on mild steel substrate is characterized in term of presented phases, microstructure, roughness, microhardness, tribological and electrochemical properties followed by detailed discussion. Then results related to the characterization of electroless Ni-P-TiO_2 nanocomposite on the mild steel are discussed. Properties of mild steel enhanced by the electroless Ni-P and Ni-P-TiO_2 nanocomposite coatings which are discussed in the last section of this chapter.

The research work of this thesis is concluded in **chapter 6**. The scope of further investigation is also included in the same chapte

Chapter 2

LITERATURE REVIEW

The second chapter has an inclusive review of the literature correlated to surface engineering, enhancement of surfaces of engineering materials, surface coating, types of surface coating, electroless coating, types of electroless coating, electroless Ni-P coating, mechanism of the electroless Ni-P coating and electroless composite coating. Electroless composite and nanocomposite coatings are also deliberated. Electrochemical and tribological studies of nanocomposite coating are also added in the second chapter. After a review of the available previous literature, the research gap between literature work and this research work has been added at the last section of this chapter.

2.1. Surface engineering

Engineering which deals with the materials surfaces, their surface properties, modification of surfaces by surface treatments is called surface engineering. Surface engineering is a process used to improve surfaces properties of engineering components thus their performance, function-ability and service life can be enhanced [1-3].

According to ASM Handbook, surface engineering is described as "operation of the materials surface and nearby surface zones of material to permit the surface to do functions which are separate from those functions required from the bulk material" [1].

According to Ian Hutchings and Philip Shipway, surface engineering is defined as "it is a process of altering or coating the surface of the engineering components to improve its properties and has a vital role to play in tribology" [4].

Reyna Areli Vazquez Aguilar says that engineering components are manufactured using surface engineering processes and advanced materials in order to minimalize wear loss [5].

According to Gary P. Halada and Clive R. Clayton, "the role of surface engineering is to create a substrate/surface system which ensures dependability of structures manufactured for use in demanding service environment" [6].

A. Matthews said, “normally, such as the importance of surface engineering to product quality and reliability, it is necessary that design engineers and other involved in optimizing performance and preventing failure have a reasonable knowledge of the main features of the coating and treatment methods at their disposal” [7].

According to Lee and Daeyeon, “surface engineering of a range of materials together with colloidal particles and porous membranes has been accomplished by exploitation of a layer-by-layer assemblage of pH-sensitive polymers and nanoparticles” [8].

In the surface engineering casebook, surface engineering is described as, “it is a speedily developing discipline which allows the design and production of metal, polymer, composite and ceramic systems, with exclusive combinations of surface and bulk properties obtainable in neither the surface nor the bulk material alone” [2].

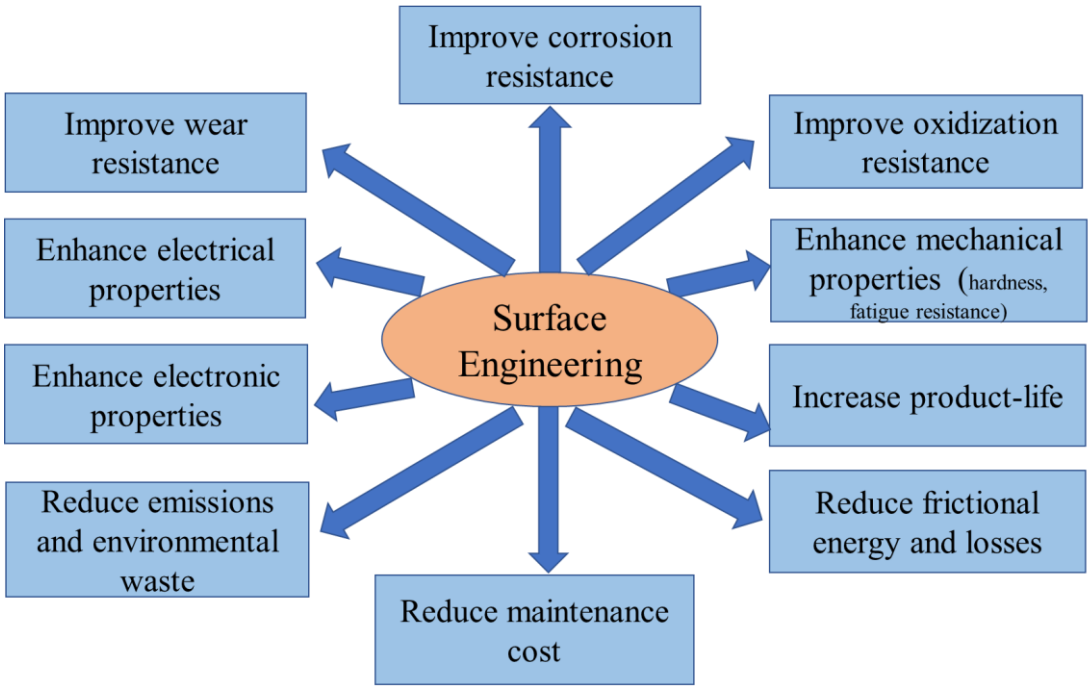

Figure 2.1: Importance of surface engineering

As above mentioned, surface engineering is defined by various researchers. According to these definitions, surface engineering is used to enhance the surface properties of materials by the modifying their surfaces. Under surface engineering processes, painting, electroplating, galvanizing, thermal and plasma spraying, nitriding, and boriding etc these all come [1-8]. Figure 2.1 is showing the importance of surface engineering in different fields.

By the use of surface engineering, the characteristics of the engineering components are changed, which are given below [1-8]:

- Enhancement of the corrosion resistance, wear resistance, oxidation resistance properties.
- Improvement of mechanical properties (hardness, fatigue resistance), electronics properties, electrical properties, and thermal insulation.
- Reduction in the maintenance cost, emission and environmental waste and frictional energy losses.
- Extend the product life.

2.2. Surface coating

A material coated to other substrates to alter the physical, metallurgical, mechanical, electrical, electrochemical and magnetic properties of the surface such as color, luster, resistance to oxidation, resistance to wear, hardness, resistance to chemical attack without affecting the bulk properties. Surface coatings have been used for hundreds of years and electroplating began in 1803. Since the last 50 years, continuous development has been taken place to increase the type and performance of coatings [9-17].
According to Sunil Takalapally et.al., "Coating" means a material applied to another material to modify the surface gloss, color, resistance to chemical attack or wear or oxidation, or permeability, without altering the properties of bulk. Basically, coatings are classified into two groups; decorative coatings and protective coatings or functional coating [18].

Patrik Karlsson said that extended service life, capability to bear greater loads, easy maintenance, low cost of maintenance, environmental gain in protection of resources, better response in kinetic systems, lesser energy consumption, resistance to corrosion, friction and wear, use of low-cost base material, etc are just some good reasons for coating machine parts and engineering components. According to him, coating techniques are categorized into three groups: solid phase, liquid phase and vapor phase [19].

According to Munger and G. Charles, "protective surface coatings are an exclusive method of corrosion and wear control. These coatings used for a long-term shield from

a wide range of eroding environments, covering form atmospheric exposures to full immersion in strong corrosive solution" [20].

According to Daniel Woldegebriel Gabretsadik, "one of the significant approaches in enchanting friction and wear resistance of surfaces is deposition of surface coatings" [21].

According to L. Bonin and V. Vitry "surface coating has been widely used in the engineering industry as a method that decreases surface reactions such as wear and corrosion and, in addition, helps better surface finishing" [22].

In surface engineering casebook, coatings techniques are grouped into two categories as given below;

- Traditional techniques
- Advanced techniques

Painting, electroplating, plasma and hypervelocity spraying, weld surfacing, nitriding and carburizing are included in traditional techniques. Chemical vapor deposition, physical vapor deposition, laser surfacing, ion mixing, and ion implantation come under advanced surface engineering techniques [2].

Figure 2.2 is showing the classification of surface engineering processes. According to A. Matthews, the film deposition processes divided into the following three categories;

- Gaseous state deposition processes
- Solution-state deposition processes
- The semi-molten state deposition process

In gaseous state coating processes include surface coating through a vapor or gaseous phase to modifying the surface of substrates. Generally, physical vapor deposition (PVD) and chemical vapor deposition (CVD) come in the gaseous state deposition processes. In solution state processes, aqueous solutions are usually used and coating can be possible on metallic and non-metallic substrates. Electroplating and electroless plating come in the solution state processes. The main benefit of the solution state coating process is that these types of coating have no lower or upper limit on thickness, unlike CVD and PVD processes, which, because of stress develop leading to debonding,

are typically used for coatings less than 10 µm thick during the hard-ceramic deposition. Within, molten and semi-molten state processes may be covered laser surface treatments, thermal spraying and electro-spark deposition [7].

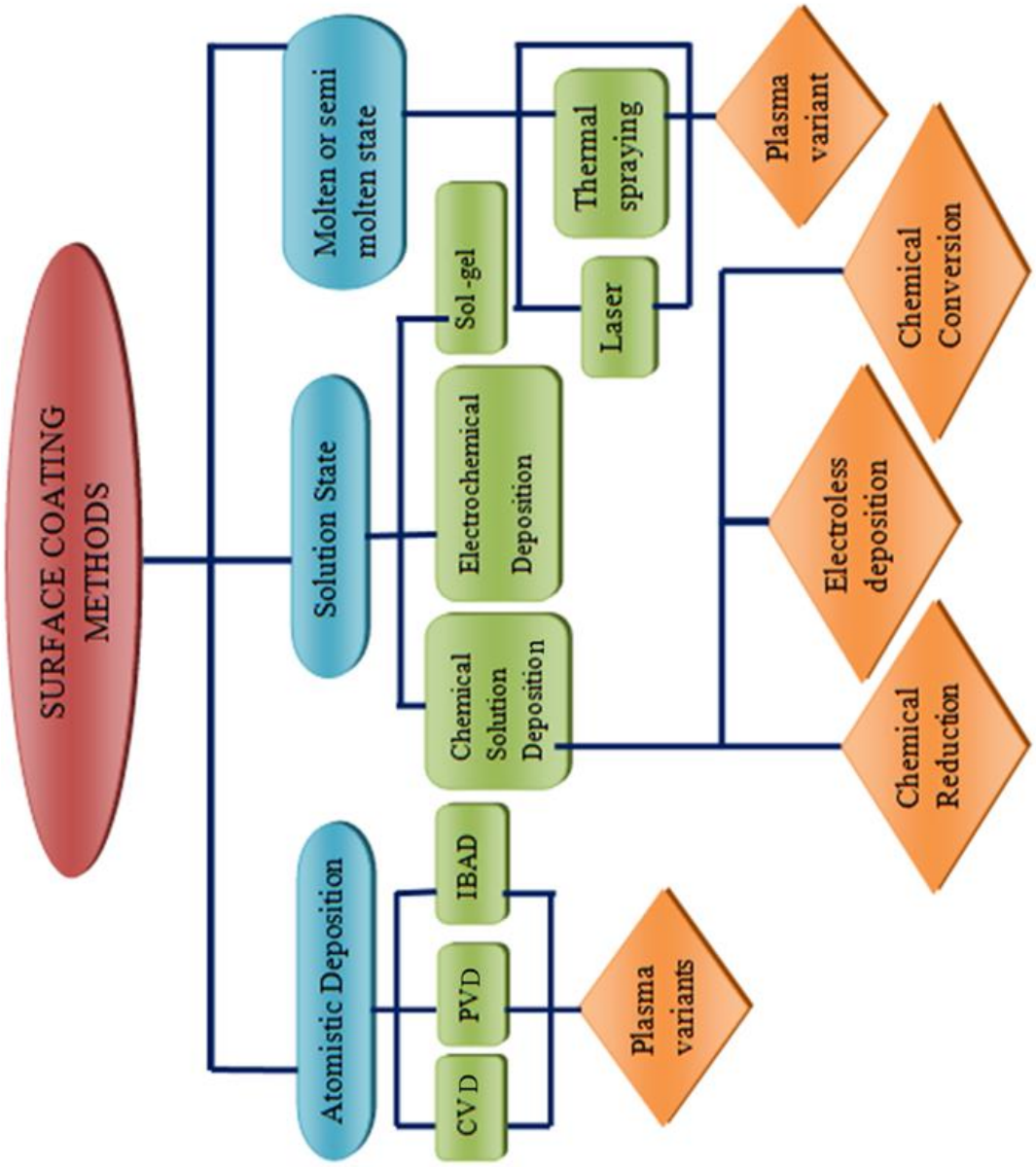

Figure 2.2: Classification of surface coating methods [7]

For the selection of coating materials, an assessment of all applicable features such as given below shall be conducted [1].

- Corrosion, oxidation, and wear protection properties.
- Necessities to health, environment, and safety.
- Belongings of application conditions, equipment, and personnel.
- Economical cast and availability of coating materials.

The current review on the surface coatings presented different types of coating techniques and characteristics of the surface coating. Surface coating against the corrosion, oxidation, friction, wear, chemical attack, environmental attack, and corrosion-wear are extensively used in various industries: food packaging, automobile, aerospace, glass, and ceramic manufacturing, cutting tools, metal processing, oil and gas production, chemical processing, paper industry, printing industries, medical, military applications and waste management [7-21].

There are uses of electroless nickel in many fields such as thermal barrier coatings (TBCs), corrosion and oxidation barrier coatings and composite coatings. In recent years various research has been done on electroless nickel deposition especially on electroless nickel deposition especially on electroless nanocomposite plating or electroless cermet with co-deposition of soft/hard particles of silicon carbide, diamond, titanium oxide, silicon nitride, and alumina.

2.3. Electroless coating

The electroless coating method is a type of solution state processes [7]. In 1844, Wurtz noted a chemical accident corresponds to the electroless deposition of nickel metal from aqueous solution in the existence of hypophosphite [23]. Electroless deposition method first time successfully used by Brenner and Riddell in the 1940's [17, 24-26]. At general american transportation corporation (GATC) during the 1954-1959 period, Gutzeit conducted research on extensive development of electroless coating by chemical reduction without using other things, as an alternative method to usual electroplating [27-28]. If the electroless coating method compared to traditional electroplating depositions, electroless plating can be used on different materials (conductive and

nonconductive) meanwhile no external electricity is applied to the constituent. The electroless coating is described by various researchers, some of those are given below;

"Electroless coating is unquestionably the most important catalytic coating process that outcomes in uniform deposits in use today" [29].

-MA Azmah Hanim

"The technique of EN deposition is one in all of the modish processes existing for the synthesis of alloy deposits. This method contains the autocatalytic reduction reaction, at the surface and solution interfaces, of cations by electrons released from presented reducing agent permitting simultaneous deposition with reduced metallic nickel so as to synthesis alloys (binary or tertiary or quaternary alloys coatings)" [30].

-P. Gillespie

"Electroless coating is also called a chemical coating. It is a method for producing a thin metallic film on all types of materials such as metal, metal-alloy, plastics or ceramics at room temperature by just dipping and holding the substrate materials in the chemical bath" [31].

- Izumi Ohno

"Electroless nickel coating is an autocatalytic chemical process in which the chemical compound used as a reducing agent is oxidized and reduced Ni^{++} ions are deposited on the material surfaces" [32].

-Ray Taher

"Electroless coating is a chemical reduction method, depends upon the catalytic reduction of a metallic ion in an aqueous solution containing a reducing agent and therefore the sequent deposition of the metallic material while not the employment of electricity" [33].

-J. N. Balaraju and S. K. Seshadri

According to Jothi Sudagar et.al. "electroless technique is an autocatalytic process within which the reduction of the metallic ions within the chemical solution and therefore the coating will be dispensed through the chemical reaction of a chemical compound present in the deposition itself, i.e. reducing agent, that provides an inside current" [34].

Preeti Makkar et.al. mentioned in their research paper, electroless plating is one of the reliable and efficient surface engineering methods used in industries to enhance the physical, metallurgical, mechanical and electrochemical properties due to its uniform deposition at the entire surface, excellent wear and corrosion resistance [35-38].

On the basis of above-mentioned definitions, it can say that electroless coating technique is an autocatalytic process in which the reduction of the metal ions within the solution and the layer deposition will be done through the oxidation of a chemical compound present in the solution itself, i.e., reducing agent, which supplies an internal current [32-43]. In simple words, the method used to deposit without external electric power called electroless plating. Electroless plating methods used to deposit metals like, Ni, Co, Pd, Cu, Au, and Ag with or without P or B are currently known [44-58]. The basic difference between cell setup of electroplating method and electroless deposition method is shown in Figure 2.3. In the experimental setup of electroplating, anode, cathode and external current source are required while in experimental setup of electroless coating, the external current source is not required [34].

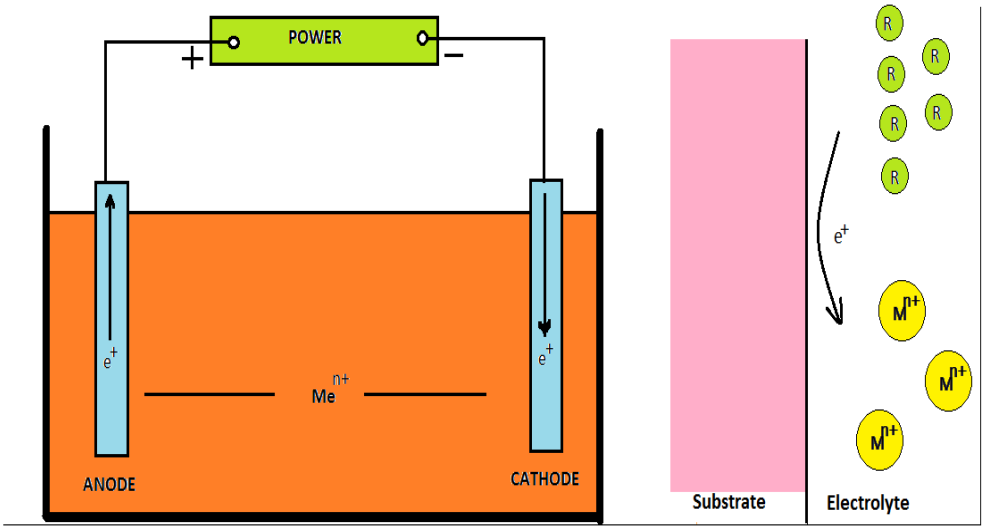

Figure 2.3: Electrodeposition cell set up (left side) and electroless deposition cell set up [34]

The electroless coating is the most important catalytic coating process in the current scenario. The main components of the electroless coating bath are a metal ions source, a reducing agent, stabilizers, buffer-solution, suitable complexing agents and energy. In case of electroless nickel coating, nickel sulphate, nickel chloride or nickel acetate are

preferred as the source of nickel cations and the four reducing agents such as sodium borohydride, sodium hypophosphite, dimethylamine borane, and hydrazine are used. As complexing agents, the additives are referred. Group VI elements (S, Te, Se etc) compounds, compounds containing oxygen (AsO_2^-, MoO_4^{--} etc), unsaturated organic acids (itaconic, maleic etc) and heavy metal cations (Sn^{++}, Sb^{+++} etc) are referred as stabilizers [34, 59-63]. In electroless nickel deposition, a surface reaction constitutes five small steps [44, 64-65];

- Diffusion of reactants to the surface;
- Adsorption of reactants at the surface;
- Chemical reaction on the surface;
- Desorption of products from the surface;
- Diffusion of products away from the surface

Mechanism of the electroless deposition are explained in term of certain characteristics of the electroless process as mentioned below [34, 44];

- Always by the evolution of H_2, the reduction of nickel happens.
- The deposit is not pure nickel because the deposit contains either P, B or N, depending on the used reducing medium.
- On the surface of certain metals, the reduction reaction takes place, but must also take place on the depositing metal.
- As a by-product of the reduction reaction, hydrogen ions are generated
- For depositing metal, the utilization of the reducing agent is not 100 percent.
- The molar ratio of deposited nickel to consumed reducing agent is generally less than or equal to one.

Electrochemically, an electroless coating reaction can be viewed as the combined response of two separate electrode reactions as given below [64];

- Partial cathodic reactions, e.g. reduction of metal ions
- Partial anodic reactions, oxidation of the reductant

Reducing agents supplied the electrons essential for the reduction of metal ions. For the electroless nickel coating with sodium hypophosphite reducing agent, the partial cathodic and anodic reactions are generally written as following manner [44, 64];

Anodic reaction (oxidation of H_2PO_2)

$H_2PO_2 + H_2O \rightarrow H_2PO_3 + 2H^+ + 2e^-$ ...…(i)

Cathodic reactions

$Ni^{++} + 2e^- \rightarrow Ni$ ……(ii)

$2H^+ + 2e^- \rightarrow H_2$ ……..(iii)

$H_2PO_2 + 2H^+ + e^- \rightarrow P + 2H_2O$ .....(iv)

2.3.1. Composition of the electroless coating bath

The chemical bath is prepared with chemicals for electroless coating as described in Table 2.1.

Table 2.1: Components/parameters of electroless bath and their work [34]

S. No.	Component/Parameter	Function
1	Source of metal-ions	Provide the metal
2	Reducing agents	Provide electrons and reduce the metallic ions
3	Complexing agents	Avoid the precipitation of metal source, Reduce the free metal ions concentration, and exert the buffering action
4	Stabilizers	Steady the bath from random breakdown by protective catalytically active deposition, and prevent the homogeneous reaction
5	Accelerators	boost the reducing agent for the reduction reactions and increase the rate of deposition
6	Buffers	Maintain the fix pH for a long time
7	pH regulators	pH adjustment
8	Temperature	Energy for catalytic reactions and deposition

Effect of Bath Loading: The ratio of the total exposed surface area of the work-piece to the volume of solution in the container is defined as bath loading.

$$\textbf{Bath loading} = \frac{\text{surface of the work piece}}{\text{volume of the solution}}$$

Commercial deposition solutions are functioned in 0.1-1.0 dm^2/l bath loading range dependent on the solution concentration in the bath [Reidel, 1997]. Figure 2.4 and 2.5 demonstrate the result of bath loading on the rate of deposition. As results revealed in Figure 2.4 and 2.5, the rate of deposition reduces with increasing bath loading. Hence, an optimal bath loading is essential to afford the suitable deposition rate as well as bath efficiency [32].

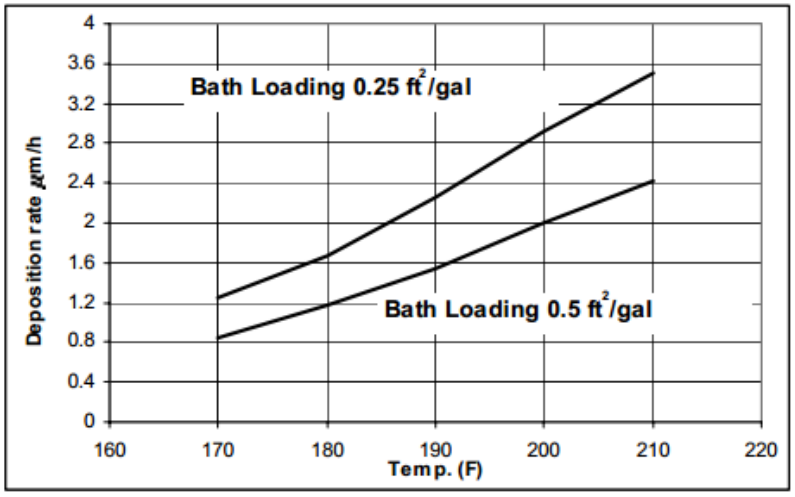

Figure 2.4: Effect on deposition rate due to the varying bath load and temperature [MFPP-Process Guide]

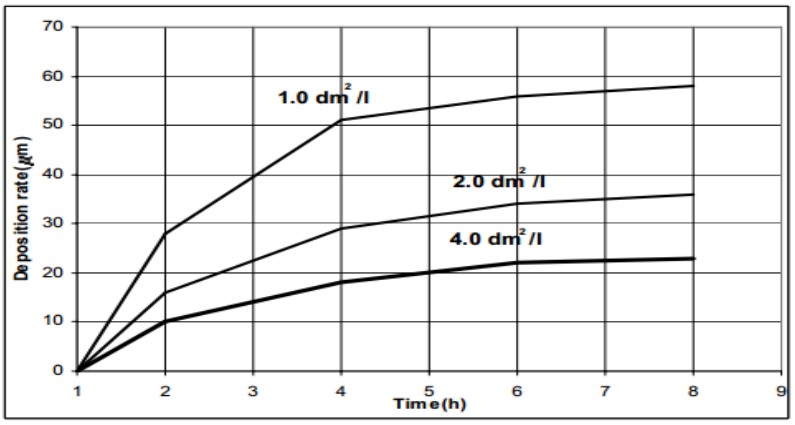

Figure 2.5: Effect on deposition rate at different bath load [Grunwald, 1983]

Taheri, Ray et. al. also said that variation in concentration of nickel salt has no clear effect on the reduction-rate of nickel but variation in concentration of hypophosphite affects the process noticeably. Even though the increase in concentrations of hypophosphite improves the nickel reduction rate, a further amount of reducing agents mustn't be used as this could cause bulk reduction of chemical solution. The suitable quantity of the hypophosphite can be selected by the bath condition observation during the deposition reaction. Less amount of H_2 is a sign of a low hypophosphite concentration and a vital H_2 evolution shows extra hypophosphite [32].

2.3.2. Types of electroless plating

Classification of the electroless coatings is shown in Figure 2.6. Electroless coatings can be categorized into three main groups like [34, 44, 66];

i. Electroless pure metal coating (pure nickel coating) [34, 66-70]
ii. Electroless alloy coating (Ni-B, Ni-P, Ni-Co-B, Ni-Cu-P etc.) [34, 44, 66, 71-83]
iii. Electroless composite coating (Ni-B-SiC, Ni-P-SiC, Ni-B-Al_2O_3, Ni-P-Dimond etc.) [34, 44, 66, 80]

Electroless coatings can be also classified on the basis of reducing agent [34];

i. Electroless Ni-P coating (reducing agent - sodium hypophosphite)
ii. Electroless Ni-B coating (reducing agent - amino boranes and sodium borohydride)
iii. Electroless pure nickel coating (reducing agent - hydrazine)

For a specific application such as electronics (semiconductor) application, electroless pure nickel coating have great use. During the deposition of electroless pure nickel plating, hydrazine is used as a reducing agent. The hardness of electroless pure nickel deposit is ~ 455 HV. This type of coatings is not much used by the industry because of hydrazine cost and hazards [44, 67-70].

Electroless alloy coating is an auto-catalytic reaction method applied to deposit a film of nickel-boron alloy or nickel-phosphorus alloy or other alloys on the surface of the solid materials, such as metal, ceramic, glass and plastic [34, 44, 66]. The electroless nickel coating is a different technique to synthesise boron or phosphorus alloy with

varying composition. Dependent on the construction and the chemistry of process, for boron, deposit compositions have been varied from 0.1 to 10 wt.% and 1 to 15 wt.% for phosphorous. This variation in the content of deposit alloys shown noteworthy advantages. Characteristics of deposited nickel-boron or nickel-phosphorus coating are relatively brittle, even, easily-solderable, hard, lubricious, and highly oxidation/corrosion resistant. These properties combination makes the coatings suitable for numerous applications and permits them to be used in the more expensive application or less willingly available alloys [80-120]. With a few differences, mostly the properties of nickel-boron are similar to that of nickel-phosphorous. Heat-treated nickel-boron alloy coating has a very high hardness similar to hard chromium. This coating also has outstanding resistance to abrasion and wear. Nickel-boron film is pricier than nickel-phosphorous while it has reduced corrosion resistance [80]. Similar to binary alloys (nickel-boron, nickel-phosphorous etc.), Pollyalloys (ternary and quaternary alloys) also deposited by the electroless coating methods. Some ternary and quaternary alloys i.e. Ni-Cu-P, Ni-Cu-B, Ni-Sn-P, Ni-W-B, Ni-W-P, Ni-P-W, Ni-Fe-P, Ni-Zn-P, Ni-Co-P, Ni-Co-Fe-P, Ni-W-Cu-P etc. have been broadly applied in different engineering components because of their electrical, superior mechanical, electronics, and magnetic properties [34, 120-133].

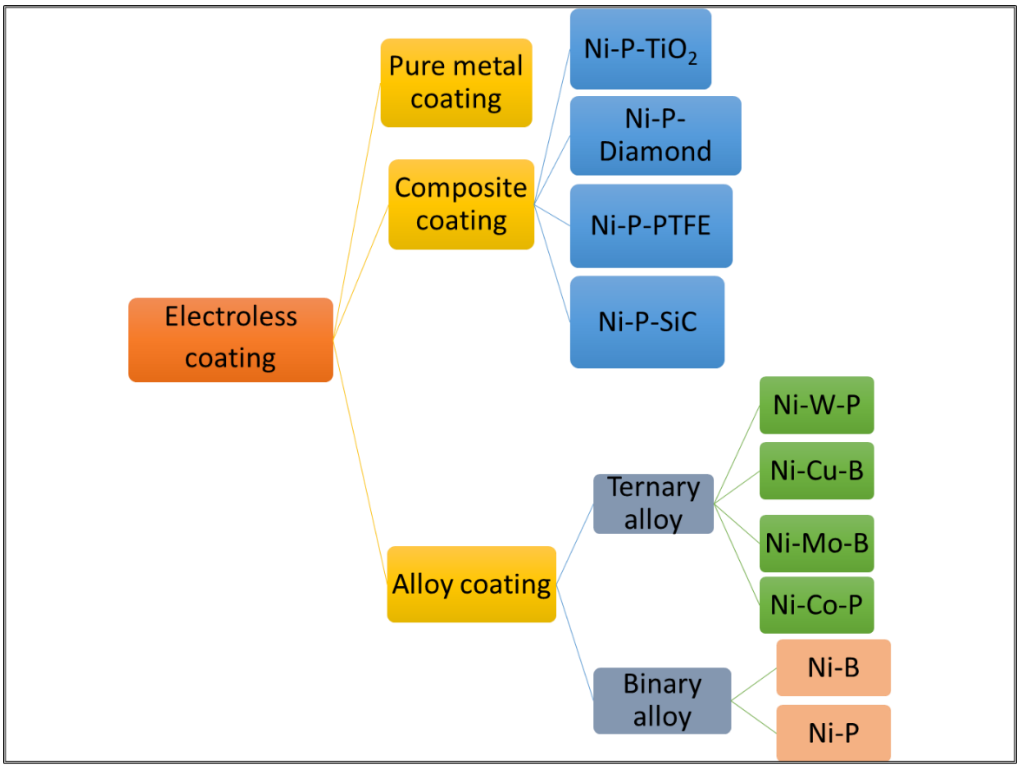

Figure 2.6: Types of the electroless coating [34, 66]

Even though electroless nickel alloy coatings can be applied for the fulfilling numerous engineering purpose, but important of enhanced properties i.e. anti-sticking, wear resistance, higher hardness, lubricity, oxidation resistance, and corrosion resistance has focused to the inclusion of several hard and soft particles in the electroless nickel-phosphorous/boron matrix [33-38, 134-157]. These particles selection based on the precise properties which are desired. For the tribological use, electroless nickel-phosphorous/boron composite coatings can be divided into two types, i.e. anti-wear composite coatings and self-lubricating composite coatings, on the basis of the categories of the incapacitated organic and/or inorganic particulate materials. The electroless nickel-phosphorous/boron composite coatings for lubrication purpose for the engineering components generally contain embedded solid particles like poly tetra fluoro ethylene (PTFE), WS_2, MoS_2, and graphite. This type of coatings has low friction coefficient compared to electroless nickel-phosphorous/nickel-boron alloys plating. In the same way, the anti-wear composite coatings are co-deposited with particles of hard material i.e. B_4C, WC, Al_2O_3, SiC, diamond, and TiO_2. Numerous Ni-P/B based composites coatings have been developed such as Ni-SiO_2-B, Ni-P-SiO_2, Ni-P-ZrO_2, Ni-P-Al_2O_3, Ni-Al_2O_3-B, Ni-P-SiC, N-P-WC, Ni-P-B_4C, Ni-Dimond-B, Ni-P-Diamond, Ni-P-PTFE, Ni-P-BN, Ni/CNT, Ni-P-CNT, Ni-P-Si_3N_4, Ni-P-Gr-SiC, Ni-P-ZnO, Ni-P-$K_2Ti_6O_{13}$ whiskers, Ni-WC-B, Ni-SiC-B, Ni-P-PTFE-SiC, Ni-P-CNT-SiC, Ni-P-TiO_2, Ni-Mo-P/PPS, Ni-P-Cr_2O_3 [34, 134-173].

2.3.3. Key benefits of electroless plating

In engineering applications, electroless plating is a plating method that has numerous advantages over the electroplating process. Some of these given below [34]:

- Deeply recessed areas and complicated shapes (e.g. through-hole) can be coated by the electroless plating process, which is tough to plate through electroplating.
- Electroless plating process does not include external electric current passing through a plating solution, while in case of electroplating external current is required [11-16, 44].
- Unlike electroplating process that can cause extreme build-ups of coating on edges and corners, electroless plating can produce a coating that has a uniform and can homogeneously cover the whole surface of a complicated shape [39].

- The electroless process can produce a coating that is homogeneous across the coating's thickness.
- It is possible to reduce the production cost through implementing the electroless method, as like in the electroplating process, it does not involve complex and arrangements that are often costly to produce and set-up.
- Electroless deposits are often much superior to that of electroplated deposits because the deposits are dense (less porous) and thus provide better protection to corrosion of steel-based substrates [34].

2.4. Electroless Ni-P coating

Since the early 1980's, electroless Ni-P alloy coating has been used progressively in numerous industries [41, 55, 174]. Few of the excellent properties of this coating are higher corrosion and oxidation resistance, deposit uniformity, wide-thickness range as well as electrical, physical and mechanical properties, good solderability, and surface lubricity [32, 89-90, 105-107, 110-113, 174-176]. Electroless nickel-phosphorus coatings are usually used either decorative or functional coatings in several industries, such as automotive, optics, plastic, petroleum, electronics, chemical, aerospace, textile, nuclear, mining, computer, food, and paper [32, 44-45, 57, 175]

An electroless Ni-P deposit is a pore-free alloy of nickel and phosphorus [65]. The quantity of P deposited is in the range <1% - 15%, dependent on bath constitutions, bath age, and working pH. Usually, electroless Ni-P deposits identify on the basis of their phosphorus content in the deposits, example: low phosphorus, medium phosphorus, high phosphorus [34].

a) **Low phosphorus (2-5% P):** Electroless Ni-P coatings with low phosphorous content have a crystalline structure. These types of deposits provide excellent wear resistance. In concentrated caustic soda, they also have outstanding corrosion resistance.

b) **Medium phosphorus (6-9% P):** As-deposited Ni-P coating is a combination of microcrystalline and amorphous nickel at medium phosphorus levels. Their resistance of abrasion and resistance are good enough for the maximum application.

c) **High phosphorus (10-15% P):** Electroless Ni-P coatings with high phosphorous content have an amorphous structure. These types of deposits are ductile and anti-corrosive. Mainly, they show anti-corrosive nature against chlorides and simultaneously they have mechanical stress.

As the above classification of electroless Ni-P deposits say that Ni-P deposits are structurally crystalline, semi-crystalline and amorphous due to the concentration of P. Ni-P nanocrystalline deposits exhibit non-magnetic nature, wear resistance, high hardness, low friction coefficient, and superior activity of electro-catalytic [32, 175-176]. An alloy of the nickel and phosphorous is thermodynamically unstable and during the heat treatment, ultimately form FCC nickel crystal and BCT Ni_3P compounds as stable structures. In the literature, many studies have been described the microstructures of the coating as deposited form and stable phases in the heat-treated form. For low phosphorus nickel and medium phosphorous nickel deposits, first of all, nickel crystal precipitated and followed by Ni_3P though in high phosphorous coating first of all Ni_3P and (or) Ni_xP_y compounds such as Ni_2P, Ni_5P_2, Ni_7P_3 and $Ni_{12}P_5$ occur. Generally, by the use of suitable heat treatment Ni-P coating's hardness can be enhanced, that can be ascribed to fine nickel crystallites and hard inter-metallic Ni_3P precipitated within crystallization of the amorphous phase [32].

2.4.1. Chemical reactions involved in the electroless Ni-P coating process

In this chapter, four mechanisms of electroless nickel-phosphorous deposition proposed by various researchers have been discussed to describe the principle reaction mechanisms involved in electroless nickel deposition. These mechanism schemes attempt to describe nickel reduction by sodium hypophosphite in acidic and alkaline bath and a secondary reaction of conversion of hypophosphite to elemental phosphorous [24-28, 56, 64].

1st mechanism:

The first proposal mechanism of electroless nickel-phosphorus deposition reaction was modified by Brenner and Riddell. They said that the actual nickel reductant is atomic hydrogen. This atomic hydrogen acts by heterogeneous catalysis at the catalytic nickel surface [24-28].

By the reaction of hypophosphite with water, the atomic hydrogen is generated:

$$H_2PO_2^- + H_2O \rightarrow H_2PO_3^- + 2H_{ad} \quad \text{.....(v)}$$

The absorbed atomic hydrogen at the catalytic surface reduces nickel ions:

$$Ni^{+2} + 2H_{ad} \rightarrow (Ni^{+2} + 2H^+ + 2e) \rightarrow Ni^0 + 2H^+ \quad \text{.....(vi)}$$

The evolution of hydrogen gas:

$$2H_{ad} \rightarrow H + H \rightarrow H_2 \quad \text{.....(vii)}$$

Gutzeit agrees with Brenner-Riddell reaction mechanism and attributes the evolution of atomic hydrogen and formation of the metaphosphate ion:

$$H_2PO_2^- \xrightarrow{cat} PO_2^- + 2H \quad \text{......(viii)}$$

The formation of hydrogen ion and an orthophosphate molecule:

$$PO_2^- + H_2O \rightarrow HPO_3^{-2} + H^+ \quad \text{.....(ix)}$$

Formational of elemental phosphorous due to the secondary reaction between atomic hydrogen and hypophosphite

$$H_2PO_2^- + H \rightarrow P + OH^- + H_2O \quad \text{.....(x)}$$

Although this mechanism has the support of several authors, it fails to describe certain other phenomena and it is not explained the reason behind less than 50 percent stoichiometric utilization of hypophosphite.

2nd mechanism:

The hydride transfer mechanism is known as the second mechanism of nickel-phosphorous deposition. The first time, this mechanism was suggested by Hersch. Hersch supposed that hypophosphite acts as the hydride ions donor. This mechanism was advanced by the Lukes [56].

At the catalytic surface, the reaction of water with hypophosphite:

In acidic solution

$$2H_2PO_2^- + 2H_2O \xrightarrow{cat} 2H_2PO_3^- + 2H^+ + 2H^- \quad \text{.....(xi)}$$

In alkaline solution

$$2H_2PO_2^- + 6OH^- \xrightarrow{cat} 2H_2PO_3^- + 2H_2O + 2H^- \quad \text{…… ……..……..(xii)}$$

Nickel ion reduction:

$$Ni^{+2} + 2H^- \rightarrow (Ni^{+2} + 2e^- + 2H) \rightarrow Ni^0 + H_2 \quad \text{……..……..(xiii)}$$

The reaction between the hydride ion and water or hydrogen ion:

Acid

$$H^+ + H^- \rightarrow H_2 \quad \text{……...……(xiv)}$$

Alkaline

$$H_2O + H^- \rightarrow H_2 + OH^- \quad \text{……(xv)}$$

Lukes said that the hydrogen ion which reveals as hydride ion was attached to P in hypophosphite. The second mechanism gives a reasonable description for joined reduction of nickel and hydrogen.

3rd mechanism:

The third mechanism of nickel-phosphorus deposition was proposed by Brenner and Riddell and modified by other researchers. This mechanism is also called electrochemical mechanism [24-26, 64].

By the reaction between water and hypophosphite, electrons are formed:

Anodic reaction

$$H_2PO_2^- + H_2O \rightarrow H_2PO_3^- + 2H^+ + 2e^- \ , \quad E^0 = 0.50\ V \quad \text{….……(xvi)}$$

Utilization of electrons generated in Eq. (xvi):

Cathodic reactions

$$Ni^{+2} + 2e \rightarrow Ni^0\ ,\ E^0 = -0.25\ V \quad \text{……..…(xvii)}$$

$$2H^+ + 2e \rightarrow H_2, E^0 = 0.000\ V \quad \text{……..…….(xviii)}$$

$$H_2PO_2^- + 2H^+ + e \rightarrow P + 2H_2O \qquad E^0 = 0.50\ V \quad \text{……(xix)}$$

On the basis of the third mechanism of nickel-phosphorus deposition, it can say that during nickel deposition, the evolution of hydrogen gas takes place. This mechanism also says that nickel ion concentration should significantly affect the rate of deposition.

4th mechanism:

Forth mechanism of nickel-phosphorus deposition was proposed by Cavallotti and Salvago and supported by Randin and Hintermann. This mechanism involves the coordination of Hydroxyl ions and hexaquonickel ion [108].

At a catalytic surface, reduction of nickel can be shown by the following reactions:

$$2H_2O \rightarrow 2H^+ + 2OH^- \quad \text{……..(xx)}$$

$$Ni(H_2O)_6^{+2} + 2OH^- \rightarrow [Ni(OH)_2]_{aq} + 2H_2O \quad \text{...……(xxi)}$$

$$[Ni(OH)_2]_{aq} + H_2PO_2^- \rightarrow NiOH_{ads}^{+} + H_2PO_3^- + H \quad \text{…….(xxii)}$$

$$NiOH_{ads} + H_2PO_2^- \rightarrow Ni^0 + H_2PO_3^- + H \quad \text{……(xxiii)}$$

Hydrogen atoms react and evolve hydrogen gas

$$H + H \rightarrow H_2 \quad \text{…….. (xxiv)}$$

Phosphorous co-deposition by the direct nitration between the catalytic nickel surface and hypophosphite:

$$Ni_{cat} + H_2PO_2^- \rightarrow P + NiOH_{ad}^{+} + OH^- \quad \text{…….(xxv)}$$

The researchers point out that silver, palladium, and copper can be also reduced with/without phosphorus co-deposition.

2.5. Electroless Ni-P composite coating

Electroless composite plating is the electroless plating which forms with co-deposition of hard or soft or non-metallic second phase particles. By the co-deposition of fine particulate matter, wear-resistant composite coatings are formed. For the formation of electroless composite deposits PTFE, RGO particles as solid lubricants and SiC, diamond, Al_2O_3 as hard particles have been used. Fluorocarbons and other small intermetallic compounds, and can co-deposited in an electroless Ni-P matrix for the

development of other electroless composite coatings. Initially, electroless composite deposition was not effective and frequently caused in the decay of the bath because of the dispersion of fine particles rises the bath loading of the electroless bath by almost 700-800 times of that of normal electroless bath and this leads to uncertainty of the bath. With the addition of appropriate stabilizers in electroless bath, nickel composite plating was ready [34, 66, 177-197]

Electroless nickel-phosphorus composite coatings can be categorized into two main groups as given in Figure 2.7.

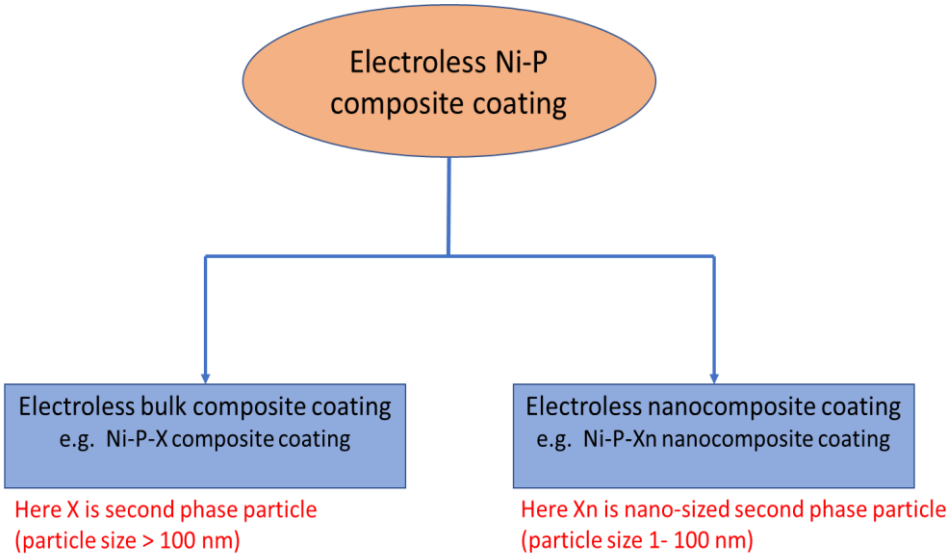

Figure 2.7: Types of electroless composite coating

Materials that incorporate nano-sized (less than 100 nanometers (nm)) particulates into a matrix material are called Nanocomposites. The effect of the inclusion of nanoparticles is an extreme improvement in toughness, thermal or electrical conductivity, mechanical strength, other mechanical and physical properties [198-200].

The co-deposition of nano-sized second phase particles (hard particles or ceramic) with the electroless coating is known as electroless nanocomposite coating. Electroless Ni-P alloy coatings show good abrasion, wear, and corrosion resistance but there is a scope for further enhancement in properties by co-depositing second phase particulate materials in a metal matrix. The idea of co-depositing several second phase particulate materials in an electroless nickel-phosphorus matrix so that taking advantage of their surface finish, hardenability, wear resistance and corrosion resistance is impelled to development of electroless nanocomposite coating. Wear-resistant electroless

nanocomposite coating can be produced by co-depositing nano-sized lubricants (solid) such as PTFE and hard materials in form of powder e.g.; silicon carbide, alumina diamond etc. The co-deposition capability of the second phase particulate materials reinforced in the metal matrix effect by the shape, density, size, concentration, polarity and technique of suspension in the solution. The properties of nanocomposite coatings extremely dependent upon the stable dispersion of second phase materials in deposition bath otherwise deposited composite coatings would have non-uniformly distributed particles. Well-dispersed second phase particles within metal matrix exhibit superior corrosion resistance, wear resistance and hardness [34, 138, 141-142, 144, 148, 151-157, 159, 201-209].

The incorporation of hard particles like, SiC and B_4C has a tendency to improve the coefficient of friction and has poor lubrication property in comparison to electroless nickel-phosphorous coating because of high mechanical interlocking force and high surface roughness of the hard particles. On the other side, adding soft particles like graphite, PTFE and MoS_2 showed a drastic reduction in coefficient of friction and exhibit self-lubrication property [152, 154, 202, 205].

Several second phase soft and hard particulate materials enhanced the tribological applicability of electroless nickel-phosphorus plating which includes, aluminum oxide, boron carbide, silicon oxide, silicon carbide, silicon nitride, molybdenum sulfide, and PTFE. In general, researchers have found that Al_2O_3 reinforcement in the deposit diminished the scaling and improved resistance against to wear of deposits as compared to the without reinforced nickel-phosphorous deposits [34, 150, 153, 155, 158, 206]. Good chemical inertness and non-sticking properties of PTFE are helpful for avoiding severe oxidation wear and adhesive wear [205]. Weiwei Chen et.al. informed that Ni-P-TiO_2 deposits show enhanced wear resistance than conventional Ni-P coating [166].

The quantity of co-depositing particles, P concentration within the matrix and heat-treatment method govern the hardness of electroless nanocomposite deposits. The deposit hardness enhanced with the improved concentration of hard second phase particles (e.g.; Si_3N_4, TiO_2, SiC) in the electroless deposit while hardness reduces with the particles of soft materials (e.g.; PTFE). Hard particulate materials are mostly responsible for a rise in hardness in case of electroless nanocomposite coatings. These nanocomposite coatings are claimed to superior hardness for materials/apparatuses

applied at ambient temperatures, e.g.; core boxes for castings, extruders for plastics, molds, metal patterns, casting dies of zinc alloys and forging dies. The heat treatment effect on the hardness of electroless nanocomposite coating has alike trend of that in electroless Ni-P alloy coating. The hardness of deposits rises with heat-treatment temperature up to 400℃ is by the creation of inter-metallic Ni_3P phase due to precipitation hardening and reduces beyond 400°C heat treatment temperature, due to a reduction in lattice defects and coarsening of Ni_3P compounds [136, 154, 174, 177, 180 190].

Though the inclusion of second phase particulates materials in nickel-phosphorous deposit marks in the enhancement of resistance against wear and friction of the deposits, the same unfavorably affects the corrosion and oxidation resistance of the deposits. Second phase particles like, B_4C, Si_3N_4, and PTFE in Ni-P coating reduced its anti-corrosion characteristics which may be due to the flaws in the matrix or may be as a result of micro-cracks formation on the surface by the impregnation of the embedded particles in the deposit. As reported in literature, some electroless nanocomposite coatings claimed good corrosion behavior [143, 155, 167, 168, 184, 202, 205]. Bigdeli et.al. stated that the inclusion of SiC particulates in electroless Ni-P deposits provided improved corrosion and oxidation protection [202]. Good corrosion-resistant performance has been also demonstrated by electroless Ni-Mo-P/PPS deposit.

2.6. Properties of electroless coatings (Ni-P coating and Ni-P-composite coating)

Electroless coatings are often used for the protection of the metal, polymer, and other materials surfaces due to coating properties like high anti-corrosion, high oxidation resistance, low friction and wear resistance. It can see in the above literature, various electroless alloy, electroless composite, and nanocomposite coatings have been developed for the enhancing the surfaces of various materials such as metals, metal alloys, magnetic materials, plastics etc. Electroless Ni-P coatings protect surfaces of materials against the friction, corrosion, abrasion, and their properties are enhanced by the co-deposition in Ni-P matrix, composite coating has improved physical, electrical, mechanical, electrochemical and tribological properties. Basic characteristics of the electroless coatings are shown in Figure 2.8. Physical, mechanical, magnetic, electrochemical and tribological properties of nickel-phosphorus and Ni-P-X (where X is second phase particles) composite coating are described below.

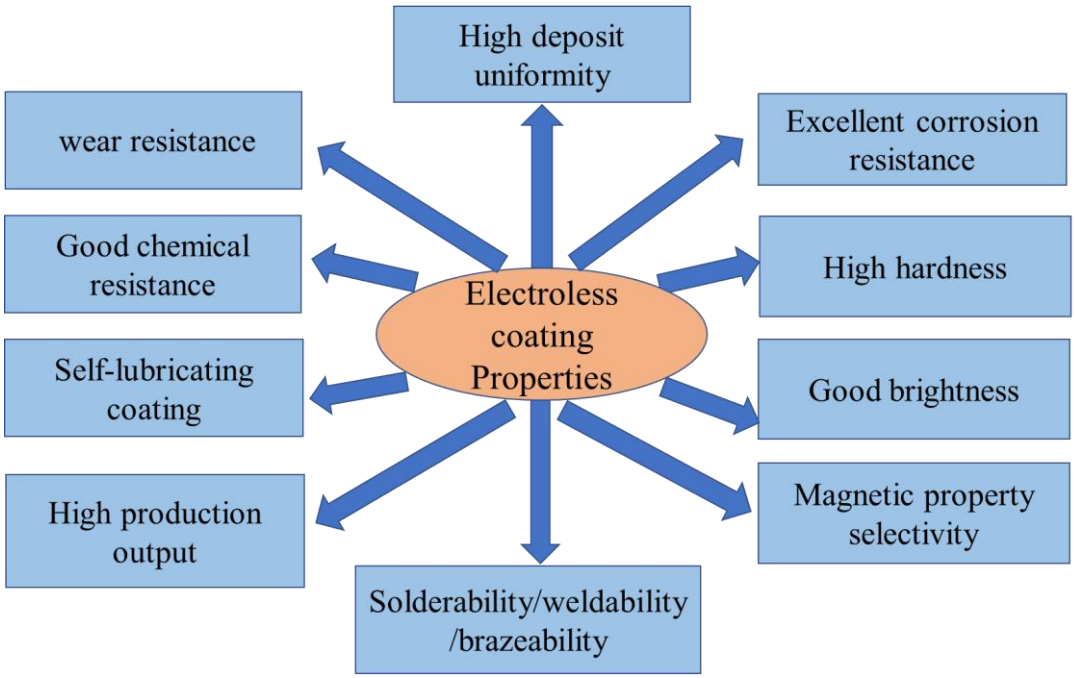

Figure 2.8: Properties of electroless coatings

2.6.1. Structure

Materials have a structure-property correlation, so for the understand the properties of materials, it is necessary to know the structure of materials. This section is started with the structure of electroless nickel-phosphorous deposit followed by structural influence due to the inclusion of the various second phase particles like SiC, TiO_2, ZrO_2 CeO_2, Si_3N_4 etc. in the Ni-P matrix.

Nickel-phosphorous deposits with various phosphorus concentration, i.e. low phosphorus (3-5 wt.% phosphorous), shows crystalline structure, medium phosphorus (6-9 wt.% phosphorous) shows the semi-crystalline structure and high phosphorus (10-15 wt.% phosphorous) shows amorphous structure [32, 34].

From SEM image (Figure 2.9), it is detected that the coating is deposited as a combination of numerous spherical globules [83]. These spherical globules have a tendency to adhere with the clean and active surface of the materials. The appearance of electroless nickel-phosphorus deposits is uniform and free of blisters, pits, cracks and pimples. The mechanism of synthesis of the coating is clear from scanning electron microscopic micrographs. During the electroless nickel-phosphorous deposition, the development of the coating starts at isolated locations on the surface and complete entire surface is then shielded by lateral growth [66, 94-97, 117].

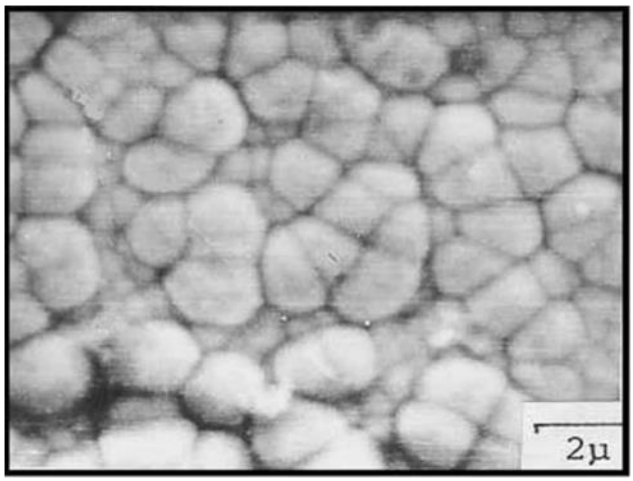

Figure 2.9: SEM image of spherical globules in Ni-P coating [83]

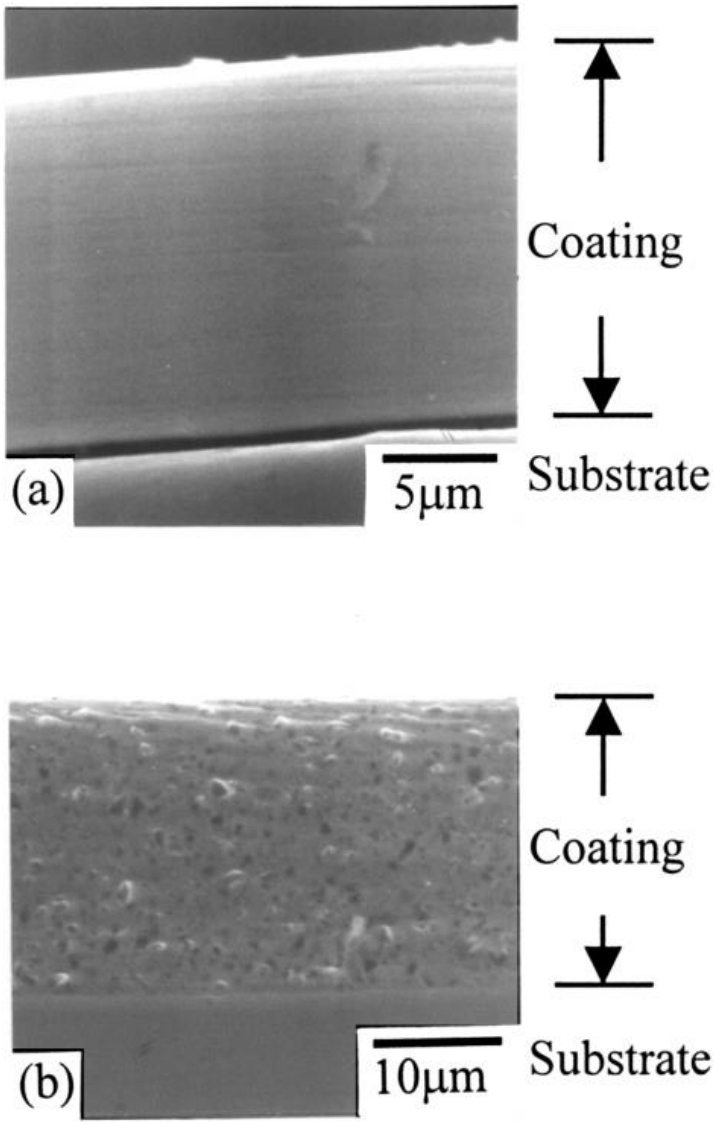

Figure 2.10: SEM images of (a) Ni-P coatings; (b) Ni-P-SiC composite coatings (100 g/l SiC suspension) [177]

In 2002, C. K. Chen et al. presented their work as electroless nickel-phosphorus plating with SiC particle were deposited on tool steel specimen and effect of post heat treatment of composite coatings. The cross-sectional scanning electron microscopic images of the nickel-phosphorus deposits and composite deposits in Figure 2.10 show that the SiC particles are homogeneously distributed in the whole Ni-P film matrix. The SiC concentration in the composite coating increased with increasing SiC powder concentration in the deposition bath. Heat treatment changed the structure of composite coatings. In both the as-deposited and the annealed below 400^{o}C states, the structure of nickel-phosphorus deposit and Ni-P-SiC composite deposit were same. Ni_5Si_2, Ni_3Si (L12) and graphite precipitate were produced by the reaction of nickel with SiC during annealing above 450^{o}C [177].

In 2006, J.N. Balaraju et. al. worked on the electroless nickel-phosphorous coating and Ni-P-CeO_2 (4-17 µm sized CeO_2), Ni-P-Si_3N_4 (2-10 µm sized Si_3N_4) and Ni-P-TiO_2 (2.4-3 µm) composite coating on stainless steel (AISI 304 grade) specimen. They concluded their study work as the inclusion of the particles of TiO_2, CeO_2, and Si_3N_4 in the nickel-phosphorous matrix does not influence the phase transformation behavior and structure of electroless Ni-P deposits [179].

In 2006, J. Novakovic et. al. presented their work on production and properties of Ni-P-TiO_2 composite deposit on brass [210]. In 2009, J. Novakovic et.al. presented their work on vacuum heat-treated electroless Ni-P-TiO_2 composite coating on steel substrate [211]. They used 200-300 nm sized TiO_2 particles for the deposition of Ni-P-TiO_2 composite deposit. The Ni-P-TiO_2 nanocomposite deposits show superior fineness, uniformity, and density. J. Novakovic et. al. presented scanning electron images of the electroless nickel-phosphorous and Ni-P-TiO_2 nanocomposite deposits in Figure 2.11 [211]. The obtained nanocomposite deposits show metallic surface of mat-gray color. All these deposits display the occurrence of micro-voids on their surface. The included TiO_2 in the nickel-phosphorous matrix shows the influence of the heterogeneity of the surface [211]. J. Novakovic et. al. [211] compared (Figure 2.12 (a)) nickel-phosphorous and nanocomposite Ni-P-TiO_2 deposits formed with various TiO_2 particles concentrations in deposition bath by XRD patterns. The electroless nickel-phosphorous deposit has amorphous nature with embedded crystalline TiO_2 particles. X-ray diffraction patterns of vacuum thermal treated (at 800°C/10 minutes) electroless nickel-

phosphorous and Ni-P-TiO_2 nanocomposite deposits with varying bath concentration shown in Figure 2.12 (b). The rapid transformation of nickel-phosphorous deposit from a disordered arrangement to an ordered arrangement of FCC nickel and BCT Ni_3P occurs during thermal treatment which founds in numerous sharp peaks. These XRD patterns have not metastable phases.

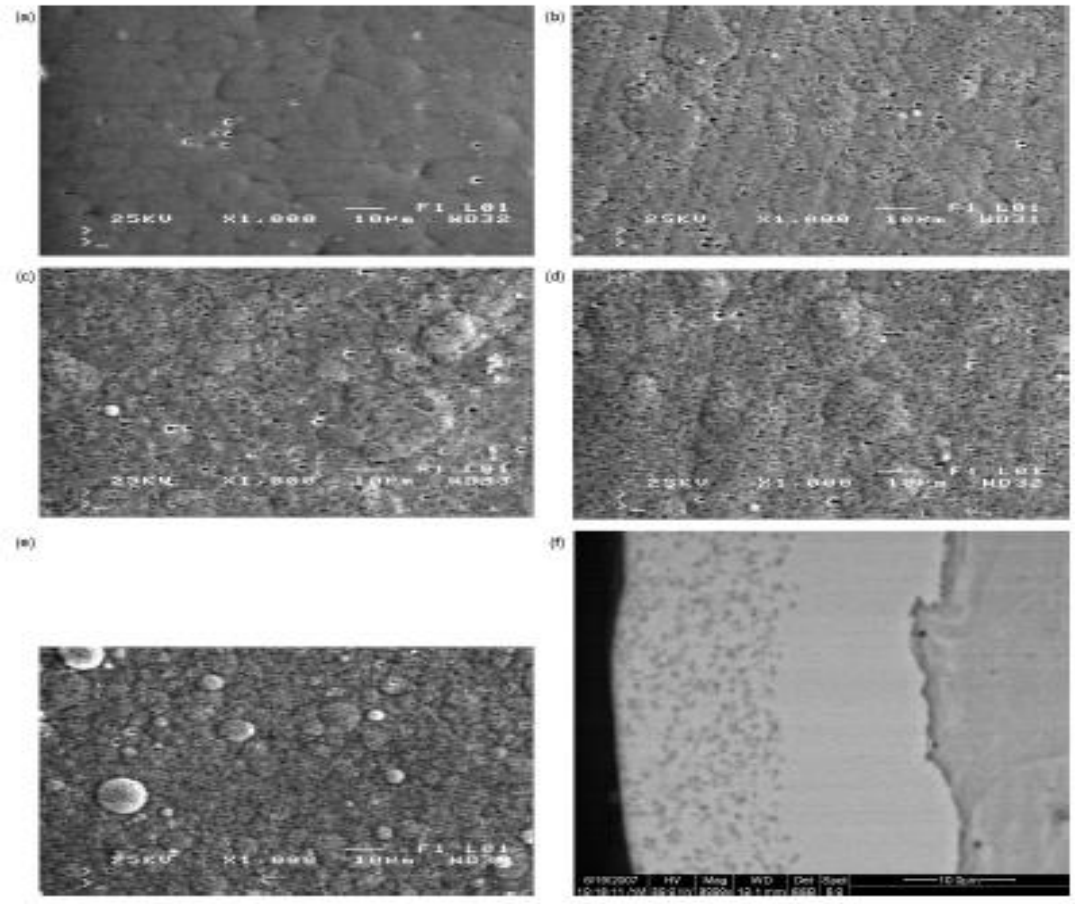

Figure 2.11: SEM images of the electroless Ni-P and Ni-P-TiO_2 nanocomposite coating with various TiO_2 bath concentrations (a) 0 g/l, (b) 0.5 g/l, (c) 1.0 g/l, (d) 1.5 g/l, (e) 2.0 g/l and (f) cross-section (3000×) [211]

In 2008, A. Abdel Aal et. al. synthesized electroless Ni-P-TiO_2 composite coating with variation in nano TiO_2 particles concentration on commercial carbon rod. The microstructure of deposited coatings shown in Figure 2.13. As they observed, the nanocomposite Ni-P-TiO_2 deposits exhibited smaller size grains compared with Ni-P deposit [169]. They also reported that the TiO_2 content in Ni-P-TiO_2 composite deposits increases with increasing TiO_2 concentration in the deposition bath. Ni-P-TiO_2 nanocomposite displayed high catalytic activity with regard to the oxidation of small

organic molecules than nickel-phosphorous and the maximum activity was shown by electrode Ni-P-TiO_2 (4.5% TiO_2) [169].

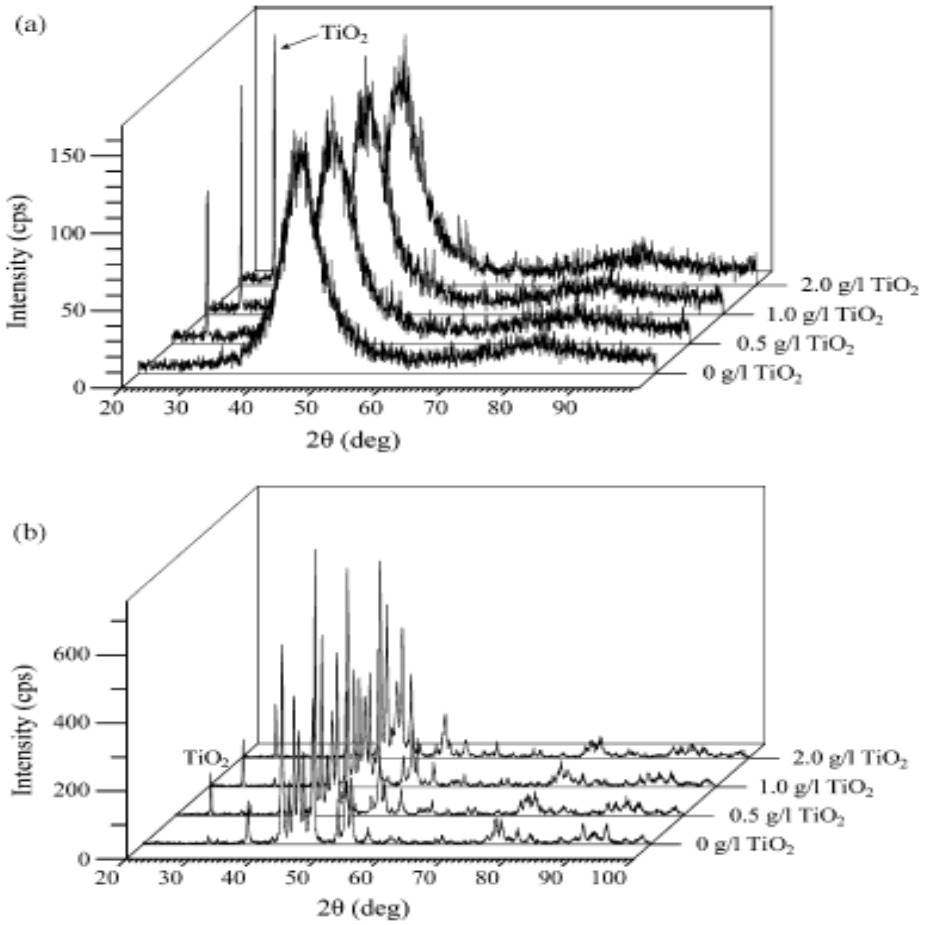

Figure 2.12: Phase analysis of the as-deposited (a) and vacuum thermal treated (b) Ni-P deposit compared to the nanocomposite Ni-P-TiO_2 deposits [211]

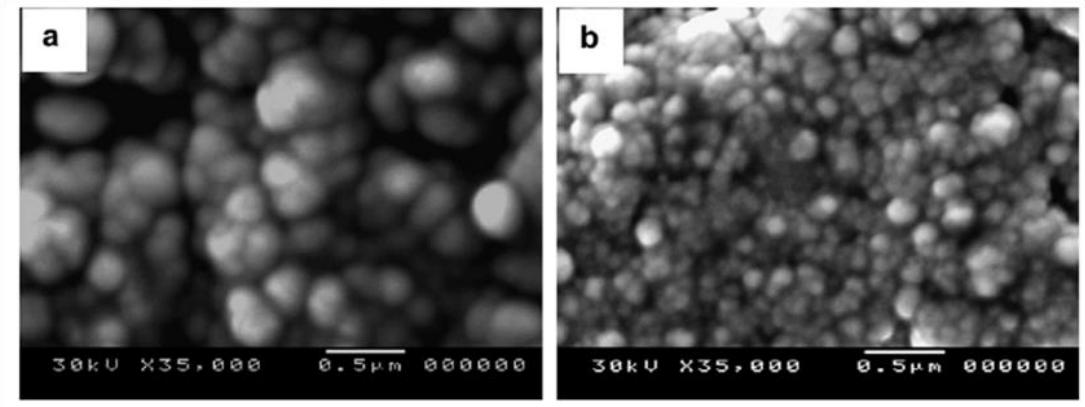

Figure 2.13: Morphology of the electroless (a) Ni-P deposit and (b) Ni-P-TiO_2 composite deposit [169]

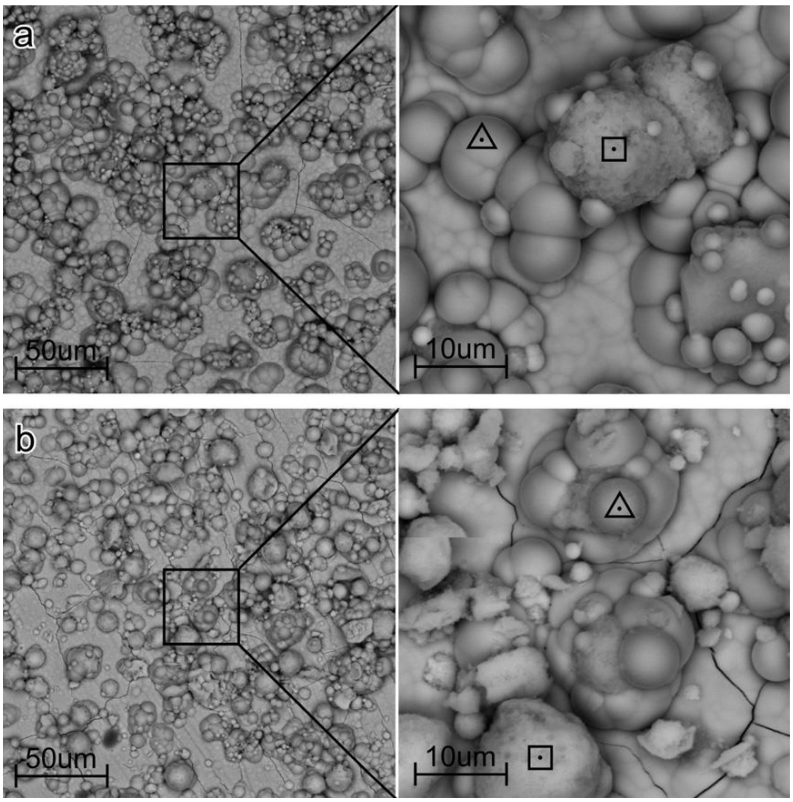

Figure 2.14: The scanning electron microscopic pictures of Ni-P-ZrO_2 nanocomposite coatings: (a) without surfactant and (b) with 2.00 x cmc concentration of DTAB [204]

In 2012, Katarzyna Zielinska et. al. [204] synthesized Ni-P-ZrO_2 nanocomposite coating on AISI 304 steel alloy. The scanning electron images of coatings are presented in Figure 2.14. In the presence of DTAB, the Ni-P-ZrO_2 nanocomposite coating changed the surface structure and became smoother. For the extensive increase in the amount of the entrenched solid particles in situations where the concentration of the surfactant is equal to or higher than cmc, some factors can account such as:

- Improved particle wettability,
- The reduction in the surface tension among H_2 bubbles present at the surface and also between the surface of the steel substrate and ZrO_2 particles,
- The improvement of the electrostatic adsorption of suspended ZrO_2 particles at the surface of the steel.

As T.R. Tamilarasan and his team (2015) mentioned in their work, on the electroless deposition of nickel-phosphorous and Ni-P-TiO_2 deposits on low carbon steel and the deposits properties due to the presence of SDS and DTAB surfactants have been also

studied by them. Surface morphology of the Ni-P-TiO_2 nanocomposite is displayed in Figure 2.15.

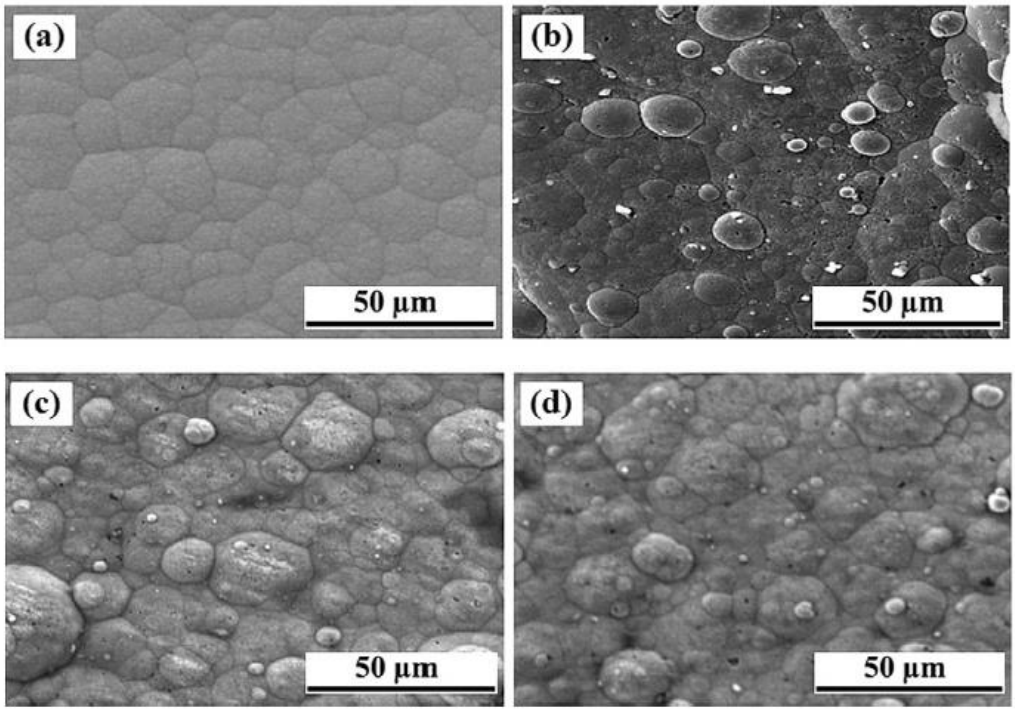

Figure 2.15: SEM images of composite coatings: (a) Ni-P deposit without surfactant, (b) Ni-P-TiO_2 nanocomposite deposit without surfactant, (c) and (d) Ni-P-TiO_2 nanocomposite deposit with surfactant [171]

For enhancing the corrosion resistance of deposits, surfactants concentrations have been optimized by them. The deposition bath with DTAB gives higher deposition rate as compared with deposition bath having SDS. The quantity of TiO_2 particles in the deposit is also high when surfactant DTAB is used. On the basis of morphological analysis of Ni-P-TiO_2 deposits, it can say that at the optimum DTAB concentration TiO_2 particles were uniformly distributed while nodular structures of TiO_2 were found for surfactant SDS. The corrosion resistance of Ni-P-TiO_2 deposit is significantly improved as an effect of the increase in Rct (charge transfer resistance) four times higher to that of nickel-phosphorous deposits [171].

In 2017, Prasanna Gadhari et. al. worked on the optimization of the deposition parameters for understand the wear behavior of Ni-P-TiO_2 composite coating. They used Taguchi orthogonal array for optimization of the deposition parameters to reduce the wear of Ni-P-TiO_2 composite deposited. Their work on surface morphology reveals the nodular structure of deposit with even dispersion of titanium particles. At 10 g/l

TiO_2 in the deposition bath, the content of titanium and phosphorus is respectively 9.97 wt.% and 7.74 wt.% in the deposit. The content titanium is 6.41 wt.% and phosphorus 8.13 wt.% (at 5 g/l TiO_2 in the electroless bath). The coating has amorphous nature as-deposited condition [212].

Above studies show the structures of electroless Ni-P deposit and Ni-P-X composite coating. These deposits have a crystalline, semi-crystalline and amorphous structure on the basis of presented constituents in the deposits. The incorporation of ZrO_2, TiO_2, CeO_2, Si_3N_4 etc. does not much influence the structure and phases of the electroless Ni-P coating.

2.6.2. Electrochemical properties

Electrochemical characteristics mean corrosion current density, polarization potential, and resistance against to corrosion and oxidation. This section started with the description related to corrosion followed by the electrochemical parameters and corrosion resistance of electroless nickel-phosphorous coating and various Ni-P-X composite coating given by the various researchers.

"The corrosion of metals is a very complex process," said by the Nicoleta Cotolan [213]. Corrosion is defined as "deuteriation of the materials and materials properties caused by chemical, electrochemical reactions that are produced between the materials and external environment". For the protection of the materials and materials properties from the corrosion, surface modification is required [214]. Electroless alloy and composite coatings modified the surface of the materials.

The resistance against corrosion of electroless nickel-phosphorous plating is a function of its constituents' composition [32, 34, 66, 89, 138, 112, 115]. Most of the electroless coatings act as naturally passive and resistant to attack in maximum environmental conditions. Passivity or corrosion resistance of these coatings is significantly affected by their P content. Other constituents of electroless nickel bath are also more important for its corrosion resistance than its P content. Heat treatment of these coatings is a most important variable which affects the corrosion [143, 167-168].

In 2010 Taher Rabizadeh et.al. (Iran) investigated corrosion resistance behavior of vacuum thermal treated electroless nickel-phosphorous coating by the help of electrochemical impedance spectroscopy (EIS) and potentiodynamic polarization in 3.5

wt.% sodium chloride electrolyte. Their electrochemical tests were done with the standard three-electrode cell using an EG & G potentiostat/galvanostat, model 273A. Ag/AgCl electrode and platinum plate were acted as a reference and counter electrodes, respectively. Polarization experiments were done by sweeping the potential at a scan rate of 1 mVs^{-1} in the range of ±400 mV vs. OCP (open circuit potential). The impedance experiments were done with Solartron Model SI 1255 HF Frequency Response Analyzer (FRA) attached to a Princeton Applied Research (PAR) Model 273A potentiostat/galvanostat [89].

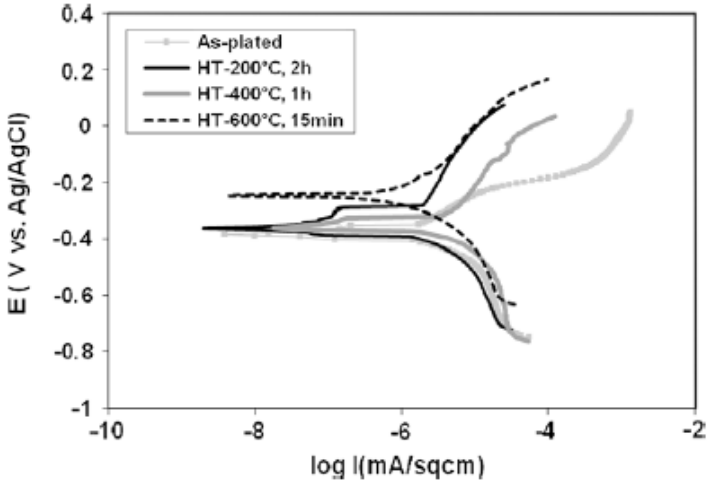

Figure 2.16: Tafel curves for as-plated and heat treated electroless nickel-phosphorous deposits in 3.5% sodium chloride electrolyte [89]

The electrochemical impedance spectroscopic results were measured at (OCP) in a range of 0.01 Hz-100 kHz frequency with an AC signal of 5 mV using electrochemical impedance spectroscopy software model 398 [89]. Their results show in Table 2.2 and Figure 2.16.

Table 2.2: Polarization parameters of coated and thermal treated electroless nickel-phosphorous coatings in 3.5% NaCl solution [89]

Coating	**Polarization potential (V vs. Ag/AgCl)**	**Current density (A/cm^2)**
Without heat-treated	376×10^{-3}	10×10^{5}
Heat-treated at 200^0C, 2 h	355×10^{-3}	6.3×10^{5}
Heat-treated at 400^0C, 1 h	320×10^{-3}	1×10^{5}
Heat-treated at 600^0C, 15 min	250×10^{-3}	2.5×10^{5}

Figure 2.17. displays the Nyquist plots got for deposited and heat-treated nickel-phosphorous coatings in 3.5% NaCl electrolyte at their respective OCPs. All Nyquist plots similarly appeared, having a single half circle in high-frequency regions indicating the charge-controlled reaction. It can be noted that these semi-circles have a similar shape, but they have different sizes. This shows that the similar fundamental procedures must be happening on all these deposits but over a various effective area in each case [89].

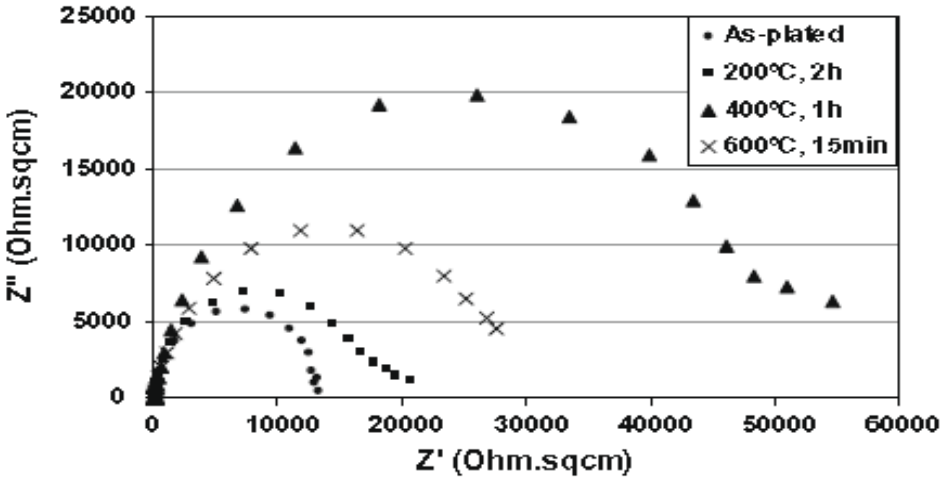

Figure 2.17: Nyquist plot for deposited and thermal treated nickel-phosphorous electroless coatings in 3.5% NaCl electrolyte [89]

In 2004, Y.S. Huong et. al. worked on electroless nickel-phosphorous composite coatings incorporated with particles of PTFE and/or SiC. The results obtained by them show that [178]:

- Both Ni-P coating and composite coatings confirmed significant enhancement of corrosion resistance in the both acidic and salty atmosphere;
- Co-deposition of either SiC or PTFE particles slightly reduced anti-corrosive property of the composite coatings in 3% NaCl electrolyte but had insignificant effects on their corrosion resistance in 1.0 N H_2SO_4;
- Ni prominent significantly enhanced resistance again the corrosion due to the enhancement of the surface autocatalytic properties and homogeneousness for Ni-P-SiC-PTFE complex composite coating.
- Correct post-thermal-treatment (400°C and 1 hr) advance the deposit density and structure, giving rise to improved corrosion resistance.

In 2008, Laizhou Song et.al. (China) studied the corrosion resistance of Ni-P-TiO_2 coating on permanent magnet NdFeB by polarization technique and EIS tests. They performed polarization measurements with ZF-3 potentiostat, ZF-4B dynamic potentiometer and ZF-10 data collection recorder, and they recorded Tafel curves at the potential 50 mV/min scan rate [215].

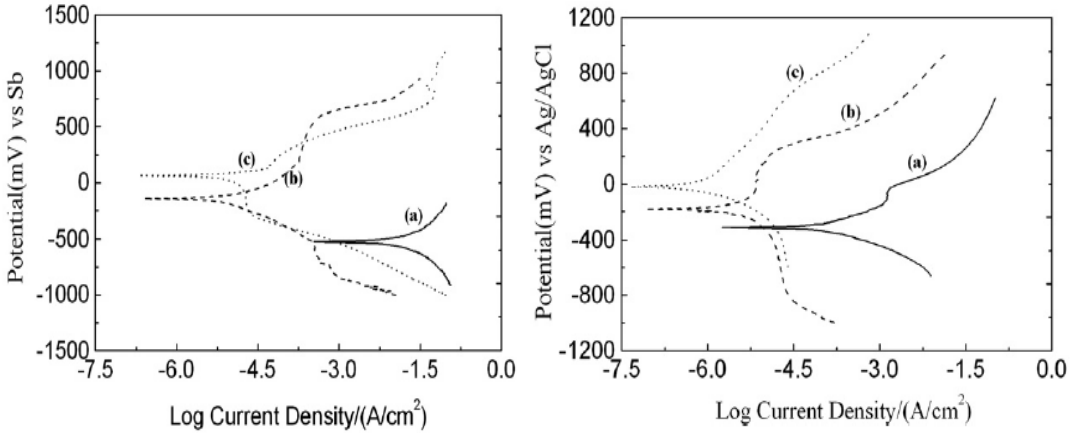

Figure 2.18: Tafel curves of (a) NdFeB magnet, (b) Ni-P coating and (c) Ni-P-TiO_2 nanocomposite coating dipped in 0.5 mol/l H_2SO_4 electrolyte and 0.5 mol/l NaCl electrolyte respectively [215]

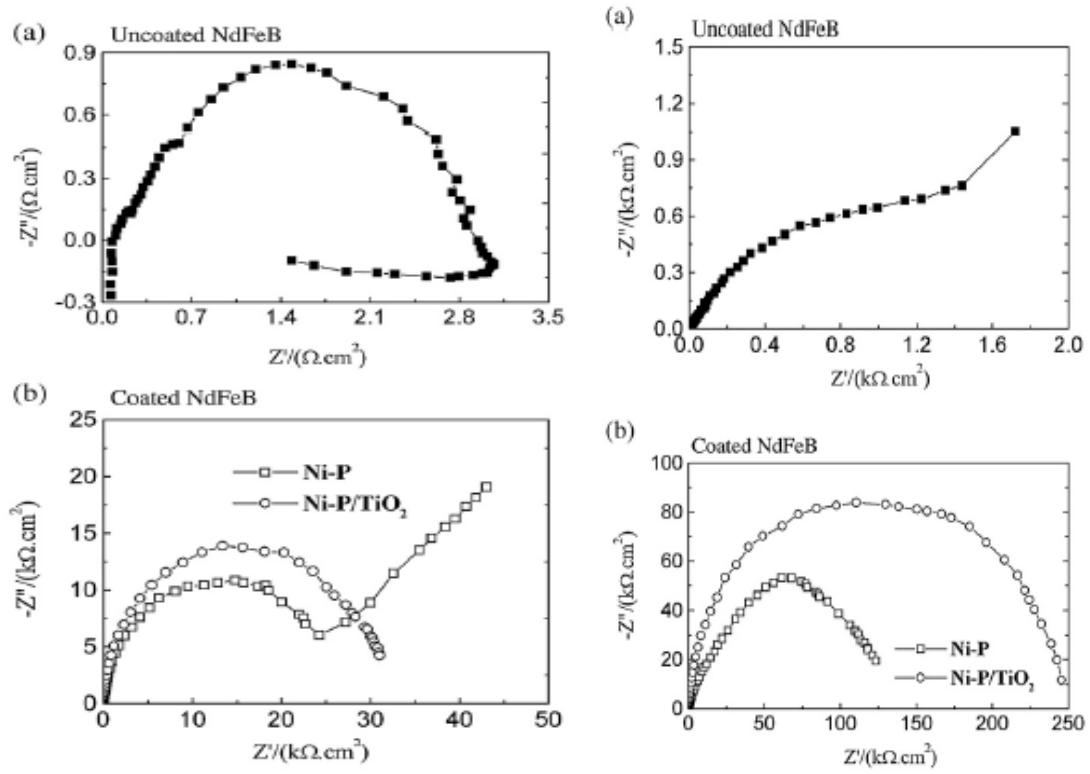

Figure 2.19: EIS results of (a) NdFeB magnet and (b) coated NdFeB in 0.5 mol/l H_2SO_4 electrolyte and 0.5 mol/l NaCl electrolyte, respectively [215]

Polarization curves of uncoated NdFeB, nickel-phosphorous and Ni-P-TiO_2 nanocomposite coating in 0.5 mol/l H_2SO_4 electrolyte and 0.5 mol/l NaCl electrolyte are presented in Figure 2.18 [215]. They conducted EIS measurements by CHI660C(USA) electrochemical analyzer/workstation at the OCP. EIS plots of NdFeB magnet and deposited NdFeB magnet in 0.5 mol/l H_2SO_4 electrolyte and 0.5 mol/l sodium hypophosphite electrolyte is shown in Figure 2.19 [215].

Table 2.3: Corrosion resistance of nickel-phosphorous deposit and Ni-P-TiO_2 nanocomposite film on NdFeB magnet [215]

Specimen	**NdFeB magnet**	**Ni-P coated magnet**	**Ni-P-TiO coated magnet**
0.5 mol/l NaCl $R_p/(k\Omega\ cm^2)$	1.83	60	120
(Deep for 1 hr) $I_{corr}/(\mu A/cm^2)$	495.45×10^2	1.44	0.22
0.5 mol/l H_2SO_4 $R_p/(k\Omega\ cm^2)$	3.33×10^{-3}	8	12.5
(Deep for 1 hr) $I_{corr}/(\mu A/cm^2)$	1.19×10^5	7.64	2.38

From Table 2.3, I_{corr} of Ni-P-TiO_2 nanocomposite coating is 2.38 $\mu A/cm^2$ in 0.5 mol/l H_2SO_4 electrolyte about 33% of that of Ni-P deposit and 0.22 $\mu A/cm^2$ in 0.5 mol/l NaCl electrolyte about 14% of that of Ni-P coating, respectively. In 0.5 mol/l H_2SO_4 and 0.5 mol/l NaCl electrolyte, the corrosion resistance of the nanocomposite coating is 12.5 $k\Omega cm^2$ and 120 $k\Omega cm^2$, around 1.6 and 2 times that of nickel-phosphorous coating, respectively. These observations indicate that Ni-P-TiO_2 nanocomposite coatings have an improved corrosion resistance than Ni-P coating [215].

In 2009, Faryad Bigdeli et al. worked on structural and corrosion properties of Ni-P-SiC nanocomposite coating on St. 367 tool steel. Nyquist plots of deposited and thermal-treated electroless nickel-phosphorous and Ni-P-SiC composite coatings are shown in Figure 2.20. Corrosion tests indicated that both nickel-phosphorous and Ni-P-SiC composite coatings demonstrated significant enhancement of corrosion resistance [202]. Better corrosion resistance was got for Ni-P-SiC composite coating over Ni-P deposit, which can be attributed to a reduction in the available effective metallic area for corrosion. Post-thermal-treatment at 400^oC for 1 hr increased the density of coating and improved corrosion resistance for the applied nickel-phosphorous and Ni-P-SiC composite coatings [202].

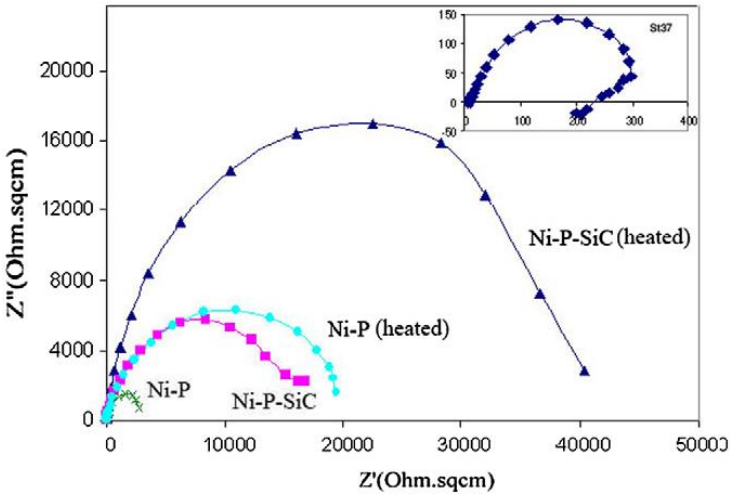

Figure 2.20: EIS results of nickel-phosphorous and Ni-P-SiC composite coatings in 3% NaCl electrolyte [202].

In 2012, M. G. Hosseini et. al. worked on the synthesis of electroless coating and electrochemical studies of Ni-PCTFE-P nanocomposite coating. Tafel curves of Ni-PCTFE-P nanocomposite coatings in 3.5% NaCl electrolyte with 0.2 mV/s scan rate are shown in Figure 2.21. Electrochemical measurements showed that increase in PCTFE concentration led to a reduction in corrosion current density and improvement in potential corrosion [205].

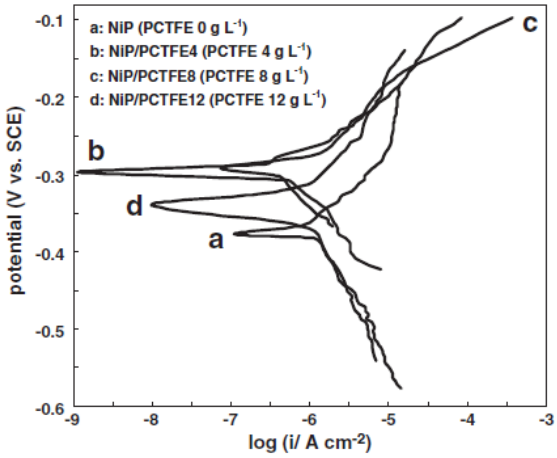

Figure 2.21: Tafel curves of electroless nickel-phosphorous deposit and Ni-PCTFE-P composite deposits in 3.5 wt.% NaCl electrolyte [205].

In 2014, Chunyang Ma et al. [154] synthesized Ni-P-SiC nanocomposite coating on mild steel and gave the corrosion study for this type of coatings. Tafel curves of the plated and thermally-treated Ni-P-SiC nanocomposite coatings in 3.5 wt.% NaCl

electrolyte at room temperature are shown Figure 2.22. Figure 2.23 shows the measured EIS data in the Nyquist plot. Nyquist plot results present that the maximum R_{ct} and the minimum CPE for Ni-P-SiC nanocomposite coatings are 188254 Ω/cm^2 and 7.244 μF/cm, respectively. The minimum corrosion current density value is got for the coatings thermally treated at 400^{o}C for 1hr.

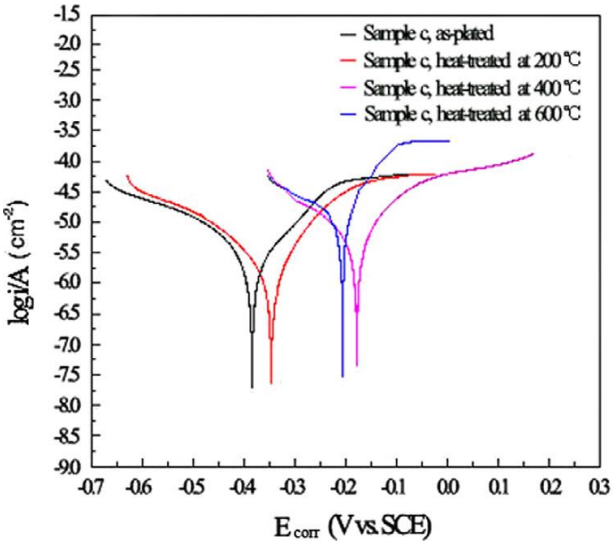

Figure 2.22: Polarization curves of plated and thermal-treated at different temperature electroless Ni-P-SiC nanocomposite coatings in 3.5 wt.% NaCl electrolyte [154]

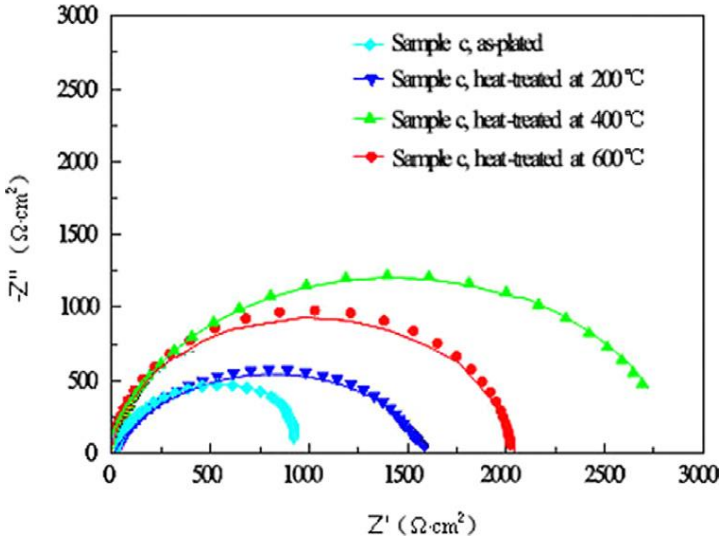

Figure 2.23: Nyquist plots of Ni-P-SiC nanocomposite coatings in 3.5 wt.% sodium chloride solution [154]

In 2015, Hong Luo et. al. developed Ni-P-WC nanocomposite coating on L80 carbon steel and analyzed the corrosion behavior of the coatings. The open circuit potentials of

the steel specimen, nickel-phosphorous plating and Ni-P-WC nanocomposite plating in 3.5 wt.% NaCl electrolyte at room temperature are presented in Figure 2.24. Tafel curves of the steel substrate, nickel-phosphorous plating and Ni-P-WC nanocomposite plating in the 3.5 wt.% NaCl solution are shown in Figure 2.25. The electrochemical tests prove that the addition of WC nanoparticles also significantly expands the coating's corrosion resistance in the NaCl solution [207].

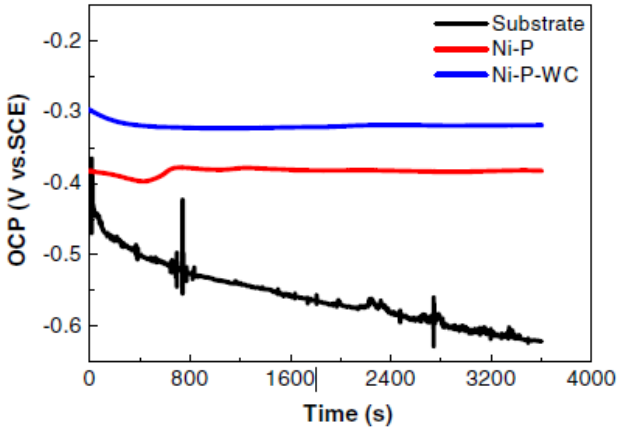

Figure 2.24: OCPs of carbon steel, nickel-phosphorus plating and Ni-P-WC composite plating in the 3.5 wt.% NaCl solution [207]

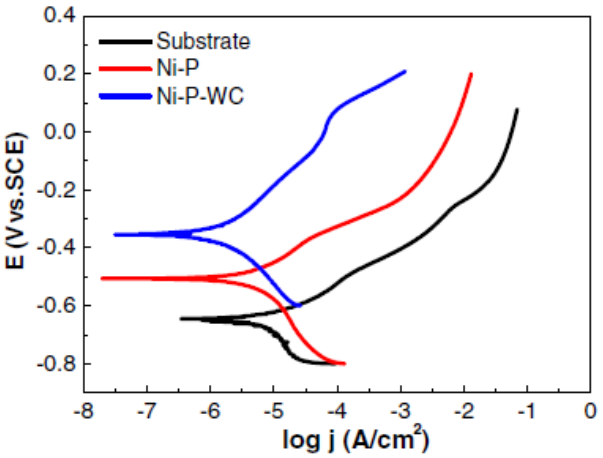

Figure 2.25: Tafel curves of the substrate, Ni-P plating and Ni-P-WC composite plating in the 3.5 wt.% NaCl electrolyte [207]

In 2016, J. A. Calderon et. al. worked on the corrosion behavior of electroless Ni-P-TiO_2, Ni-P-SiC and Ni-P-Dimond nanocomposite films on commercially pure magnesium substrate (99.9 percent). Figure 2.26 shows the polarization curves during the erosion-corrosion tests of nickel-phosphorus coating and nickel-phosphorus-

ceramic nanocomposite coatings. The impedance plots obtained at OCP for the nickel-phosphorus coating and nickel-phosphorus-ceramic nanocomposite coatings at high and low concentrations of TiO_2, SiC and Dimond nanoparticles are shown in Figure 2.27. The incorporation of the TiO_2, SiC and Dimond nanoparticles into the nickel-phosphorus matrix decreases the increases the deposition rate by around 5 times with respect to the Ni-P coating and corrosion rate of the coating by 4 times [209].

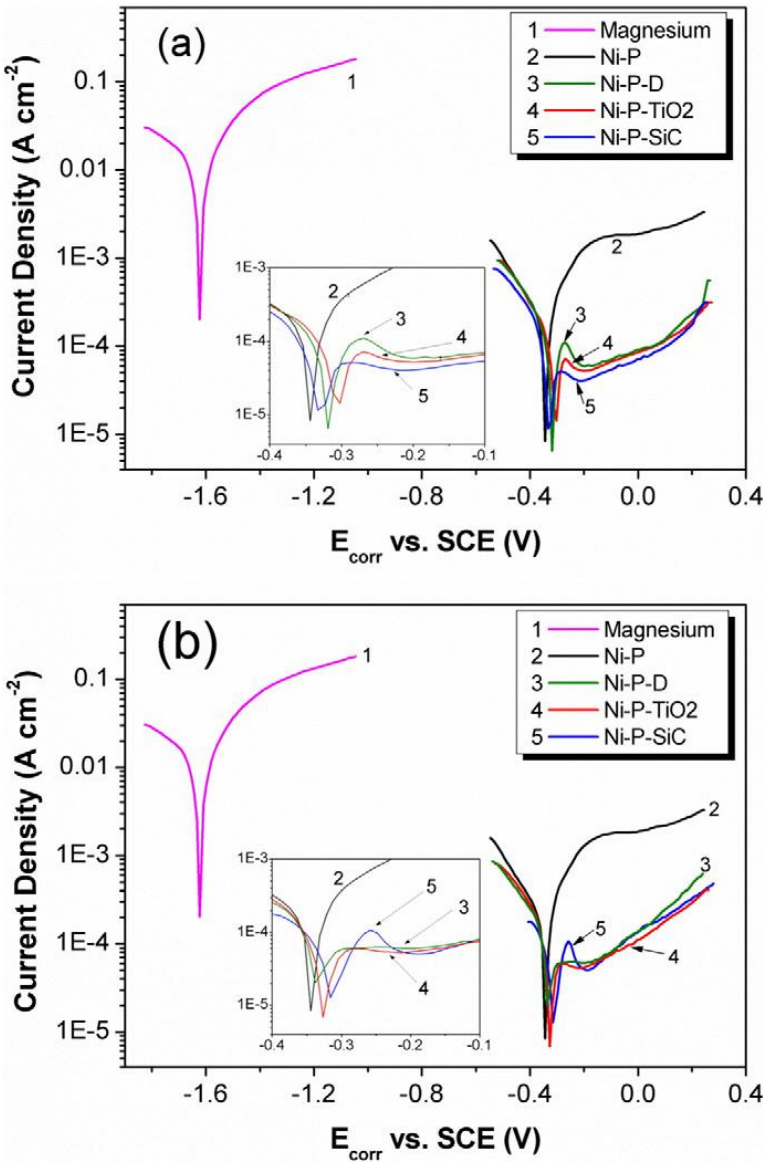

Figure 2.26: Polarization curves during erosion-corrosion experiment in an electrolyte of 0.6 mol/l sodium chloride + 20% w/w SiO_2 particles for Ni-P-ceramic nanocomposite coatings with various nanoparticles concentrations (a) 0.2 g/l concentration (low) and (b) 2.0 g/l concentration (high) [209]

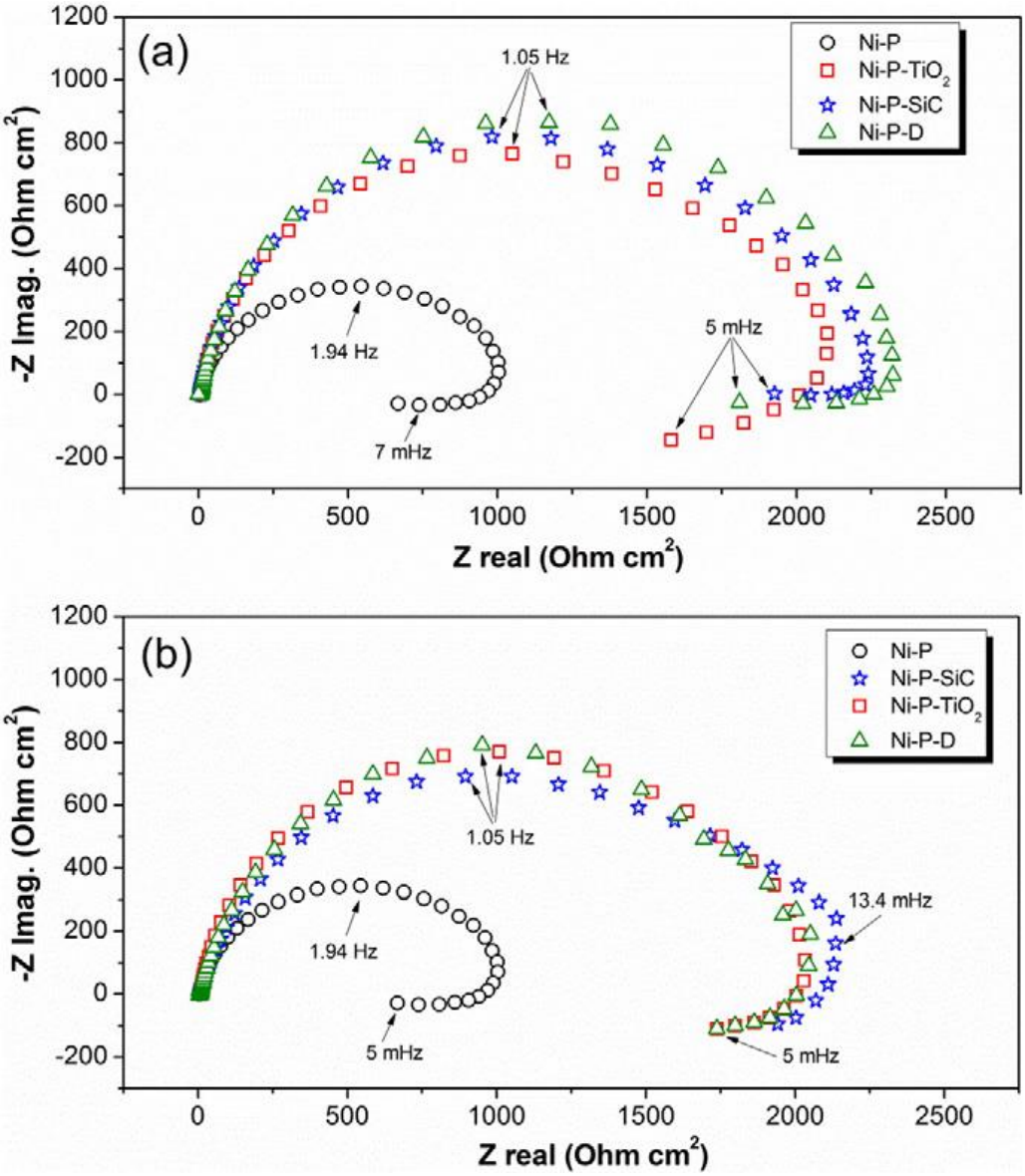

Figure 2.27: Nyquist plots during erosion–corrosion experiment in an electrolyte of 0.6 mol/l sodium chloride + 20% w/w SiO_2 particles) for Ni-P and Ni-P-ceramic nanocomposite coatings with various nanoparticles concentrations (a) 0.2 g/l concentration (low) and (b) 2.0 g/l concentration (high) [209]

In 2017, Nadtinam Promphet et. al. prepared an electroless Ni-P-TiO_2 sol-RGO coating on steel. They improved corrosion resistance properties and electrical conductivity of steel by the Ni-P-TiO_2 sol-RGO deposition on steel. Corrosion characteristics and relative conductivity of uncoated steel and coated steel are shown in Figures 2.28 and 2.29 respectively [181].

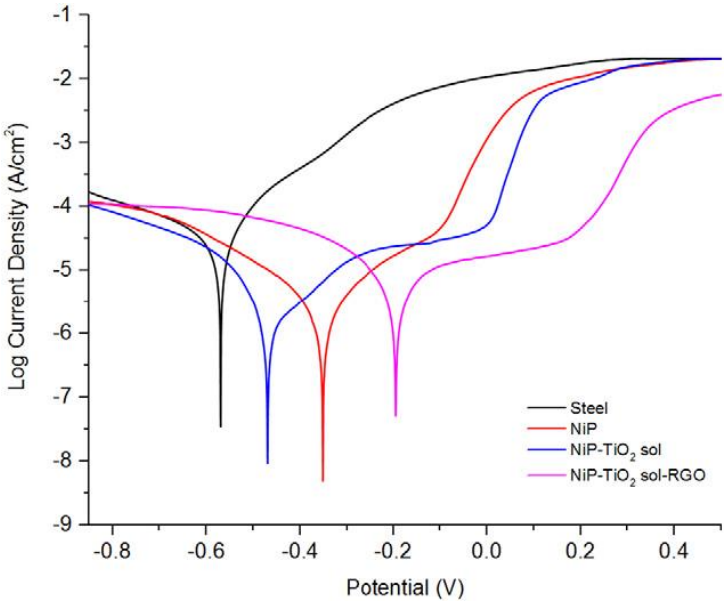

Figure 2.28: Potentiodynamic polarization curves of steel (black), Ni-P (red), Ni-P-TiO_2 sol (blue) and Ni-P-TiO_2 sol-RGO (pink) coatings in 3.5 wt% NaCl electrolyte [181]

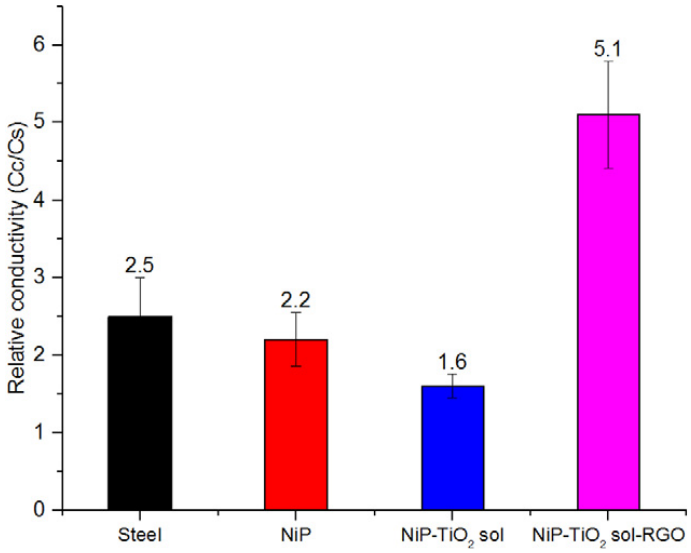

Figure 2.29: Relative conductivity of the Ni-P, Ni-P-TiO_2 sol, and Ni-P-TiO_2 sol-RGO coated surfaces, respectively. The error bars correspond to the standard deviation obtained from five measurements (n = 5) [181]

As above corrosion studies given by various researchers are reviewed, electroless coating is provide higher resistance against corrosion compare to uncoated substrates (e.g. steel, aluminum etc.). These coatings protect the materials by providing a dense coating (pore-free). Corrosion resistance of the nickel-phosphorus plating with high

phosphorus and passivity is excellent due to its amorphous nature. Amorphous Ni-P deposits have improved corrosion resistance than corresponding polycrystalline Ni-P deposits. Generally, the corrosion resistance of the composite deposits is lower than that of electroless Ni-P deposits. In case of some coatings such as electroless Ni-P-TiO_2, Ni-P-Si_3N_4, Ni-P-SiC, and Ni-P-CeO_2 composite coatings, by EIS, demonstrated improved corrosion resistance than the electroless nickel-phosphorous deposit [143, 155, 184, 202, 205].

2.6.3. Mechanical properties

In case of mechanical evaluation of coatings, hardness, wear resistance and coefficient of friction are studied by various researchers. As was already discussed in the literature by various researchers, a principal reason for using electroless coatings is to protect materials not only from the corrosion and oxidation but also from wear. Wear is not directly related to the hardness of materials but high hardness materials have less plastic deformation. Hardness, wear, wear resistance of electroless nickel-phosphorous plating and Ni-P-X composite plating (here X is second phase particles) studies given by various researchers are mention in this section.

Hardness is defined as a property of materials which provide the resistance to penetration by an indenter under load and pressure. Micro and nano-hardness have also been developed for measuring the hardness of coatings and thin films [216]. The main factor contributing to improved resistance to mechanical abrasion of electroless coatings is hardness [110].

According to Staffan Johansson, wear is defined as a process of removal of material from the surface of the substrates which experiencing relative motion to each other and wear loss is occurs mostly at the outer surface [217].

It is necessary to make a surface modification of materials for reducing the wear loss from the materials. In the as-deposited and hardened condition, electroless nickel-phosphorous deposit and electroless composite deposits showed the excellent wear and abrasion resistance. Different laboratory experiments mentioned in literature have shown coating with high hardness to have wear and erosion-wear resistance near to hard chromium in different tribological conditions. Electroless nickel-phosphorous and composite coatings can be used to replace hard chromium and high alloy materials

because of its excellent wear resistance. Post-heat-treatment of high nickel-phosphorous coatings provide the high wear resistance due to the formation of Ni_xP_y compounds [66, 86, 106, 107].

The hardness of the electroless nickel-phosphorous and composite coatings is the most important property for many engineering and industrial application. The microhardness of electroless nickel deposits is from 500 to 700 HV. This microhardness value is around equal to 45 to 58 Hardness (R_C scale) and equal to numerous hardened alloy steels [32, 34, 66, 95, 105]. Approximately 1100 HV microhardness equal to the hardness of commercial chromium coatings is achieved by the thermal-treatment of these coatings. The hot hardness of electroless nickel deposits is shown in Figure 2.30. As the figure shows, excellent hardness is achieved by heat-treated at 500°C [95].

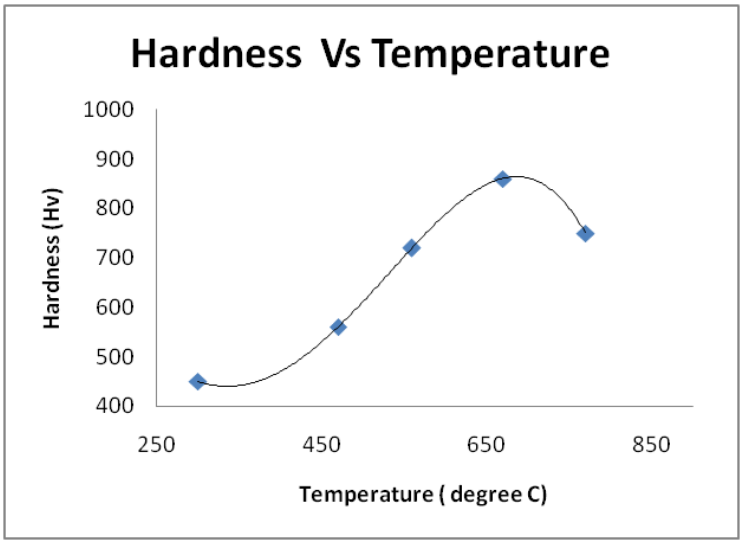

Figure 2.30: Hardness vs temperature [95]

Table 2.4: Microhardness of the as-plated and vacuum thermally-treated nickel-phosphorous and Ni-P-TiO_2 composite coatings [210]

Bath load (TiO_2), g/l	**Microhardness, HV**	
	Plated	**Vacuum thermally treated**
Brass	240±7	202±30
0	643±10	1173±35
2.5	651±12	1433±47
5.0	651±9	1384±50
10.0	648±13	1275±42

In 2006, J. Novakovic et.al. (Greece) observed Vickers micro-hardness of substrate and coating through microhardness tester with a Vickers diamond indenter (Leitz Wetzlar tester). Observation was carried out on the vacuum thermal treated electroless Ni-P-TiO_2 nanocomposite coated brass substrate providing 40 gm load for 20 s. The results are shown in Table 2.4 with variation of wt.% TiO_2 particles in the coating as plated and vacuum treated [210].

In 2007, Y. Y. Liu et. al. worked on the investigation of mechanical properties of Ni-P-WC nanocomposite plating on medium carbon steel. Microhardness of samples Ni-P plating, Ni-P-WC nanocomposite plating, and the vacuum heat-treated Ni-P-WC nanocomposite deposits at 600°C, 400°C, and 200°C are shown in Figure 2.31. The microhardness of Ni-P-WC nanocoating coating is 19% better than that of the nickel-phosphorous plating. Figure 2.32 presents the graphs between the friction coefficients and sliding time for Ni-P plating, Ni-P-WC nanocomposite plating, and the vacuum heat-treated Ni-P-WC nanocomposite deposits at 600°C, 400°C, and 200°C. It was observed that the tungsten carbide nanoparticles were able to significantly enhance the microhardness and wear resistance and decrease coefficient of friction [151].

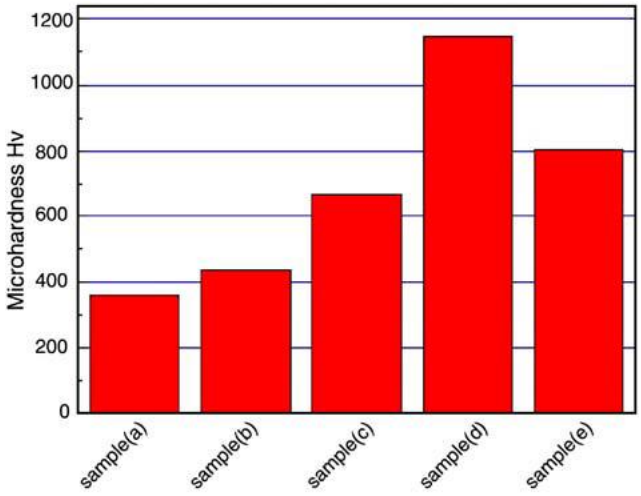

Figure 2.31: Vickers hardness of (a) Ni-P coating, (b) Ni-P-W nanocomposite coating, and the vacuum annealed Ni-P-WC nanocomposite coatings at (c) 200°C, (d) 400°C, and (e) 600°C [151]

In the Ni-P-WC nanocomposite coatings, abrasive wear phenomena occurred due to the existence of the tungsten carbide nanoparticles, while the combined fatigue and adhesive wear mechanism observed for the nickel-phosphorous coating. 1150 HV microhardness and 0.13 friction coefficient were found in the thermally treated

nanocomposite coating due to the development of Ni_3P phase and duping of the reinforced nanoparticles. [151].

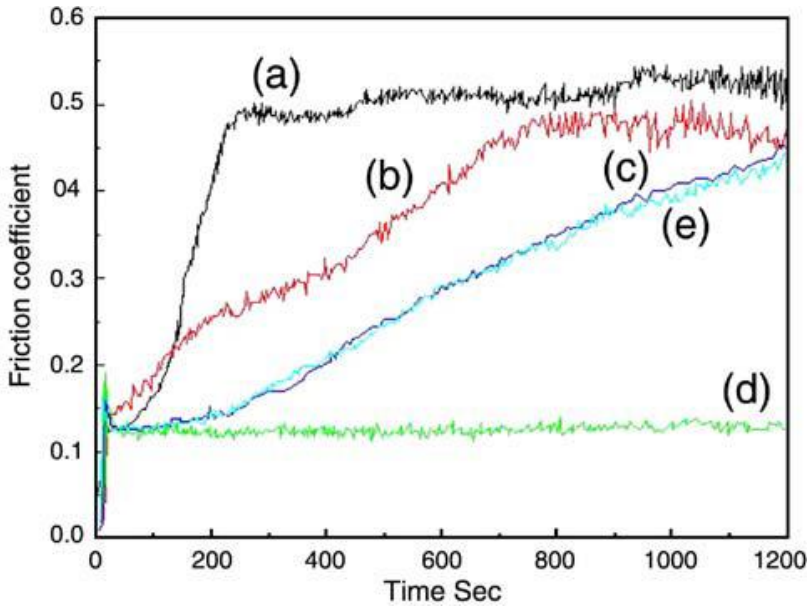

Figure 2.32: Friction coefficient of electroless (a) Ni-P coating, (b) Ni-P-W, and the vacuum annealed Ni-P-WC nanocomposite coatings at (c) 200°C, (d) 400°C, and (e) 600°C under dry sliding wear conditions [151]

In 2009, J. Novakovic and P. Vassiliou **(**Greece**)** observed micro-hardness of substrate and coating through microhardness tester with a Vickers diamond indenter (Leitz Wetzlar tester). The observation was carried out on the vacuum thermal treated electroless Ni-P-TiO_2 nanocomposite coated steel applying 100 gm load for 10 s. The results are shown in Table 2.5 with variation of wt.% TiO_2 particles in the coating as a plated and vacuum treated [211].

Table 2.5: Microhardness of as-plated and vacuum heat-treated nickel-phosphorous and Ni-P-TiO_2 composite coatings [211]

TiO_2 particles (wt.%)	**Microhardness (HV)**	
	Plated	Thermally heated
0	673±18	1194±30
3.7	745±21	1210±33
5.0	767±23	1306±43
6.2	780±32	1350±51
8.8	797±35	1434±62

In 2010, Taher Rabizadeh et.al. (Iran) observed microhardness (VHN) of vacuum thermal treated electroless Ni-P coated API-5L X65 steel substrates using a Vickers diamond indenter at 100 gm load for 20 s. They resulted that microhardness of thermally-treated Ni-P electroless coatings is increased [Figure 2.33] [89].

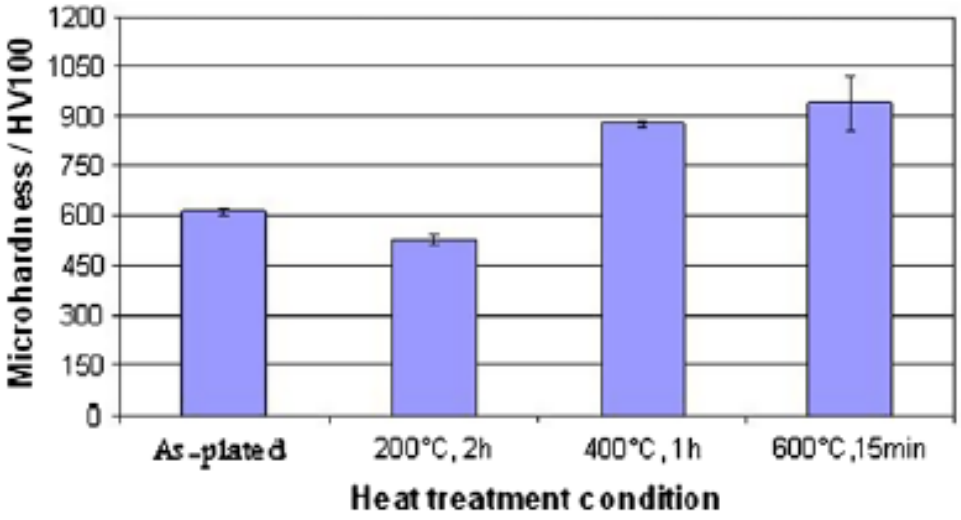

Figure 2.33: Microhardness of nickel coating and thermally-treated Ni-P electroless deposits [89]

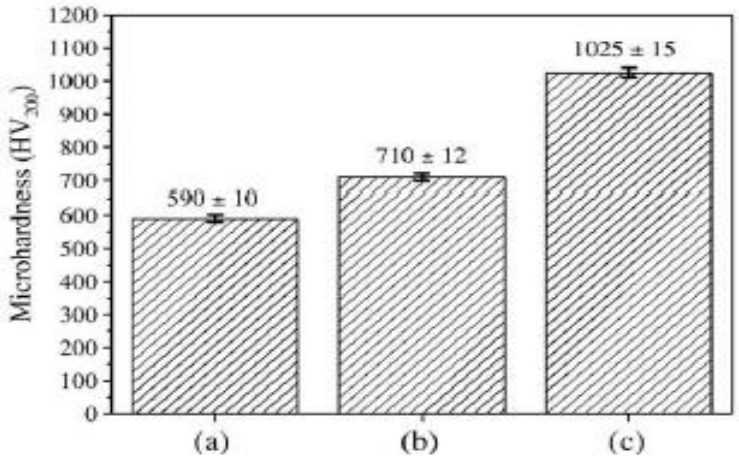

Figure 2.34: Microhardness of: (a) conventional nickel-phosphorus plating, (b) conventional Ni-P-TiO_2 nanocomposite plating, and (c) novel Ni-P-TiO_2 nanocomposite plating [166]

In 2010, Weiwei Chen et.al. worked on the novel electroless deposition of Ni-P-TiO_2 nanocomposite plating on commercial AZ31 Mg alloy. They observed micro-hardness (VHN) of electroless Ni-P-TiO_2 nanocomposite coated Mg alloy substrate by using a load of 200 gm with a holding time of 15 s. They reported that the novel Ni-P-TiO_2 coating process resulted in a significantly improved micro-hardness. Figure 2.34

demonstrates that micro-hardness of the new Ni-P-TiO_2 nanocomposite coating (1025±15 HV_{200}) is better than micro-hardness of conventional Ni-P-TiO_2 coating (710±12 HV_{200}) [166]. Similarly, the wear resistance of the novel composite plating has also been enhanced significantly (Figure 2.35).

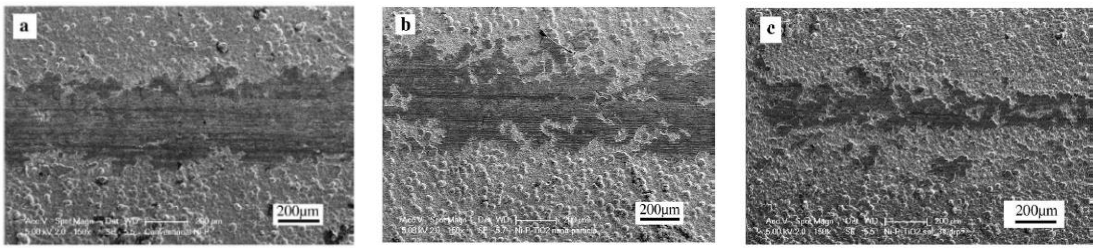

Figure 2.35: Wear track images on: (a) conventional nickel-phosphorus plating, (b) conventional Ni-P-TiO_2 nanocomposite plating, and (c) novel Ni-P-TiO_2 nanocomposite plating [166]

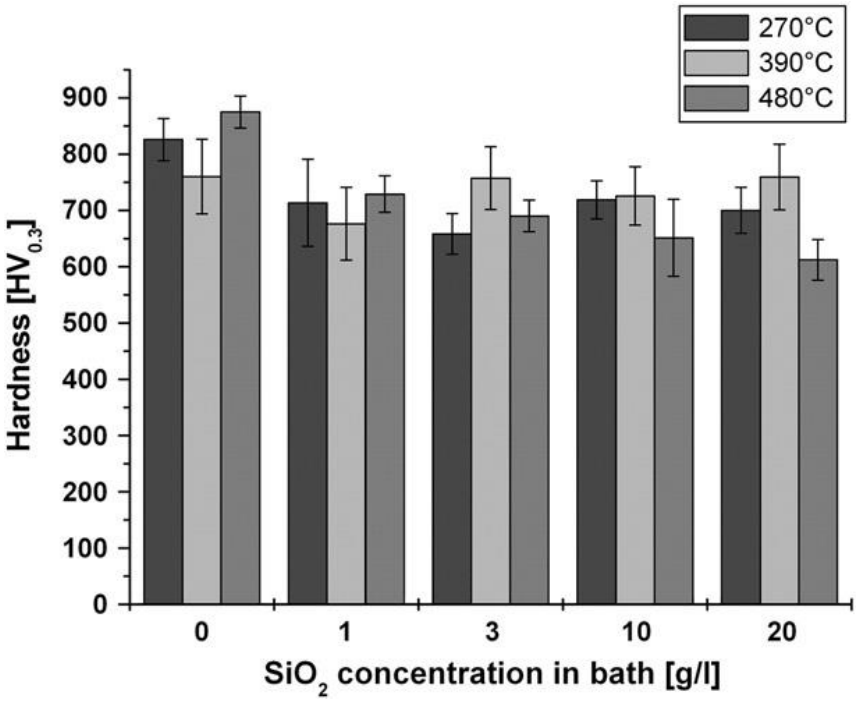

Figure 2.36: Hardness of the electroless Ni-P-SiO_2 nanocomposite deposits with various concentration of SiO_2 in the deposition bath and temperature of thermal treatment [156]

In 2010, Yoram De Hazan et. al. worked on the deposition and wear behavior of Ni-P-SiO_2 nanocomposite coating on 100Cr6 steel. The hardness ($HV_{0.3}$) of the Ni-P-SiO_2 composite deposits after thermal treatment at 270°C / 10 hrs, 390°C / 2 hrs and 480°C

/ 1 hr are presented in Figure 2.36 as a function of SiO_2 content in the deposition bath. Figure 2.37 shows the pin-on-disc wear resistance of the Ni-P-SiO_2 composite deposits as a function of SiO_2 content in the deposition bath and temperature thermal treatment. The microhardness of the thermally-treated composite deposit is reduced compared to the Ni-P coating. Simultaneously an enhancement in wear resistance by factors of 1.5 and 2 is found after thermal treatment at 270°C and 390°C, respectively [156].

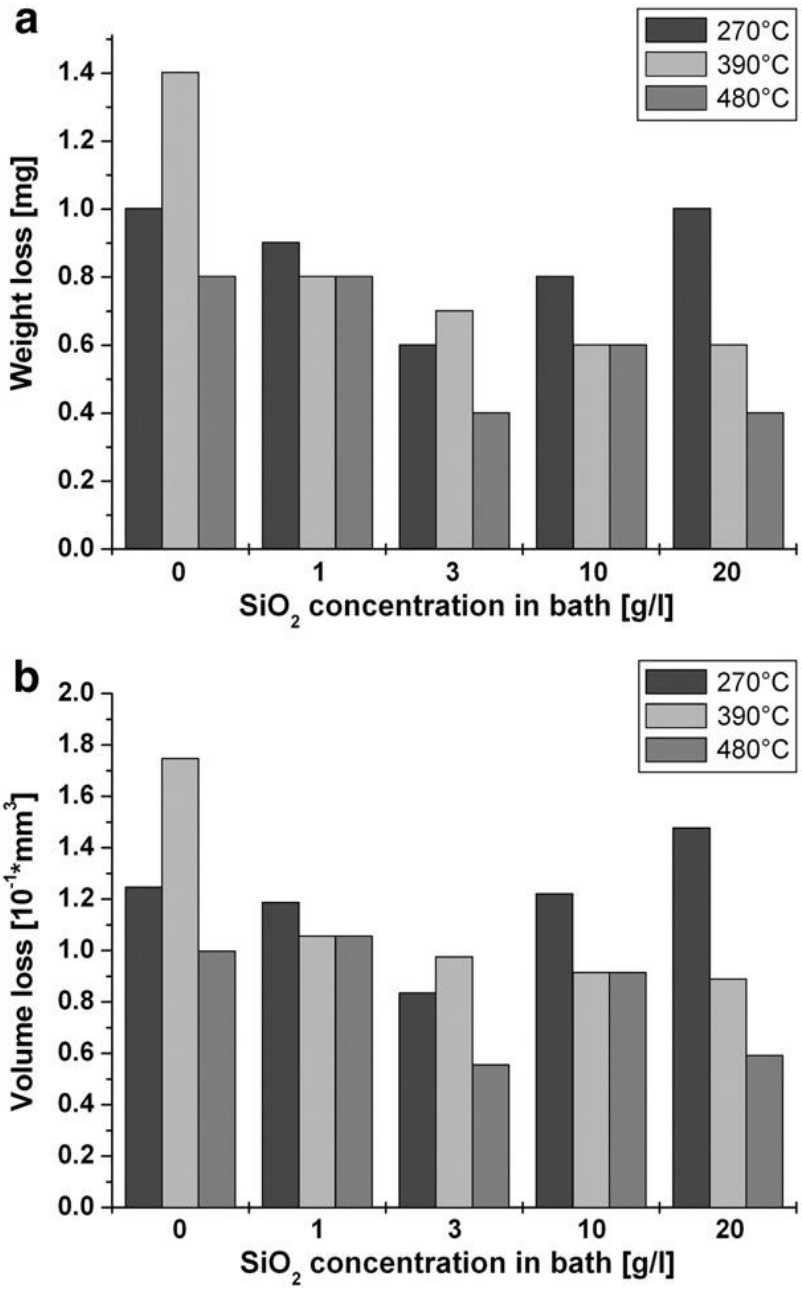

Figure 2.37: Wear loss of Ni-P-SiO_2 nanocomposite deposits (a) gravimetric, and (b) volumetric with various SiO_2 concentration in the deposition bath and heat treatment temperature [156]

In 2013 and 2014, Preeti Makkar et. al. worked on the preparation of nanosized TiO_2 powder and synthesis of Ni-P-TiO_2 nanocomposite plating on mild steel discs. As compared to nickel-phosphorus plating, Ni-P-TiO_2 nanocomposite plating displays the improved wear resistance and microhardness [36, 37]. Improved microhardness and wear resistance of Ni-P-TiO_2 nanocomposite coating are shown in Figures 2.38 and 2.39. After thermal treatment, the wear resistance and microhardness of the deposits are enhanced significantly. Superior wear resistance and microhardness are observed for Ni-P-TiO_2 nanocomposite coatings over Ni-P coatings.

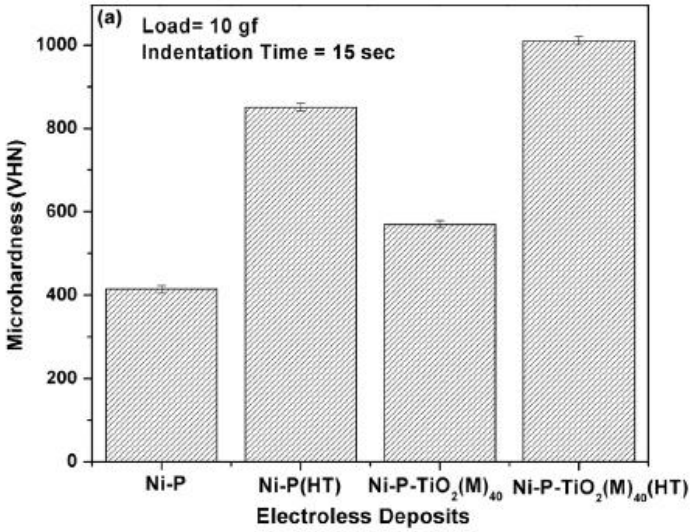

Figure 2.38: Microhardness of EL nickel-phosphorus deposit and Ni-P-TiO_2 nanocomposite deposit (M)40 in 'as coated' and thermally treated condition [36]

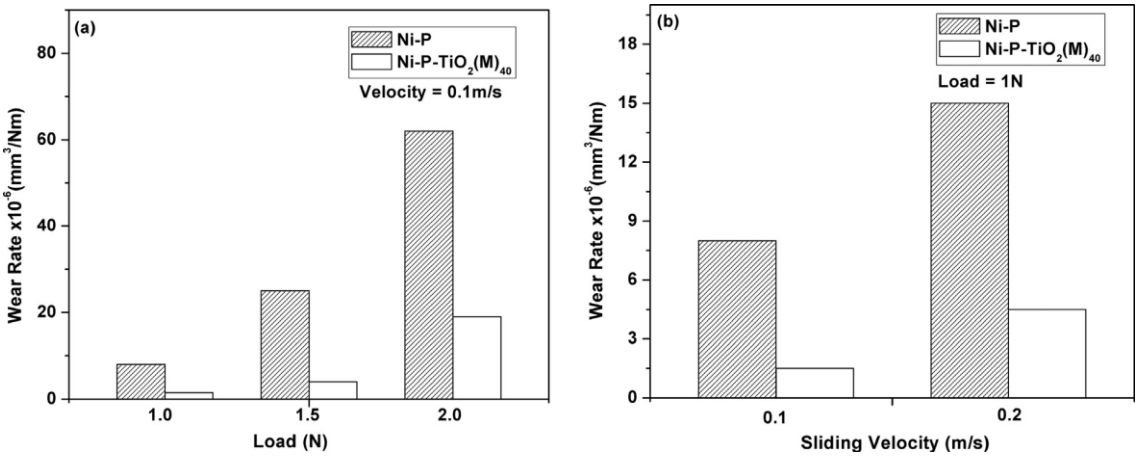

Figure 2.39: Wear rate of EL nickel-phosphorus and Ni-P-TiO_2 (M)40 nanocomposite coatings in thermally treated condition at (a) different loads (b) different velocities [37]

In 2014, S. Karthikeyan et. al. worked on the mechanical properties of Ni-P-Al_2O_3 nanocomposite coating on AISI 1040 steel plate. Figure 2.40 shows the variation of microhardness of as plated and thermally treated nickel-phosphorus coating and Ni-P-Al_2O_3 nanocomposite plating with varying sodium hypophosphite concentration [206].

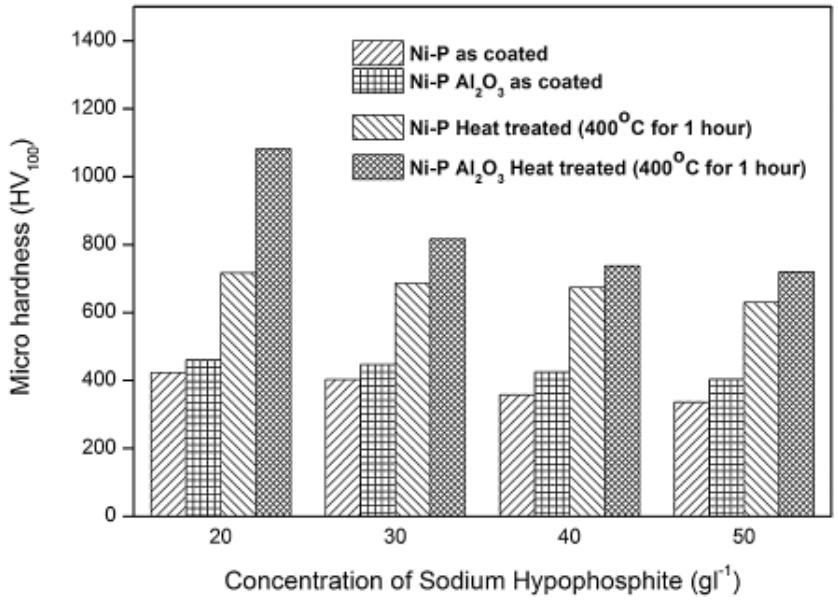

Figure 2.40: Microhardness of the plated and thermally-treated nickel-phosphorus plating and Ni-P-Al_2O_3 composite plating with sodium hypophosphite concentration and heat treatment [206]

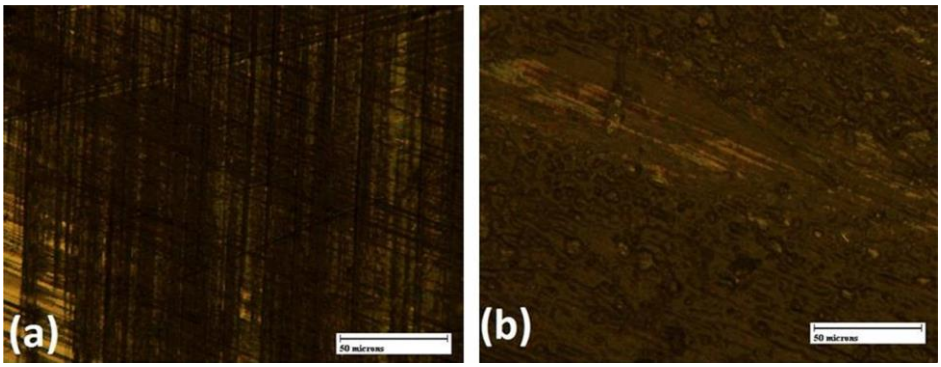

Figure 2.41: Optical microstructure images of the wear track of the (a) Ni-P plating (b) Ni-P-Al_2O_3 composite plating [206]

The optical microstructure image (Figure 2.41) displays the worn surface of nickel-phosphorous plating and Ni-P-Al_2O_3 composite plating exposed to a pin-on-disc wear test. The worn surfaces show the presence of patches in nickel-phosphorous plating and Ni-P-Al_2O_3 composite plating in Figure 2.41. Hardness increased from 410 HV to 460

HV (increase in 12.19%) for Ni-P-Al_2O_3 composite plating in as coated condition. Further enhancement of hardness to 1083 HV after thermal treatment and enhanced wear resistance was observed. The specific wear rate is reduced by 52.62% and 32.38% for coated and thermal-treated Ni-P-Al_2O_3 composite coating [206].

In 2015, Xiaoyan Wu et. al. prepared electroless Ni-P-TiO_2 nanocomposite coating on 211Z aluminum alloy and they investigate the properties of nickel-phosphorus and Ni-P-TiO_2 nanocomposite coatings on aluminum alloy. They reported that the nanoparticles of TiO_2 are able to refine the mechanical properties of aluminum alloy with the given heating technique which lead to the increment of microhardness about 1325 HV in this study. The reason can be considered in the context of the formation of hard Ni_3P phase in which the effectiveness of TiO_2 nanoparticles in composite coating strengthened due to the precipitation and dispersion strengthening [172].

In 2015, Huihui Wu et. al. prepared Ni-P-GO composite plating on mild steel. The Ni-P-GO composite deposition procedure is similar to the deposition process used in convention Ni-P plating. Figure 2.42 illustrations the microhardness of the nickel-phosphorus plating and Ni-P-GO composite plating. The electroless Ni-P-GO composite plating (780 HV) had a higher hardness than the nickel-phosphorus (416 HV) [163].

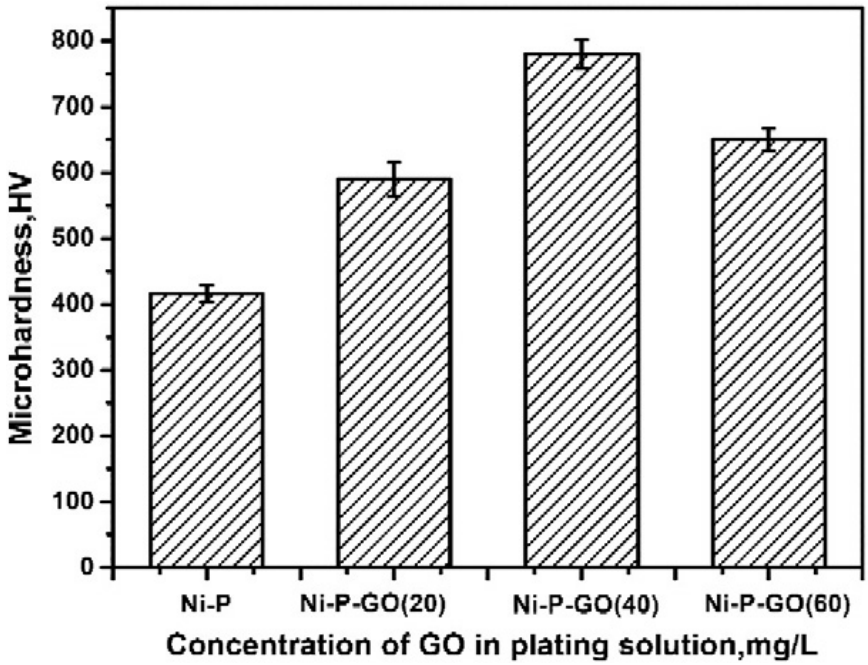

Figure 2.42: Comparison of the microhardness of nickel-phosphorus and Ni-P-GO composite deposits with various GO concentration [163]

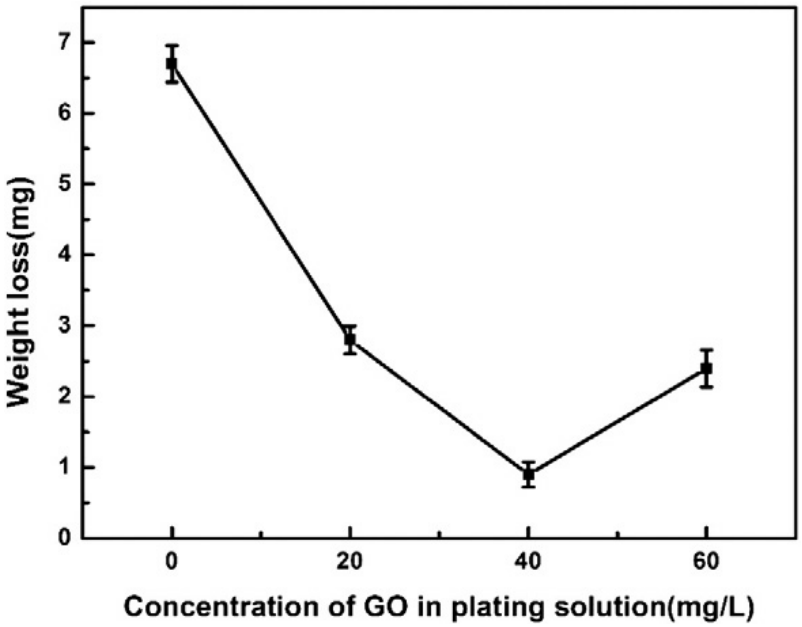

Figure 2.43: Comparison of wear mass loss of Ni-P-GO composite deposits with various GO concentrations [163]

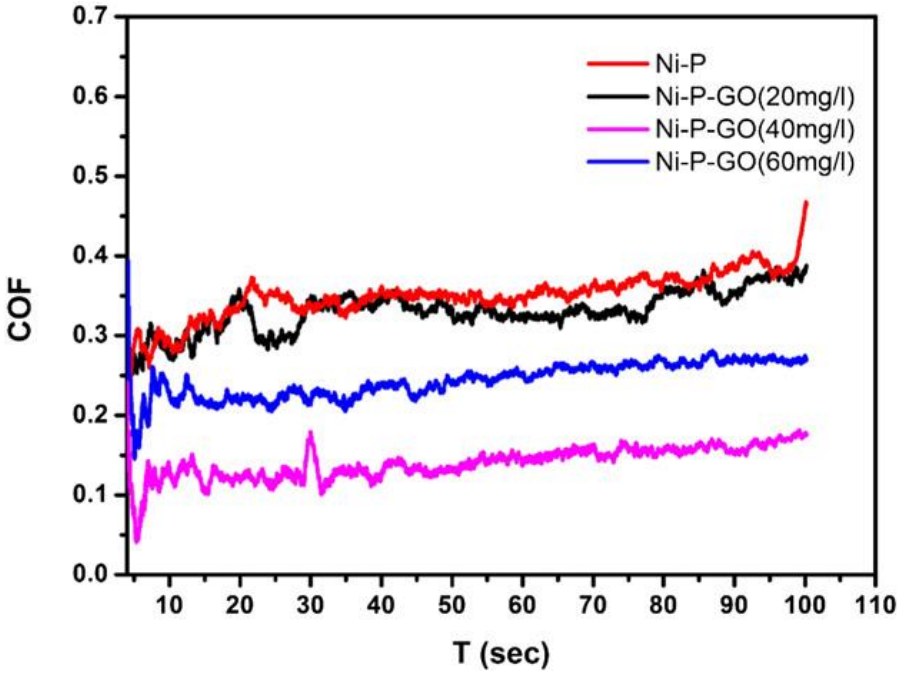

Figure 2.44: The coefficient of friction of nickel-phosphorus deposit and Ni-P-GO composite deposits with variation in GO concentration [163]

Figure 2.43 represents the graph between the wear mass loss and GO concentration for the Ni-P-GO composite coating. Figure 2.44 shows the coefficient of friction of the electroless Ni-P-GO composite deposits with respect to the effect of GO concentration in the coating bath under 10 N. Their findings shows that GO positively affected the

friction properties of the coating. Friction coefficient and particle concentration showed a direct relationship. However, excess GO results lead to reduce of the coating properties. The best anti-wear and microhardness properties of the Ni-P-GO composite deposits were obtained at 40 mg/l in the electroless bath formulation for the substrate [163].

In 2016, Ulas Matik et. al. studied the structural and tribological properties of coated and thermally-treated Ni-P-Si_3N_4 composite deposits on iron-based powder metallurgy compacts. Results of Vickers hardness show that average microhardness of the PM substrate, nickel-phosphorous deposit, and Ni-P-Si_3N_4 nanocomposite deposit is 112 HV_{100}, 612 HV_{100} and 784 HV_{100}, respectively (Figure 2.45). Figure 2.46 illustrations the effect of heat treatment temperature on the friction coefficient of nickel-phosphorous and Ni-P-Si_3N_4 nanocomposite deposits. The wear loss curves as a function of thermal treatment temperature for nickel-phosphorous deposit and Ni-P-Si_3N_4 nanocomposite deposit before and after the thermal treatment were presented in Figure 2.47. Wear tests results that the average friction coefficient of uncoated PM substrate is 0.57 N. Their observations show that the co-deposition of particles of micro-sized Si_3N_4 in the coating improved the wear resistance and microhardness of composite deposits. Thermally-treated (at 400°C) nickel-phosphorus and Ni-P-Si_3N_4 deposits have the highest wear resistance and hardness [180].

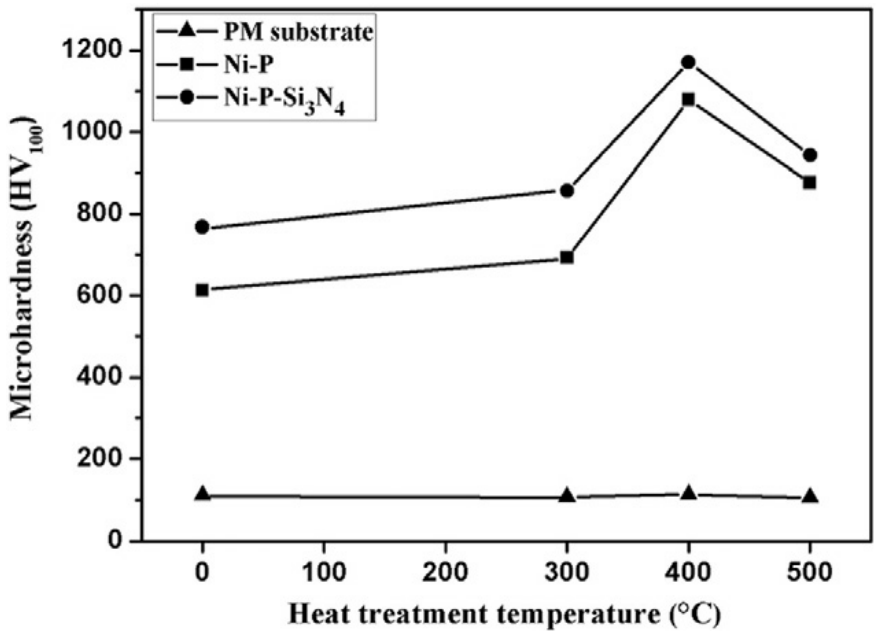

Figure 2.45: The effect of temperature of thermal treatment on the hardness of electroless nickel-phosphorous and Ni-P-Si_3N_4 composite deposits [180]

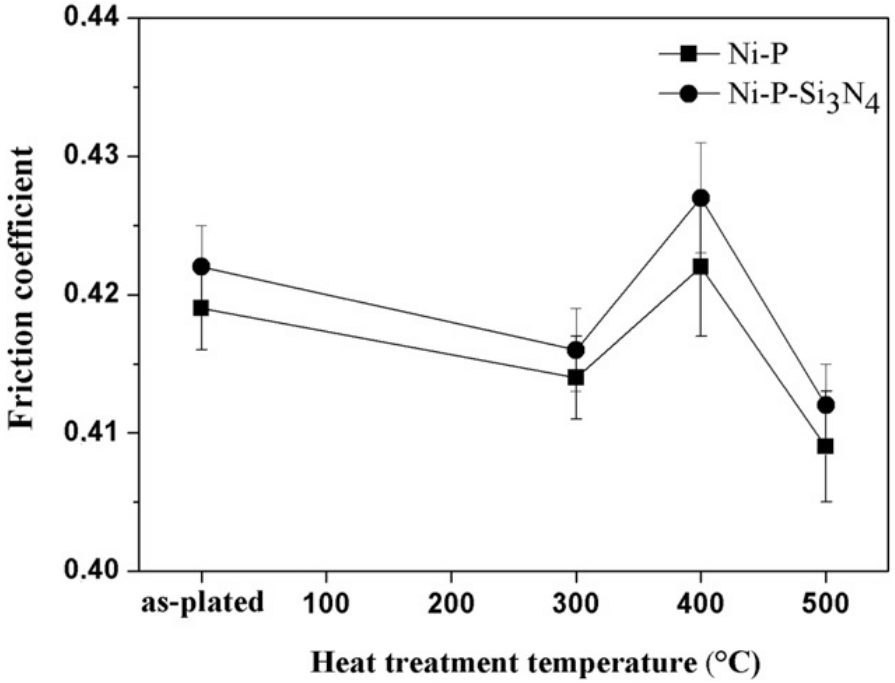

Figure 2.46: Effect of temperature of thermal treatment on the friction coefficient of nickel-phosphorous and Ni-P-Si_3N_4 composite deposits [180]

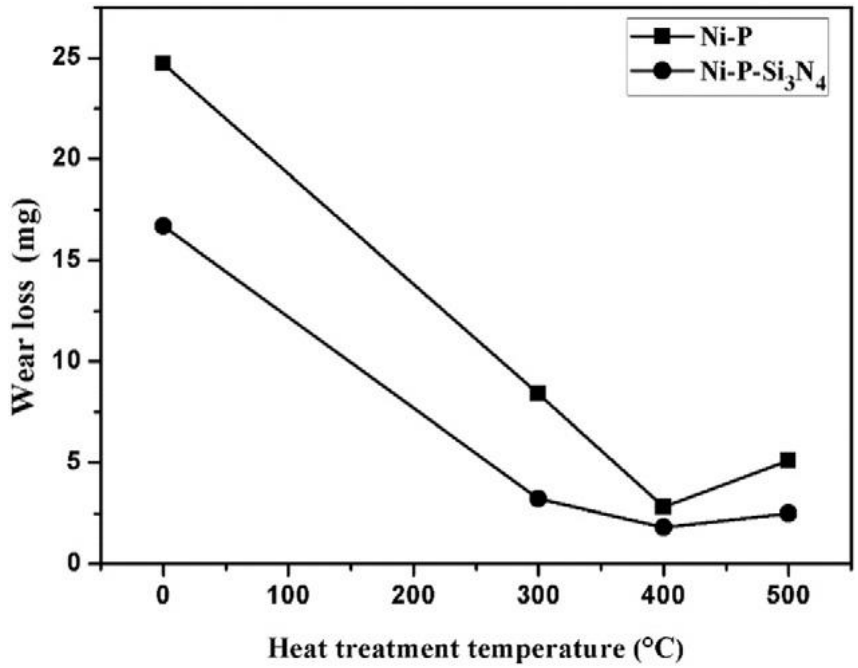

Figure 2.47: The effect of temperature of thermal treatment on wear resistance of electroless nickel-phosphorous and Ni-P-Si_3N_4 composite deposits [180]

In 2016, A. Sadeghzadeh Attar et. al. worked on the improvement in tribological behavior of Ni-P-SiO_2 nanocomposite coating on low carbon steel alloy. Comparison

of the microhardness of Ni-P-SiO_2 nanocomposite coating with the microhardness of steel and electroless nickel-phosphorous coating given in Figure 2.48 [208].

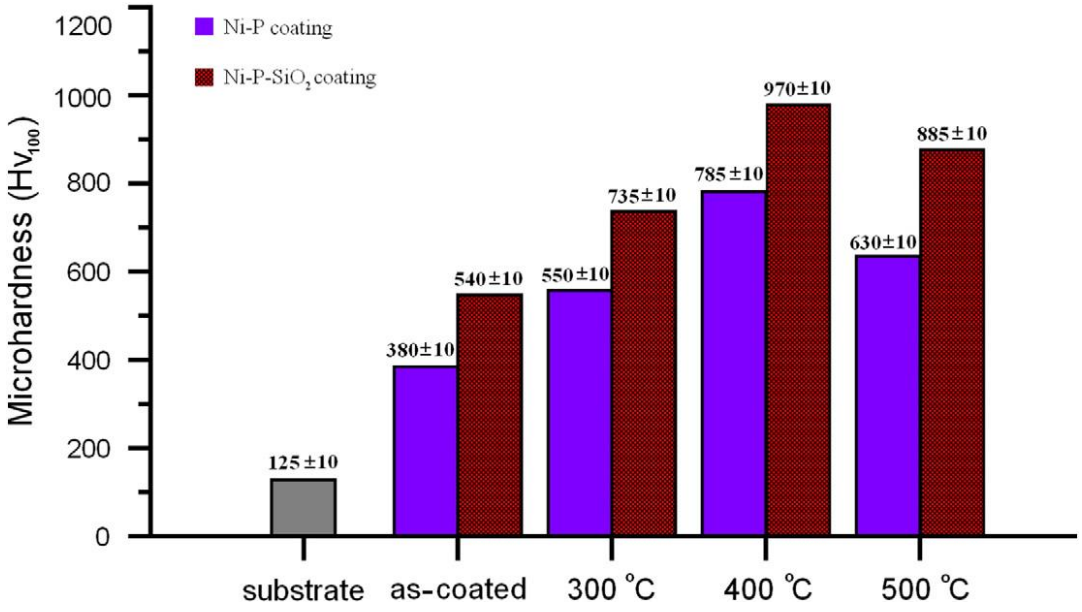

Figure 2.48: Comparison of microhardness for steel deposited and annealed electroless nickel-phosphorous and Ni-P-SiO_2 nanocomposite [208]

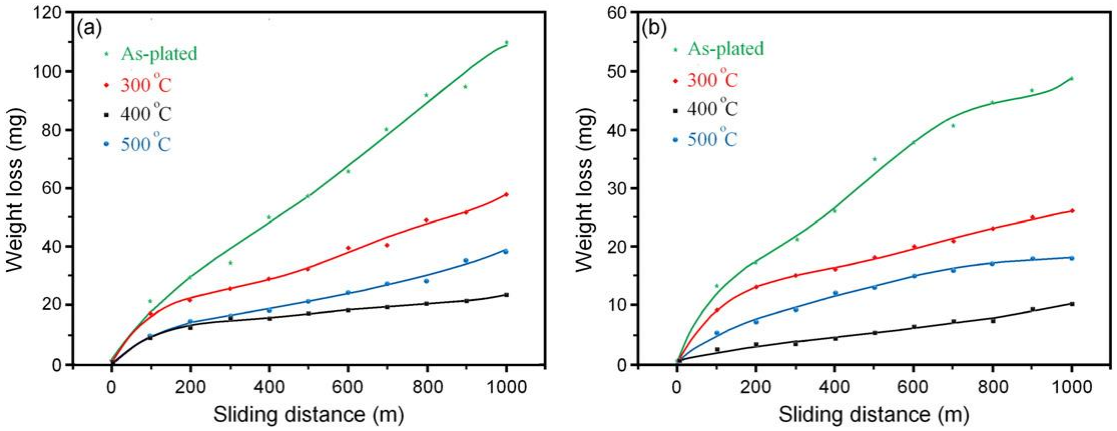

Figure 2.49: Weight loss with the sliding distance for deposited and annealed with temperatures (a) electroless nickel-phosphorous and (b) novel Ni-P-SiO_2 nanocomposite coatings temperatures [208]

Comparison of the weight loss for the electroless nickel-phosphorous deposit and Ni-P-SiO_2 nanocomposite deposits are presented in Figure 2.49. The scanning electron micrographs of wear scratch on the surface of the Ni-P coated steel and Ni-P-SiO_2 nanocomposite coated steel heat-treated at 400°C are shown in Figures 2.50 (a) and (b), respectively. The microhardness and wear-resistance of electroless coatings are

enhanced by the inclusion of SiO_2 nanoparticles and the presence of hard crystalline nickel precipitates and Ni_3P, which hinder the growth of grains and hinder the movement of dislocations. After the study of wear mechanism, abrasive wear was found as the dominant mechanism for wear of this type of coatings [208].

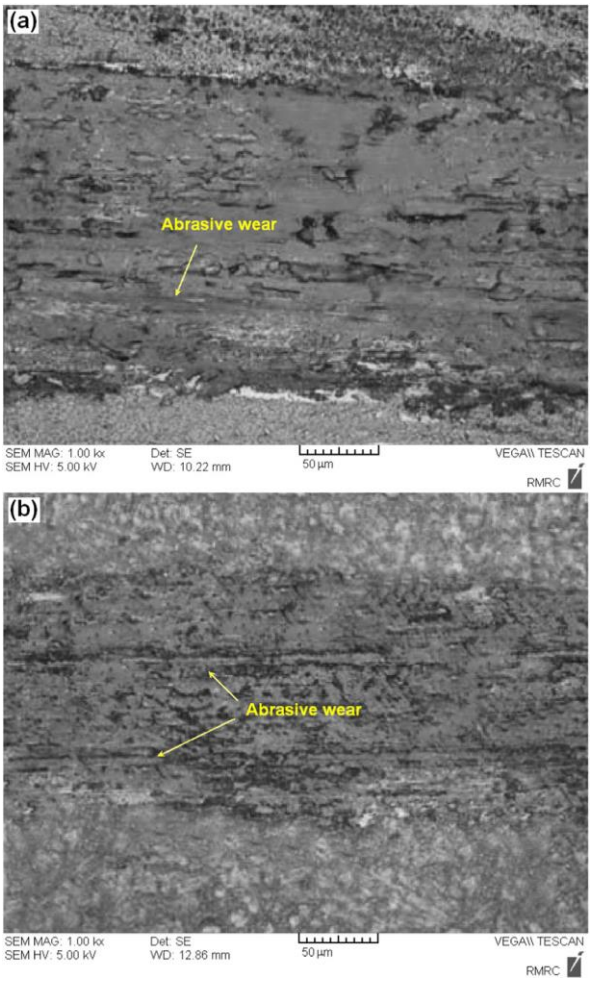

Figure 2.50: Micrographs of worn (a) electroless Ni-P coated surface and (b) novel Ni-P-SiO_2 composite coated and heat-treated surface [208]

As above studies say that electroless nickel-phosphorous and Ni-P-X composite coating have established as hard coatings for tribological applications. The hardness of the electroless nickel-phosphorous coating is increased with co-deposition of second phase particles within the Ni-P matrix. The electroless nickel-phosphorous deposit hardness improved with the increased concentration of hard SiC, Si_3N_4, Al_2O_3 particles in the deposit. The wear resistance of electroless composite deposit increases with increase in SiC incorporation concentration. The wear resistance of the electroless nickel-phosphorous coatings further increased by the co-deposition of both ZrO_2 and W

particulates. So, it is concluded that electroless composite coatings improve the mechanical properties of substrates [135-136, 151, 154, 156, 163, 173-174, 177, 180, 190, 206, 208].

2.6.4. Other properties

In 2007, S. M. A. Shibli et. al. presented work on 90-130 nm sized TiO_2 reinforcement on Ni-P electroless plates. Enhanced the quantity of electro-active sites, roughness factor and hydrogen adsorption capability due to the reinforcement of the plates with TiO_2. The TiO_2-reinforced plates showed high electrocatalytic action during HER [218].

In 2003, Yoram Hazan et. al. presented their work as homogeneous functional Ni-P-ceramic nanocomposite coating through constant dispersion in electroless nickel solutions. They used nanosized particles of CeO_2, ITO, α-Fe_2O_3, and TiO_2 as second phase particles in the deposition of nanocomposite coatings. Baths containing ITO nanoparticles exhibited no deposition reactions and other baths containing a-Fe_2O_3 have not co-deposition of the nanoparticle. In contrast, uniform Ni-P-CeO_2 and Ni-P-TiO_2 nanocomposites up to 22 vol.% nanoparticles are synthesized [209].

In 2013, Zhao, Qi, et. al. work on antibacterial properties of electroless Ni-P-TiO_2 coating. They used nanosized TiO_2 powder (25 nm) for depositing the nanocomposite coating. The bacterial adhesion examines in reducing bacterial attachment presented that the Ni-P-TiO_2 deposits achieved antibacterial characteristics better than the nickel-phosphorous deposit and uncoated stainless steel [219].

2.7. Applications

Electroless deposition today has many applications, for example, in corrosion prevention and electronics. Materials with unique properties, such as nickel-phosphorus (corrosion resistance) and cobalt-phosphorus (magnetic properties) based alloys are easily obtained by electroless deposition. If the components being plated are of complex shape electroless deposition may produce coatings with a high degree of uniformity [42, 44].

Electroless nickel-phosphorus can produce coatings with varying properties because it has the ability to easily control the phosphorus content, so according to it alters deposit

properties, such as corrosion resistance and wear resistance. Electroless nickel phosphorus is by far the most widely used electroless process in the industry; it has been successfully used in computers and electronics to the automotive, aerospace, and oil and chemical industries. Some recent uses of electroless coating include application in MEMS, electromagnetic interference (EMI), in powder metallurgy, as membrane reactors, minimizing fouling in heat exchangers and reduction of bacterial adhesion [32, 34, 42, 44-45, 66].

The Ni-P composite coatings containing ceramic particles as the reinforcing phase find wide applications, especially as anti-wear and self-lubricant materials. The main application of electroless composite coatings is for machining and finishing tools requiring maximum wear resistance, and hard surface [34, 66].

The incorporation of TiO_2 nanoparticles into the Ni-P matrix is likely to take advantage of the different properties of Ni-P alloy and TiO_2, including good wear and good corrosion resistance and anti-bacterial properties. Because the electroless Ni-P-TiO_2 coatings are metal-based, their thermal conductivity, anti-abrasive property, mechanical strength and adhesion strength to the substrate are superior to standard PTFE coatings. Therefore Ni-P-TiO_2coatings have great potential applications in reducing biofouling formation in heat exchangers, pipelines, ship hulls and many other devices that suffer from biofouling problems. Electroless Ni-P-TiO_2 nanocomposite coatings on aluminum alloys, carbon steel or low-grade stainless steels, mild steel, brass, sintered NdFeB permanent magnet are used in chemical process industry, seawater cooling, food industry, oil and gas industry, pumping systems, automotive industry, aerospace industry, electronics industry, foundry tooling, mould protection, textile industry etc [34, 36, 44, 45, 66, 211, 215, 219]

As above mentioned-literature are showing, electroless deposition process has the ability to produce uniform coatings on the entire surface. Electroless deposition avoids the excessive build-up at projection & Edges. Electroless nickel-phosphorous alloy and composite coatings are used as a functional or protective coating because of their unique combination of physical, electrochemical and mechanical properties. Nano TiO_2 particles also have unique properties combination and non-hazardous nature. Nano TiO_2 particles can be used for thin film formation or thin coating deposition due to it's

anisotropic structure. The corrosion and wear studies on nano TiO_2 embedded electroless Ni-P composite coating are limited till date.

2.8. Identification of Research Gap

After a review of the available previous literature, the research gap between literature work and this research work has been given below

- In past research work, deposition of electroless Ni-P-TiO_2 nanocomposite was done on carbon rod, AZ31 Mg alloy, stainless steel, and Al alloys. Currently, work on of Ni-P-TiO_2 nanocomposite coating with co-deposition of nano TiO_2 particulate on mild steel is limited.
- In the past research work, the effect of variation in concentration of nano TiO_2 particles in the electroless bath has not been done. So, this parameter is selected for the present study.
- Morphological study of Ni-P-TiO_2 nanocomposite coated sample is very important due to the texture of the surface influences the properties of the deposits. The effect of the texture of nano TiO_2 coating on mild steel has been rear studied previously. So morphological study with surface texture is chosen for further study.
- Effects of the concentration of TiO_2 nanoparticles on the tribological and electrochemical properties of electroless Ni-P-TiO_2 nanocomposite on mild steel has not been studies.

2.9. Objectives

The primary objectives of this research work are to deposit electroless Ni-P-TiO_2 nanocomposite coatings on the surface of mild steel specimen with a variation of nano TiO_2 content and study the properties of obtained coatings. Various characterization technique such as X-ray diffraction analysis, FESEM with EDS and area mapping, microhardness measurements, potentiostat tests and wear tests were implemented to conduct this research work.

The present work therefor contemplates the following study in respect of electroless Ni-P-TiO_2 nanocomposite coating on mild steel.

- Effect of varying concentration of nickel sulphate (in the deposition bath) on mechanical, electrochemical and tribological properties of electroless Ni-P-TiO_2 nanocomposite coated mild steel.
- Effect of varying concentration of sodium hypophosphite (in the deposition) on mechanical, electrochemical and tribological properties of electroless Ni-P-TiO_2 nanocomposite coated mild steel.
- Effect of varying concentration of TiO_2 nanoparticles on surface morphology and surface texture of electroless Ni-P-TiO_2 nanocomposite coated mild steel
- Effect of varying concentration of TiO_2 nanoparticles on mechanical properties of electroless Ni-P-TiO_2 nanocomposite coated mild steel.
- Effect of varying concentration of TiO_2 nanoparticles on electrochemical properties of electroless Ni-P-TiO_2 nanocomposite coated mild steel
- Effect of varying concentration of TiO_2 nanoparticles on tribological properties of electroless Ni-P-TiO_2 nanocomposite coated mild steel.

Chapter 3

PARAMETERS OPTIMIZATION

The electroless coating is an autocatalytic deposition process. In this process, a metal source (to be deposited) and reducing agent are used. Some chemical reactions occur in the chemical bath. These chemical reactions influenced by pH of the solution, the temperature of the deposition bath and bath loading of the solution.

Before starting the deposition of Ni-P-TiO_2 nanocomposite coating on mild steel, optimization of effective parameters such as temperature, pH, deposition time period is an important step. Electroless nanocomposite coating is an autocatalytic chemical reduction method which has not required external electric sources. So suitable coating process parameters such as the pH of the bath, the temperature of bath and deposition-time are required. Optimization of parameters for the coating process is a necessary action.

In this chapter, the essential parameters for electroless Ni-P coating and Ni-P-TiO_2 nanocomposite coating have been decided.

3.1. Important parameters of the electroless coating process

Following parameters affect the electroless Ni-P and Ni-P-TiO_2 nanocomposite coating process [30-32, 44]:

i. Bath concentration or bath loading

ii. pH of the chemical bath

iii. The temperature of the chemical bath

iv. Time-period of the coating process

Autocatalytic reactions, such as electroless Ni-P and Ni-P-TiO_2 nanocomposite coatings, required energy in order to proceed. In the electroless process, the required energy is coming in the form of heat. Heat (energy) is measured in terms of temperature, hence temperature during the plating is the principal variable. A number of chemical reactions involved in the electroless Ni-P coating and Ni-P-TiO_2 nanocomposite coating

technique are sensitive to pH of the electroless coating bath. The time duration of the electroless Ni-P coating has a profound effect on the rate of deposition. The concentration of second phase particles (nano TiO_2 particles) is an essential parameter for the Ni-P-TiO_2 nanocomposite coating.

3.1.1. Bath concentration or bath loading

Chemical bath for the electroless deposition is made with the combination of deionized water, nickel salt, reducing agent and a complexing agent. There is autocatalytically reduction of the Ni^{++} with the reducing agent in the electroless deposition. Nickel concentration and hypophosphite (reducing agent) concentration are very important parameters affecting the rate of deposition of Ni-P coating and Ni-P-TiO_2 nanocomposite coating.

$$3\ NaH_2PO_2 + 3\ H_2O + NiSO_4 \longrightarrow 3\ NaH_2PO_3 + H_2SO4 + Ni + 2\ H_2\uparrow \quad \text{.....(i)}$$

$$Ni^{++} + H_2PO_2^- + H_2O \longrightarrow Ni^0 + H_2PO_3^- + 2\ H^+ \quad \text{.....(ii)}$$

$$3\ H_2PO_2^- \longrightarrow H_2PO_3^- + H_2O + 2\ OH^- + 2\ P \quad \text{.....(iii)}$$

As above equation (i) shows, three moles of hypophosphite is consumed by the one mole of Ni ion. Optimize concentration of nickel salt with reducing agent is required to develop adhere deposition [32, 44]. The concentration of second phase particles (nano TiO_2) also affects the rate of deposition and properties of Ni-P-TiO_2 deposit. The TiO_2 nanoparticles dispersed within nickel-phosphorous matrix on the surface of the substrate.

Bath loading for the electroless process is defined as the ratio of the exposed surface of the substrate divided by the volume of chemical solution. According to Reidel et.al., for the commercial bath bath-loading range (0.1 - 1.0 dm^2/l) depends on the chemical bath solution [40].

3.1.2. pH of the solution

The pH value of bath solution is defined by the richness of the concentration of H^+ ions in the solution. The pH of the solution is varied with the concentration of hydrogen ions in solution. In the coating bath, pH value of the solution is decreased by the accumulation of H^+ ions.

$$2H^+ + 2e^- \longrightarrow H_2 \uparrow$$

In an above chemical reaction, hydrogen gas is liberated by reaction between generated H^+ ions in the bath. Hydrogen gas formation hinders chemical reactions on the surface of the substrate. Hence, pH of the solution is another parameter of the electroless coating process which affects the appearance of electroless nickel-phosphorous and Ni-P-TiO_2 nanocomposite deposits on a substrate of mild steel. According to many types of research, no significant Ni-P coatings were obtained from Ni-P bath solution with low pH value (pH 1, 2, 3) as well as with very high pH value (pH 12, 13, 14). Optimization of pH of the solution is a must for deposition of significant coatings [32, 40, 44].

3.1.3. The temperature of the bath

The temperature of the electroless nickel-phosphorous deposition bath is an effective parameter which affects the rate of deposition. Electroless deposition is a self-catalytic process, thus sufficient temperature of the solution is required for the generation of a chemical reaction while very high temperature is also not suitable for coating because the bath becomes unstable. On the basis of literature, the rate of deposition was low at a temperature below 65℃, in this temperature range the bath chemical reactions were not taking place. Increase the rate of deposition with the increase in temperature up to 95℃. In the electroless deposition process, water is used as the solvent for the chemical bath. Water boils at 100℃, so the maximum temperature of the deposition bath is 100℃. Hence optimization of the temperature of the solution is required for the study [32, 44].

3.1.4. Time-period of coating process

The time period of the electroless coating affects the rate of deposition. The rate of deposition in initial hours differs from the rate of deposition in the last hours because the rate of chemical reactions is changing with time. For deposition of the significant coating, optimization of deposition period is demanded. In the literature, studies related to the effect of the time-period of the coating process on deposition-rate are found. Figure 3.1 shows the effect of deposition time-period on the rate of deposition. As shown, the rate of deposition decreases with increasing time. After a certain time period,

the deposition rate is constant. Thus, an optimum bath load is required to produce the acceptable deposition rate [32].

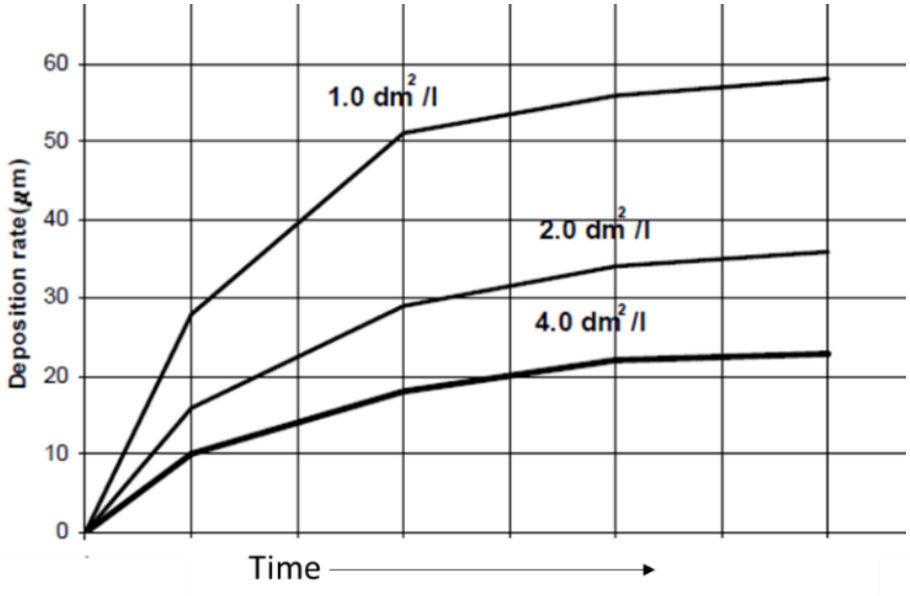

Figure 3.1: Effect of deposition time-period on deposition rate [Grunwald, 1983] [32]

3.2. Optimization of parameters

The parameters detailed in the previous section for the deposition of the electroless Ni-P alloy and Ni-P-TiO_2 nanocomposite coating. In this section, optimization of parameters required to achieve the adhered coating is carried out. Following parameters of temperature, pH and time period for deposition of Ni-P and Ni-P-TiO_2 nanocomposite coatings are selected:

Table 3.1: Selected parameters for the study

The temperature of chemical bath	70°C, 80°C, 90°C
pH of the chemical bath	1, 2, 3, 4, 5, 6, 7, 8, 9, 10, 11, 12, 13, 14
Time-period for the deposition process	30 minutes, 60 minutes, 90 minutes, 120 minutes

For the above parameters shown in Table 3.1, the concentration composition of the bath is 30 g/l nickel sulphate and 20 g/l sodium hypophosphite.

In this parameter-optimization study, Ni-P coatings on the substrates of mild steel with varying temperature (70℃, 80℃ and 90℃), pH (1-13) and time period for deposition process (30 minutes, 60 minutes, 90 minutes and 120 minutes) were done by chemical bath deposition (electroless coating) method as discussed below. The chemical bath for the electroless coatings constituted with $NiSO_4$ as a source of nickel in the solution, sodium hypophosphite as a reducing agent to reduce the nickel from nickel ions. It also constituted with lactic acid as a complexing agent to prevent precipitation of nickel sulphate and sodium hypophosphite. Setup for electroless coating is shown in Figure 3.2. The pH and temperature were measured at regular intervals for the optimization of pH of solution and temperature of the solution. The pre-treated mild steel substrate was dipped in the chemical bath for the particular period of time for deposition of the coating. The sample then removed outside of chemical bath and washed with distilled water and dried.

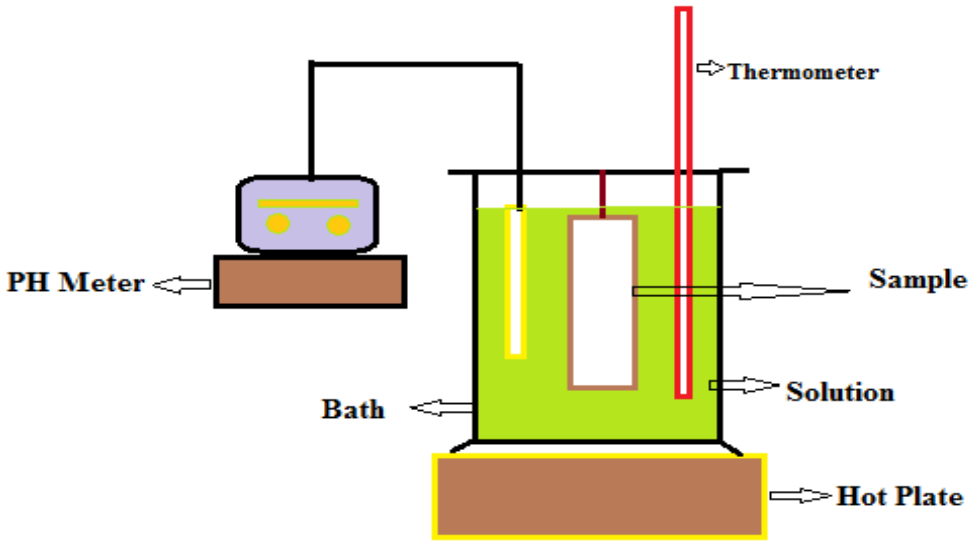

Figure 3.2: Electroless Ni-P coating set up

3.2.1. Bath concentration or bath loading

Bath concentration for the electroless deposition form with the salt of the source of metal to be deposited, a reducing agent to reduce this salt to obtain metallic ion in the bath. Ni-P deposition takes place by the reduction of nickel sulphate with the sodium hypophosphite in a provided chemical bath. The nickel salt and sodium hypophosphite were consumed in the chemical bath of the electroless coating so their concentration in

the chemical bath was decreasing with increase in deposition time. There were many researchers who did a coating of Ni-P and Ni-B on mild steel with variation in the composition of a chemical bath. Bath concentrations used by the various researchers are given in Table 3.2. C. Y. Wang et.al. mentioned in their work, the concentration of nickel salt and sodium hypophosphite was 30 g/l, and 25 g/l respectively for the preparation of the electroless bath [150]. A. Abdel Al. et. al. prepared an electroless bath with 30 g/l nickel salt concentration and 15 g/l sodium hypophosphite [169]. Preeti Makkar et. al. constituted the electroless bath with 30 g/l nickel sulphate and 20 g/l sodium hypophosphite with 20 g/l complexing agent [36]. The concentration of sodium hypophosphite in the deposition bath differs in above previous research work done by the various researchers. The content of P in the Ni-P deposit is varied by the variation of the concentration of sodium hypophosphite in the deposition bath.

Table 3.2: Bath composition used by the various researchers

S. No	Researchers	Concentration			
		$NiSO_4$ (g/l)	NaH_2PO_2 (g/l)	Temp (°C)	pH
1	C.Y. Wang et.al.	30	25	85	4.6
2	A. Abdel Aal et.al.	30	15	90 ± 2	4.7- 4.9
3	Preeti Makkarn et.al.	30	20	90	9

On the basis of research work done by various researchers, bath concentration was selected for the optimization of pH of the solution, the temperature of solution and time-spend of the coating process. Chemical composition for the electroless coating is shown in Table 3.3.

Table 3.3: Chemical composition and parameters of the electroless bath for Ni-P coating

S. No.	Chemicals/parameters	Concentration
1	Nickel Sulphate	30 g/l
2	Sodium Hypophosphite	20 g/l
3	Lactic Acid	35 ml/l
4	Temperature	70°C, 80°C, 90°C
5	pH	1-13

Variation in concentration of nickel sulphate and sodium hypophosphite with the second phase particles (nano TiO_2) in the electroless bath for the study of structural, corrosion tribological behavior of Ni-P-TiO_2 nanocomposite deposit was done in the main experimental work. Here, in this work, the optimization of pH of a chemical bath, the temperature of the chemical bath and time-spend of deposition process was done.

Bath loading for the deposition of Ni-P and Ni-P-TiO_2 nanocomposite coating was calculated by the given formula

Bath loading = Exposed surface area / Total volume of solution

In this optimization work, 2 cm x 1 cm sample size was used. Calculated exposed surface area for both sides of the plate was 4 cm^2 and 200 ml solution was used for the coating of one sample. Calculation for the determining the bath loading is given below:

Bath loading = 4 cm^2 / 200 ml

= 0.4 dm^2 / 0.2 l

= 0.2 dm^2/l

The calculated value of bath load for these experiments is 0.2 dm^2/l, which is lying in the range of bath loading value given in the literature (0.1 to 1.0 dm^2/l) [40].

3.2.2. pH of the chemical bath

For the optimization of pH of the solution, the concentration of the chemicals in the bath were selected from the above optimization study of bath concentration. For the optimization purpose, deposition of the Ni-P coating on mild steel substrate was done by the variation of pH from 1 to 14. Obtained coating thickness and weight at different pH are given in Table 3.4. As the deposition results shown in Table 3.4, deposition did not occur at pH 1. Some amount of Ni-P deposits deposited at pH 2 and pH 3. As the pH reached at 4 and 5, the thickness of the coating is very high after then thickness decreased. It means the appropriate pH for coating is pH 4 in the acidic electroless bath. In alkaline electroless bath at pH 9, good coating results were obtained. At very high pH (pH 12-14) coating process was uncontrolled because of involvement of fast chemical reactions and no deposition was obtained.

Table 3.4: Obtained coating thickness and weight with different pH (1-14 pH)

pH of solution	Coating Weight (mg)			Coating Thickness (micron)		
	70℃	**80℃**	**90℃**	**70℃**	**80℃**	**90℃**
1	-0.07	-0.64	0.12	-0.7	-0.4	1.2
2	0.11	3.20	0.86	1.2	16	6
3	0.94	3.40	0.94	6	15	14
4	4.94	5.76	4.00	20	26	21
5	3.48	5.19	3.90	16	24	20
6	3.63	4.76	3.83	18	23	20
7	3.73	3.27	3.25	16	15	12
8	2.88	2.90	1.01	11	11	6
9	3.89	3.91	0.67	12	16	3
10	0.86	2.83	Coating was not found	2.5	8	Coating was not found
11	coating was not found	1.66	Coating was not found	coating was not found	3	coating was not found
12	coating was not found	1.34	coating was not found	coating was not found	2.8	coating was not found
13	coating was not found	coating was not found	coating was not found	coating was not found	coating was not found	coating was not found
14	process was not controlled	process was not controlled	process was not controlled	process was not controlled	process was not controlled	process was not controlled

Comparison of the coating weight and thickness of deposits at different pH (1-12) with 70℃, 80℃ and 90℃ chemical bath temperature is presented in Figure 3.3(a) and (b) respectively. As comparison graphs show at 70℃, 80℃ and 90℃ with pH 4 has highest coating thickness and weight in acidic bath and at 80℃ with pH 9 has highest coating thickness and weight in the alkaline bath. Very low pH and temperature not suitable for obtaining required coating thickness and weight because at low temp and pH autocatalytic reduction of the metal salt in the electroless bath is not started, so no deposition or very less deposition occurred. Reduction of the metal salt in the bath took place very fast at high temp and pH. Due to this, more metallic ions accumulated in the bath and the proper coating did not take place.

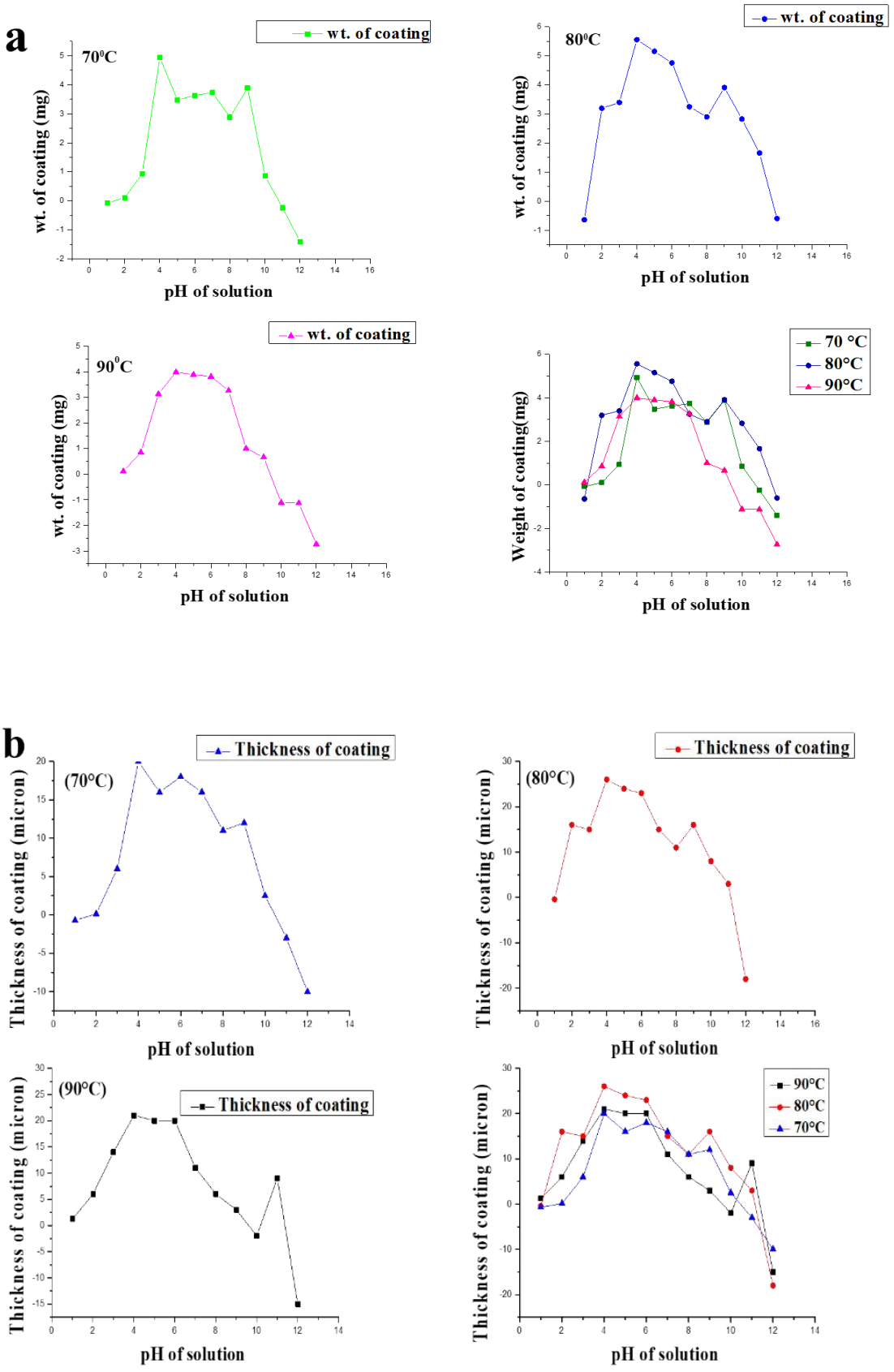

Fig. 3.3. (a) Weight of deposited electroless Ni-P coatings; and (b) thickness of deposited electroless Ni-P coatings, as a function of temperature and pH

For the studies of microhardness of the Ni-P coating with a variation of pH, Vickers microhardness tester was used. Measurements of microhardness were carried out on the coated substrate by applying a 10 gm load for 15 s because thickness of the obtained coatings (given in Table 3.4) are in micrometer. An average value of microhardness was reported after repeating five measurements for microhardness. Microhardness value of obtained Ni-P coatings on mild steel specimen is given in Table 3.5.

Table 3.5: Vickers microhardness of obtained coatings with different pH (1-14)

pH of solution	**Microhardness (VHN)**		
	70 ℃	**80 ℃**	**90 ℃**
1	133	132	135
2	177	298	288
3	280	330	301
4	319	446	420
5	319	363	338
6	318	361	320
7	319	356	315
8	204	220	190
9	325	397	295
10	242	337	198
11	258	240	183
12	143	233	180
13	132	176	Not deposited
14	Not deposited	Not deposited	Not deposited

Microhardness evaluation was done to understand the effect pH value of solution on the microhardness of electroless Ni-P coating on the mild steel substrate. Figure 3.4 shows the effect of pH of the solution on the microhardness of the electroless Ni-P coating on mild steel. Mild steel (uncoated) has microhardness ~132 $VHN_{10.}$ The maximum microhardness achieved for electroless Ni-P coatings on mild steel has been reached at pH 4 with 70℃, 80℃, and 90℃. Microhardness value of the electroless Ni-P coating on mild steel at pH 4 and 80℃ (acidic bath) is ~ 446 VHN_{10}. ~397 VHN_{10} is the microhardness of the Ni-P coating on mild steel at pH 9 and 80℃ (alkaline bath).

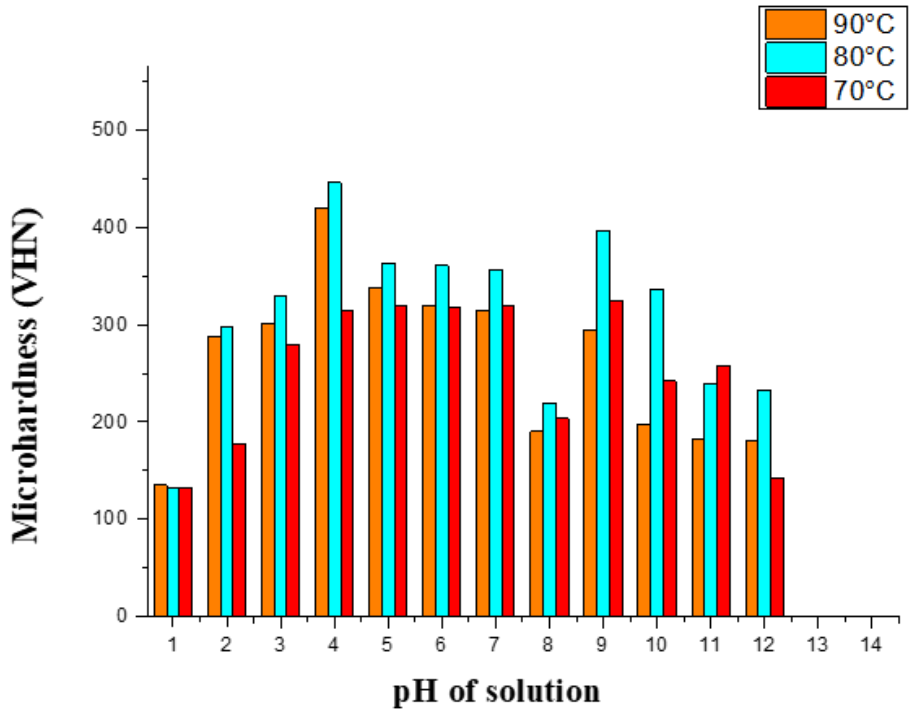

Figure 3.4: Comparison of microhardness values for obtained Ni-P coatings on mild steel at different pH (1-12)

From the above studies, it is concluded that pH for the acidic electroless bath is 4 and for alkaline bath 9 to obtain, significant coating thickness and microhardness of Ni-P coating, which are the important parameters of this work.

3.2.3. Temperature of chemical bath

Next parameter for the optimization is the temperature of the chemical bath. Temperature is varying as 70℃, 80℃ and 90℃ for the acidic and alkaline electroless deposition bath. The thickness and weight of the obtained coating deposited by use of the acidic bath and alkaline bath with 70℃, 80℃ and 90℃ bath temperature are given in Table 3.6 and 3.7. The thickness of Ni-P deposits by the electroless deposition at 80℃ with pH 3, pH 4 and pH 5 are 15 µm, 26 µm & 24 µm respectively. These are the higher thickness of deposits in case of acidic deposition. In the case of alkaline deposition, 16 µm is the highest coating thickness. It was obtained in the alkaline bath with 80℃ and pH 9.

Table 3.6: Obtained coating thickness and weight at different temperature (70°C, 80°C and 90°C) by the acidic bath

Temperature of solution (°C)	Coating weight (mg) at different pH value			Coating thickness (micron) at different pH value		
	3	4	5	3	4	5
70	0.94	4.94	3.48	6	20	16
80	3.40	5.76	5.19	15	26	24
90	3.14	4.00	3.90	14	21	20

Table 3.7: Obtained coating thickness and weight at different temperature (70°C, 80°C and 90°C) by the alkaline bath

Temperature of solution (°C)	Coating weight (mg) at different pH value			Coating thickness (micron) at different pH value		
	8	9	10	8	9	10
70	2.88	3.89	0.86	11	12	2.5
80	2.90	3.91	2.83	11	16	8
90	1.01	0.67	0	6	3	0

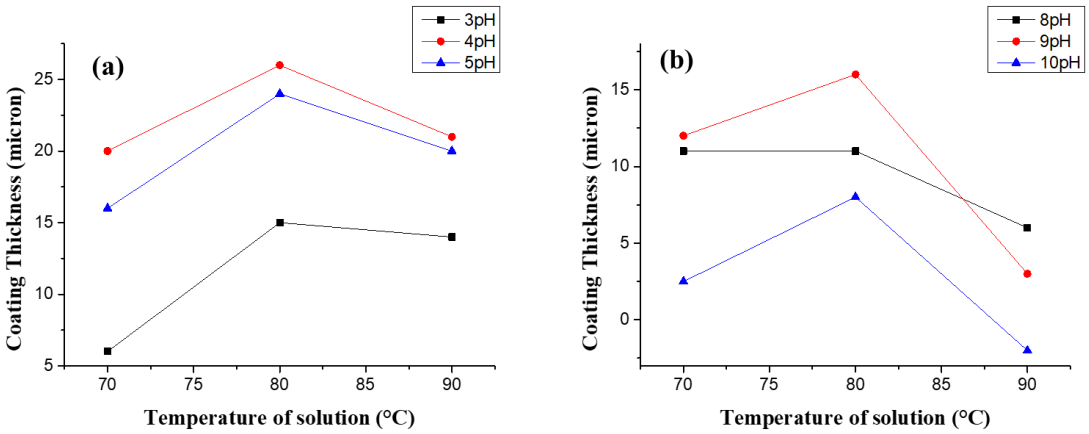

Figure 3.5: The thickness of Ni-P deposits by electroless deposition of (a) acidic bath & (b) alkaline bath, as a function of temperature

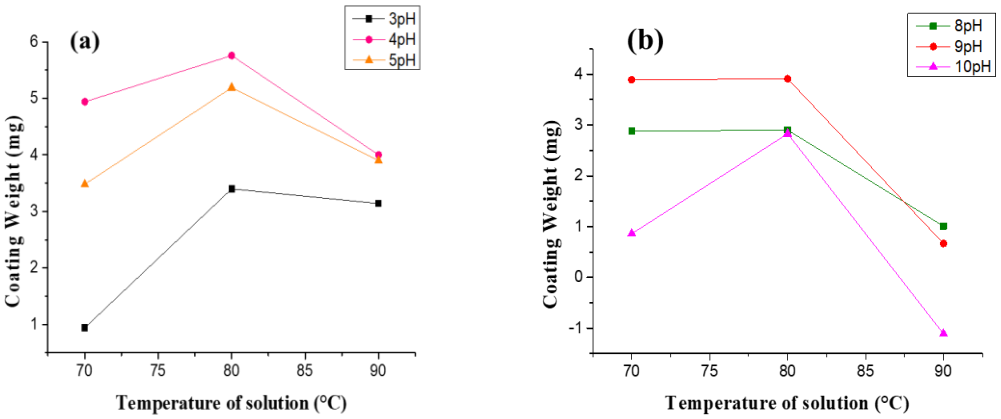

Figure 3.6: The weight of Ni-P deposits by electroless deposition of (a) acidic bath and (b) alkaline bath, with varying temperature

Comparative studies for deposited coating thickness and weight at 70°C, 80°C and 90°C are given in Figure 3.5 and 3.6. The comparison of coating thickness obtained by the deposition in the acidic medium and alkaline medium has been presented in Figure 3.5 (a) and (b), respectively. As graphs show, the coating thickness is higher at 80°C as compare to at 70°C and 90°C in both deposition medium. Figure 3.6 (a) and (b) are showing the comparison of the weight of deposits deposited in acidic medium and alkaline medium respectively. Similar to coating thickness, coating weight is also higher in the case of deposition with 80°C.

Table 3.8: Vickers microhardness of obtained coatings with different temperature (70°C, 80°C and 90°C)

Temperature of solution (°C)	**Microhardness (VHN) at different pH value**					
	In acidic bath			**In alkaline bath**		
	3	**4**	**5**	**8**	**9**	**10**
70	280	314	319	204	325	242
80	330	446	363	220	397	337
90	301	420	338	190	295	198

Values of microhardness of various deposits deposited at different temperature (70°C, 80°C and 90°C) are mentioned in Table 3.8. Microhardness values of the Ni-P coatings deposited in the acidic bath at 80°C with pH 3, pH 4 and pH 5 are 330 VHN_{10}, 446 VHN_{10}, and 363 VHN_{10} respectively and the microhardness of coatings deposited in the

alkaline bath at 80℃ with pH 8, pH 9 and pH 10 are 220 VHN_{10}, 397 VHN_{10}, and 337 VHN_{10} respectively.

Comparison of microhardness for obtained coatings at 70℃, 80℃ and 90℃ by acidic bath & alkaline bath deposition is presented in Figure 3.7 (a) and (b). Significant coating thickness is obtained at 80℃, so microhardness of this deposit is high.

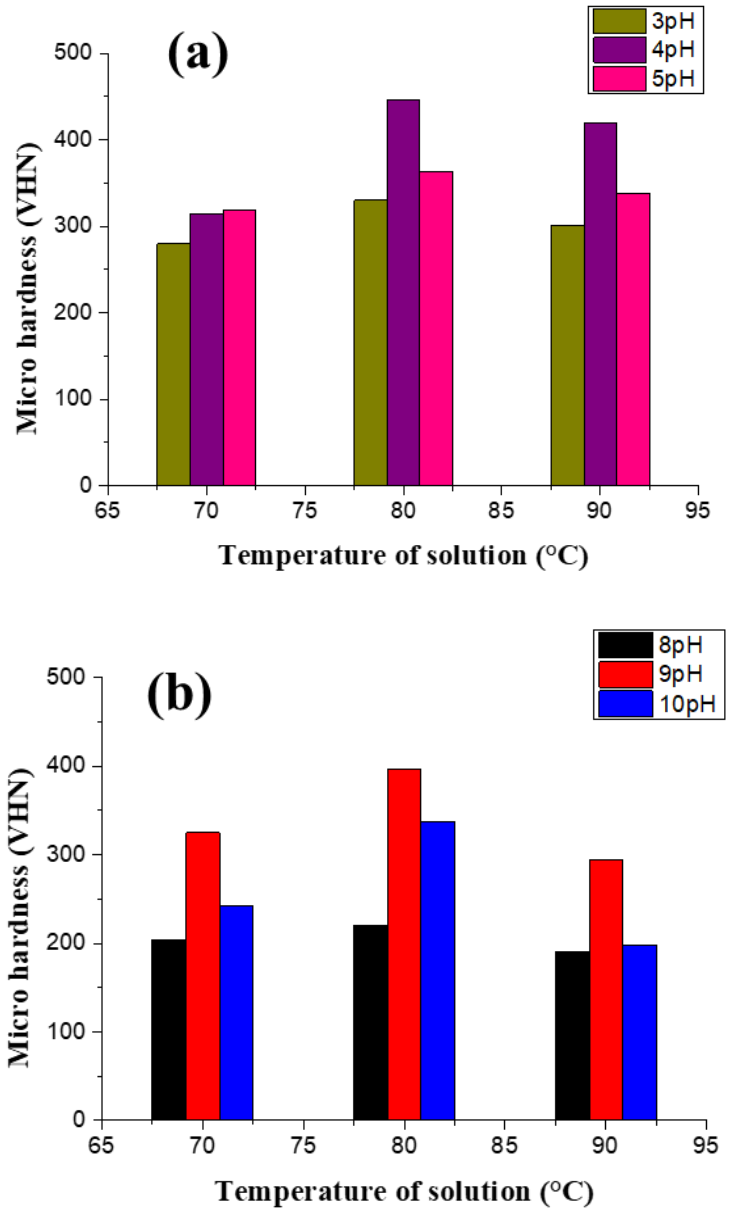

Figure 3.7: Comparison of microhardness values for obtained coatings at 70℃, 80℃ and 90℃ by (a) acidic bath and (b) alkaline bath

As result obtained from the optimization of chemical bath temperature with help of coating thickness, weight, and microhardness measurement, 80℃ is the optimal

temperature for the deposition of electroless Ni-P coating in the acidic medium and alkaline medium.

3.2.4. Time-period for coating process

By the optimization of pH and temperature of the chemical bath for the electroless nickel-phosphorus deposition, pH 4 and 80°C temperature was fixed during the optimization of time-spend for this coating process. During the optimization of time-period for electroless coating, the thickness of deposits measured after 30 minutes, 60 minutes, 90 minutes and 120 minutes of deposition. 80°C bath temperature and pH 4 of the solution are maintained during the deposition. These tests were repeated in three times. The average thickness of deposits after 30 minutes was 10 µm. The thickness of deposits after 60 minutes, 90 minutes and 120 minutes of deposition were 18 µm, 22 µm, and 22.5 µm respectively. As results observed, it can say that coating thickness is increased with an increase in deposition-time. Figure 3.8 shows, in the initial first hour, the rate of deposition of the coating is high as compared to the second hour. In the last 30 minutes thickness is increased only 2 µm. 90 minutes of deposition is sufficient for the achieving good coating thickness.

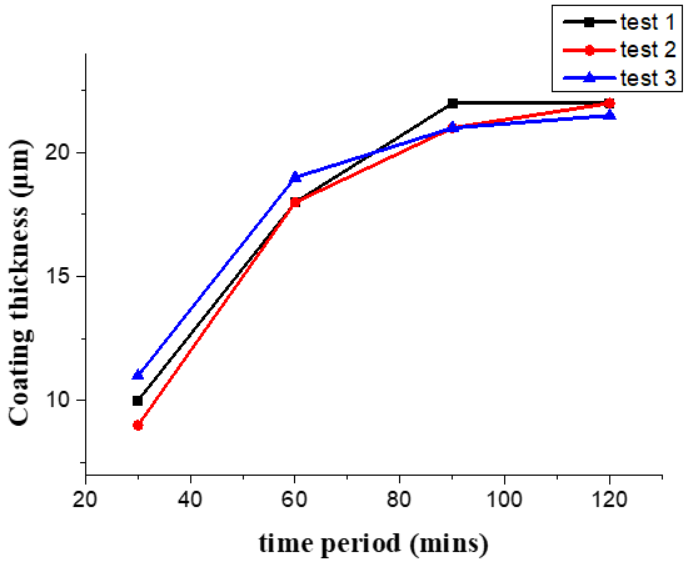

Figure 3.8: Comparison of the obtained Ni-P coating thickness after 30 minutes, 60 minutes, 90 minutes, and 120 minutes (at 4 pH and 80°C)

On the basis of above studies done for the parameters optimization of an electroless chemical bath, selected pH of the solution is 4 for acidic bath and 9 for alkaline bath,

the temperature of the solution is 80℃ and 90 minutes are time-period of the coating process.

For the study of structure and phase identification of Ni-P coating on mild steel deposited with above selected parameters, X-rays diffraction method was used. The surface morphology and chemical analysis of Ni-P coated mild steel was carried out by using FESEM with EDS technique.

The study of the structural changes in the produced coating was performed with help of X-ray diffraction technique. The X-ray diffraction patterns of Ni-P for the acidic bath (with pH 4) as well as the alkaline bath (with pH 9) both exhibited a single peak corresponding to Ni (1 1 1) phase and more diffused peaks revealed amorphous nature of coatings. X-ray diffraction analysis of Ni-P coatings for acidic and alkaline as shown in Figure 3.9 (a) and (b), confirmed that the Ni phase was present in both the samples. The X-Ray diffraction pattern of the electroless Ni-P coating obtained from acidic bath has a single broad peak centered at 43.6566, 2Θ, indicating the amorphous nature of the coating and having high phosphorous content in the deposit. The X-Ray diffraction pattern of the electroless Ni-P coating obtained from alkaline bath has a single sharp peak centered at 43.8266, 2Θ, indicating the semi-crystalline nature of the coating and having low phosphorous content in the deposit. When the pH value of the electroless bath is increased then the percentage of phosphorous content is decreased in the deposit. Amorphous nature of electroless Ni-P coating is showing when P content in the coating is higher [10, 11].

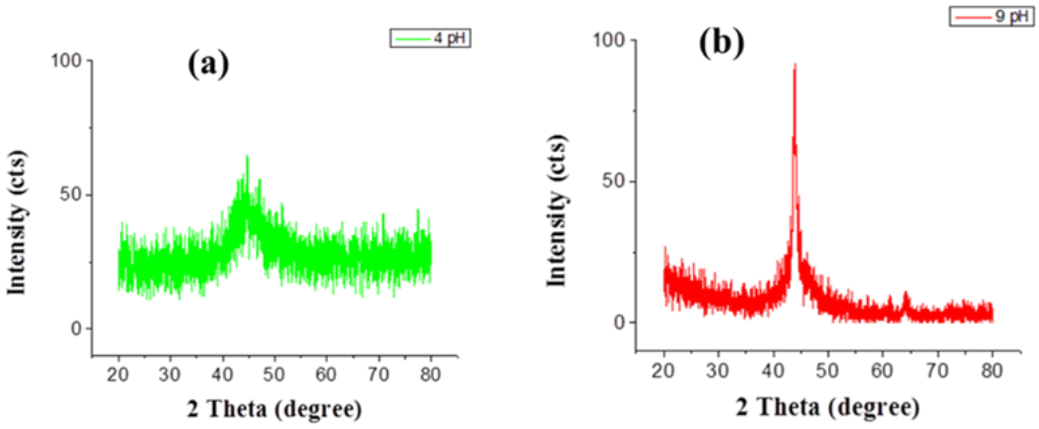

Figure 3.9: X-ray diffraction pattern of electroless Ni-P coatings obtained using (a) bath with pH 4; and (b) bath with pH 9

The studies of surface morphology of Ni-P deposits were studied by using scanning electron microscopic analysis, which was used for the surface analysis of the deposits. FESEM images of Ni-P deposits on mild steel obtained at pH 4 and pH 9 are shown in Figure 3.10 (a) and (b). FESEM micrographs show that Ni-P coating was deposited on mild steel substrate in form of spherical globules of Ni-P. The globules had a tendency to adhere with the clean upper surface of the mild steel substrate. At first, globules were formed at some random place on the mild substrate after then these globules grew in the lateral direction on the substrate. As the first layer of globules growth completed, the second layer of globules deposited on the previous layer. By this continuous process, a coherent uniform Ni-P coating developed on mild steel substrate [83]. EDS results of Ni-P coatings deposited with pH 4 and pH 9 are given in Table 3.9. The concentration of Ni is increased and the concentration of P decreases in the Ni-P deposits when the pH value of the solution is increased.

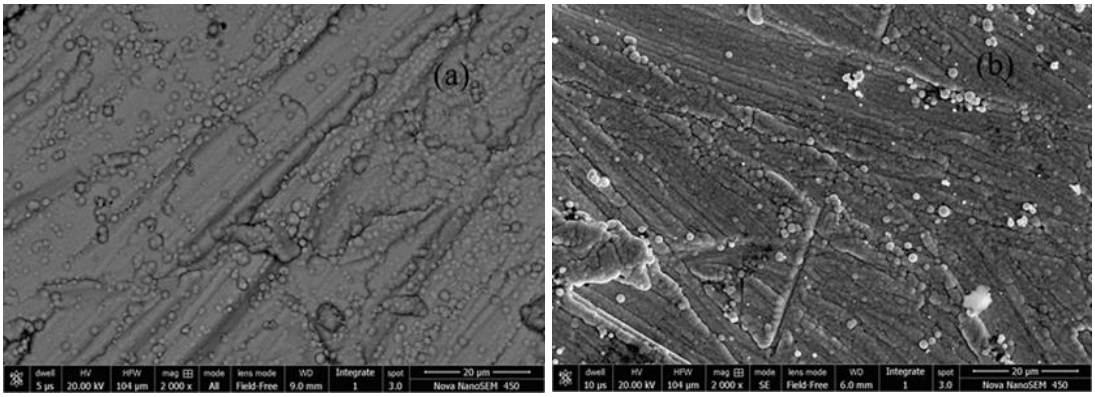

Figure 3.10: FESEM images for electroless Ni-P coating at (a) pH 4 and (b) pH 9

Table 3.9: The weight percent of elements in Ni-P alloy coating and on mild steel

Sample	**wt.% Ni**	**wt.% P**
Ni-P alloy coating with pH 4	84.4	15.6
Ni-P alloy coating with pH 9	90.6	9.4

Ni-P coatings were fruitfully developed on the mild steel substrate with help of electroless plating technique using a hypophosphite reduced bath. Electroless Ni-P coatings reveal good adherence to the mild steel substrate and were deposited as a

thickness of ~20 µm. Selected parameters for deposition of the Ni-P coating on mild steel are given in Table 3.10.

Table 3.10: Selected parameters of the electroless Ni-P coating on mild steel

Coating Parameters	**Ni-P deposition with acidic bath**	**Ni-P deposition with alkaline bath**
pH of solution	pH 4	pH 9
Temperature of solution	80°C	80°C
Time period of the coating process	90 minutes	90 minutes

XRD result obtained for Ni-P coating with acidic bath exhibited a single broad peak corresponding to Nickel (1 1 1) phase, indicated the amorphous nature of coatings and XRD pattern obtained for Ni-P coating with alkaline bath exhibited a sharp peak of nickel, indicate the semi-crystalline nature of the coating. Increase in pH of solution showing Ni-P deposits having semi-crystalline nature. On the basis of literature coating at low pH has a high content of phosphorous compared to the coating at high pH and the high phosphorous coating has an amorphous structure and low phosphorous coating has a semi-crystalline structure. If thickness, weight, and microhardness of coating are compared for deposition in the acidic and alkaline bath then deposit deposited with acidic bath has superior results so for further deposition experiments of this research work was done by the use of the acidic chemical bath.

As the conclusion of this chapter, it can say that optimize pH of the chemical bath is 4, optimize temperature of the chemical bath is 80°C and optimize time-spend of the coating process are 90 minutes for deposition of significant electroless coatings. For the further deposition of Ni-P and Ni-P-TiO_2 nanocomposite coating for studying corrosion-behavior, tribological research and structural analysis, the above parameters are used.

Chapter 4

EXPERIMENTAL

In the present chapter, the procedure used to perform the experiments is discussed. The chapter starts with the chemical analysis of raw material as received and substrate preparation for deposition of the electroless nanocomposite coating. Development of Ni-P-TiO_2 nanocomposite coating with a variation of the bath constituents is mentioned followed by characterizations of the developed nanocomposite coatings. In the characterization part, XRD analysis, SEM analysis, surface roughness, microhardness, corrosion and wear studies are included.

In the present study, the effect of electroless Ni-P coating and Ni-P-TiO_2 nanocomposite coating on mild steel carried out for the structural, mechanical, corrosion resistance and tribological properties.

4.1. Compositional analysis of mild steel

The confirming that the mild steel used as a substrate in coating processes is chemically sound or not, the compositional analyses are done by spectroscopic analysis and by chemical root.

4.1.1. By instrumentation

The sample used for chemical analysis was cut from rectangular mild steel sheet in the size of 30 mm x 30 mm x 1 mm. The chemical analysis of the mild steel substrate was done using Optical Emission Spectrometer (Bench type). The result of the chemical analysis of mild steel sample is summarized in Table 4.1, a slight variation in composition was observed from the desired composition.

Table 4.1: Chemical Composition of mild steel sample (wt.%)

Al	Mn	B	C	Cu	Nb	S	Si	P	W	Ni	Fe
0.0576	0.0599	0.0079	0.1623	0.0325	0.0402	0.0139	0.50	0.0289	0.0837	0.025	98.97

4.1.2. By chemical analysis

Carbon percent in the mild steel substrate was done using chemical analysis method in metallurgical analysis lab

% of carbon = 0.16

The weight percentage of iron and carbon was found to be 98.97% and 0.1623% which is very close to the standard composition of mild steel (0.05% to 0.25% carbon content).

4.2. Substrate preparation

This process included the cutting of the substrate from a mild steel sheet. The substrate size was taken as 20 mm x 10 mm x 1 mm (100 samples). The substrates were then filed or grinded to eliminate the sharp edges. The substrates were drilled on one side of its corner to hang in the solution.

4.2.1. Substrate surface pretreatment

To obtain good adhesion of electroless deposition to the surface of the substrate it is essential that the surface should be thoroughly cleaned [220]. Therefore, all the mild steel substrates were subjected to the following pre-treatment method [220]:

i. Degreasing in acetone.
ii. It was then washed with deionized water and immersed in the light acidic solution.
iii. It was then rinsed with deionized water and immersed in a 3% NaOH solution.
iv. It was again rinsed with deionized water and then treated with 10 g/l $SnCl_2$ solution (for sensitization purpose).
v. It was again rinsed with deionized water followed by dipping in 0.6 g/l $PdCl_2$ solution (for activation purpose).

Now the substrate is ready for the electroless coating process.

The pretreatment process of electroless Ni-P and Ni-P-TiO_2 nanocomposite coating on mild steel is shown in Figure 4.1.

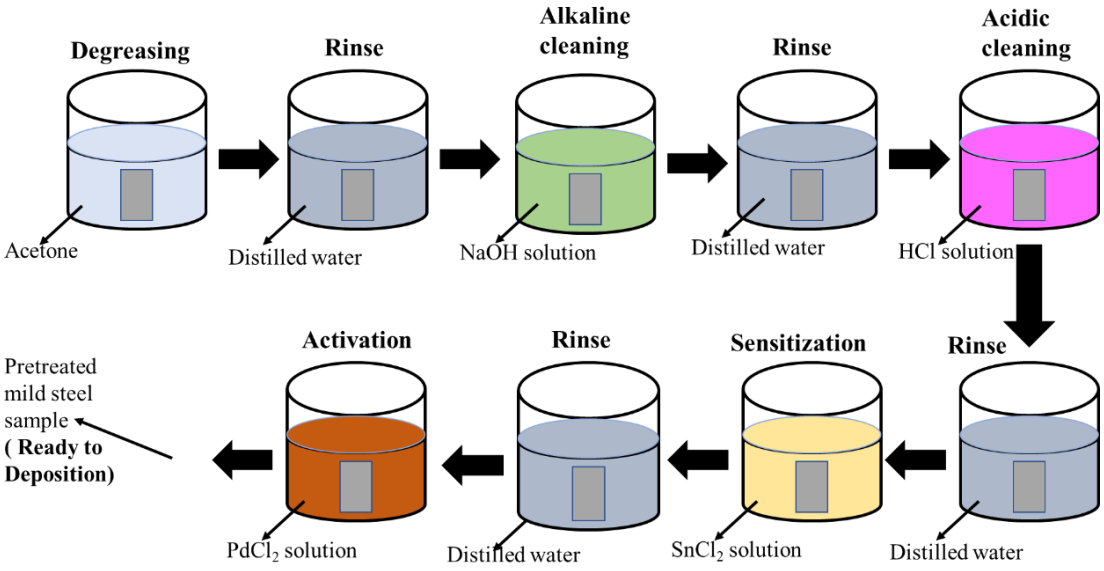

Figure 4.1: Procedure for substrate surface pre-treatment

4.3. Deposition of Ni-P-TiO_2 nanocomposite coating

Development of the different electroless Ni-P-TiO_2 nanocomposite coatings by varying concentration of nickel salt, reducing agent and second phase particulate material in the coating bath was done.

The process of deposition of electroless Ni-P-TiO_2 nanocomposite coating on the mild steel is in two steps:

Step I: Pre-treatment of the substrate

Step II: Deposition of Ni-P-TiO_2 nanocomposite coating on the mild steel substrate.

Pretreatment of the substrate is very essential due to this coating is a type of chemical bath deposition and a good adhered uniform surface is getting after properly pretreatment. Pretreatment process for mild steel substrate described in section 4.2.1. After pretreatment of the mild steel substrate, it is ready to the electroless deposition.

For the deposition of Ni-P-TiO_2 nanocomposite coating on mild steel, made a chemical reduction bath containing nickel salt, a complexing agent, a reducing agent, and nano TiO_2 powder is as shown in Figure 4.2. Ni-P-TiO_2 nanocomposite coatings on the mild steel substrate were done by chemical bath deposition (electroless coating) method as follows:

i. 200 ml of distilled water was heated at 90°C with hot plate cum stirrer and then it was mixed with Nickel Sulphate and Sodium hypophosphite and then the solution is added with lactic acid. The pH and temperature were measured at regular intervals this stage (to maintain the optimized pH value of 4 and temperature of 90°C).

ii. The pre-treated mild steel substrate was dipped in the chemical bath for prescribed time i.e. 90 minutes for deposition of the coating.

iii. Then the sample was taken out from the chemical bath and rinsed with deionized water and dried.

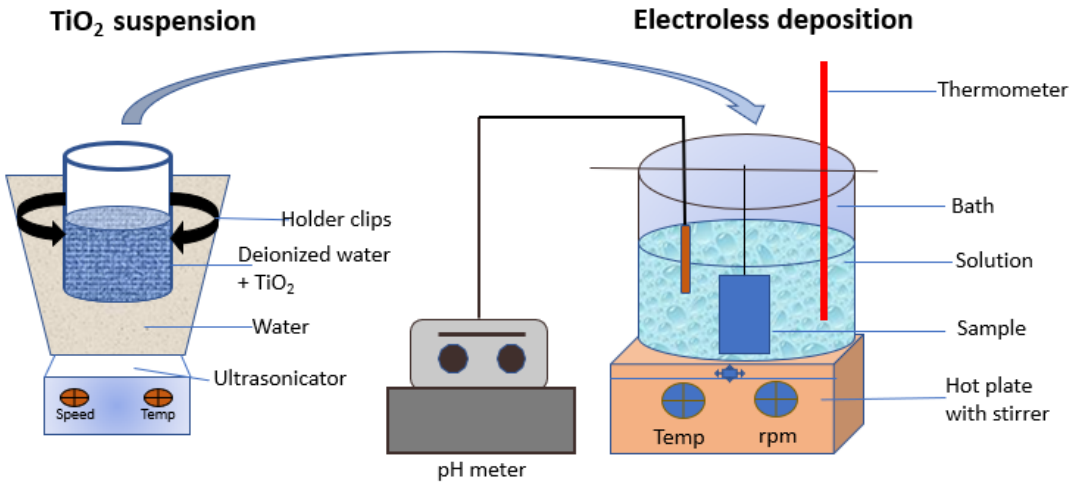

Figure 4.2: Electroless nanocomposite coating set up

4.3.1. Mechanism of Ni-P-TiO_2 nanocomposite coating

Deposition of electroless Ni-P-TiO_2 nanocomposite coating is a surface reaction, divided into elementary steps, such as diffusion of Ni^{+2} and $H_2PO_2^-$ to the surface, adsorption of Ni^{+2} and $H_2PO_2^-$ at the surface of activated mild steel, chemical reaction on the mild steel surface desorption of HPO_3^-, H_2, and H^+ from the surface and last diffusion of HPO_3^-, H_2, and H^+ away from the mild steel surface. Reduction of nickel with hypophosphite is always conducted by the release of H_2. As a by-product of reduction reaction, hydrogen ions are generated. Chemical reactions involved in the electroless coating prosses are given below [44].

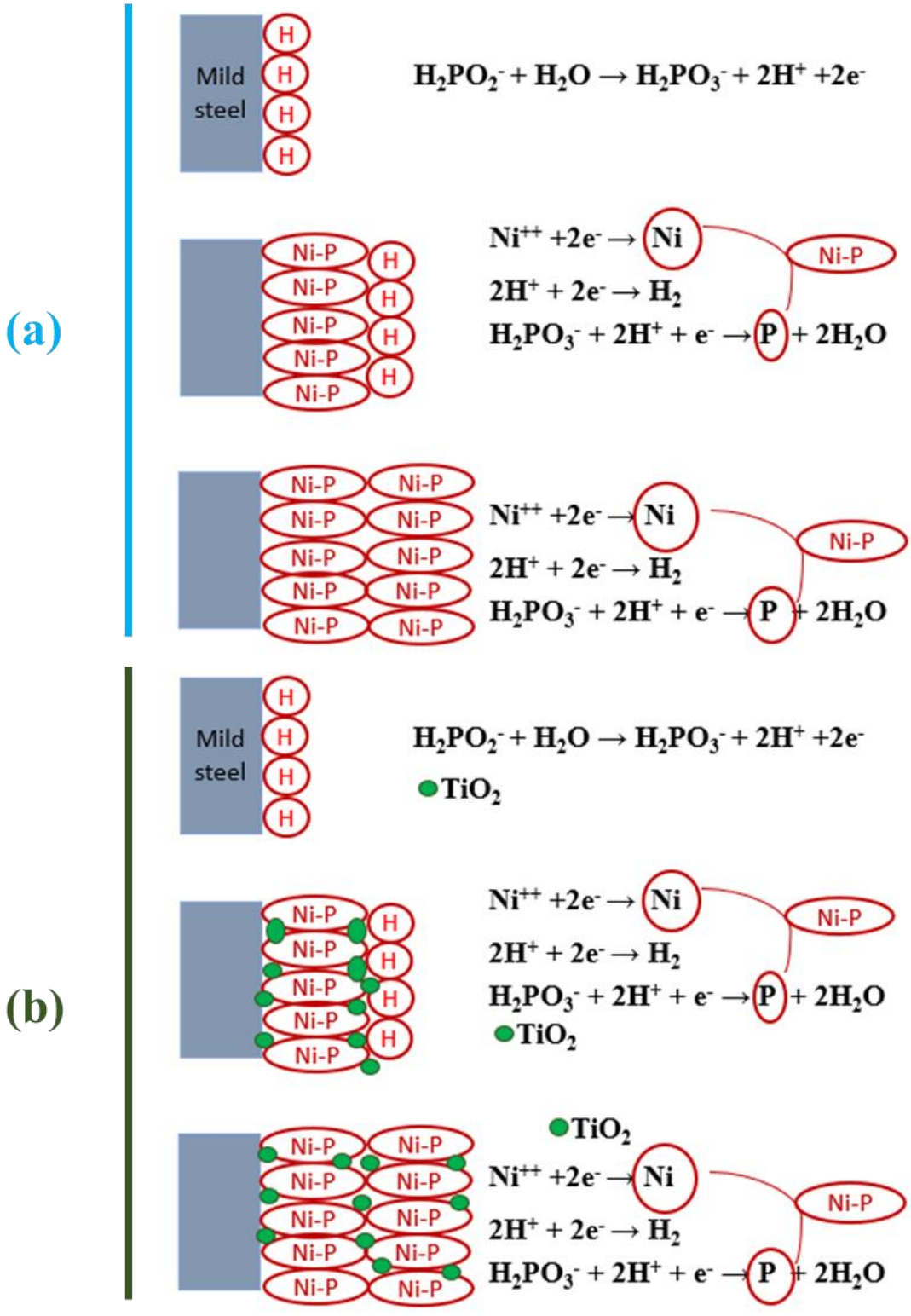

Figure 4.3: Mechanism of electroless deposition of (a) Ni-P coating and (b) Ni-P-TiO_2 nanocomposite coating on mild steel

Mechanism of the electroless deposition on the mild steel surface is shown in Figure 4.3. when hypophosphite ion reacts with water, atomic hydrogen form and these atomic hydrogens adsorbed in the surface of mild steel.

$$H_2PO_2^- + H_2O \rightarrow H_2PO_3^- + 2H^+ + 2e^- \quad \text{.....(i)}$$

$$Ni^{+2} + 2e \rightarrow Ni^0 \quad \text{.....(ii)}$$

$$2H^+ + 2e \rightarrow H_2 \quad \text{.....(iii)}$$

$$H_2PO_2^- + 2H^+ + e \rightarrow P + 2H_2O \quad \text{.....(iv)}$$

Then co-deposition of nickel-phosphorus (Ni-P) by the reduction for atomic hydrogen of Ni^{+2} ion and $H_2PO_2^-$ ion. Again, atomic hydrogen (H) adsorption in the formed Ni-P deposit. These atomic hydrogens also formed by the reaction of the hypophosphite ion with water. Again, co-deposition of Ni-P in the Ni-P deposit by new reaction for atomic hydrogen of Ni^{+2} ion and $H_2PO_2^-$ ion. TiO_2 nanoparticles were simply co-deposited with Ni-P coating.

A number of experiments done for the obtaining the electroless nanocomposite coating with a variation of concentration of TiO_2 content, a nickel source, and reducing agent are shown in Figure 4.4. Electroless bath chemical composition and parameters for Ni-P-TiO_2 nanocomposite coatings are given in Table 4.2, 4.3 and 4.4, with variation of concentration of nickel sulphate 25 g/l, 30 g/l, and 35 g/l, concentration of sodium hypophosphite20 g/l, 30 g/l, and 40 g/l and concentration of TiO_2 nanopowder 0.4 g/l, 0.8 g/l, 1.2 g/l, 1.6 g/l, and 2 g/l respectively.

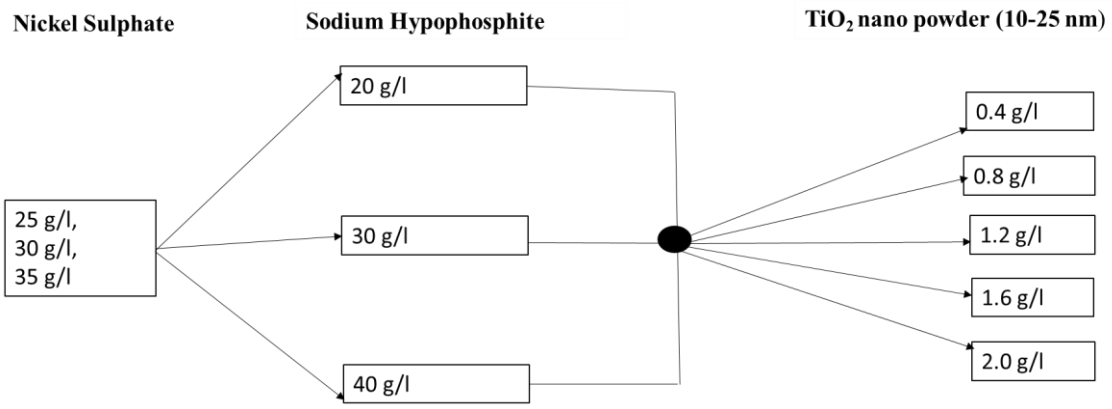

Figure 4.4: Chemical bath compositions: variation in concentration of nickel sulphate, sodium hypophosphite, and TiO_2 nanoparticles

Table 4.2: Electroless bath chemical composition for composite coating (only variation in concentration of nickel-source)

S. No.	Chemicals	Concentration
1.	**Nickel sulphate**	**25 g/l, 30 g/l, 35 g/l**
2.	Sodium hypophosphite	30 g/l
3.	Lactic acid	35 ml/l
4.	TiO_2 nano powder (10-20 nm)	2.0 g/l
5.	pH of solution	4
6.	Temperature of bath	90±2°C
7.	Bath loading	0.002 m^2/l

Table 4.3: Electroless bath chemical composition for composite coating (only variation in concentration of reducing-agent)

S. No.	Chemicals	Concentration
1.	Nickel sulphate	30 g/l
2.	**Sodium hypophosphite**	**20 g/l, 30 g/l, 40 g/l**
3.	Lactic acid	35 ml/l
4.	TiO_2 nano powder (10-20 nm)	2.0 g/l
5.	pH of solution	4
6.	Temperature of bath	90±2°C
7.	Bath loading	0.002 m^2/l

Table 4.4: Electroless bath chemical composition for composite coating (only variation in concentration of second phase particles)

S. No.	Chemicals	Concentration
1.	Nickel sulphate	35 g/l
2.	Sodium hypophosphite	30 g/l
3.	Lactic acid	35 ml/l
4.	**TiO_2 nano powder (10-20 nm)**	**0.4, 0.8, 1.2, 1.6, and 2.0 g/l**
5.	pH of solution	4
6.	Temperature of bath	90±2°C
7.	Bath loading	0.002 m^2/l

4.3.2. Coating thickness and weight measurement

The coating thickness and coating weight was measured by digital micrometer with precision 0.001 mm and digital weighing balance with a precision of 0.1 mg respectively. After obtained a well-adhered coating on mild steel substrate, the thickness and weight of the electroless deposited coating were measured by taking the difference of thickness and weight of the substrate with and without coating. The following formulas were used to calculate the coating thickness and weight:

$$\textbf{Coating Thickness (mm)} = t_2 - t_1 \qquad \ldots\ldots\ldots\ldots\ldots\ldots\ldots\ldots (4.a)$$

$$\textbf{Coating weight (mg)} = w_2 - w_1 \qquad \ldots\ldots\ldots\ldots\ldots\ldots\ldots\ldots (4.b)$$

Where t_1 and t_2 are thickness measured in mm by digital micrometer before and after coating respectively. w_1 and w_2 are weight measured in mg by weight balance before and after the deposition respectively.

4.4. Characterization techniques for obtained coatings

Surface texture and microstructure of coating have an enormous effect on its corrosion and wear performance. Therefore, it was necessary to do XRD analysis, scanning electron microscopy and surface roughness analysis before conducting microhardness, electrochemical and wear tests. XRD analysis and FESEM analysis of coatings were helpful to understand the information related to presented phases and morphological information such as particles size, shape, and distribution in the deposit on the mild steel surface.

4.4.1. X-ray diffraction (XRD)

X-rays diffraction analysis is a technique worked for studying the structure (crystalline or amorphous) and parented phases in the materials. The XRD testing was carried out on XRD testing machine (Model: Panalytical X Pert Pro) using Cu as the anode material with K alpha wavelength of 1.540598Å. The size of the samples was 20 mm x 10 mm

x 1 mm. The scan range was 20˚ to 80˚ and the scan rate was 2˚ per minute. X-ray diffractometer machine is shown in Figure 4.5.

In this research work, X-rays diffraction analysis was used for the generating X-ray diffraction spectra for electroless Ni-P coating on mild steel and Ni-P-TiO_2 nanocomposite coatings on mild steel with a variation in concentration of nickel sulphate, concentration of sodium hypophosphite and concentration of second phase particles (nano TiO_2).

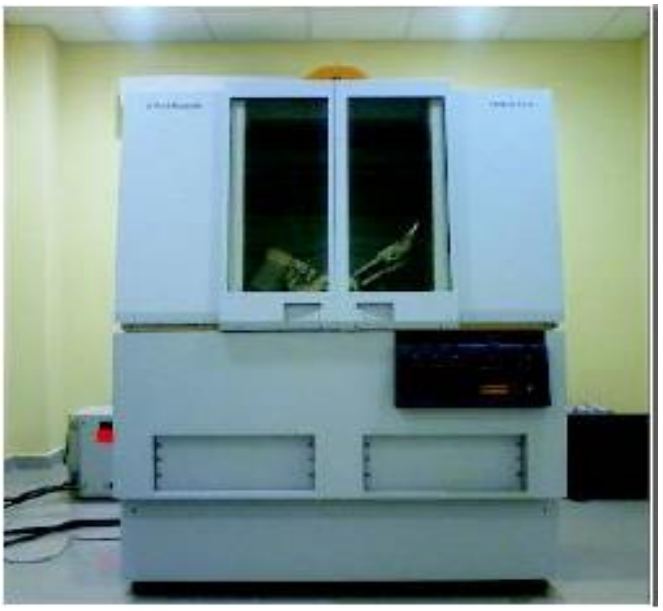

Figure 4.5: X-Ray Diffractometer (Panalytical X Pert Pro)

The size of the Ni-P globules and developed strain within the nickel-phosphorous matrix due to the inclusion of second phase particles (TiO_2 particles) calculated by formula (4.c) and formula (4.d) respectively [206, 221-222].

$$L = \frac{x\lambda}{\beta.cos\theta} \qquad \text{..... (4.c)}$$

$$\frac{\beta cos\theta}{\lambda} = \frac{1}{L} + \frac{\varepsilon sin\theta}{\lambda} \qquad \text{.....(4.d)}$$

Where L is particle size, $\boldsymbol{\lambda}$ is the used X-ray wavelength, x is the correction faction (~ 0.9), β is the FWHM of observed Peaks, Ɛ is the effective strain and Ɵ is the Bragg's angle.

4.4.2. Field emission scanning electron microscope (FESEM)

FESEM was conducted to study the surface morphology (shape, size, and distribution of the presented elements) of the Ni-P and Ni-P-TiO_2 nanocomposite coated mild steel as well the effect of inclusion of second phase particles (nano TiO_2) on morphological changes. Different electron microscopic analysis such as mapping and spot analysis (EDS) were performed with FESEM for studying the distribution of the elements in particular area and wt.% and atm.% of presented elements in a particular spot.

Microstructural characterization study was done to observe the microstructure of the sample surface. This was done by using field emission scanning electron microscope with energy dispersive X-ray spectroscopy at the materials research center, MNIT Jaipur, and IIT Kanpur. Figure 4.6 shows the SEM equipment. The FESEM micrographs of the samples were obtained. The images were taken in secondary electron (SE) mode. FESEM with EDS and mapping analysis was done for the various coated samples, which are given in Table 4.5.

Table 4.5: Coated samples which are used for the FESEM analysis

Sample	**Chemical concentration**	**Parameters**
Ni-P coating	Nickel sulphate: 30 g/l Sodium hypophosphite: 20 g/l Lactic Acid: 35 g/l	pH of solution: 4 Temperature of solution: 80℃ Time period for coating process: 90 minutes
Ni-P-TiO_2 nanocomposite coating	Nickel sulphate: 25 g/l, 30 g/l, 35 g/l Sodium hypophosphite: 20 g/l, 30 g/l, 40 g/l Lactic Acid: 35 g/l TiO_2 nano powder: **0**.4 g/l, 0.8 g/l, 1.2 g/l, 1.6 g/l, 2.0 g/l	pH of solution: 4 Temperature of solution: 80℃ Time period for coating process: 90 minutes

Fig 4.6: Scanning electron microscopy (Nova Nano FESEM 450)

4.4.3. Microhardness testing

In this research work, hard nano TiO_2 particles are used as second phase particles to develop electroless Ni-P-TiO_2 nanocomposite on mild steel. Microhardness tests were performed with the purpose of understanding the effect of Ni-P and Ni-P-TiO_2 nanocomposite deposition on the microhardness of mild steel.

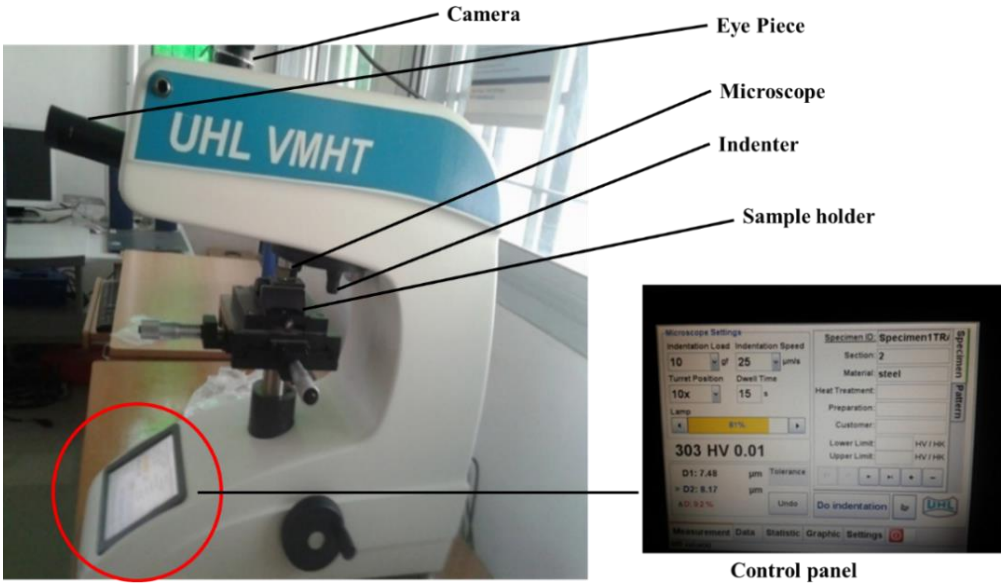

Figure 4.7: Microhardness tester

The microhardness of the mild steel and both types of coatings was measured using a Vickers microhardness tester (Model: UHT VMHT) with the diamond indenter. A 10 gm load is applied on the steel and coated steel samples for 15 second and microhardness measurements are taken. An average of five measurements was reported as the microhardness value. Set-up of Vickers microhardness tester is shown in Figure 4.7.

4.4.4. Surface texture analysis

The advantage of electroless Ni-P coating and Ni-P-TiO_2 nanocomposite coating is that these types of coatings provide a uniform deposit thickness on the surface of the specimen. In this research, Ni-P-TiO_2 nanocomposite coatings are deposited on the mild steel surface with the use of nano TiO_2 particles as second phase particles. For measuring the roughness of nanocomposite coatings, AFM tests were performed.

The surface roughness of electroless Ni-P coating and electroless Ni-P-TiO_2 nanocomposite coatings were studied by atomic force microscopy (model: Multimode Scanning Probe Microscope). AFM (Multimode Scanning Probe Microscope) is shown in Figure 4.8.

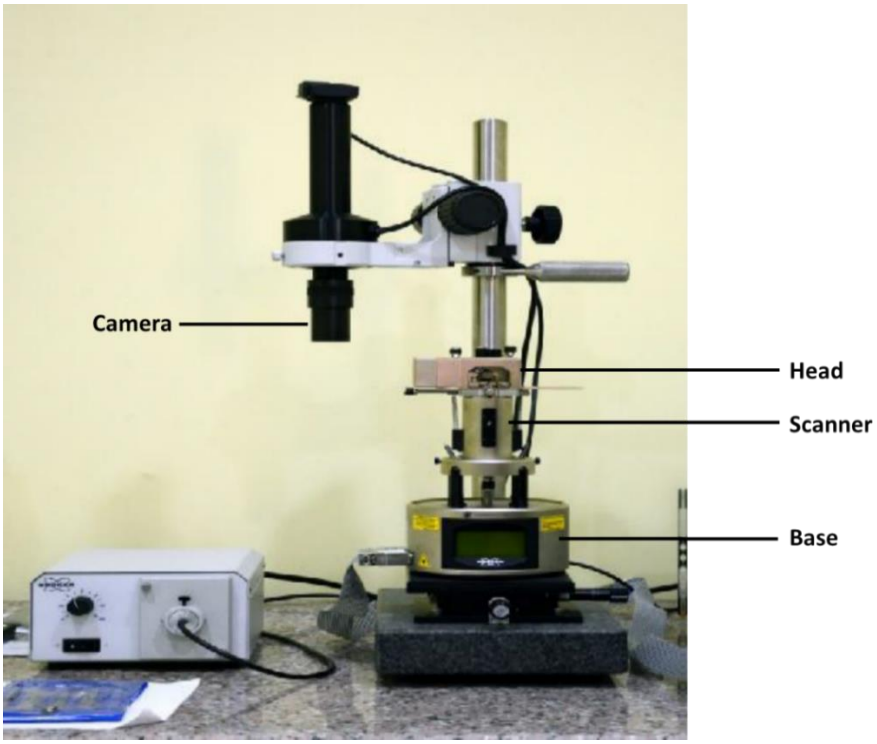

Figure 4.8: AFM (Multimode Scanning Probe Microscope)

4.4.5. Corrosion test

Mild steel usually possesses poor corrosion resistance in the corrosive environment. In previous studies done by various researchers, Ni-P coatings were deposited on mild steel by the electroless method. Ni-P coated mild steel showed quite improved corrosion resistance in the corrosive environment. For knowing the effect of Ni-P-TiO_2 nanocomposite coating on corrosion resistance property, electrochemical tests were performed on coated samples.

Corrosion resistance characterization of the mild steel and coated mild steel samples was carried out by the computer-controlled instrument Gamry 600^{TM} Potentiostat/Galvanostat with specific software for the treatment of obtained corrosion data. Tafel electrochemical measurements were taken on the specimen during their exposure to an aqueous solution of 3.5% NaCl at room temperature in the range of -0.5 to 0.5 V open circuit potential and a constant scan rate of 1 mV/s. For comparison, the corrosion test has been applied for the mild steel substrate, Ni-P coating, and Ni-P-TiO_2 nanocomposite coating. Potentiostat used for corrosion test is showing in Figure 4.9.

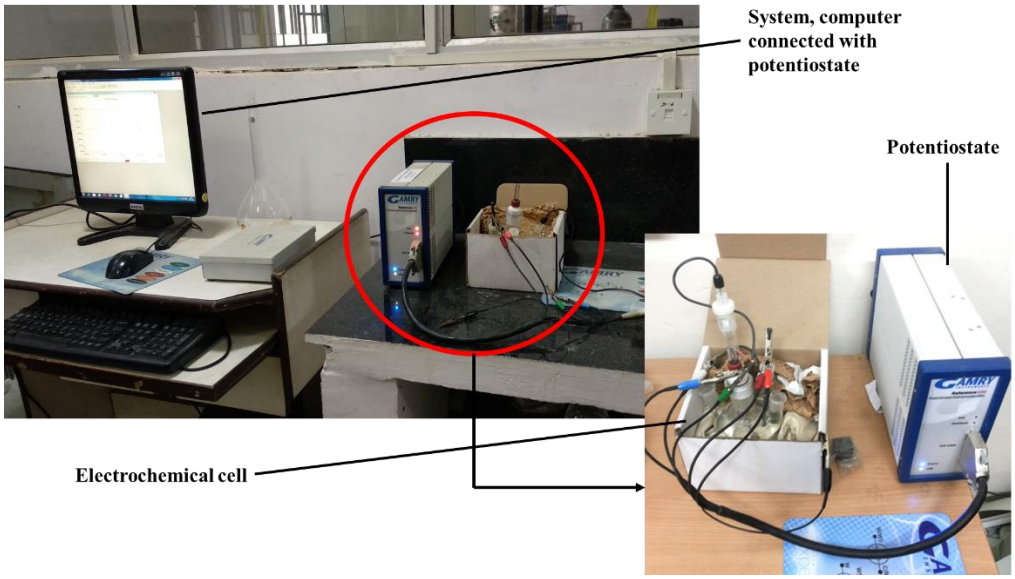

Figure 4.9: Potentiostat used for corrosion test

Tafel plot obtained from electrochemical potentiodynamic polarization was used to measure corrosion rate with the help of Tafel slop at anodic polarization β_a, Tafel slops at cathodic polarization β_c, corrosion potential $E_{corr,}$ and corrosion current density I_{corr} . The Tafel plot is based on the mixed potential theory.

The polarization resistance (R_p) and corrosion rate were determined using the relationships given below [171, 215]:

$$R_p = \frac{\beta}{I_{corr}} \qquad \text{.....(4.e)}$$

$$\beta = \frac{\beta a \beta c}{2.3(\beta a + \beta c)} \qquad \text{..... (4.f)}$$

β (constant) and corrosion rate were calculated with the help of following equations:

$$\textbf{Corrosion Rate (mpy)} = \frac{0.13 I_{corr}(Eq.wt.)}{d} \qquad \text{.....(4.g)}$$

4.4.6. Wear analysis

Nanocomposite coatings produced by inclusion of the second phase particles into the nickel-phosphorous matrix to enhance the hardness, corrosion resistance and tribological characteristics of the material. Wear analysis required to understand the effect of inclusion of TiO_2 into the matrix of Ni-P on the wear resistance property of nickel-phosphorous coating. Wear resistance properties of Ni-P-TiO_2 nanocomposite coating are also affected by the concentration of the chemicals such as sodium hypophosphite, nickel sulphate and nano TiO_2 particles in the deposition bath.

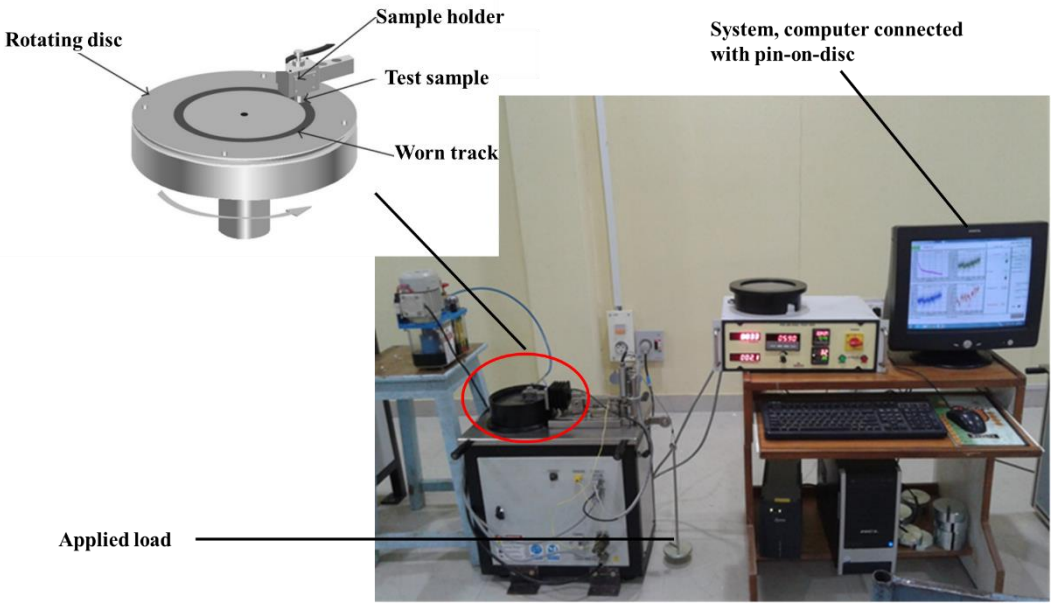

Figure 4.10: Pin-on-disc apparatus using in the wear test

Wear resistance of electroless Ni-P coating and electroless Ni-P-TiO_2 nanocomposite coatings were studied Pin on Disc Wear Tester. Wear tests were performed with 0.2 m/s (55 rpm) sliding speed for sliding wear monitoring and prediction, the temperature of 35°C, under 5 N load and 500 m sliding distance. Pin-on-disc setup is showing in Figure 4.10.

Pin-on-disc tests were performed on mild steel (uncoated substrate), Ni-P coated mild steel, and Ni-P-TiO_2 nanocomposite coated mild steel for the wear analysis. Ni-P-TiO_2 nanocomposite coatings on mild steel were developed with variation of nickel sulphate (25 g/l, 30 g/l and 35 g/l), sodium hypophosphite (20 g/l, 30 g/l and 40 g/l) and nano TiO_2 particles (0.4 g/l, 0.8 g/l, 1.2 g/l, 1.6 g/l and 2.0 g/l). These all coating samples were used for wear analysis.

Chapter 5

RESULTS AND DISCUSSION

This chapter deals with results related to the characterization of electroless Ni-P alloy coating and Ni-P-TiO_2 nanocomposite coatings on the mild steel and its discussion. Electroless nanocomposite coating obtained after deposition process have been studied in different groups. Groups of coated samples for characterization study are made on the basis of variation in concentration of nickel salt, reducing agent and second phase particles (TiO_2). The characterization of deposited coating is done with X-ray analysis, FESEM, microhardness, surface texture analysis, corrosion resistance study and wear study.

There are three sections in the fifth chapter. The first section of this chapter deals with the characterizations of electroless Ni-P coating on the mild steel specimen. Characterizations of electroless Ni-P-TiO_2 nanocomposite coatings on the mild steel are discussed in the second section, while the comparison of enhanced properties of the mild steel by the deposition of Ni-P coating and Ni-P-TiO_2 nanocomposite coatings is discussed in the third section.

5.1. Deposition of electroless Ni-P coating on mild steel and its characterization

In this section, results related to the properties of Ni-P deposit on mild steel, which was deposited from the acidic chemical bath in which sodium hypophosphite used as the reducing agent, are discussed. Phase analysis, morphological study with elemental analysis, microhardness, surface finish, corrosion resistance and wear resistance of the deposited Ni-P coating on mild steel are discussed in this section. It is necessary to understand the influence in properties of the coating due to the inclusion of hard second phase particles (nano TiO_2) in the Ni-P coating before starting the discussion about the characterization of obtained Ni-P-TiO_2 nanocomposite coatings on the mild steel, analysis of characterizations of Ni-P coating.

The thickness of the developed Ni-P coating on mild steel is ~20 µm. X-rays diffraction analysis was done to find the phases present in the Ni-P coating on the mild steel, XRD Pattern obtained from the X-rays diffraction test with Cu K_α target performed on the Ni-

P coated mild steel are shown in Figure 5.1. A peak was observed at position (2θ) 44.3142°. According to the JCPDF data, this peak is found of Nickel exhibited (1 1 1) preferred orientation and d-spacing value 2.04707Å. In the X-ray diffraction pattern of nickel-phosphorous coating, single broad peak with many diffused peaks revealed amorphous nature of the coating.

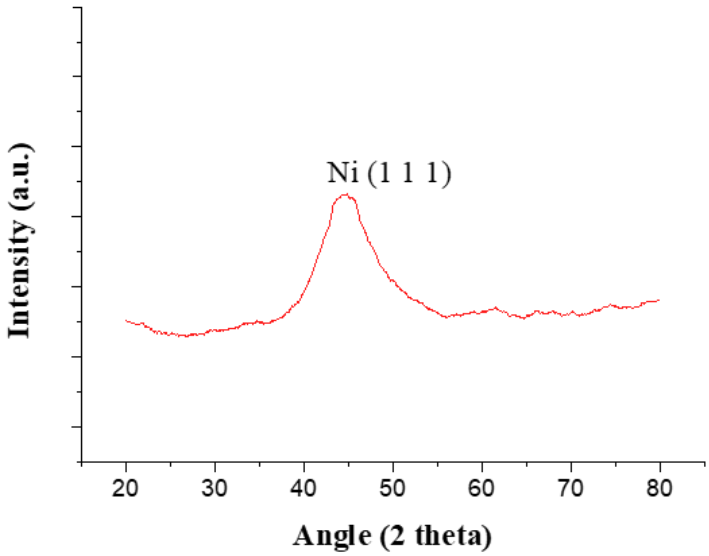

Figure 5.1: XRD pattern of Ni-P coating on mild steel

Guojin Lu et.al (2002) were reported FCC (1 1 1) peak corresponding due to the Nickel during the analysis of XRD spectra of the Ni-P based alloys [113]. A similar type of broad peak of Nickel in XRD analysis of Ni-P alloy coating due to the high (19%) P content was also reported by Maura Crobu et.al [112].

In Figure 5.2, FESEM micrograph shows that Ni-P coating deposited on mild steel substrate in the form of spherical globules of Ni-P. On the surface structure of Ni-P coated mild steel, pores are not present or visible between the globules. The surface of the mild steel is fully covered by the numerous spherical globules. Ni-P globules in Ni-P alloy coatings were reported by Maura et.al., Guojin et.al and many other researchers who had worked in the field of Ni-P coatings [112, 113, 119].

The results obtained from EDS analysis for Ni-P coating are presented in Figure 5.3. From EDS spectra of Ni-P coating, peaks of nickel and phosphorus were observed which leads to the coating composition. Results confirmed the presence of Ni and P in

the obtained Ni-P coating. EDS analysis indicated that Ni-P coating consisted of 84.4 wt.% Ni and 15.6 wt.% P. On the basis of phosphorous content in the Ni-P deposit, the coating can be characterized as high phosphorous electroless coating so the film found is amorphous in nature.

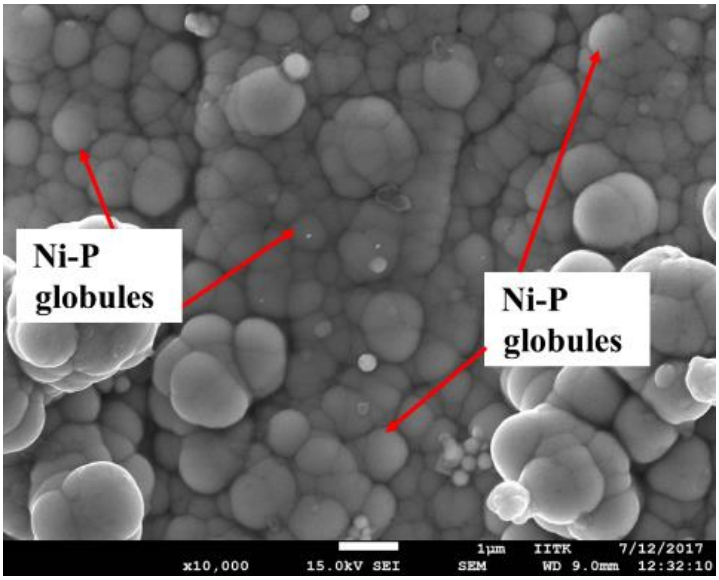

Figure 5.2: FESEM image of electroless Ni-P coating on mild steel specimen at 10000X

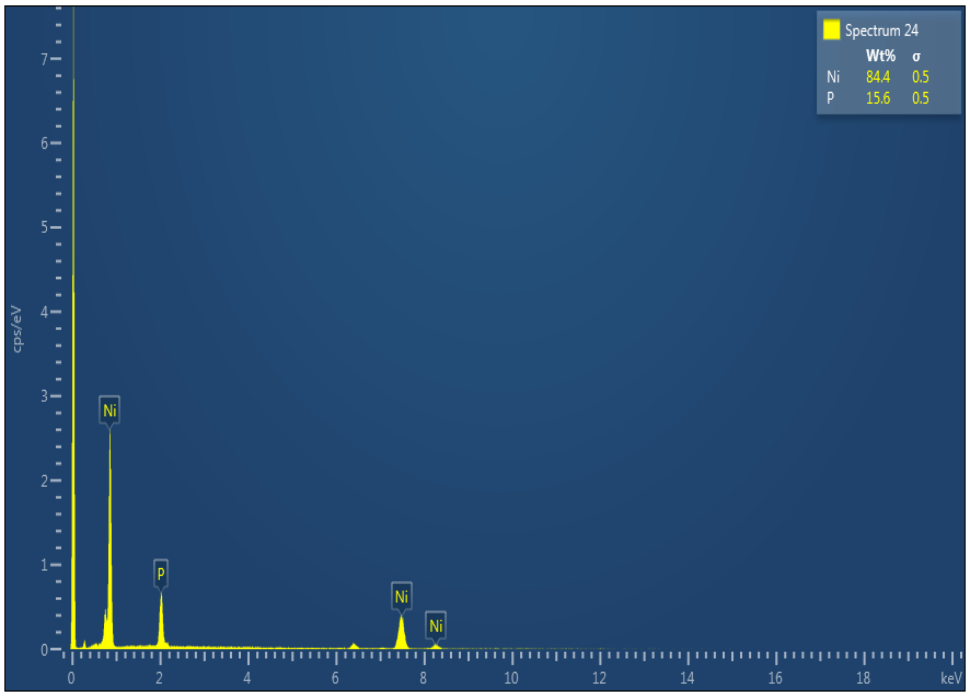

Figure 5.3: EDS Pattern of Ni-P coating on mild steel specimen

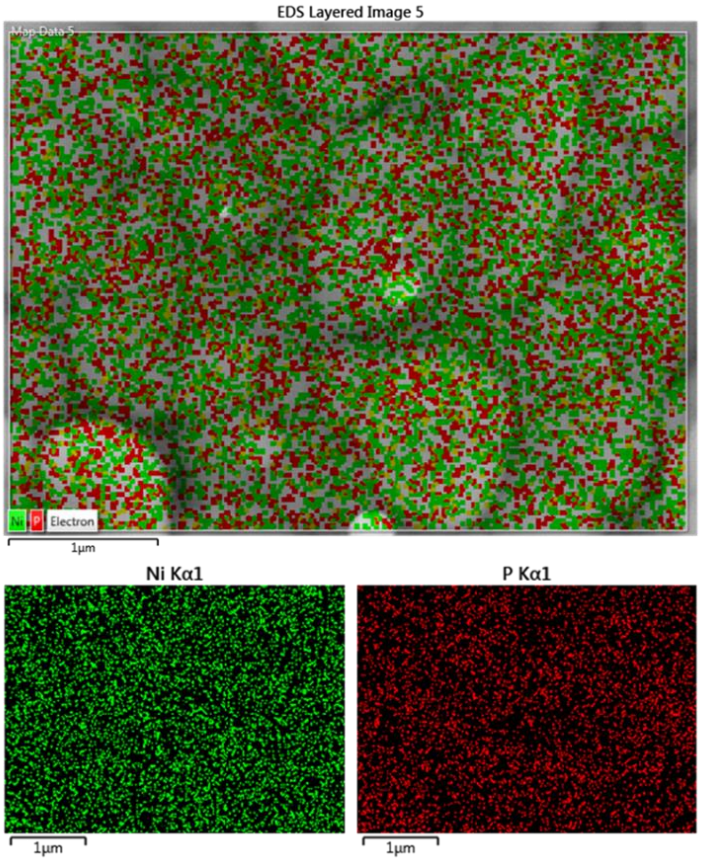

Figure 5.4: Ni-P matrix in Ni-P coated mild steel

Uniform dispersion of deposition of the nickel and phosphorous in form of Ni-P globules on the coated surface is shown in Figure 5.4. These results are obtained by the SEM with mapping analysis. Dispersion of nickel and phosphorus was found as 88.2 wt.% and 11.8 wt.% respectively through the mapping analysis of Ni-P coating on mild steel.

Vickers microhardness of uncoated sample (mild steel) and coated with 20 µm thick electroless Ni-P coating sample at 10 gm indentation load with 15 s dwell time was found by tests performed on Vickers's microhardness tester. Five repeated readings are taken on the surface of mild steel and Ni-P coated mild steel and the obtained average values are used for further use. The average value of microhardness in uncoated mild steel and in the Ni-P coated mild steel are calculated as ~ 132 VHN_{10} and ~ 400 VHN_{10} respectively. Comparison of the microhardness hardness values of mild steel and Ni-P coated mild steel is presented in Figure 5.5. This figure shows the enhancement in the microhardness of mild steel by the Ni-P coating on the surface due to the uniform and

adheres deposition of Ni-P coating. The deposited Ni-P coating has a hard surface, this hard Ni-P deposit resists the penetration by the indentation.

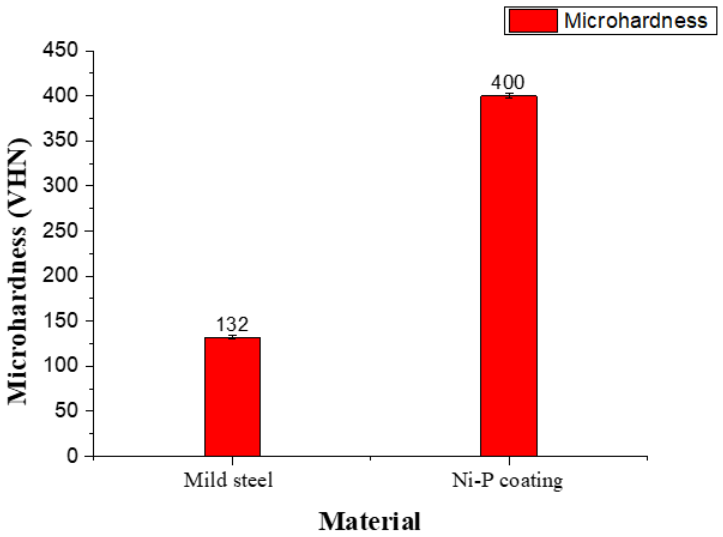

Figure 5.5: Comparison of Vickers microhardness of uncoated and Ni-P coated mild steel

If the main aim is to understand the nature of the surface of engineering solid materials, the surface texture is a very important factor. In the working/functional performance of several engineering components, the surface texture of solids plays an important role. Measurements related to surface texture were made with a Multi-Mode AFM in contact mode.

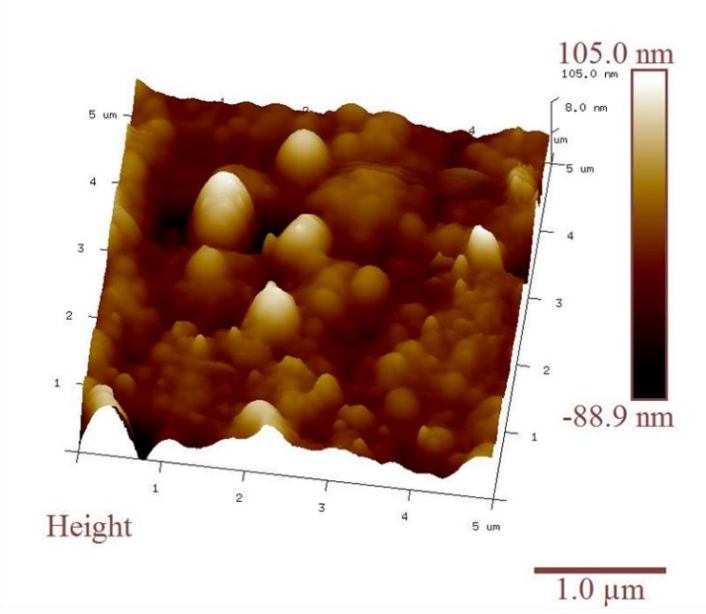

Figure 5.6: AFM images of surface roughness of Ni-P coating

The surface roughness parameters were calculated from the analysis of AFM images as shown in Figure 5.6. The mean square root roughness (Rq) value and average roughness (Ra) value along with 20 µm coating thickness of electroless Ni-P coating are 23.5 nm and 17.4 nm respectively.

The corrosion studies of electroless Ni-P coated mild steel were carried out in 3.5% sodium chloride solution. Tafel plot obtained from electrochemical potentiodynamic polarization was used to measure corrosion rate with the help of Tafel slop at anodic polarization β_a, Tafel slop at cathodic polarization β_c, corrosion potential $E_{corr,}$ and corrosion current density I_{corr}. The Tafel plot is based on a mixed potential theory of corrosion.

Figure 5.7 shows the Tafel curve obtained from polarization studies for Ni-P coated mild steel in 3.5% NaCl aqueous solution. The corrosion density (I_{corr}) of Ni-P coated mild steel substrate is 70.23 µA/cm^2 and electrode-potential (E_{corr}) is -701 mV. Calculated corrosion rate with the help of electrochemical parameters is 6.61 mpy.

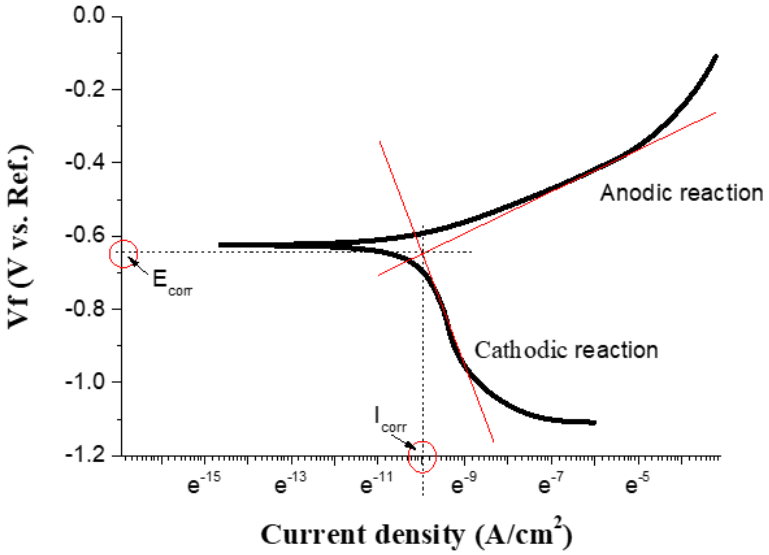

Figure 5.7: Tafel curve for Ni-P coating in 3.5% NaCl solution

Y. S. Huang et. al. evaluated corrosion characteristics of electroless Ni-P and electroless composite coating in 1.0 N H_2SO_4 and 3% NaCl electrolyte solutions. Figure 5.8 shows the Tafel curves of electroless Ni-P deposit, electroless Ni-P-SiC, and Ni-P-PTFE composite deposits [178]. They observed that the electroless Ni-P coating and electroless composite coatings showed lower corrosion currents (I_{corr}) and more positive

corrosion potentials (E_{corr}) than the mild steel substrate in 1.0 N H_2SO_4 and 3% NaCl. Their observation indicates that Ni-P coatings have better corrosion resistance results compare to the uncoated mild steel substrate [178]. The corrosion results obtained from electrochemical studies for Ni-P coated mild steel in 3.5% sodium chloride electrolyte are well supported with the electrochemical results obtained by Y. S. Huang et.al.

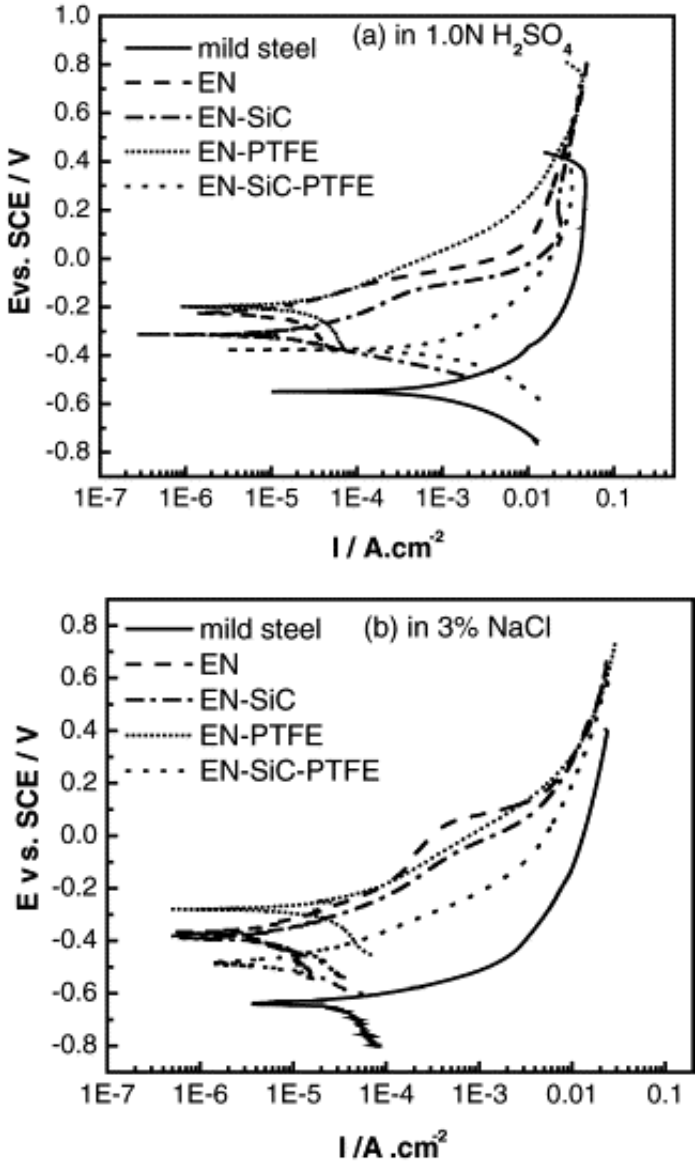

Figure 5.8: The polarization curves of electroless Ni-P and electroless composite coatings in (a) 1.0 N H_2SO_4 and (b) 3% NaCl electrolyte [178]

For the study, wear resistance and adhesion of the obtained electroless Ni-P coating on mild steel pin-on-disc tests were performed. The effect of sliding distance and time on the wear of Ni-P coating at 500 gm load is shown in Figure 5.9. Wear was determined by the weight loss method. Initially, the weight of coated mild steel was measured then

the pin-on-disc test was performed, after this again weight of the tested sample was measured. For the measurement of the weight loss, final weight subtracted from the initial weight. Weight loss measured for the Ni-P coated mild steel was 0.009 gm at minimum load (500 gm) and 500 m sliding distance.

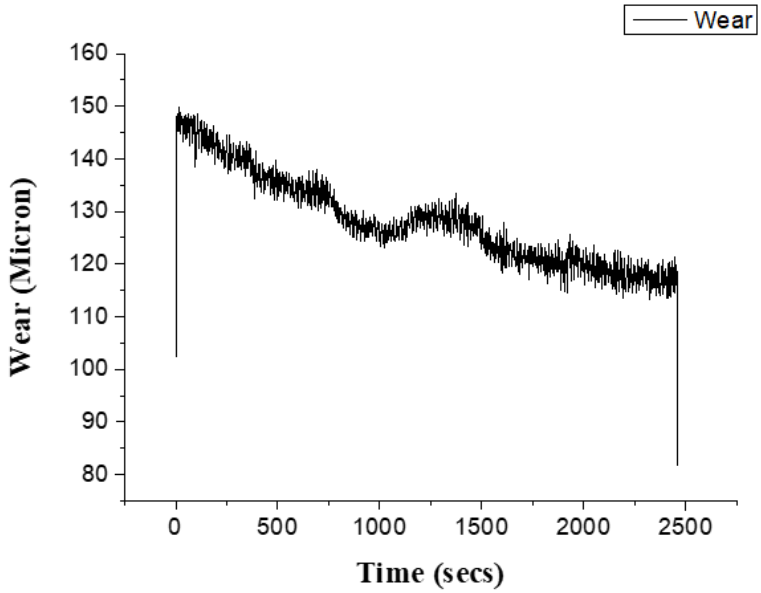

Figure 5.9: Wear versus time graph for Ni-P coated mild steel at load 500 gm

Formulas are given below for the determination of wear rate [206, 223];

$$\boldsymbol{Wear\ rate = volume\ loss\ /sliding\ distance} \quad \text{. ……..……(5.a)}$$

$$\boldsymbol{Volume\ loss = mass\ loss/density} \quad \text{……...……(5.b)}$$

From the formulas (5.a) and (5.b);

$$\boldsymbol{Wear\ rate = (mass\ loss/\ density)/\ sliding\ distance} \quad \text{……(5.c)}$$

Wear rate = 0.001125 / 500 mm^3/m

= 0.00225 mm^3/m

Wear rate of electroless Ni-P coating on mild steel during pin-on-disc wear test was 0.001125 mm^3/m.

The above observation studies have been taken into consideration for the study of Ni-P coating on mild steel. Since mild steel is a structurally soft material and uses in the

different structural application, so when it is coated with Ni-P coating, its properties enhanced. In this section, the obtained results have been discussed. The XRD analysis of Ni-P coating was showing amorphous nature of deposit due to high phosphorous content in it. EDS analysis of Ni-P coating revealed that coating best suited to the corrosive environment due to its amorphous structure and its nodular surface morphology. As surface roughness results obtained from the AFM analysis has shown that roughness of Ni-P coating on mild steel is in nanometer (59.6 nm) and high surface finish. Microhardness analysis confirms that the hardness and wear resistance of mild steel is increase after the Ni-P coating due to the amorphous nature and high surface finish of the coating. Hence, these properties make mild steel coated with Ni-P for structural application.

5.2. Electroless Ni-P-TiO_2 nanocomposite coatings and their characterization

In this section, nano TiO_2 particles (10-20 nm) were added in the electroless bath for deposition of Ni-P-TiO_2 nanocomposite coating on mild steel. Now-a-days TiO_2 has gained much interest in research communities due to its large variety of applications in engineering materials. Structure of nano TiO_2 particles is anisotropic. Due to the anisotropic structure of TiO_2, grain orientation induced by directional dynamic ripening and in texture thin film. Effect of concentration of nano TiO_2 in particles Ni-P-TiO_2 nanocomposite coating is studied in this section along with different $NiSO_4$ (source of nickel) and $Na.H_2PO_2$ (reducing agent) concentration.

Discussion about the characterization of Ni-P-TiO_2 nanocomposite coating on mild steel is further categorized in three sections on the basis of variation in concentration of the constituents of the electroless bath such as (a) nickel sulphate, (b) sodium hypophosphite and (c) TiO_2 (second phase particles) in the deposition bath. Effects of the above chemical's concentrations on the structural properties, surface texture, electrochemical properties, and mechanical properties (microhardness and wear) Ni-P-TiO_2 nanocomposite coating on mild steel are also discussed in this section.

Nickel sulphate used as the source of nickel cations in the chemical bath. During the plating process, chemical reduction of nickel-salt by the sodium hypophosphite took place. The reduction process of nickel in the Ni-P-TiO_2 nanocomposite deposition bath is always involved by the generation of hydrogen gas.

Anodic Reaction:

$$H_2PO_2^- + H_2O \rightarrow H_2PO_3^- + 2H^+ + 2e^- \quad \text{..... (i)}$$

Cathodic Reaction:

$$Ni^{+2} + 2e \rightarrow Ni^0 \quad \text{.....(ii)}$$

$$2H^+ + 2e \rightarrow H_2 \quad \text{......(iii)}$$

$$H_2PO_2^- + 2H^+ + e \rightarrow P + 2H_2O \quad \text{.....(iv)}$$

Overall reaction:

$$2NiSO_4 + 4Na.H_2PO_2 + H_2O \xrightarrow{cat} 2Ni^0 + P + 2HPO_3^{-2} + H_2PO_3^- + 3H^+ + 2Na_2SO_4 + \frac{3}{2}H_2 \quad \text{.....(v)}$$

In these reactions, the reactants Ni^{+2} and $H_2PO_2^-$; products H^+ and $H_2PO_3^-$ are mainly influence the deposition reaction. In this plating process, nickel deposition was decreased and phosphorus content was increased by increasing H^+. Almost three phosphite ions were formed for each nickel ion reduction. Nickel sulphate and sodium hypophosphite concentration affect the deposition of Ni-P-TiO_2 nanocomposite coating on mild steel. By the incorporation of TiO_2 nanoparticles in the deposition bath, obtained deposit become composite because of the absence of molecular bonding between the Ni-P matrix and the embedded TiO_2 nanoparticles. TiO_2 particles size and distribution, TiO_2 catalytic inertness, bath reactivity, charge on the particles and compatibility of TiO_2 with the Ni-P matrix play the important roles for the successful development of the Ni-P-TiO_2 nanocomposite coating [224]. This study is necessary to understand the effect on the electroless Ni-P-TiO_2 nanocomposite deposits and their properties due to the different concentration of sodium hypophosphite, nickel sulphate, and nano TiO_2 particles.

First of all, the thickness and weight of deposited Ni-P-TiO_2 nanocomposite coatings on mild steel measured by the use of digital micrometer (with the precision 0.001 mm) and specific weighing balance (with the precision of 0.1 mg) respectively. Five repeated readings have been used and taken average to measure the thickness of deposited nanocomposite coatings. Measurements of coating thickness and coating weight are given in Table 5.1.

Table 5.1: Thickness and weight of deposited Ni-P-TiO_2 nanocomposite coatings on mild steel

Experimen No.	TiO_2 content (g/l)	$NiSO_4$ (g/l)	$Na.H_2PO_2$ (g/l)	Coating Weight (mg)	Coating Thickness (both side) (Microns)
1	0.4	25	20	1.6	17
2	0.4	25	30	1.6	17
3	0.4	25	40	1.5	16
4	0.4	30	20	1.6	17
5	0.4	30	30	2.0	19
6	0.4	30	40	1.9	19
7	0.4	35	20	1.8	18
8	0.4	35	30	2.4	21
9	0.4	35	40	2.7	22
10	0.8	25	20	1.7	18
11	0.8	25	30	1.8	18
12	0.8	25	40	1.6	17
13	0.8	30	20	1.6	17
14	0.8	30	30	1.9	20
15	0.8	30	40	2.0	20
16	0.8	35	20	1.8	18
17	0.8	35	30	2.7	22
18	0.8	35	40	2.7	22
19	1.2	25	20	1.8	18
20	1.2	25	30	2.0	19
21	1.2	25	40	1.8	18
22	1.2	30	20	1.8	18
23	1.2	30	30	2.4	21
24	1.2	30	40	2.7	22

25	1.2	35	20	2.0	19
26	1.2	35	30	2.7	22
27	1.2	35	40	2.8	22
28	1.6	25	20	2.0	19
29	1.6	25	30	2.1	20
30	1.6	25	40	2.0	19
31	1.6	30	20	1.8	18
32	1.6	30	30	2.4	21
33	1.6	30	40	2.7	22
34	1.6	35	20	2.2	20
35	1.6	35	30	3.1	23
36	1.6	35	40	2.8	22
37	2	25	20	2.0	19
38	2	25	30	2.4	21
39	2	25	40	2.0	19
40	2	30	20	2.1	19
41	2	30	30	2.7	22
42	2	30	40	3.1	23
43	2	35	20	2.1	20
44	2	35	30	3.6	24
45	2	35	40	3.0	23

Electroless Ni-P-TiO_2 nanocomposite coatings with 16-24 µm thickness were successfully deposited on the mild steel substrate with different chemicals concentration. The thickness of obtained Ni-P-TiO_2 nanocomposite coatings is varying with the concentration of nickel sulphate, sodium hypophosphite, and TiO_2 concentration, as shown in Figures 5.10, 5.11 and 5.12. As Figures 5.10, 5.11 and 5.12, the thickness of Ni-P-TiO_2 nanocomposite deposits is increased when nano TiO_2 concentration increased in the deposition bath. Figure 5.10 also represents that the thickness of deposits is enhanced by the increase in the concentration of nickel sulphate.

Figure 5.11 shows that sodium hypophosphite concentration in the electroless bath also affects the thickness of Ni-P-TiO_2 deposits. Although increase in sodium hypophosphite concentration in electroless bath increase the rate of reduction, the extra amount of sodium hypophosphite should not be used as it may cause a reduction to take place in the bulk of solution and deposition at the surface of the mild steel is not as sufficient as required.

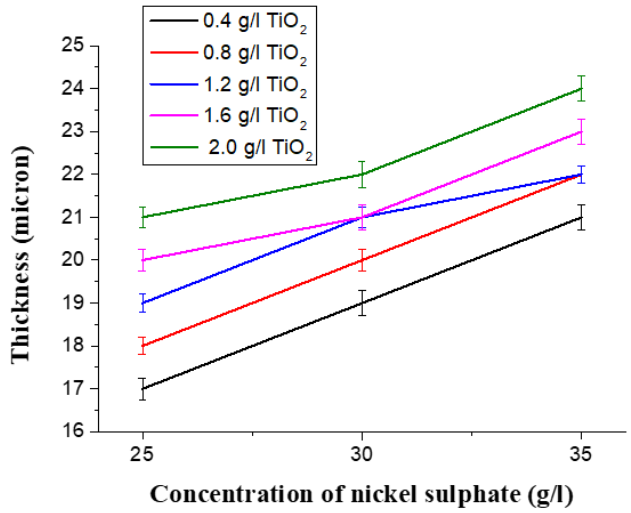

Figure 5.10: Coating thickness of obtained Ni-P-TiO_2 nanocomposite on mild steel with different nickel sulphate concentration along with the TiO_2 concentration in the deposition bath

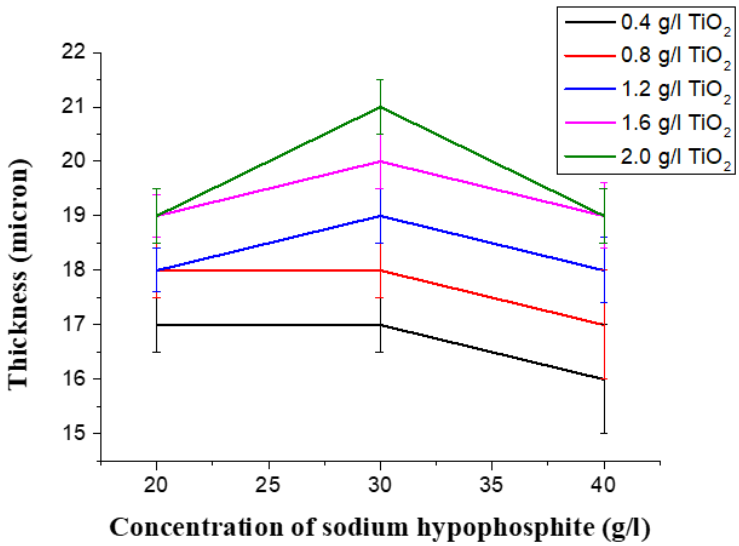

Figure 5.11: Coating thickness of obtained Ni-P-TiO_2 nanocomposite on mild steel with different sodium hypophosphite concentration along with TiO_2 concentration in the deposition bath

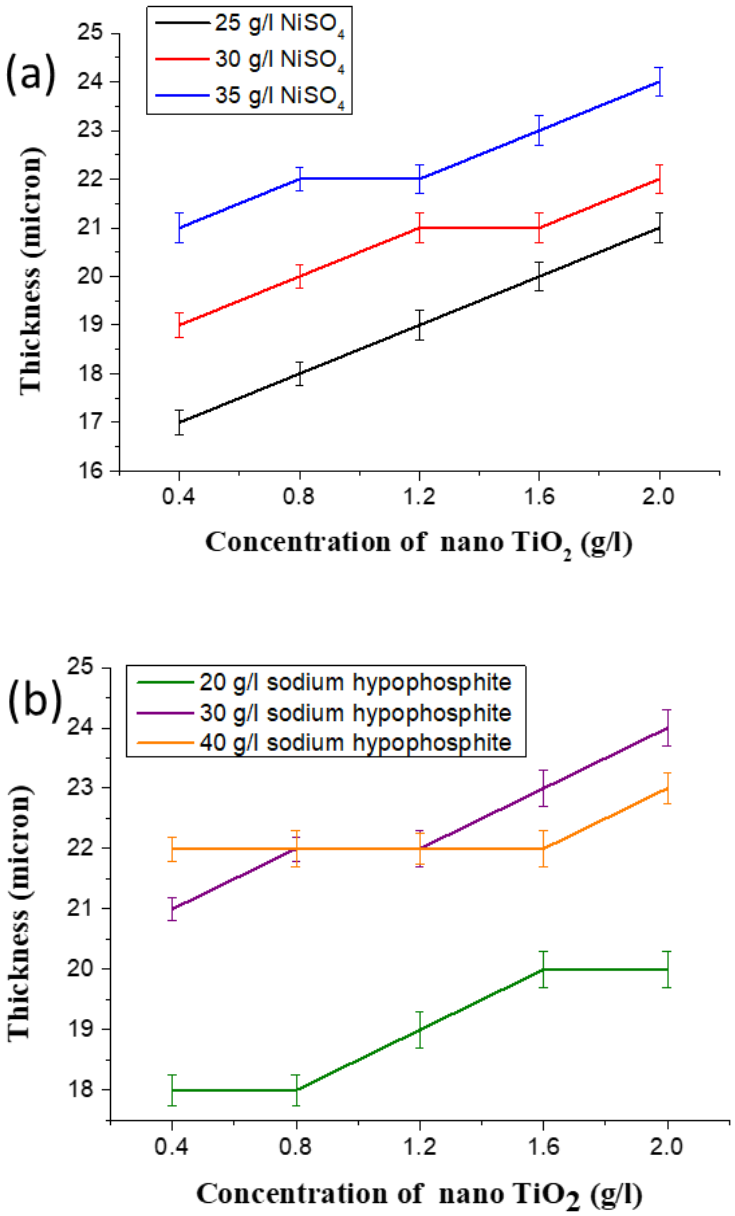

Figure 5.12: Coating thickness of obtained Ni-P-TiO_2 nanocomposite on mild steel with various concentration of nano TiO_2 along with (a) nickel sulphate and (b) sodium hypophosphite concentration in the deposition bath

For characterization of these coating by phase analysis, morphological analysis, surface texture analysis, microhardness, corrosion study and wear study are discussed below on the basis of variation in concentration of nickel sulphate, sodium hypophosphite, and TiO_2 (second phase particles) in the chemical bath.

5.2.1. Variation in concentration of $NiSO_4$

As a source of nickel ions, nickel sulphate was used in the electroless Ni-P-TiO_2 nanocomposite coating bath. Nickel sulphate provided nickel for the deposition of Ni-P-TiO_2 coating on mild steel. Here, different characterization studies of Ni-P-TiO_2 nanocomposite coatings on mild steel deposited with different concentration of $NiSO_4$ in the chemical deposition bath are discussed. In this section, observations obtained and their discussion related to the changes in the morphology, hardness, corrosion resistance and wear resistance due to the variation of concentration of $NiSO_4$ in the chemical deposition bath.

In this section, characterization of three kinds of Ni-P-TiO_2 nanocomposite coatings on mild steel deposited with 25 g/l, 30 g/l and 35 g/l nickel sulphate (variation in concentration of nickel sulphate in the deposition bath), 35 ml/l lactic acid, 30 g/l sodium hypophosphite and 2 g/l TiO_2 at optimized parameters pH 4 and 80°C are discussed.

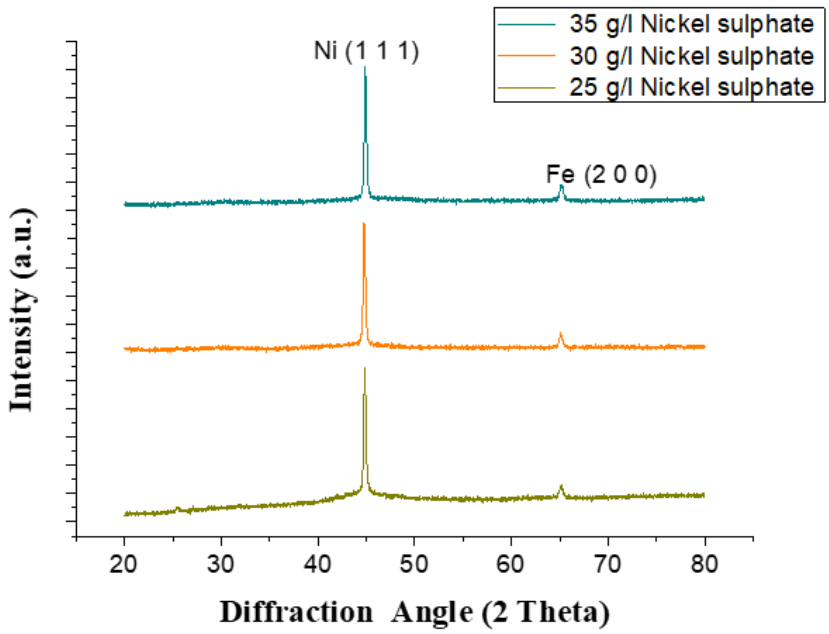

Figure 5.13: Comparison of XRD patterns of Ni-P-TiO_2 coated mild steel samples deposited with 25 g/l, 30 g/l, and 35 g/l $NiSO_4$

X-ray diffraction patterns of the deposited Ni-P-TiO_2 nanocomposite coatings on mild steel with 25 g/l, 30 g/l, and 35 g/l nickel sulphate concentration are shown in Figure 5.13. Ni-P-TiO_2 nanocomposite coating with 25 g/l $NiSO_4$ (in deposition bath) exhibited

a peak corresponding to Ni (1 1 1) phase at 44.90° and the sharp small peak at 65.10° results from the iron substrate. XRD patterns of these three coatings (deposited with 25 g/l, 30 g/l, and 35 g/l $NiSO_4$ concentration in deposition bath) are similar. No phase change is carried out there. So, it can say that change in structure and properties of Ni-P-TiO_2 nanocomposite coating with variation in concentration of nickel sulphate in the deposition bath is not observed by X-ray diffraction analysis.

EDS results with FESEM micrographs of the Ni-P-TiO_2 nanocomposite coatings on mild steel substrates with 25 g/l, 30 g/l and 35 g/l nickel sulphate are shown in Figures 5.14 (a), 5.14 (b) and 5.14 (c). FESEM micrographs of nanocomposite coatings show the spherical Ni-P globulus with TiO_2 particles. Ni-P-TiO_2 nanocomposite coating completely covers the steel surface. There is no pore present within the deposit, so the deposited coating is not porous.

In Figure 5.14 (a), with the help of EDS analysis of Ni-P-TiO_2 nanocomposite coating (deposited with 25 g/l $NiSO_4$ in deposition bath), 74.9 wt.% of Nickel, 15.8 wt.% of Phosphorous, 2.9 wt.% of Titanium and 6.4 wt.% Oxygen is observed. In Figure 5.14 (b), EDS results of Ni-P-TiO_2 nanocomposite coatings (deposited with 30 g/l $NiSO_4$ in the deposition bath), 76.7 wt.% of Nickel, 14.5 wt.% of Phosphorous, 2.8 wt.% of Titanium and 6.0 wt.% Oxygen are shown. In Figure 5.14 (c), EDS results of Ni-P-TiO_2 nanocomposite coatings with 35 g/l $NiSO_4$ are shown as 80.3 wt.% of Nickel, 13.4 wt.% of Phosphorous, 3.5 wt.% of Titanium and 2.8 wt.% Oxygen.

Table 5.2: Results obtain from the EDS analysis of Ni-P-TiO_2 nanocomposite coating on Mild steel deposited with (a) 25 g/l, (b) 30 g/l and (c) 35 g/l $NiSO_4$ concentration in the deposition bath

Concentration of $NiSO_4$ in the deposition bath (g/l)	**wt. % of elements in deposited coatings**			
	Ni	P	Ti	O_2
25	74.9	15.8	2.9	6.4
30	76.7	14.5	2.8	6.0
35	80.3	13.4	3.5	2.8

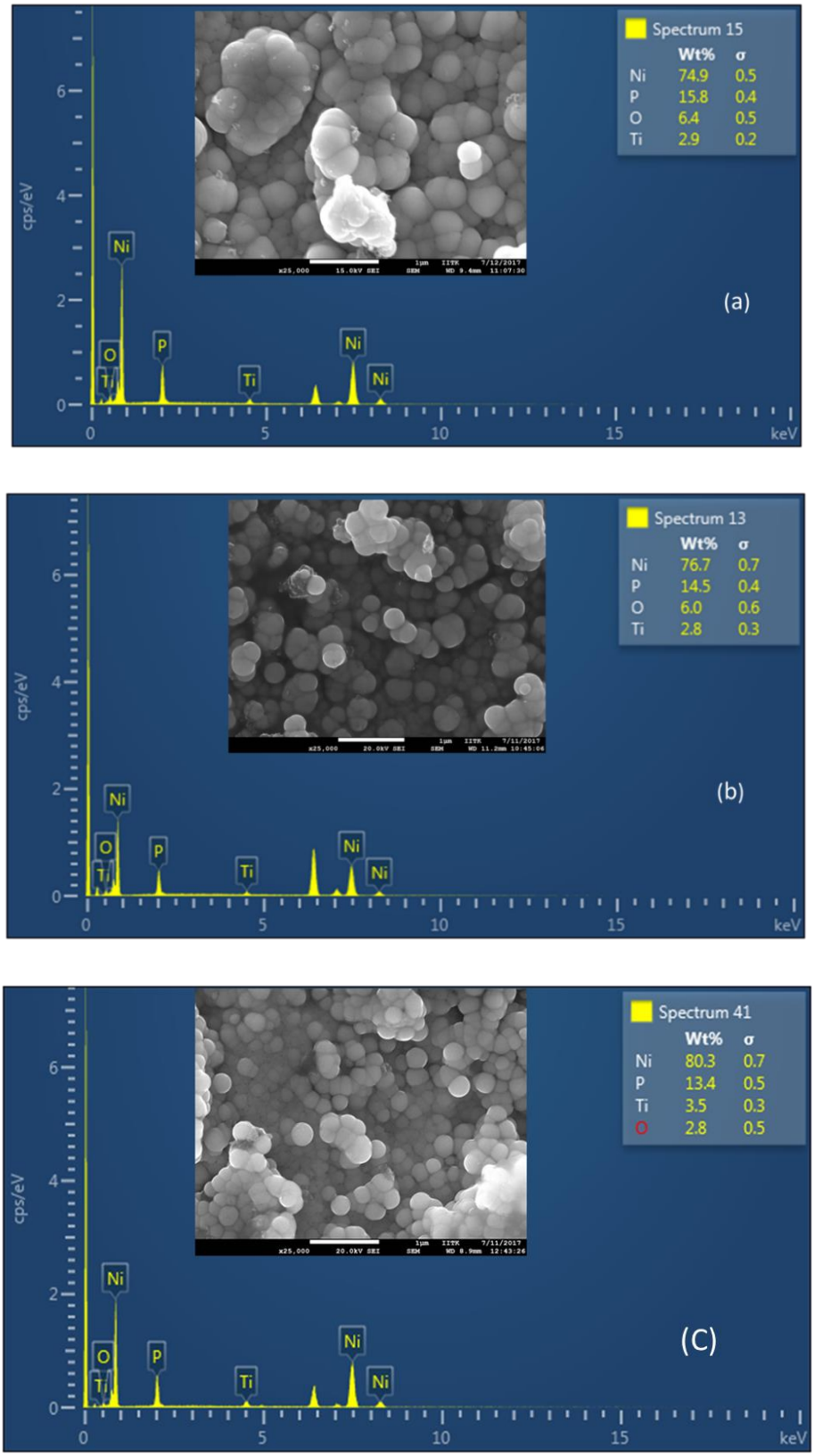

Figure 5.14: FESEM image with EDS Pattern of electroless Ni-P-TiO_2 nanocomposite coating on mild steel substrate with (a) 25 g/l, (b) 30 g/l, and (c) 35 g/l $NiSO_4$ concentration

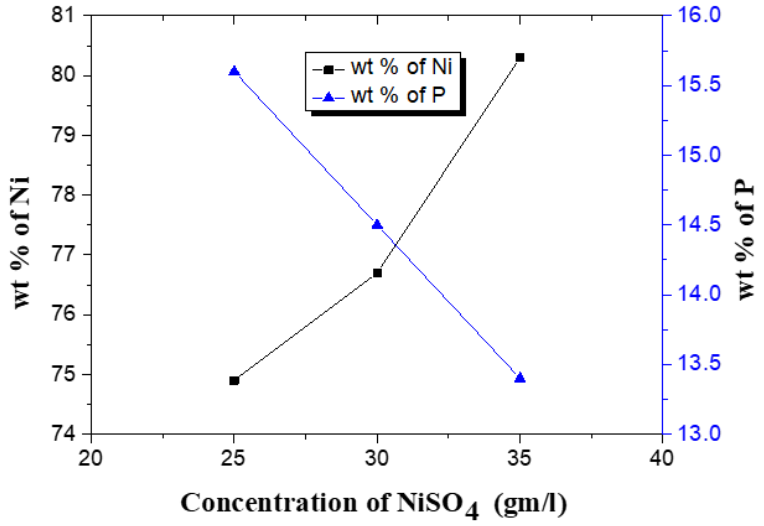

Figure 5.15: Concentration (wt.%) of Ni and P in the deposited Ni-P-TiO_2 nanocomposite coatings on mild steel with a variation of concentration of $NiSO_4$ in the deposition bath

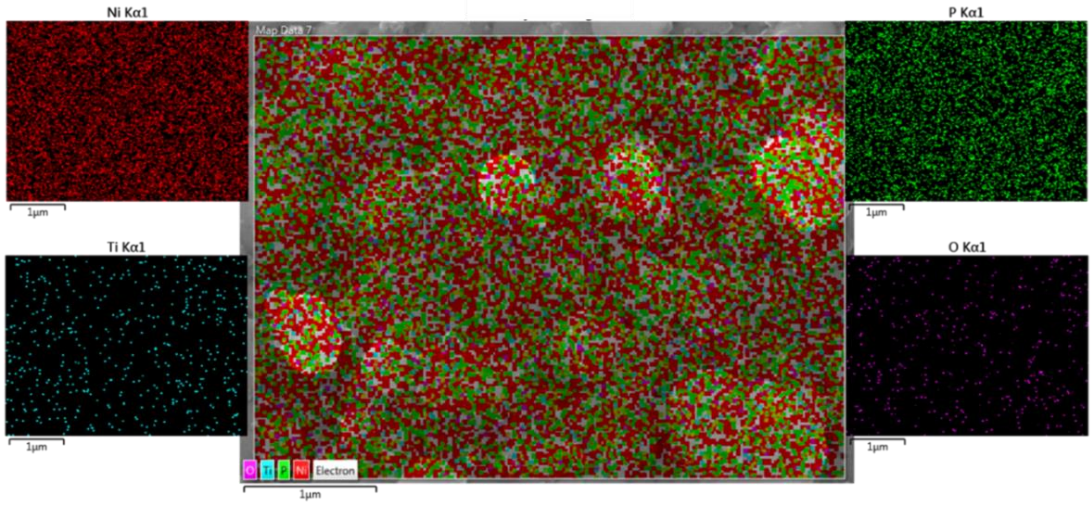

Figure 5.16: FESEM image with area mapping of constituents present in electroless Ni-P-TiO_2 nanocomposite coating on the mild steel substrate

In Table 5.2, it can be observed that Ni content increases from 74.9 to 80.3 wt.% and P content decreases from 15.8 to 13.8 wt.% in these coatings. Figure 5.15 shows the change in wt.% of Ni and P in the obtained Ni-P-TiO_2 nanocomposite coatings on mild steel with variation in concentration of $NiSO_4$ (25 g/l, 30 g/l and 35 g/l). It means when the concentration of $NiSO_4$ is increased in deposition bath, Ni content is increased and P content is decreased in the obtained coatings. FESEM micrograph with elemental

mapping of Ni-P-TiO_2 nanocomposite coating on mild steel substrate is shown in Figure 5.16. and observed the homogeneous distribution of Ni, P, Ti and O in the deposit.

Microhardness results of the Ni-P-TiO_2 nanocomposite coatings on mild steel with variation in concentration of $NiSO_4$ (25 g/l, 30 g/l and 35 g/l) are given in Figure 5.17. Microhardness of the deposited Ni-P-TiO_2 nanocomposite coatings on mild steel with 25 g/l, 30 g/l and 35 g/l $NiSO_4$ are ~ 450 VHN_{10}, ~ 495 VHN_{10} and ~ 517 VHN_{10} respectively.

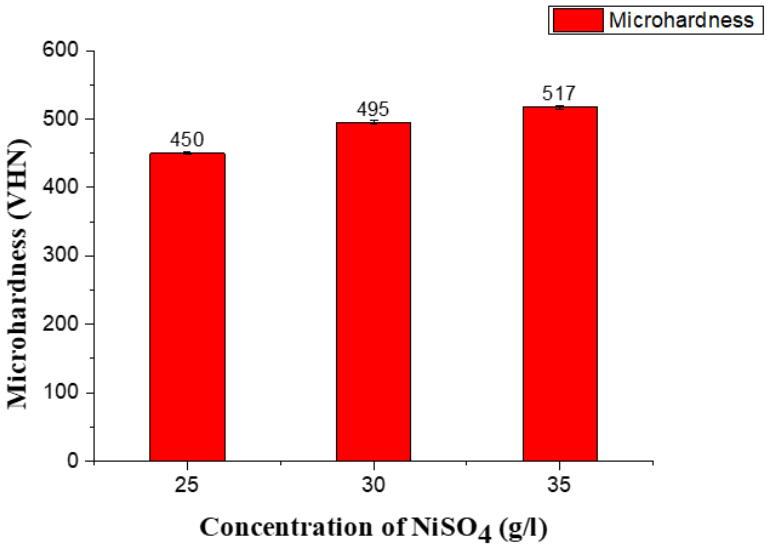

Figure 5.17: Comparison of Vickers microhardness of electroless Ni-P-TiO_2 nanocomposite coatings with different $NiSO_4$ bath concentrations

As Figure 5.18 shows, microhardness value of these coatings is increased when nickel sulphate concentration increased. Microhardness of Ni-P-TiO_2 nanocomposite coatings depends on the content of P in the deposit. As EDS results shown in the previous study, P content in deposits is decreased when nickel-sulphate concentration increased in the deposition bath. As described in the literature, low phosphorous electroless nickel coatings are microcrystalline, medium phosphorous nickel coatings are semi-crystalline and high phosphorus electroless nickel coatings are amorphous in nature [32, 34]. When phosphorus content in the deposits decreases, the crystallinity of deposit increases. It means low phosphorous coatings have a large number of grain and grain boundaries as compared to high phosphorus coatings. Grain boundaries hinder the cracks propagation in deposits. So, decreased P content in the deposits gives the improved microhardness of the coatings.

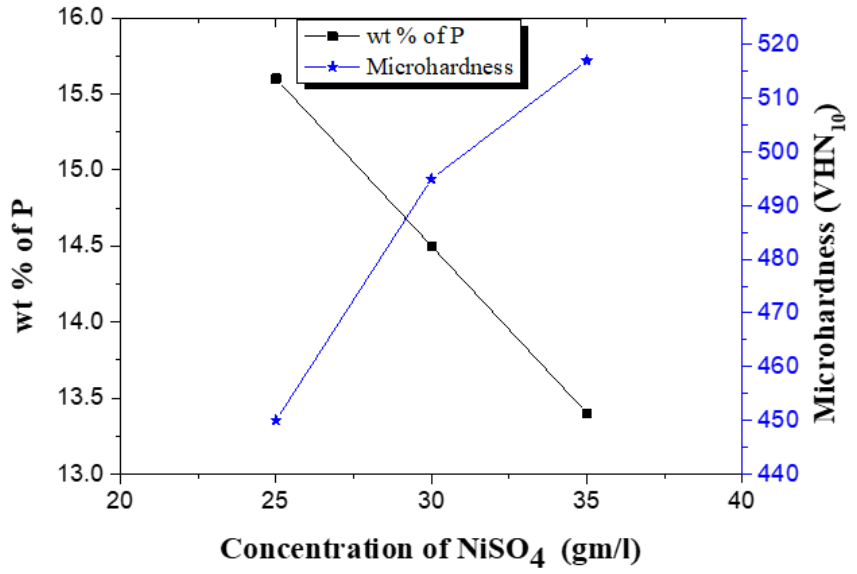

Figure 5.18: Microhardness of the Ni-P-TiO_2 nanocomposite coatings on mild steel deposited with variation of wt.% of P and concentration of $NiSO_4$

The corrosion results obtained from electrochemical studies of Ni-P-TiO_2 composite coatings (25 g/l, 30 g/l, and 35 g/l nickel sulphate concentration) in 3.5% sodium chloride aqueous solution are shown in Figures 5.19, 5.20, and 5.21.

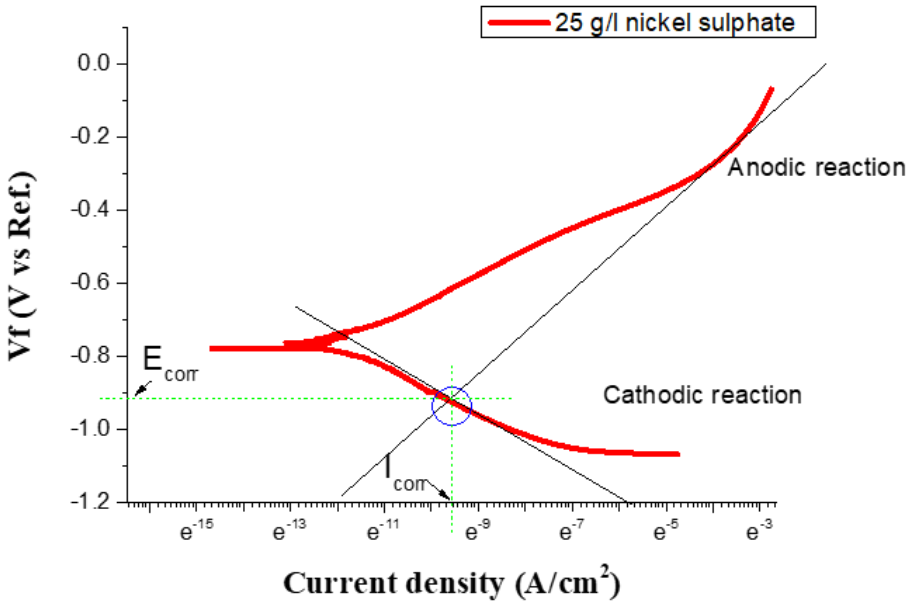

Figure 5.19: Tafel curve of Ni-P-TiO_2 composite coating (with 25 g/l nickel sulphate) in 3.5% NaCl solution

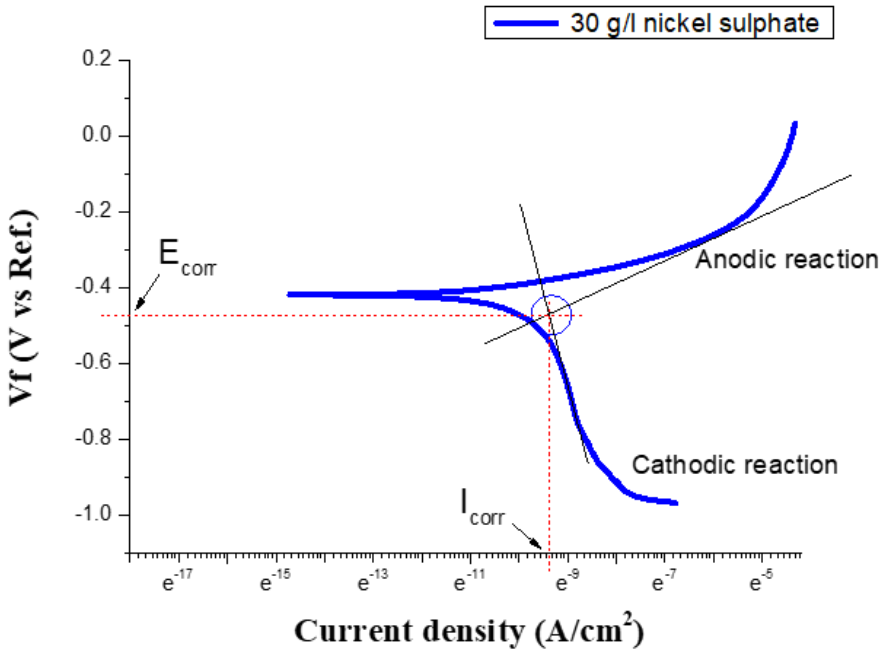

Figure 5.20: Tafel curve of Ni-P-TiO_2 composite coating (with 30 g/l nickel sulphate) in 3.5% NaCl solution

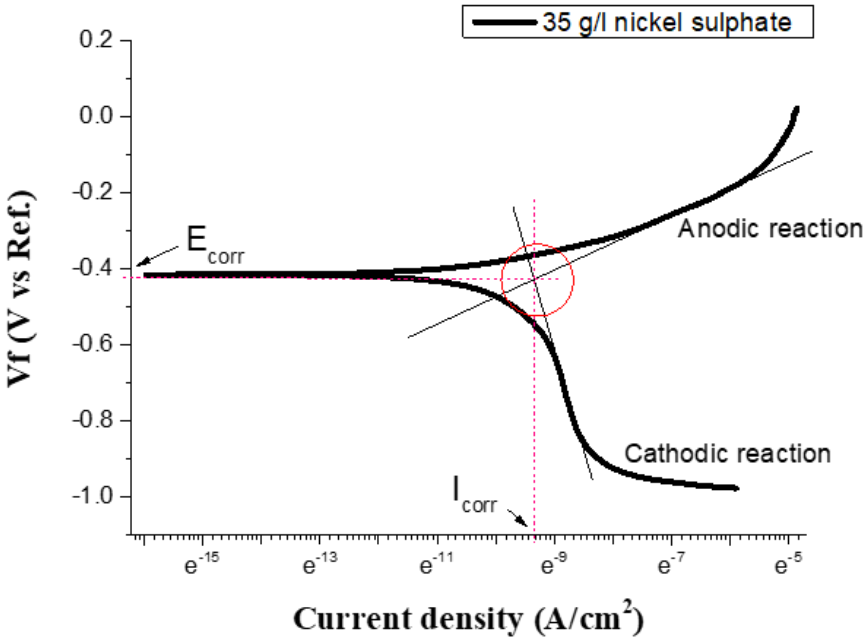

Figure 5.21: Tafel curve of Ni-P-TiO_2 nanocomposite coating (with 35 g/l nickel sulphate) in 3.5% NaCl solution

Figure 5.22 shows the comparison of Tafel plots of the three kinds of Ni-P-TiO_2 nanocomposite coatings (deposited with 25 g/l, 30 g/l, and 35 g/l nickel sulphate

concentration). Electroless Ni-P-TiO_2 nanocomposite coating with 35 g/l nickel sulphate has high corrosion current density (62.78 µA) as compare to Ni-P-TiO_2 nanocomposite coating with 25 g/l and 30 g/l nickel sulphate

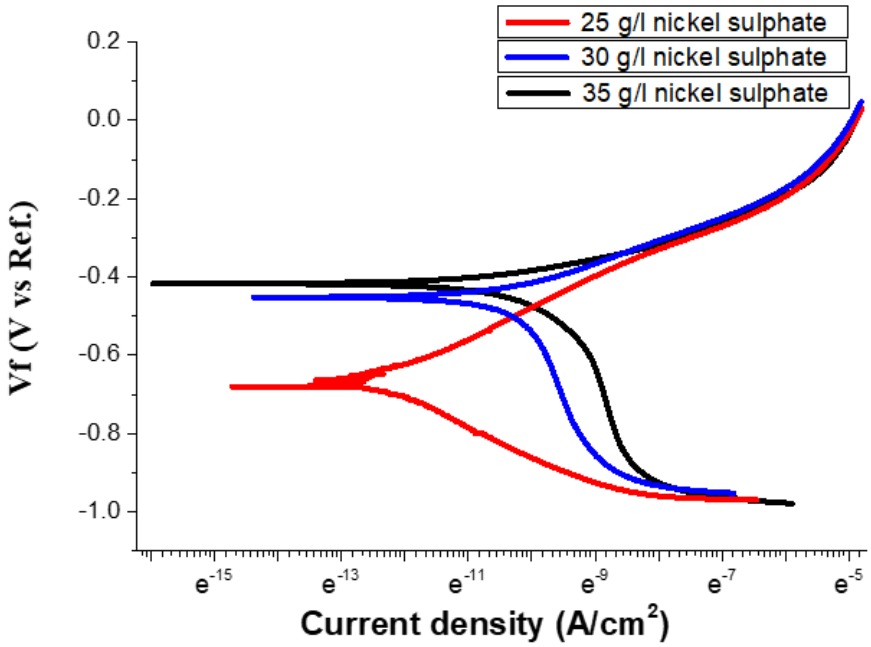

Figure 5.22: Corrosion characteristics of as plated Ni-P-TiO_2 nanocomposite coatings with various $NiSO_4$ bath concentrations

Tafel plots obtained from the electrochemical potentiodynamic polarization of these coatings were used to measure corrosion rate with the help of Tafel slop at anodic polarization β_a, Tafel slop at cathodic polarization β_c, corrosion potential $E_{corr,}$ and corrosion current density I_{corr}. The Tafel plot is based on a mixed potential theory. Table 5.3 has shown the electrochemical results of the coatings derived from the Tafel plots of Ni-P-TiO_2 nanocomposite coatings with the variation of nickel sulphate concentration (25 g/l, 30 g/l, and 35 g/l). As shown in Table 5.3, Corrosion current density I_{corr} of these coatings are decreasing when nickel sulphate concentration increased. Corrosion current density I_{corr} is inversely proportional to polarization resistance (R_p) [215]. So, Ni-P-TiO_2 nanocomposite coating with low nickel-sulphate concentration has improved corrosion resistance. The corrosion rate of nanocomposite coatings slightly increased with increase in the concentration of nickel sulphate in the coating bath.

Table 5.3: Electrochemical results of Ni-P-TiO_2 nanocomposite coatings (25 g/l, 30 g/l, and 35 g/l nickel sulphate concentration) derived from Tafel plots

Sr. No.	Sample with various $NiSO_4$ concentration	E_{corr} (mV)	I_{corr} (µA)	Corrosion Rate (mpy)
1	Ni-P-TiO_2 nanocomposite coating with 25 g/l nickel sulphate	-961	55.23	5.205
2	Ni-P-TiO_2 nanocomposite coating with 30 g/l nickel sulphate	-425	57.80	5.447
3	Ni-P-TiO_2 nanocomposite coating with 35 g/l nickel sulphate	-489	62.78	5.917

As above studies show, the corrosion resistance of the obtained Ni-P-TiO_2 nanocomposite coatings on mild steel is decreased when the concentration of $NiSO_4$ in the deposition bath is increased while microhardness of the Ni-P-TiO_2 nanocomposite coatings on mild steel is improved by increased concentration of $NiSO_4$ in the deposition bath during the deposition of the Ni-P-TiO_2 nanocomposite coatings. Reason for the improvement on microhardness and deterioration on the corrosion resistance of electroless Ni-P-TiO_2 nanocomposite coatings with increasing the concentration of $NiSO_4$ in the deposition bath is low phosphorus content in the obtained deposits. As EDS results are showing, phosphorus content decreased in the obtained coatings with increased concentration $NiSO_4$ in the deposition bath. Ni-P-TiO_2 nanocomposite coating with low phosphorus content have more grain and grain boundaries. These grain boundaries hinder the cracks propagation but provide the sites for corrosion initiation. For studying the effect of concentration of $NiSO_4$ during the deposition of Ni-P-TiO_2 nanocomposite coatings on mild steel on wear resistance of coatings, tribological tests were performed.

Pin-on-disc tests were performed for determining the loss of Ni-P-TiO_2 nanocomposite coatings due to the wear. During the wear tests, room temperature is ~30°C and relative humidity is 85% approximately. Descriptive curves amid for wear with time for electroless Ni-P-TiO_2 nanocomposite coatings (deposited with 25 g/l, 30 g/l, and 35 g/l nickel sulphate concentration) at sliding velocity of 0.2 m/s with 5 N load are shown in

Figures 5.23, 5.24 and 5.25. Wear during the pin-on-disc tests of coatings are calculated by weight loss methods. Wear rate of electroless Ni-P-TiO_2 nanocomposite coatings (deposited with 25 g/l, 30 g/l, and 35 g/l nickel sulphate concentration) is calculated by the formula (5.c) which is mentioned in section 5.1.

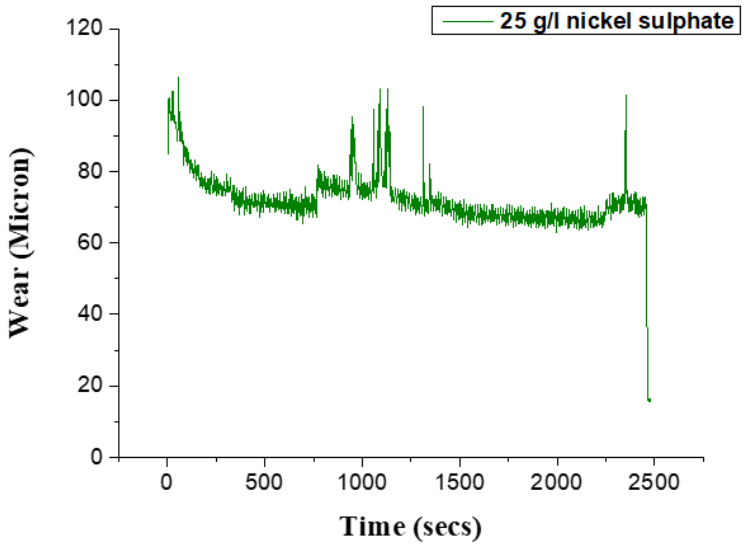

Figure 5.23: Wear (micron) with time at room temperature and sliding velocity 0.2 m/s at 5 N for Ni-P-TiO_2 nanocomposite coating obtained with 25 g/l $NiSO_4$ in the bath

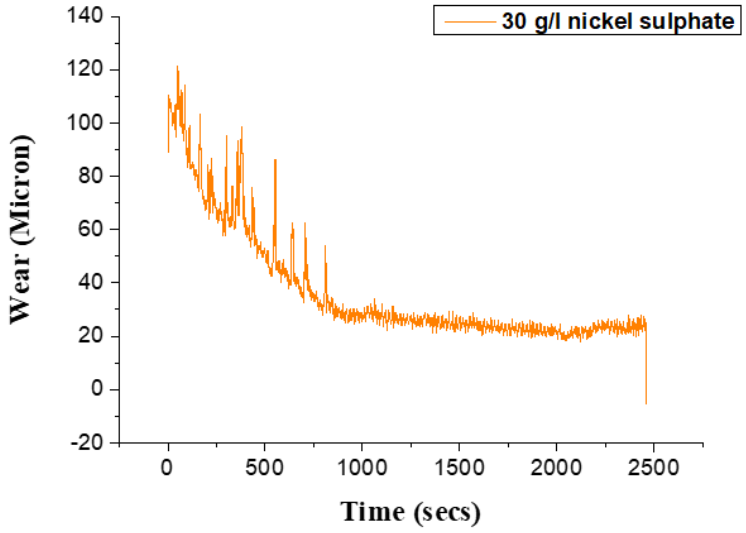

Figure 5.24: Wear (micron) with time at room temperature and sliding velocity 0.2 m/s at 5 N for Ni-P-TiO_2 nanocomposite coating obtained with 30 g/l $NiSO_4$ in the bath

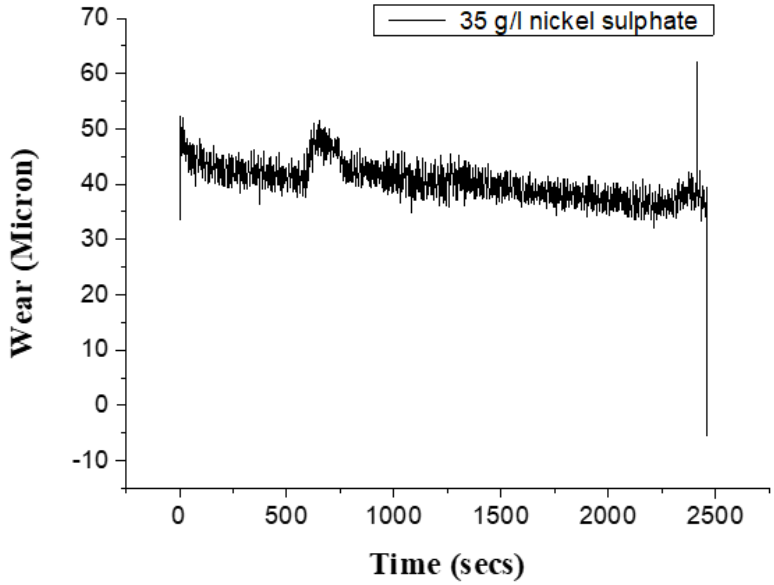

Figure 5.25: Wear (micron) with time at room temperature and sliding velocity 0.2 m/s at 5 N for Ni-P-TiO_2 nanocomposite coating obtained with 35 g/l $NiSO_4$ in the bath

Table 5.4: Comparison of wear of Ni-P-TiO_2 nanocomposite coatings (25 g/l, 30 g/l, and 35 g/l nickel sulphate concentration) determine from the pin-on-disc tests

S. No.	Sample	Thickness of coating (µm)	Wear loss (gm)	Wear rate (mm^3/m)
1	Ni-P-TiO_2 nanocomposite coating with 25 g/l nickel sulphate	21	0.010	0.002857
2	Ni-P-TiO_2 nanocomposite coating with 30 g/l nickel sulphate	22	0.007	0.002000
3	Ni-P-TiO_2 nanocomposite coating with 35 g/l nickel sulphate	24	0.005	0.001428

As results are shown in Table 5.4, wear loss of Ni-P-TiO_2 nanocomposite coatings with 25 g/l, 30 g/l and 35 g/l nickel sulphate are 0.010 gm, 0.007 gm and 0.005 gm respectively. As analysis shown in Figure 5.26, wear loss is decreased with increased concentration of $NiSO_4$ in the bath. because of decreased wt.% of P in the obtained coatings and improved microhardness. Wear resistance property of the material is inversely propositional to the wear loss. Wear resistance of nanocomposite coatings are

increased when the concentration of $NiSO_4$ is increased because of decreased wt.% of P in the obtained coatings and improved microhardness.

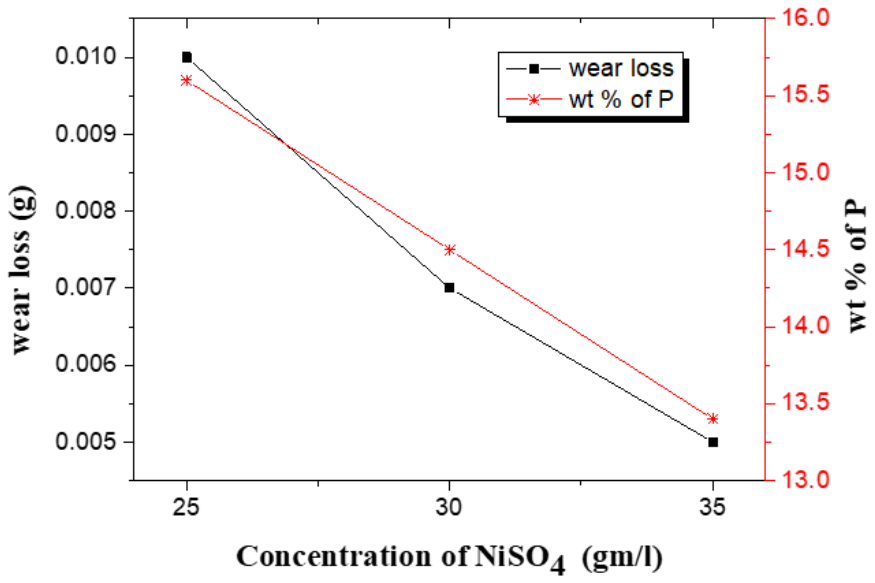

Figure 5.26: Wear loss of the Ni-P-TiO_2 nanocomposite coatings on mild steel deposited with variation of wt.% of P and concentration of $NiSO_4$ in the deposition bath

5.2.2. Variation in concentration of sodium hypophosphite

As a reducing agent, sodium hypophosphite was used in the electroless Ni-P-TiO_2 nanocomposite bath. Sodium hypophosphite reduces the nickel ions from the nickel sulphate and provides the phosphorous for the deposition of Ni-P-TiO_2 nanocomposite coating on mild steel. Here, different characterization studies of Ni-P-TiO_2 nanocomposite coatings on mild steel deposited with different concentration of sodium hypophosphite in the chemical deposition bath are discussed. This section is content the observed observations and their discussion related to the changes in the morphology, hardness, corrosion resistance and wear resistance due to the variation of concentration of sodium hypophosphite in the chemical deposition bath.

In this section, characterization of three kinds of Ni-P-TiO_2 nanocomposite coatings on mild steel deposited with 35 g/l nickel sulphate, (a) 20 g/l, (b) 30 g/l, and (c) 40 g/l sodium hypophosphite (variation in sodium hypophosphite concentration), 35 ml/l lactic acid, and 2 g/l TiO_2 at optimize parameters pH 4 and 80°C are discussed.

X-ray diffraction patterns of the Ni-P-TiO_2 nanocomposite coating with 20 g/l, 30 g/l, and 40 g/l sodium hypophosphite are shown in Figure 5.27. Ni-P-TiO_2 nanocomposite coatings exhibited a peak corresponding to Ni (1 1 1) phase at 44.90° and the sharp small peak at 65.10° results from the mild steel substrate. As shown in Figure 5.27, the intensity of nickel peak in deposits is reduced when the concentration of sodium hypophosphite is increased in deposition bath and height of Fe peak is also reduced with increased concentration of sodium hypophosphite. It means Ni-P-TiO_2 nanocomposite coating on mild steel deposited with a high concentration of sodium hypophosphite has reduced crystallinity.

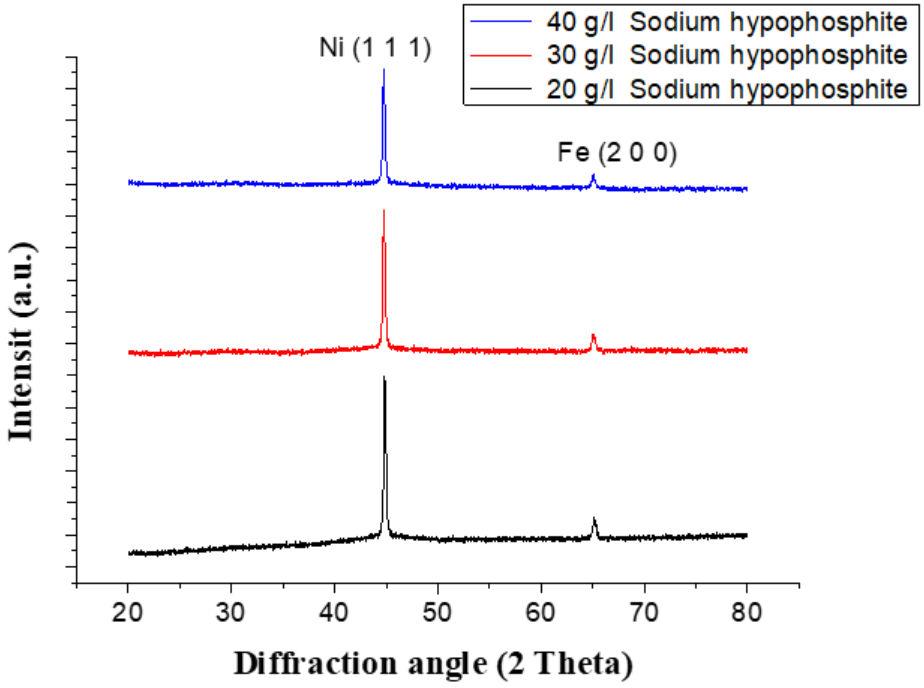

Figure 5.27: Comparison of XRD patterns of Ni-P-TiO_2 coated samples with various concentrations of sodium hypophosphite (20 g/l, 30 g/l, and 40 g/l)

EDS results with FESEM micrographs of the Ni-P-TiO_2 nanocomposite coatings on mild steel substrates with 20 g/l, 30 g/l, and 40 g/l sodium hypophosphite are shown in Figures 5.28 (a), (b) and (c). FESEM micrographs of nanocomposite coatings show the spherical Ni-P globulus with embedded TiO_2 particles. Ni-P-TiO_2 nanocomposite coating completely covers the steel surface. There is no pore present within the deposit, so the deposited coating is dense.

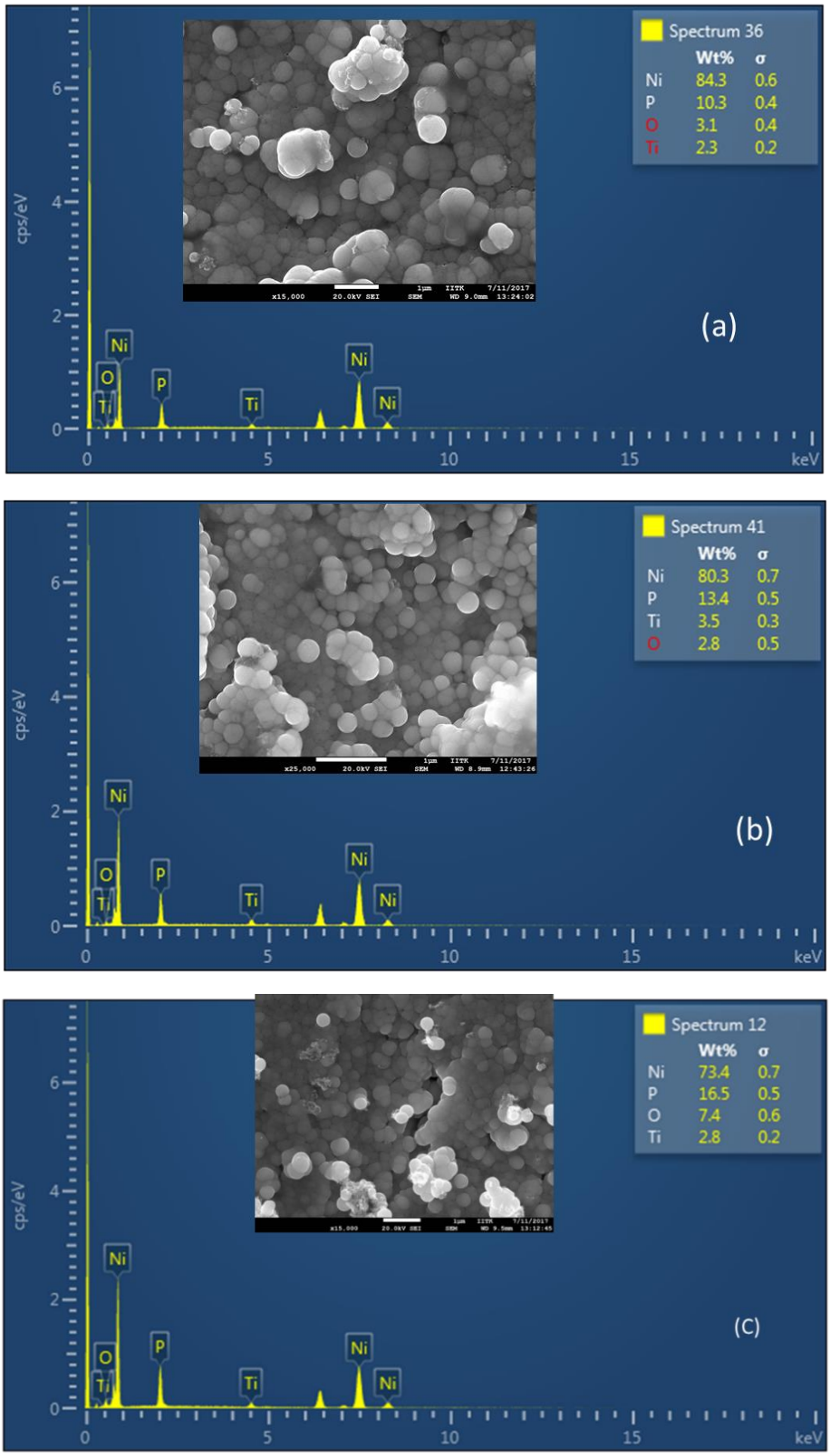

Figure 5.28: FESEM image with EDS Pattern of electroless Ni-P-TiO_2 nanocomposite coating on mild steel substrate with (a) 20 g/l, (b) 30 g/l and (c) 40 g/l sodium hypophosphite concentration

In Figure 5.28 (a), with the help of EDS of Ni-P-TiO_2 nanocomposite coatings with 20 g/l sodium hypophosphite, 84.3 wt.% of Nickel, 10.3 wt.% of Phosphorous, 2.3 wt.% of Titanium and 3.1 wt.% Oxygen is observed. In the Figure 5.28 (b), EDS results of Ni-P-TiO_2 nanocomposite coatings with 30 g/l sodium hypophosphite, 80.3 wt.% of Nickel, 13.4 wt.% of Phosphorous, 3.5 wt.% of Titanium and 2.8 wt.% Oxygen are shown. In Figure 5.28 (c), EDS results of Ni-P-TiO_2 nanocomposite coatings with 40 g/l sodium hypophosphite are shown as 73.4 wt.% of Nickel, 16.5 wt.% of Phosphorous, 2.8 wt.% of Titanium and 7.4 wt.% Oxygen.

Table 5.5: Results obtained from the EDS analysis of Ni-P-TiO_2 nanocomposite coating on Mild steel deposited with (a) 20 g/l, (b) 30 g/l and (c) 40 g/l sodium hypophosphite concentration in the deposition bath

Concentration of sodium hypophosphite in the deposition bath (g/l)	wt.% of elements in deposited coatings			
	Ni	P	Ti	O_2
20	84.3	10.3	2.3	3.1
30	80.3	13.4	3.5	2.8
40	73.4	16.5	2.8	7.4

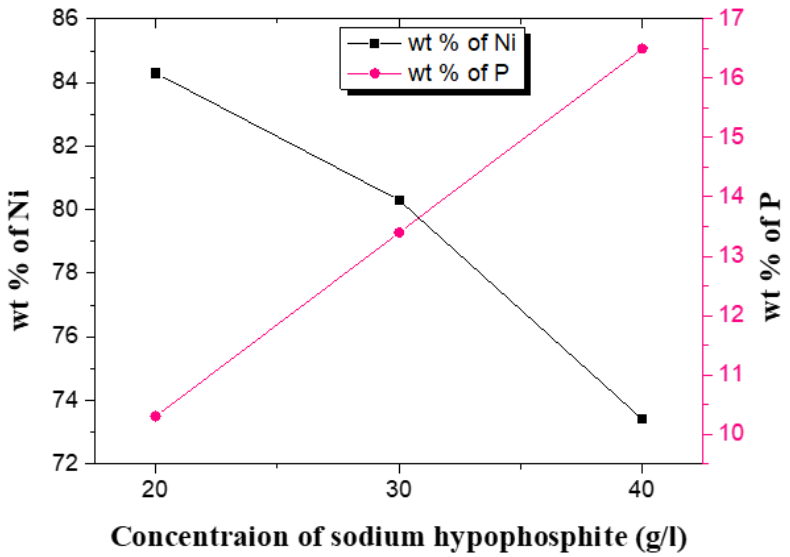

Figure 5.29: Concentration (wt.%) of Ni and P in the deposited Ni-P-TiO_2 nanocomposite coatings on mild steel with a variation of concentration of sodium hypophosphite in the deposition bath

In Table 5.5, it can be observed that Ni content decreased from 84.3 to 73.4 wt.% and P content increased from 10.3 to 16.5 wt.% in these coatings. Figure 5.29 shows the change in wt.% of nickel and phosphorous in the obtained Ni-P-TiO_2 nanocomposite coatings on mild steel with variation in concentration of sodium hypophosphite (20 g/l, 30 g/l and 35 g/l). It means when the concentration of sodium hypophosphite is increased in deposition bath, Ni content is decreased and P content is increased.

FESEM micrograph with area mapping of Ni-P-TiO_2 nanocomposite coating on mild steel substrate is presented in Figure 5.30. The homogeneous distribution of Ni, P, Ti and O in the deposit are shown in this Figure.

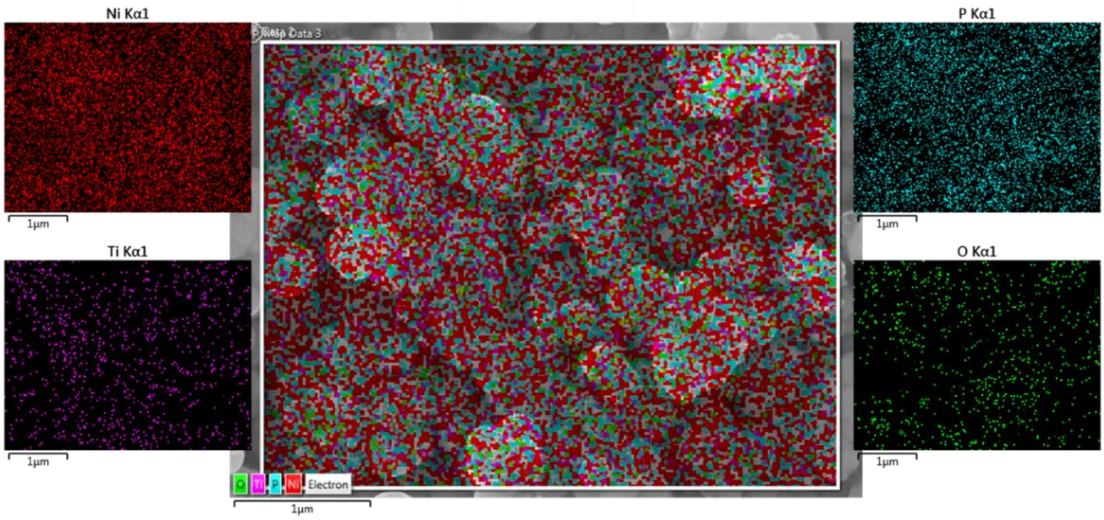

Figure 5.30: FESEM image with area mapping of constituents present in electroless Ni-P-TiO_2 nanocomposite coating on the mild steel substrate

Microhardness results of Ni-P-TiO_2 nanocomposite coatings on mild steel with variation in concentration of sodium hypophosphite (20 g/l, 30 g/l, and 40 g/l) are given in Figure 5.31. Microhardness of the deposited Ni-P-TiO_2 nanocomposite coatings on mild steel with 20 g/l, 30 g/l, and 40 g/l sodium hypophosphite are ~520 VHN_{10}, ~517 VHN_{10}, and ~488 VHN_{10} respectively.

As Figure 5.32 shows, microhardness value of these coatings is decreased when concentration increased. Microhardness of Ni-P-TiO_2 nanocomposite coatings depends on the content of P in the deposit. As EDS results shown in this section, P content in deposits is increased when sodium hypophosphite concentration increased in the deposition bath. Deposit with high P content gives the poor microhardness of the

coatings. Ni-P alloy with high P content acts as a brittle material and offers cracks initiation and their propagation in the surface of the material during the indentation [221].

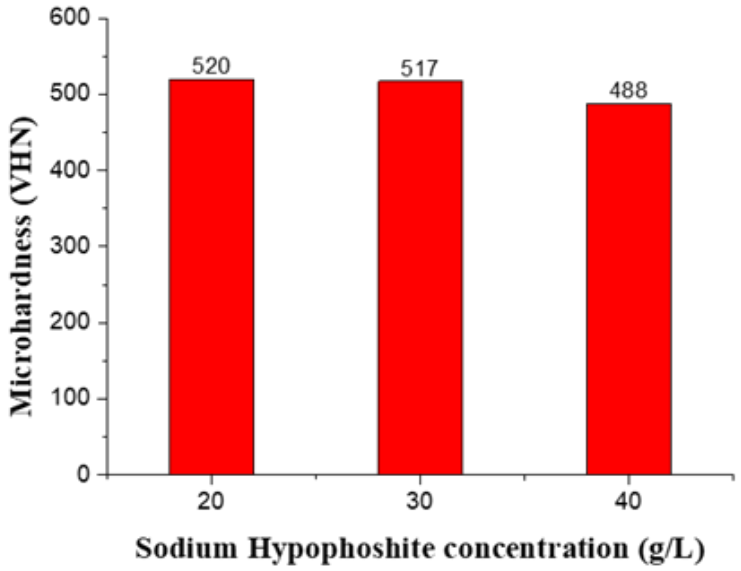

Figure 5.31: Comparison of Vickers microhardness of electroless Ni-P-TiO_2 nanocomposite coatings with various sodium hypophosphite bath concentrations

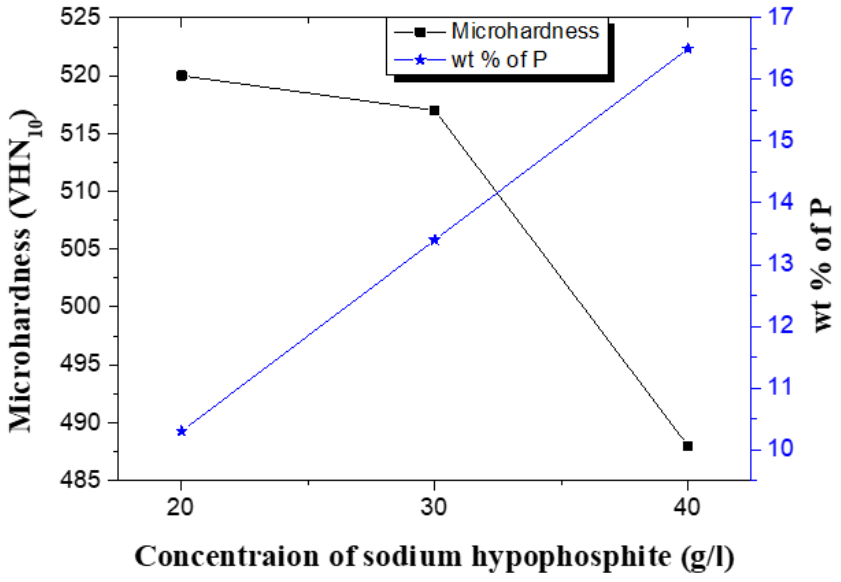

Figure 5.32: Microhardness of the Ni-P-TiO_2 nanocomposite coatings on mild steel deposited with variation of wt.% of P and concentration of sodium hypophosphite

The corrosion results obtained with the help of polarization studies of Ni-P-TiO_2 composite coatings (20 g/l, 30 g/l, and 40 g/l sodium hypophosphite concentration) in 3.5% sodium chloride aqueous solution are shown in Figures 5.33, 5.34 and 5.35.

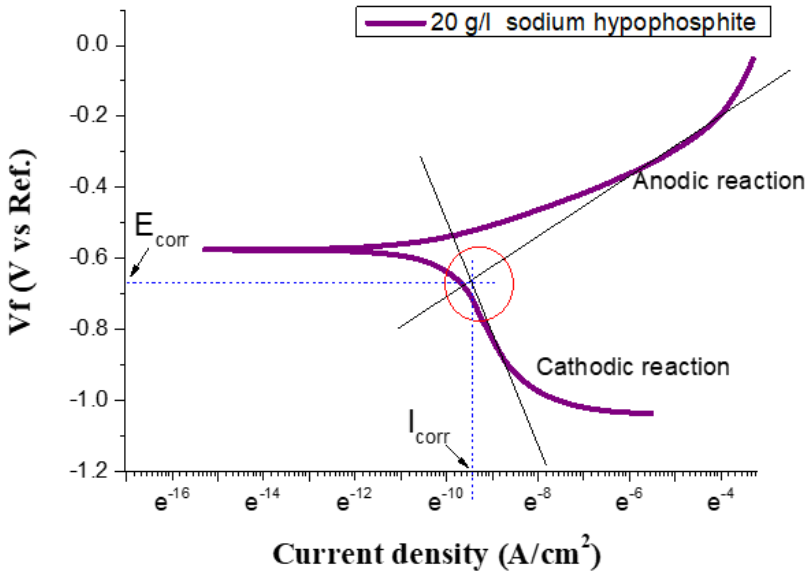

Figure 5.33: Tafel curve of Ni-P-TiO_2 nanocomposite coating (with 20 g/l sodium hypophosphite) in 3.5% NaCl solution

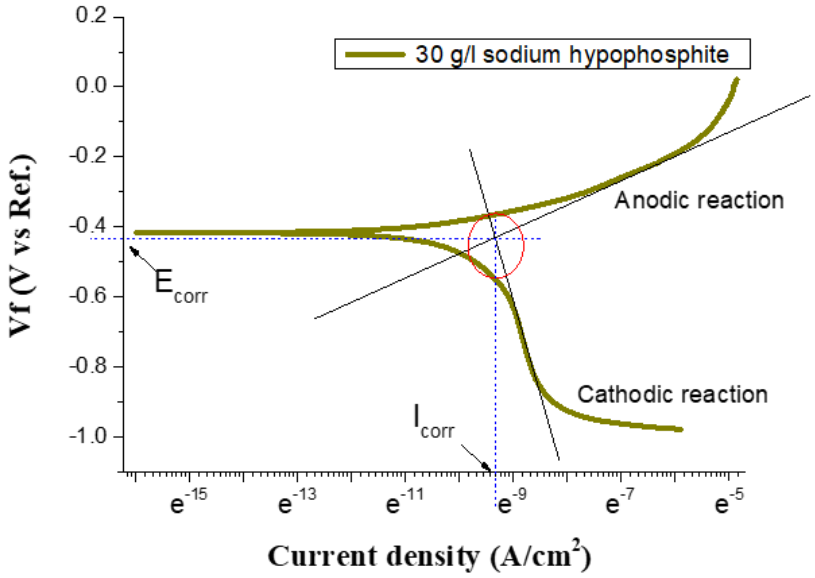

Figure 5.34: Tafel curve of Ni-P-TiO_2 nanocomposite coating (with 30 g/l sodium hypophosphite) in 3.5% NaCl solution

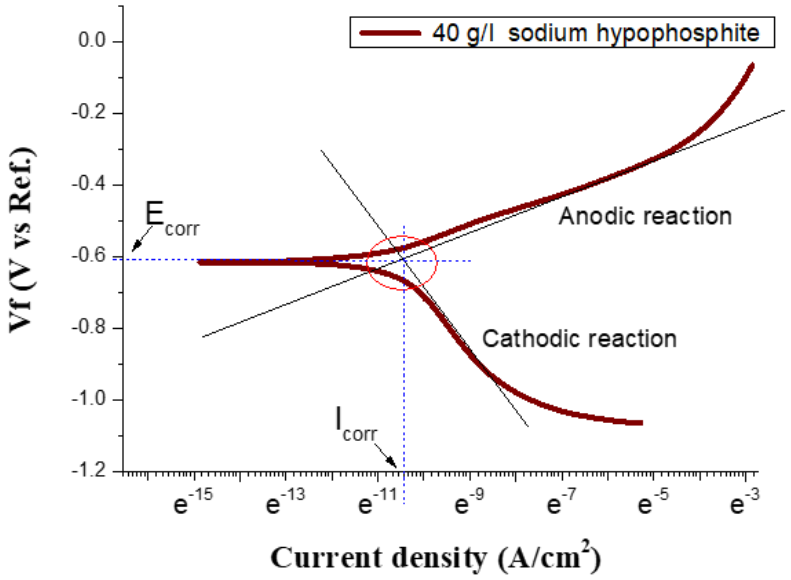

Figure 5.35: Tafel curve of Ni-P-TiO_2 nanocomposite coating (with 40 g/l sodium hypophosphite) in 3.5% NaCl solution

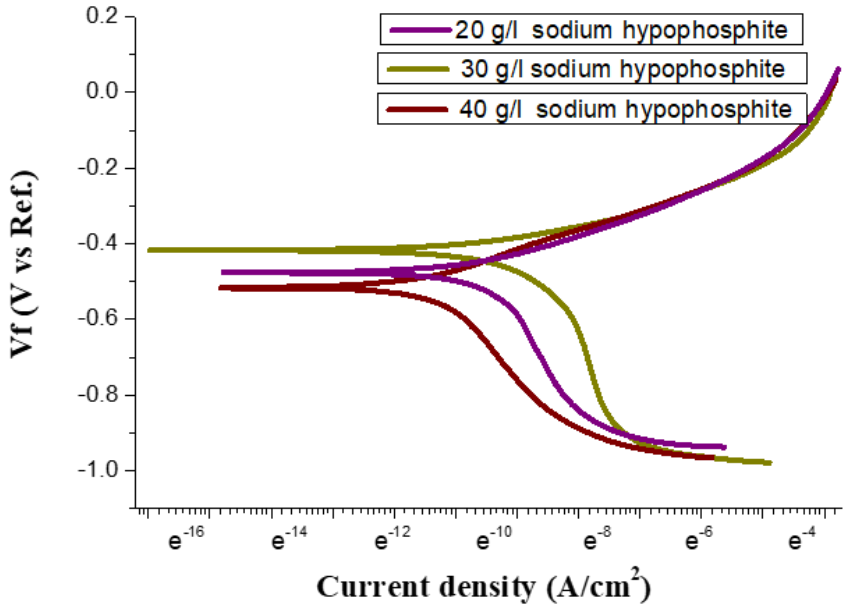

Figure 5.36: Corrosion characteristics of as plated Ni-P-TiO_2 nanocomposite coatings with various sodium hypophosphite concentrations in the bath

Figure 5.36 shows the comparison of Tafel plots of the three types of Ni-P-TiO_2 nanocomposite coatings (deposited with 20 g/l, 30 g/l and 40 g/l sodium hypophosphite concentration). Similar polarization mechanism was seen for these coating in 3.5%

NaCl solution. These nanocomposite coatings have more positive corrosion potential than the Ni-P coating and mild steel substrate. Electroless Ni-P-TiO_2 nanocomposite coating with 20 g/l sodium hypophosphite has high corrosion current density (63.32 µA) as compare to Ni-P-TiO_2 nanocomposite coating with 30 g/l and 40 g/l sodium hypophosphite.

Table 5.6: Electrochemical results of Ni-P-TiO_2 nanocomposite coatings (20 g/l, 30 g/l, and 40 g/l sodium hypophosphite concentration) derived from the Tafel plots

S. No.	Sample with various sodium hypophosphite concentration	E_{corr} (mV)	I_{corr} (µA)	Corrosion Rate (mpy)
1	Ni-P-TiO_2 nanocomposite coating with 20 g/l sodium hypophosphite	-687	63.32	5.967
2	Ni-P-TiO_2 nanocomposite coating with 30 g/l sodium hypophosphite	-551	62.78	5.917
3	Ni-P-TiO_2 nanocomposite coating with 40 g/l sodium hypophosphite	-601	40.19	3.787

Tafel plots obtained from the electrochemical potentiodynamic polarization of these coatings were used to measure corrosion rate with the help of Tafel slop at anodic polarization β_a, Tafel slop at cathodic polarization β_c, corrosion potential $E_{corr,}$ and corrosion current density I_{corr}. The Tafel plot is based on a mixed potential theory. Table 5.6 has shown the electrochemical results of the coatings derived from the Tafel plots of Ni-P-TiO_2 nanocomposite coatings with a variation of sodium hypophosphite concentration (20 g/l, 30 g/l, and 40 g/l). The corrosion rate of nanocomposite coatings slightly decreased with increased in concentration of sodium hypophosphite in deposition bath. As given in Table 5.6, Corrosion current density I_{corr} of these coatings are increasing when sodium hypophosphite concentration increased. Corrosion current density I_{corr} is inversely proportional to polarization resistance (R_p) [215]. So, Ni-P-TiO_2 nanocomposite coating with high sodium hypophosphite concentration has improved corrosion resistance. The reason behind better corrosion resistance of the Ni-P-TiO_2 nanocomposite coating deposited with high sodium hypophosphite

concentration is that the amorphous microstructure of deposits due to the highest phosphorus content. The amorphous microstructure is more homogeneous and there are no grain boundaries [225].

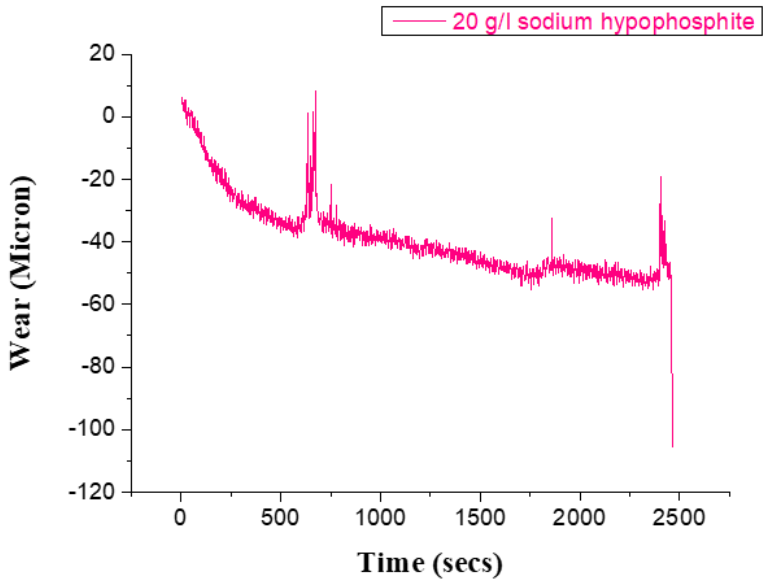

Figure 5.37: Wear (micron) with time at room temperature and sliding velocity 0.2 m/s at 5 N for Ni-P-TiO_2 composite coating (with 20 g/l $Na.H_2PO_2$)

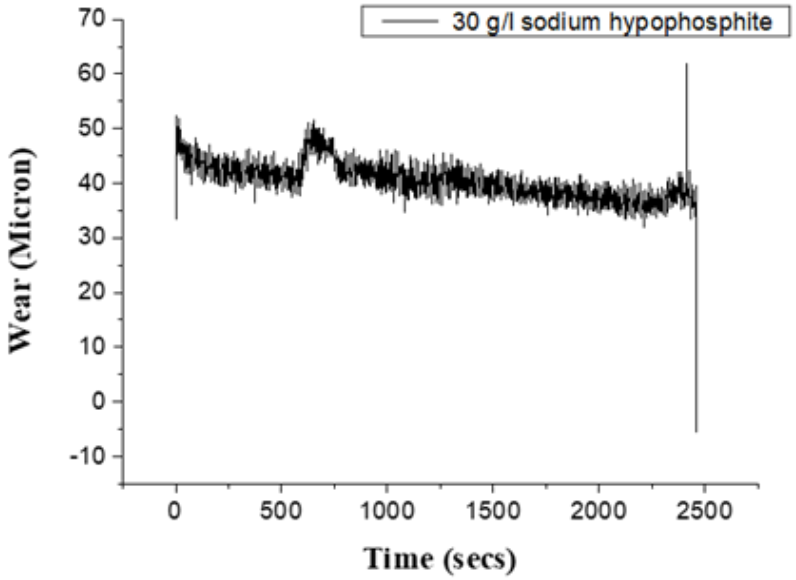

Figure 5.38: Wear (micron) with time at room temperature and sliding velocity 0.2 m/s at 5 N for Ni-P-TiO_2 composite coating (with 30 g/l $Na.H_2PO_2$)

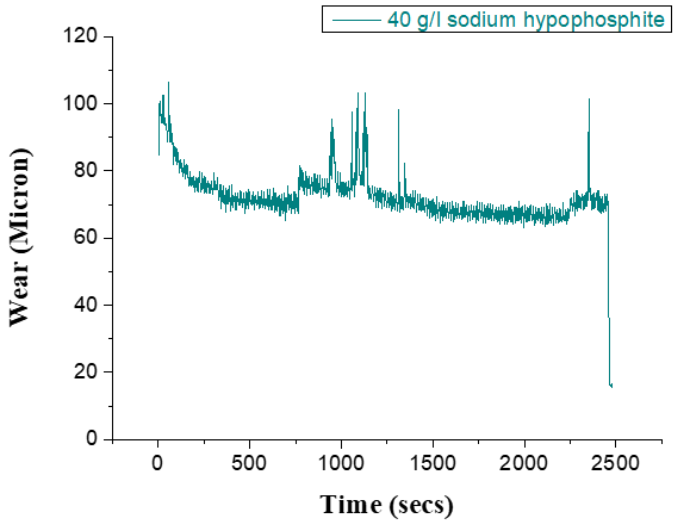

Figure 5.39: Wear (micron) with time at room temperature and sliding velocity 0.2 m/s at 5 N for Ni-P-TiO_2 composite coating (with 40 g/l $Na.H_2PO_2$)

Table 5.7: Comparison of wear of Ni-P-TiO_2 nanocomposite coatings (20 g/l, 30 g/l, and 40 g/l sodium hypophosphite concentration) determine from the pin-on-disc tests

S. No.	Sample	Thickness of coating (µm)	Wear loss (gm)	Wear rate (mm^3/m)
1	Ni-P-TiO_2 nanocomposite coating with 20 g/l sodium hypophosphite	20	0.004	0.0011428
2	Ni-P-TiO_2 nanocomposite coating with 30 g/l sodium hypophosphite	24	0.005	0.0014290
3	Ni-P-TiO_2 nanocomposite coating with 40 g/l sodium hypophosphite	23	0.009	0.0025714

For determining the wear loss of Ni-P-TiO_2 nanocomposite coatings, Pin-on-disc tests were performed on coated samples. During the wear tests, room temperature is ~30°C and relative humidity is 85% approximately. Descriptive curves amid for wear with time for electroless Ni-P-TiO_2 nanocomposite coatings (deposited with 20 g/l, 30 g/l, and 40 g/l sodium hypophosphite concentration) at a sliding velocity of 0.2 m/s with 5 N load are shown in Figures 5.37, 5.38, and 5.39. Wear during the pin-on-disc tests of coatings are calculated by weight loss methods. Wear rate of electroless Ni-P-TiO_2

nanocomposite coatings (deposited with 20 g/l, 30 g/l, and 40 g/l sodium hypophosphite concentration) is calculated by the formula (5.c) which is mentioned in section 5.1.

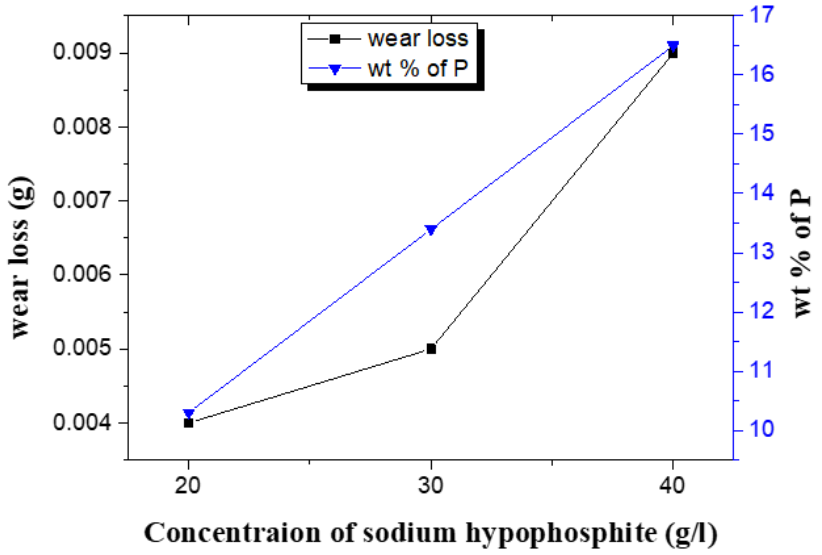

Figure 5.40: Wear loss of the Ni-P-TiO_2 nanocomposite coatings on mild steel deposited with variation of wt.% of P and concentration of sodium hypophosphite in the deposition bath.

As results are shown in Table 5.7, wear loss of Ni-P-TiO_2 nanocomposite coatings on mild steel deposited with 20 g/l, 30 g/l and 40 g/l sodium hypophosphite are 0.004 gm, 0.005 gm and 0.009 gm respectively. As analysis shown in Figure 5.40, wear loss is increased with increased concentration of sodium hypophosphite in the bath. Minimum wear rate (0.0011428 mm^3/m) is observed for the electroless Ni-P-TiO_2 nanocomposite coating deposited with 20 g/l sodium hypophysis. Wear resistance property of the material is inversely propositional to the wear rate. Wear resistance of nanocomposite coatings are decreased when the concentration of sodium hypophosphite is increased because of improved wt.% of P in the obtained coatings and diminution in microhardness.

5.2.3. Variation of the concentration of nano TiO_2 particles

Nano TiO_2 particles were used as second phase particles in the electroless Ni-P-TiO_2 nanocomposite bath. Nano TiO_2 particles were co-deposited with Ni-P matrix. Second phase particles play important role in the development of nanocomposite coatings and

their properties. Here, different characterization studies of Ni-P-TiO_2 nanocomposite coatings on mild steel deposited with various concentrations of nano TiO_2 particles in the chemical deposition bath are discussed. This section is content obtained observations and their discussion related to the changes in the morphology, surface roughness, hardness, corrosion resistance and wear resistance due to the variation of concentration of nano TiO_2 particles in the chemical deposition bath.

Up to 20 µm thick electroless Ni-P-TiO_2 nanocomposite coatings on mild steel were successfully deposited on the mild steel substrate. For characterization of these coating by XRD analysis, morphological analysis, microhardness, corrosion and wear studies are given below:

The X-ray diffraction pattern of Ni-P exhibited a single broad peak corresponding to Ni (1 1 1) phase at 44.70° and more diffused peaks revealed the amorphous nature of the coating. While Ni-P-TiO_2 composite coatings exhibited a single sharp peak corresponding to Ni (1 1 1) phase at 44.90° and more diffused peaks revealed the semi-crystalline nature of coatings. The sharp small peak at 65.10° results from the iron substrate.

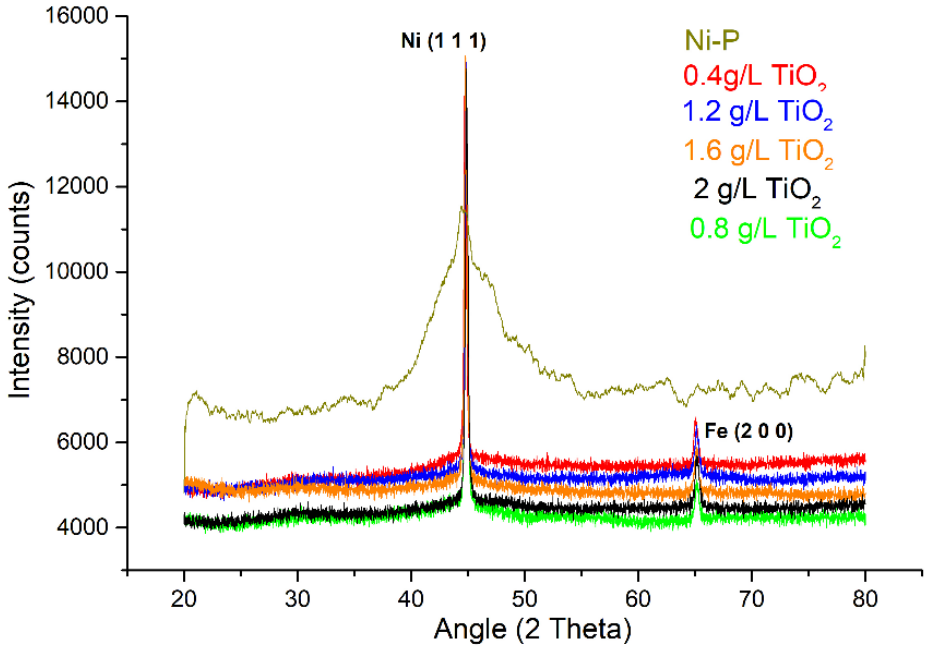

Figure 5.41: Comparison of XRD patterns of Ni-P-TiO_2 coated samples with various concentrations of TiO_2 (0.4 g/l, 0.8 g/l, 1.2 g/l, 1.6 g/l and 2 g/l)

The various X-ray diffraction patterns compared in Figure 5.41, also shows the shifting of position (2θ) towards right i.e. at a higher angle in case of Ni-P-TiO_2 nanocomposite coatings. The reason for shifting of the peak may be due to the atomic radius of nano TiO_2 particles being very small as compared to the atomic radius of Ni-P globules. When these particles were incorporated in Ni-P matrix they decrease the interplanar spacing, as a result, the lattice parameter decreased which shifts the peak towards the right.

The size of the Ni-P globules and developed strain within the Ni-P matrix due to the inclusion of second phase particles (TiO_2 particles) are calculated by the equation (5.d) and equation (5.e) respectively [206, 221-222].

$$L=(x\lambda) / (\beta.\cos\theta) \quad (5.d)$$

$$\beta.\cos\theta / \lambda = 1 / L + \varepsilon.\sin\theta / (\lambda) \quad (5.e)$$

Where L is particle size, λ is the used X-Ray wavelength, x is the correction faction (~ 0.9), β is the FWHM of observed Peaks, Ɛ is the effective strain and Ɵ is the Bragg's angle.

Table 5.8: Results of XRD analysis of Ni-P-TiO_2 coated samples with different concentration of TiO_2 (0.4 g/l, 0.8 g/l, 1.2 g/l, 1.6 g/l and 2 g/l)

S. No.	Coated samples with different concentration of TiO_2 (g/l)	d-spacing (Å)	2Ɵ (degree)	FWHM (degree)	Ni-P globules size (nm)	Strain (Ɛ)
1	0.4	2.02420	44.7350	0.1092	786.7	-0.000514
2	0.8	2.02286	44.8020	0.1151	738.2	-0.000600
3	1.2	2.02265	44.8102	0.1279	671.6	-0.000602
4	1.6	2.02272	44.7694	0.14404	611.7	-0.000661
5	2	2.01886	44.8597	0.1092	787.0	-0.000514

Results were obtained from the XRD analysis, given in Table 5.8. Size of Ni-P globules is decreased when increasing the wt.% of second phase particle in the Ni-P matrix and developed strain in Ni-P matrix is negligible. So, from Figure 5.42, it is concluded that developed strain is not much affected by the co-deposition of TiO_2 particles.

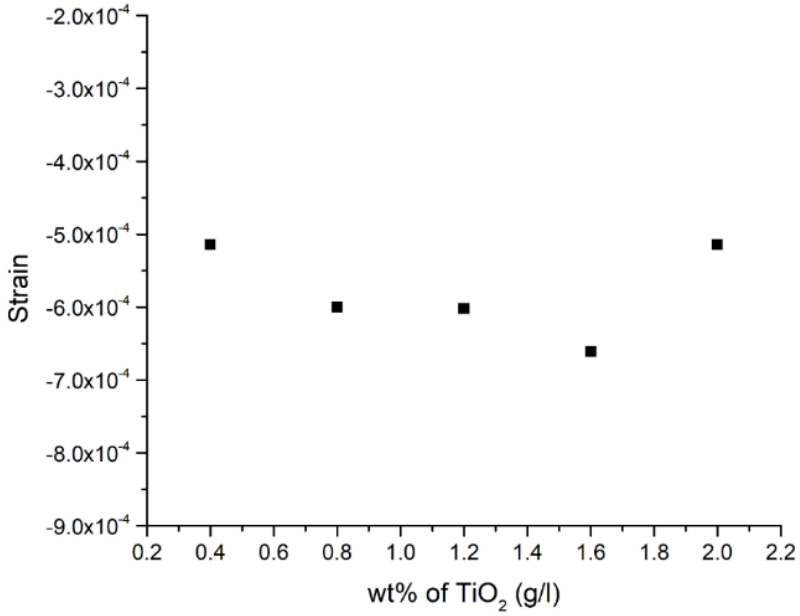

Figure 5.42: Developed strain within the Ni-P-TiO_2 nanocomposite coatings (with 0.4 g/l, 0.8 g/l, 1.2 g/l, 1.6 g/l and 2 g/l nano TiO_2 particles concentration)

FESEM equipped with EDS was used for the study of the surface morphology of Ni-P-TiO_2 nanocomposite coatings. The EDS technique was used to obtain the quantitative and qualitative analysis of Ni-P-TiO_2 composite coatings. FESEM micrographs show that Ni-P coating was deposited on mild steel substrate in the form of spherical globules of Ni-P. The globules had a tendency to adhere to the clean upper surface of the mild steel substrate [220, 225]. FESEM micrographs (Figures 5.43, 5.45, 5.47, 5.49 and 5.51) of Ni-P-TiO_2 nanocomposite coating confirmed the uniform co-deposition of nano TiO_2 particles in entire the Ni-P matrix of Ni-P-TiO_2 composite coatings. It can be seen Ni-P globules were covered by nano TiO_2 particles film, so it indicated that mild steel substrate can be protected by Ni-P-TiO_2 nanocomposite coatings better than Ni-P coating.

The results from EDS analysis for Ni-P-TiO_2 nanocomposite coatings with different wt.% of TiO_2 such as 0.4 g/l, 0.8 g/l, 1.2 g/l, 1.6 g/l, and 2 g/l are presented in Figures

5.43, 5.45, 5.47, 5.49 and 5.51 respectively. The EDS spectra for Ni-P-TiO_2 nanocomposite coatings have shown peaks of Ni, P, Ti and O which leads to the coating composition. The result confirmed the co-deposition of nano TiO_2 particles in Ni-P matrix on the mild steel substrate. EDS analysis clearly showing when increasing concentration TiO_2 in the coating bath then TiO_2 wt.% increase in deposited coating.

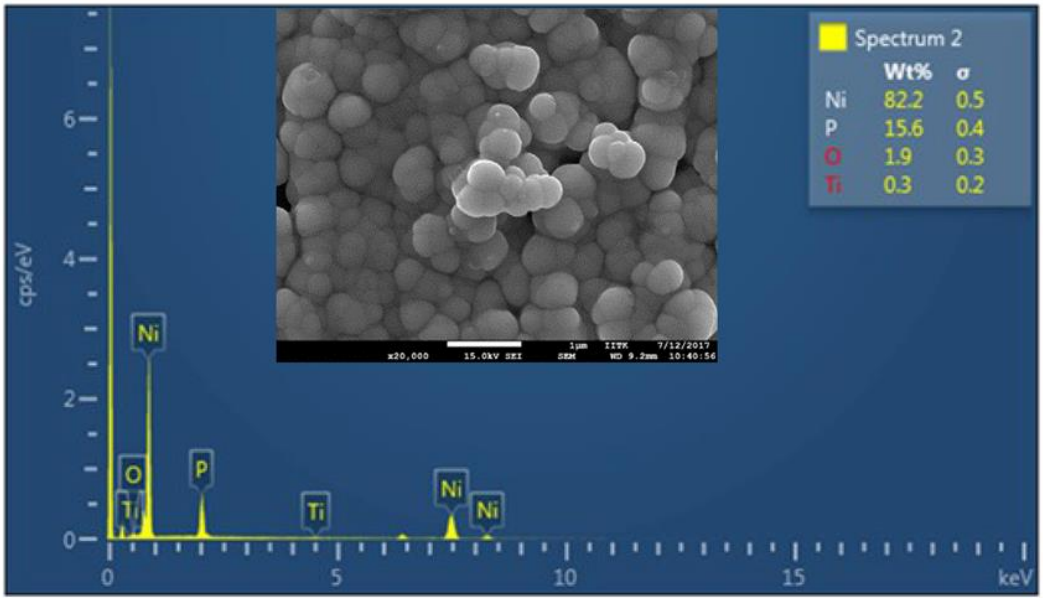

Figure 5.43: FESEM image with EDS pattern of electroless Ni-P-TiO_2 nanocomposite coating on mild steel substrate with 0.4 g/l TiO_2 concentration

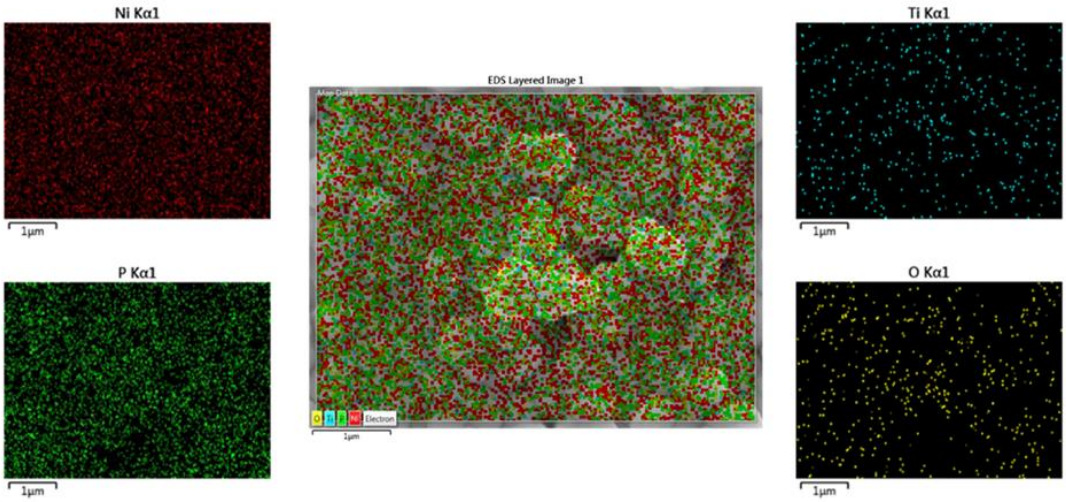

Figure 5.44: Dispersion of TiO_2 nanoparticles in Ni-P matrix (0.4 g/l TiO_2 concentration)

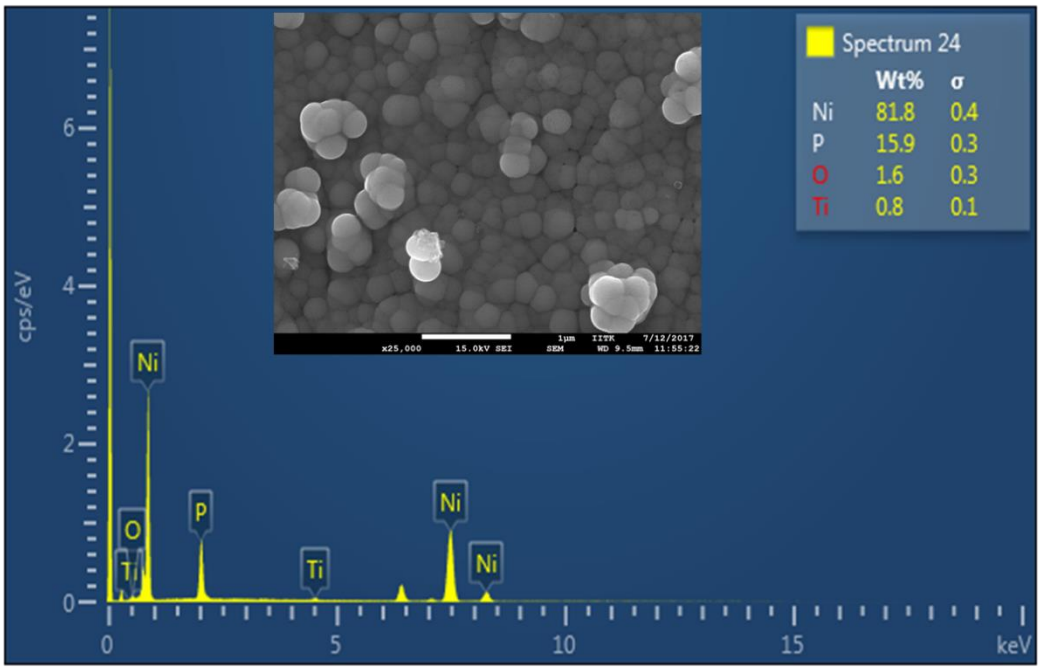

Figure 5.45: FESEM image with EDS pattern of electroless Ni-P-TiO_2 nanocomposite coating on mild steel substrate with 0.8 g/l TiO_2 concentration

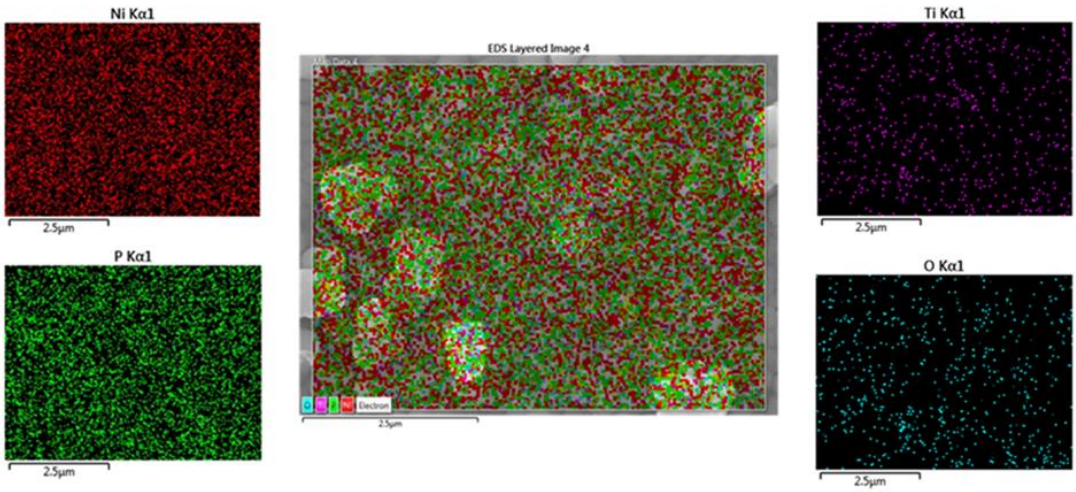

Figure 5.46: Dispersion of TiO_2 nanoparticles in Ni-P matrix (0.8 g/l TiO_2 concentration)

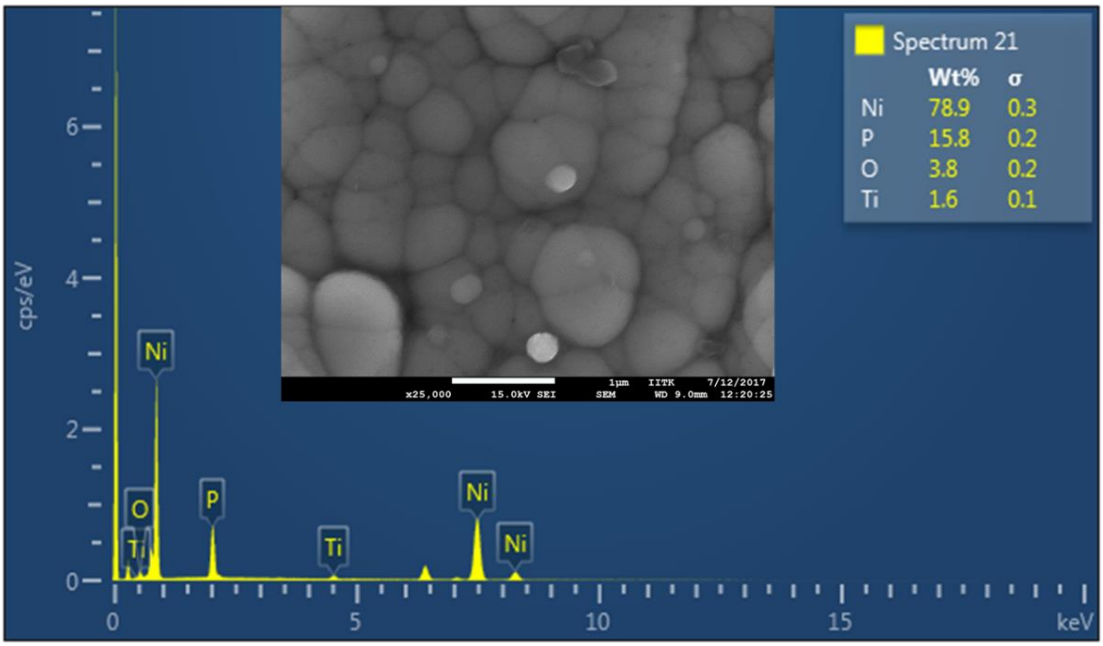

Figure 5.47: FESEM image with EDS pattern of electroless Ni-P-TiO_2 nanocomposite coating on mild steel substrate with 1.2 g/l TiO_2 concentration

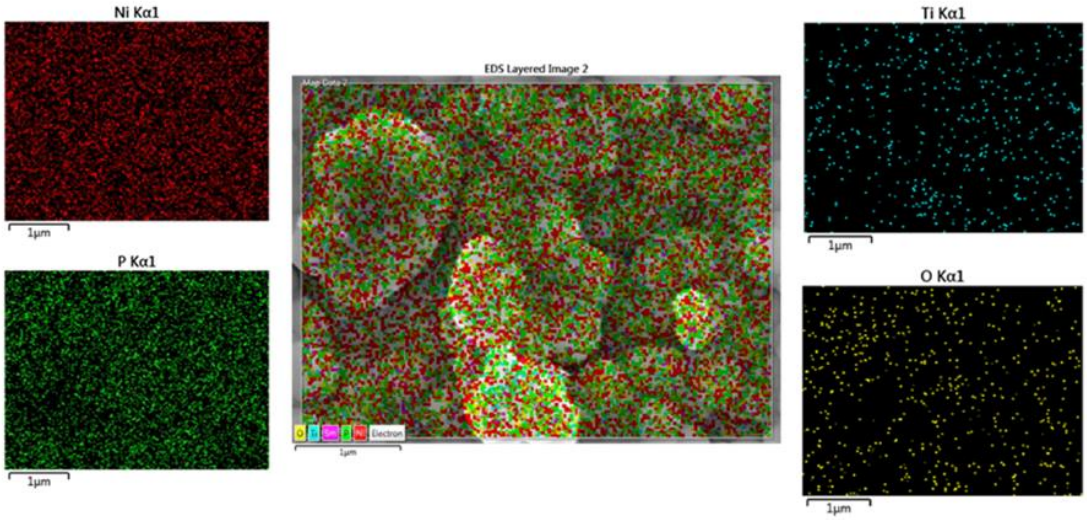

Figure 5.48: Dispersion of TiO_2 nanoparticles in Ni-P matrix (1.2 g/l TiO_2 concentration)

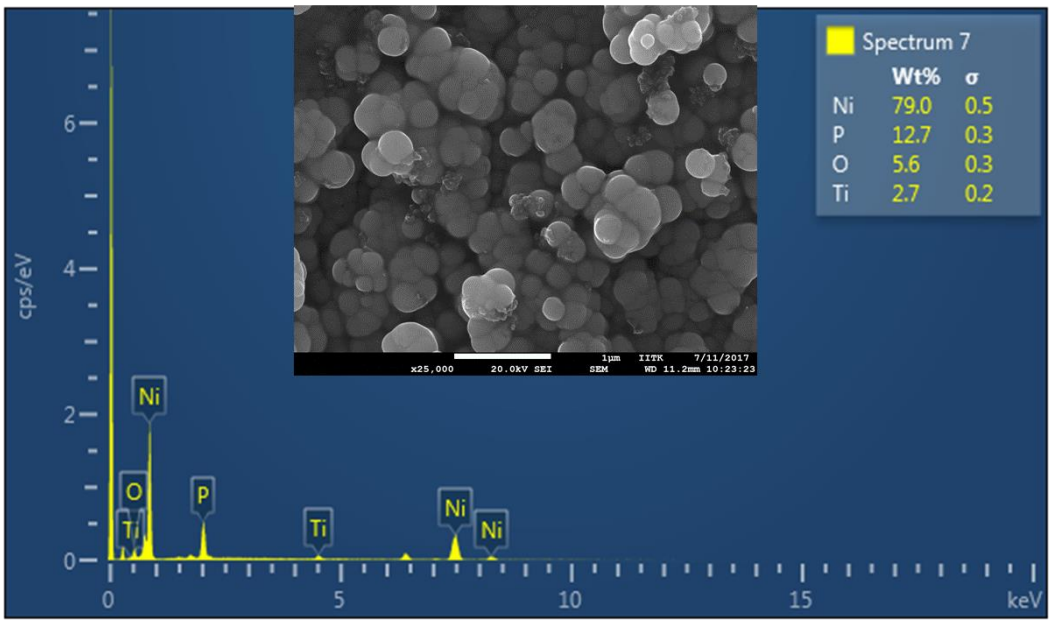

Figure 5.49: FESEM image with EDS pattern of electroless Ni-P-TiO_2 nanocomposite coating on mild steel substrate with 1.6 g/l TiO_2 concentration

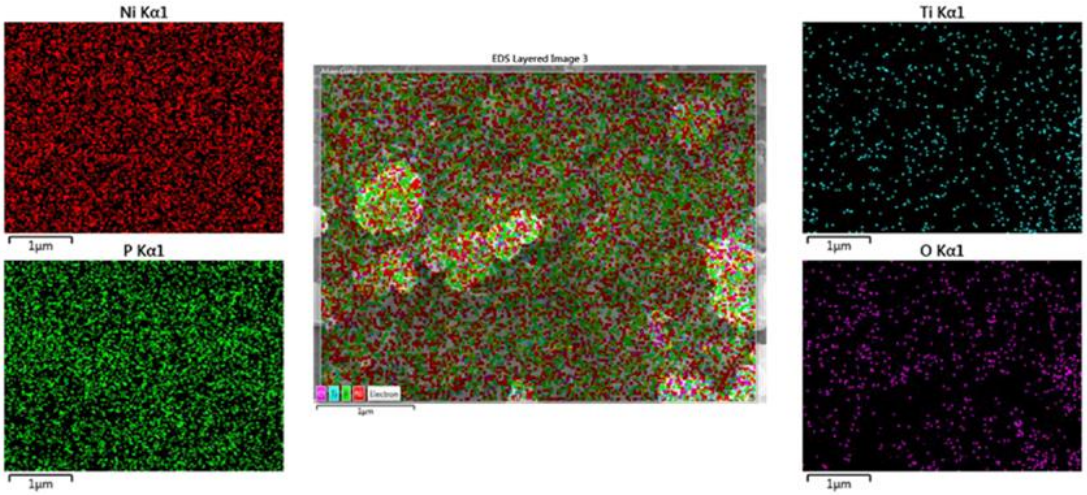

Figure 5.50: Dispersion of TiO_2 nanoparticles particles in Ni-P matrix (1. 6 g/l TiO_2 concentration)

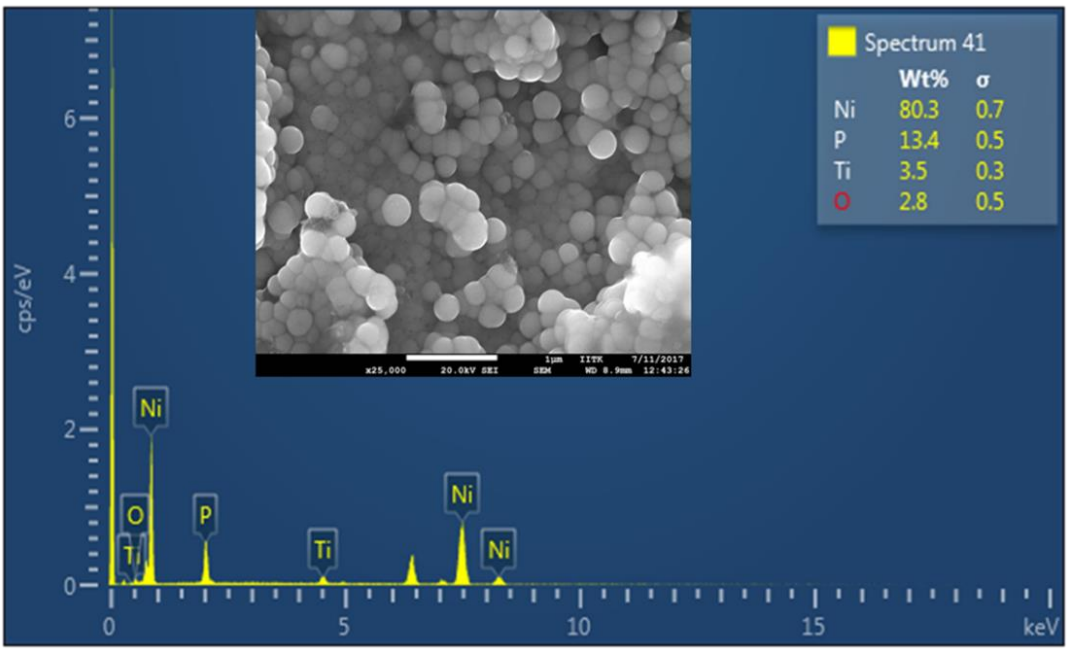

Figure 5.51: FESEM image with EDS pattern of electroless Ni-P-TiO_2 nanocomposite coating on mild steel substrate with 2 g/l TiO_2 concentration

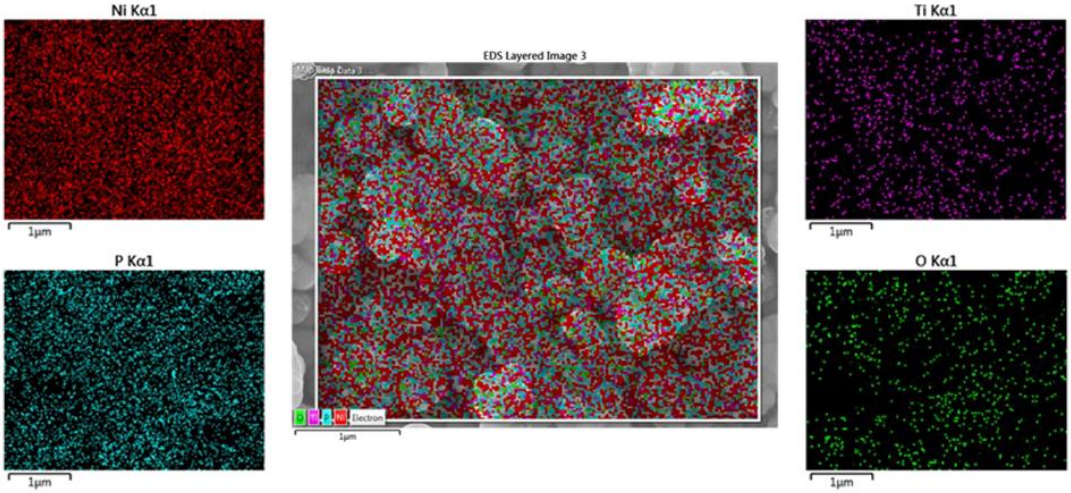

Figure 5.52: Dispersion of TiO_2 nanoparticles in Ni-P matrix (2 g/l TiO_2 concentration)

Figures 5.44, 5.46, 5.48, 5.50 and 5.52 show phosphorous were well alloyed in the matrix of nickel on the mild steel substrate. The good dispersion of nano TiO_2 particles in Ni-P metal matrix (5.44, 5.46, 5.48, 5.50 and 5.52), it revealed the uniform distribution of embedded nano TiO_2 in Ni-P-TiO_2 nanocomposite coatings. It can be seen Ni-P globules were covered by nano TiO_2 particles so it inferred that mild steel

substrate can be better protected by Ni-P-TiO_2 nanocomposite coating rather than Ni-P coating.

Figure 5.53 shows the variation in microhardness of Ni-P-TiO_2 nanocomposite coating at a different concentration of TiO_2 particles in the electroless bath. The microhardness of Ni-P-TiO_2 nanocomposite coatings is increasing with the increase in the content of TiO_2 in the deposit. The hardness of electroless nickel composite deposit depends on both phosphorus content and amount of the second phase particles. In general, the hardness of the electroless Ni-P increase with the decrease of P content and the increase of second phase particles [224-225]. Hardness is improved by the strengthening mechanism. The second phase hard TiO_2 incorporated into the coating matrix which provides the dispersion strengthening effect and an additional barrier to the movement of dislocation. At low TiO_2 concentration, Microhardness increase with increasing TiO_2 content. 2.0 g/l TiO_2 particles enhanced nanocomposite coating processes the highest microhardness of 517 VHN_{10}.

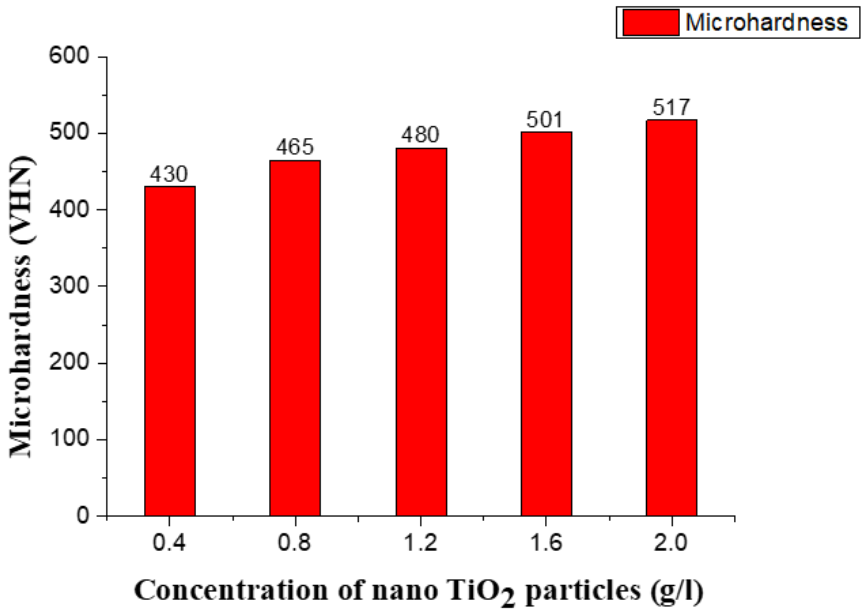

Figure 5.53: Comparison of Vickers microhardness of electroless Ni-P-TiO_2 nanocomposite coatings with various TiO_2 concentrations in the deposition bath

Tafel graphs of electroless Ni-P-TiO_2 nanocomposite coatings with 0.4 g/l, 0.8 g/l, 1.2 g/l, 1.6 g/l and 2.0 g/l nano TiO_2 concentration obtained from potentiostat (Gamry 600^{TM}) tests are shown in Figures 5.54, 4.55, 4.56, 4.57 and 4.58. Electrochemical

parameters such as corrosion potential, corrosion current density, anodic slop, and cathodic slop were determined from the potentiostat tests.

Table 5.9 summarize the electrochemical corrosion parameters derived from the Tafel curves for all the tested samples. The corrosion current density and potential of electroless Ni-P-TiO_2 nanocomposite coating with 0.4 g/l TiO_2 (minimum concentration of TiO_2) obtained as 55.25 µA/cm^2 and -472 mV. With the highest concentration of TiO_2 (2 g/l) the corrosion potential and the current density values were -551.2 mV and 62.78 µA/cm^2. It is clear from the above values that the increase of TiO_2 concentration in the plating bath significantly affects the corrosion behavior.

Tafel plot obtained from electrochemical potentiodynamic polarization was used to measure corrosion rate with the help of Tafel slop at anodic polarization β_a, Tafel slop at cathodic polarization β_c, corrosion current density I_{corr} and corrosion potential $E_{corr.}$

The Corrosion Rate (CR) is calculated by equation (5.f) [171]

$$\text{Corrosion Rate (mpy)} = (0.13I_{corr}\,(\text{Eq.wt.}))/d \qquad (5.f)$$

Where d is the density of substrate and Eq. wt. is the equivalent weight of the substrate.

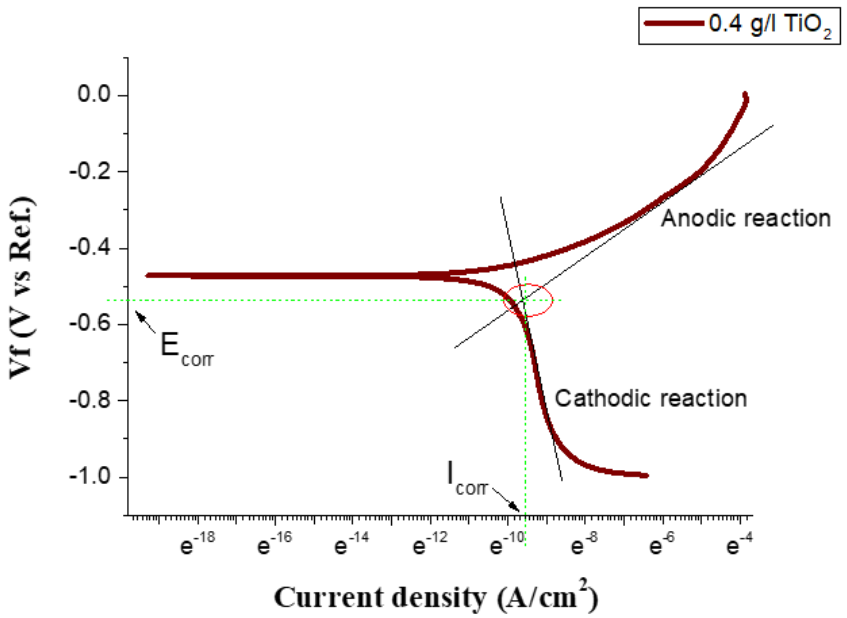

Figure 5.54: Tafel curve of Ni-P-TiO_2 nanocomposite coating (with 0.4 g/l TiO_2) in 3.5% NaCl solution

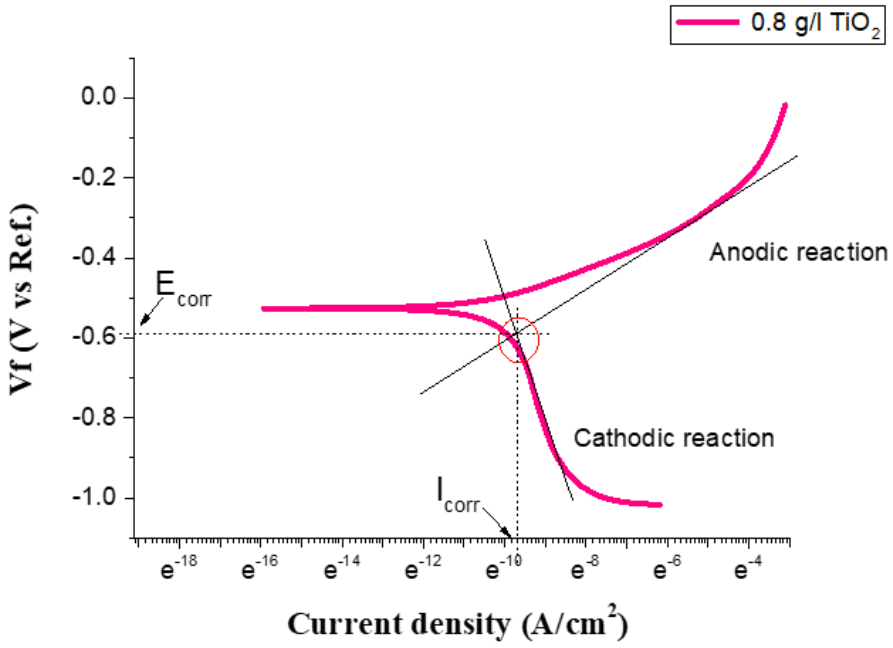

Figure 5.55: Tafel curve of Ni-P-TiO_2 nanocomposite coating (with 0.8 g/l TiO_2) in 3.5% NaCl solution

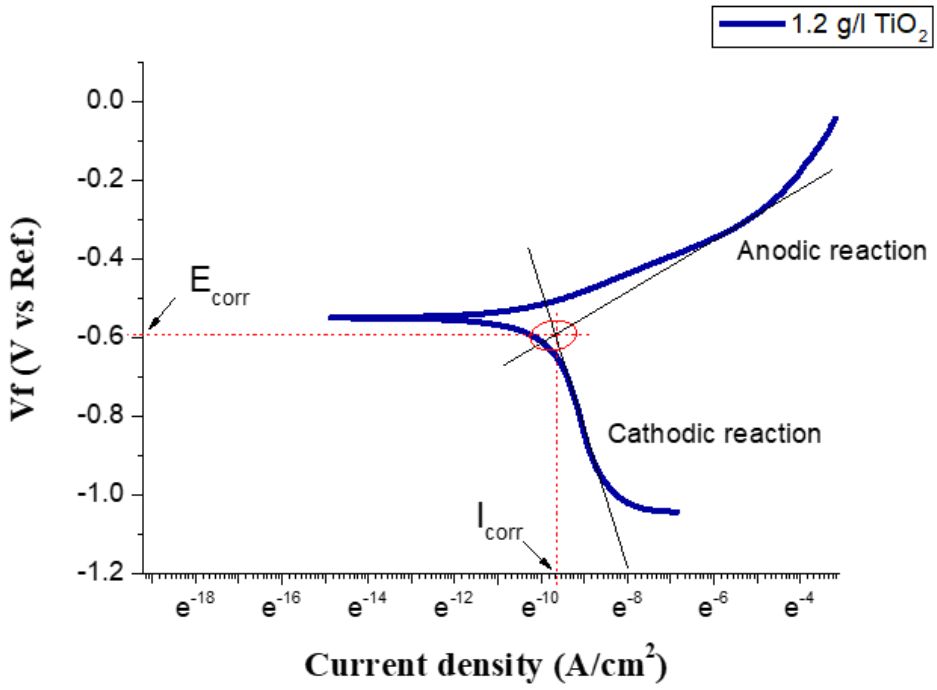

Figure 5.56: Tafel curve of Ni-P-TiO_2 nanocomposite coating (with 1.2 g/l TiO_2) in 3.5% NaCl solution

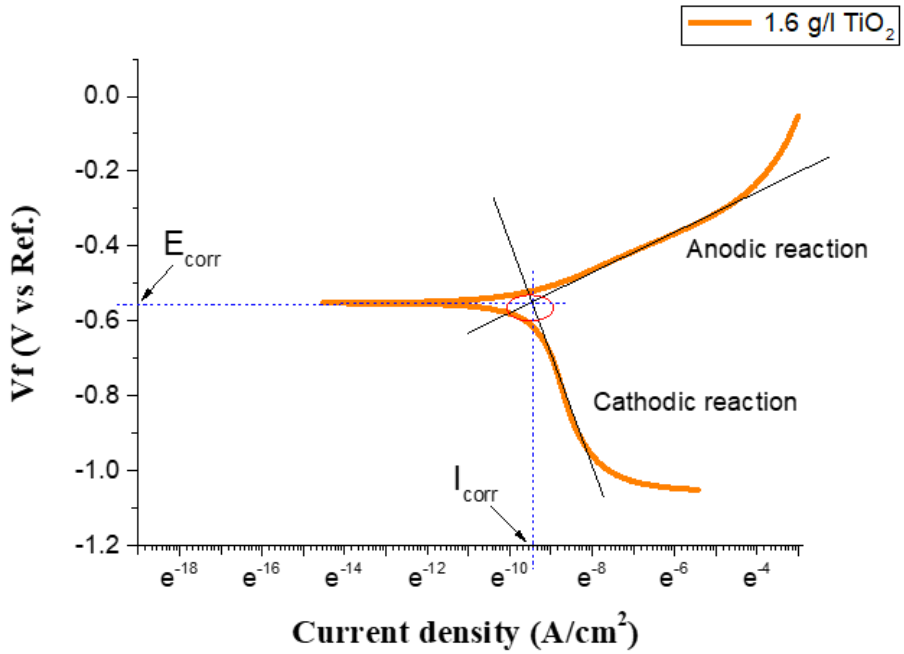

Figure 5.57: Tafel curve of Ni-P-TiO_2 nanocomposite coating (with 1.6 g/l TiO_2) in 3.5% NaCl solution

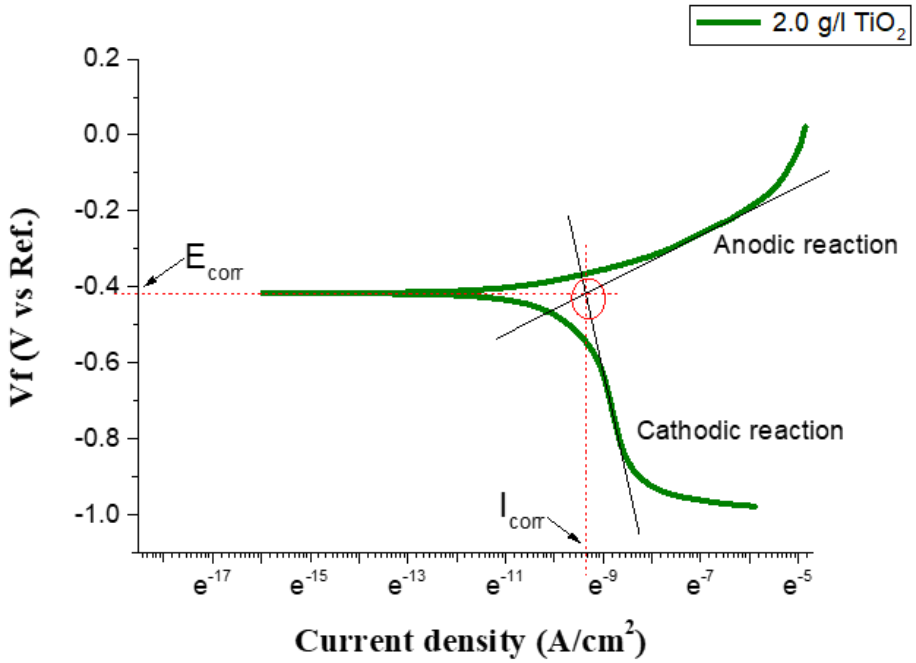

Figure 5.58: Tafel curve of Ni-P-TiO_2 nanocomposite coating (with 2 g/l TiO_2) in 3.5% NaCl solution

Table 5.9: Corrosion characteristics of as plated Ni-P-TiO_2 nanocomposite coatings with different TiO_2 bath concentrations

S. No.	Sample with TiO_2 variation (g/l)	E_{corr} (mV)	I_{corr} (µA)	Corrosion Rate (mpy)
1	0.4	-472.4	55.25	5.159
2	0.8	-525.7	51.72	4.829
3	1.2	-550.3	47.23	4.451
4	1.6	-529.6	58.52	5.515
5	2	-551.2	62.78	5.917

Figure 5.59 shows the electrochemical results obtained from the Tafel curves with respect to TiO_2 bath concentration for five 0.4 g/l TiO_2, 0.8 g/l TiO_2, 1.2 g/l TiO_2, 1.6 g/l TiO_2 and 2 g/l TiO_2 in 3.5 wt.% nickel chloride solution.

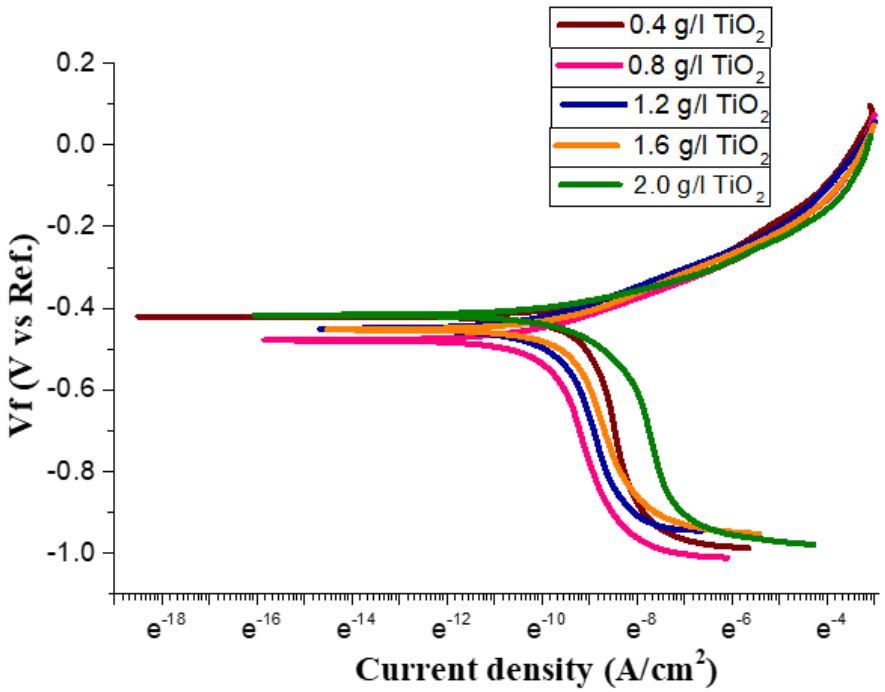

Figure 5.59: Comparative study of Tafel curves of Ni–P–TiO_2 nanocomposite coatings with 0.4 g/l TiO_2, 0.8 g/l TiO_2, 1.2 g/l TiO_2, 1.6g/l TiO_2 and 2 g/l TiO_2 in 3.5% NaCl solution

Basically, electroless Ni-P-TiO_2 nanocomposite coating deposited with less TiO_2 concentration (1.2 g/l) has the highest corrosion resistance than Ni-P-TiO_2 nanocomposite coating with higher TiO_2 concentration (2.0 g/l). Reason for the decrease in corrosion resistance value with increase in TiO_2 particles incorporation in the composite coating, when TiO_2 particles are co-deposited then the formation of passive layer might be disturbed [34, 66, 215, 224-225].

With the increase in TiO_2 concentration, the crystallinity of the composite coating is increased. The amorphous coating offers better protection against the corrosion than equivalent polycrystalline materials because amorphous materials are free from grain and grain boundaries. The SEM images clearly showing the distribution of TiO_2 in the Ni-P matrix. When the TiO_2 concentration is increased in the electroless bath, the high TiO_2 distribution in Ni-P matrix which provides high microhardness and low corrosion resistance.

If the main aim is to understand the nature of the surface of engineering solid materials, the surface texture is a very important factor. In the working/functional performance of several engineering components, the surface texture of solids plays an important role. Surface texture (surface finishing, roughness) of materials plays a vital role when these materials involved in tribological applications.

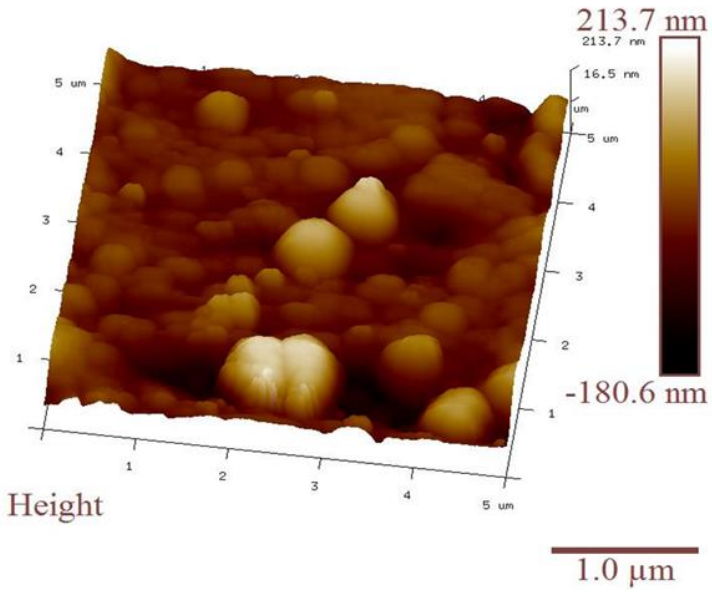

Figure 5.60: AFM image of surface roughness of Ni-P-TiO_2 nanocomposite coating with 0.4 g/l TiO_2

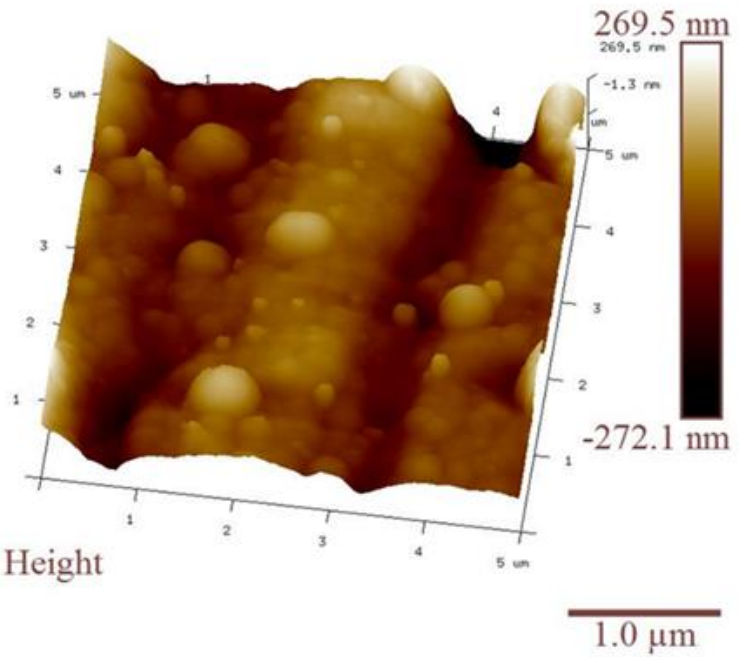

Figure 5.61: AFM image of surface roughness of Ni-P-TiO_2 nanocomposite coating with 0.8 g/l TiO_2

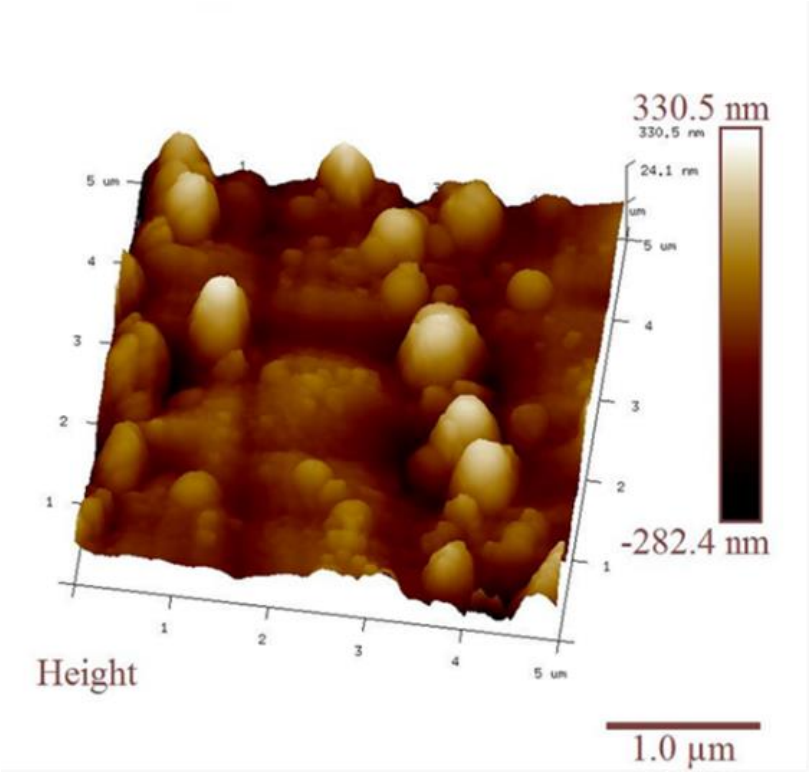

Figure 5.62: AFM image of surface roughness of Ni-P-TiO_2 nanocomposite coating with 1.2 g/l TiO_2

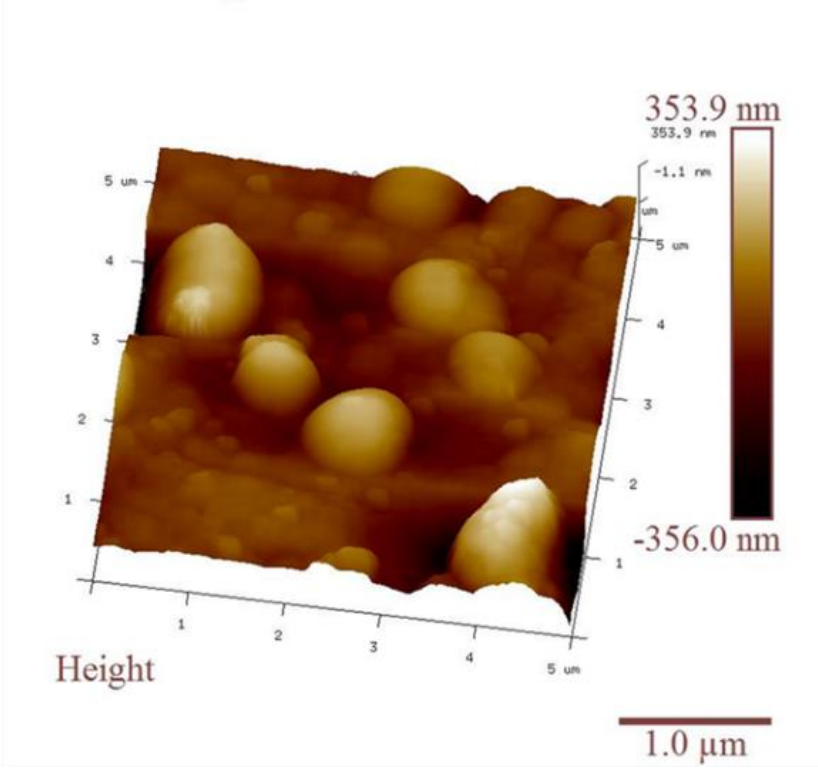

Figure 5.63: AFM image of surface roughness of Ni-P-TiO_2 nanocomposite coating with 1.6 g/l TiO_2

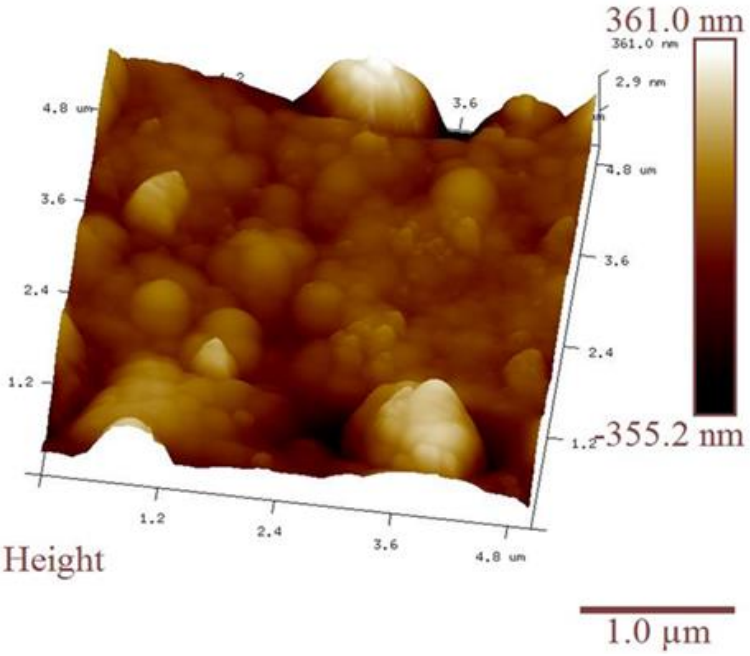

Figure 5.64: AFM image of surface roughness of Ni-P-TiO_2 nanocomposite coating with 2 g/l TiO_2

The surface roughness parameters were calculated from the analysis of AFM images of Ni-P-TiO_2 nanocomposite coatings with 0.4 g/l TiO_2, 0.8 g/l TiO_2, 1.2 g/l TiO_2, 1.6 g/l TiO_2, and 2 g/l TiO_2 as shown in Figures 5.60, 5.61, 5.62, 5.63, and 5.64 respectively.

Table 5.10: Roughness values of Ni-P-TiO_2 composite coatings with 0.4 g/l TiO_2, 0.8 g/l TiO_2, 1.2 g/l TiO_2, 1.6 g/l TiO_2 and 2 g/l TiO_2, calculated from atomic force microscopy

S. No.	Sample	R_a (nm)	R_q (nm)	Thickness of coating (µm)
1	Ni-P-TiO_2 nanocomposite coating with 0.4 g/l TiO_2	30.8	44.7	21
2	Ni-P-TiO_2 nanocomposite coating with 0.8 g/l TiO_2	50.5	67.9	22
3	Ni-P-TiO_2 nanocomposite coating with 1.2 g/l TiO_2	54.3	80.9	22
4	Ni-P-TiO_2 nanocomposite coating with 1.6 g/l TiO_2	59.1	79.0	23
5	Ni-P-TiO_2 nanocomposite coating with 2 g/l TiO_2	59.6	85.4	24

These measurements were made with a Multi-Mode AFM in contact mode. Mean square root roughness (Rq) and average roughness (Ra) values along with the coating thickness of electroless Ni-P-TiO_2 nanocomposite coatings with varying concentration of TiO_2 particles shown in Table 5.10.

Comparison of root means square roughness (R_q) and average roughness (R_a) of Ni-P-TiO_2 nanocomposite coatings on mild steel with different TiO_2 concentration is shown in Figure 5.65. The surface roughness of Ni-P-TiO_2 nanocomposite coatings on mild steel is dependent upon several parameters such as particle size of TiO_2 and its distribution, concentration of bath loading, deposit-thickness, smoothness of the mild steel substrate. As comparison shows in Figure 5.65, the roughness of Ni-P-TiO_2 nanocomposite coatings on mild steel is increased when nano TiO_2 particles concentration is increased in the deposition bath. Size of used nano TiO_2 particles is 10-25 nm. The inclusion of second phase particles within the electroless Ni-P metal matrix tends to increase the degree of surface roughness, especially in the case of hard second

phase particles. TiO_2 particles come in the category of hard and wear resistance particles.

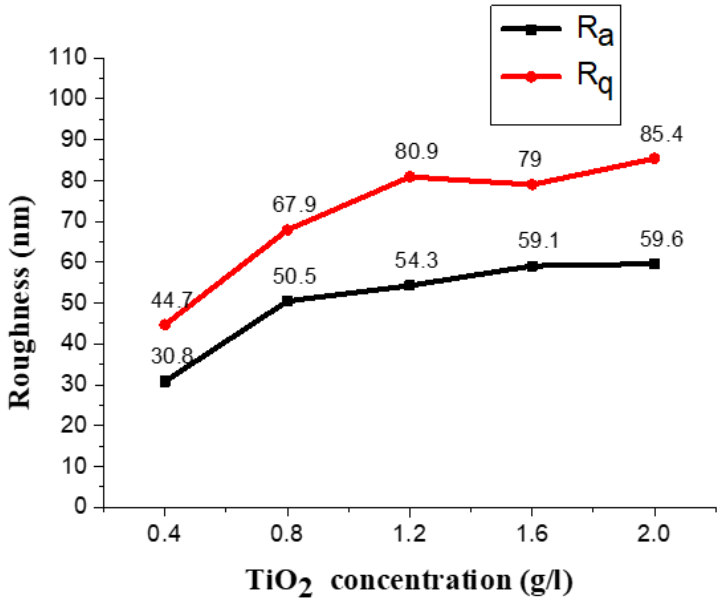

Figure 5.65: Variation of root mean square roughness (R_q) and average roughness (R_a) for electroless Ni-P-TiO_2 nanocomposite coatings with the different TiO_2 concentration

Pin-on-disc tests were done for determining the wear loss of Ni-P-TiO_2 nanocomposite coatings. During the wear tests, room temperature is ~30°C and relative humidity is 85%. Descriptive curves amid for wear with time for electroless Ni-P-TiO_2 nanocomposite coatings (deposited with 0.4 g/l, 0.8 g/l, 1.2 g/l, 1.6 g/l, and 2 g/l nano TiO_2 concentration) at sliding velocity of 0.2 m/s with 5 N load are shown in Figures 5.66, 5.67, 5.68, 5.69, and 5.70. Wear during the pin-on-disc tests of coatings are calculated by weight loss methods. Wear rate of electroless Ni-P-TiO_2 nanocomposite coatings (deposited with 0.4 g/l, 0.8 g/l, 1.2 g/l, 1.6 g/l, and 2 g/l TiO_2 nanoparticles concentration) is calculated by the formula (5.c) which is mentioned in section 5.1.

As Table 5.11 shows, wear loss of Ni-P-TiO_2 nanocomposite coatings with 0.4 g/l, 0.8 g/l, 1.2 g/l, 1.6 g/l and 2 g/l nano TiO_2 is 0.010 gm, 0.008 gm, 0.006 gm, 0.006 gm, and 0.005 gm respectively. Wear loss is decreased with increased concentration of nano TiO_2 particles in the electroless bath.

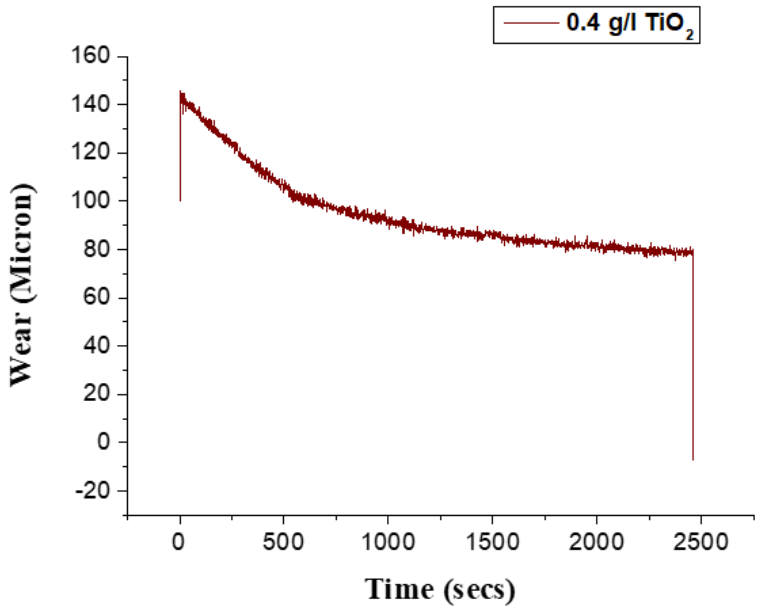

Figure 5.66: Wear (micron) with time profile at room temperature and sliding velocity 0.2 m/s at 5 N for Ni-P-TiO_2 composite coating (with 0.4 g/l TiO_2)

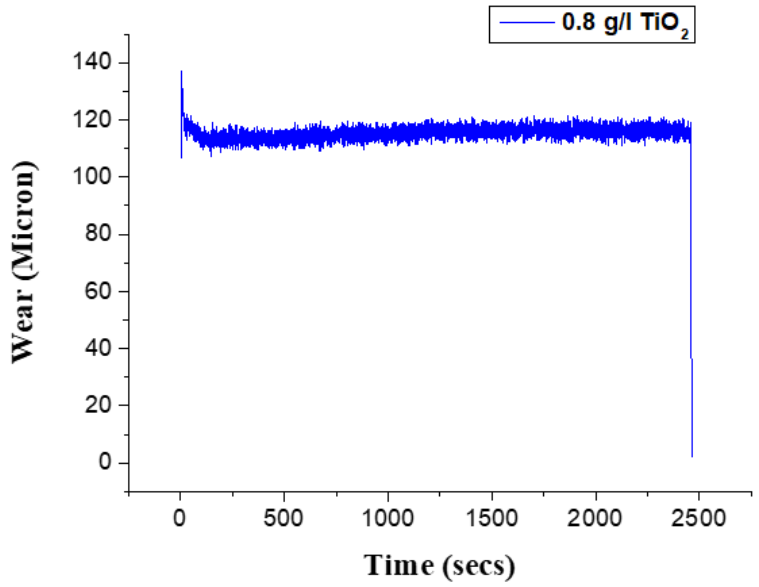

Figure 5.67: Wear (micron) with time profile at room temperature and sliding velocity 0.2 m/s at 5 N for Ni-P-TiO_2 composite coating (with 0.8 g/l TiO_2)

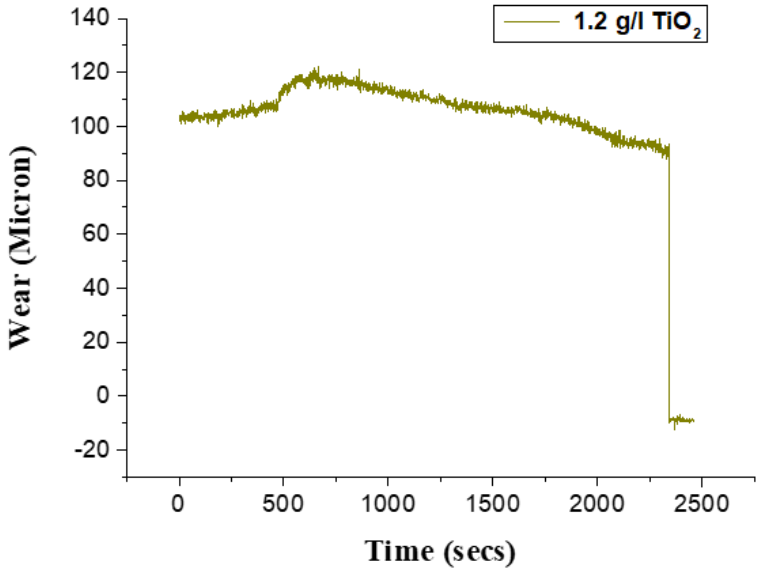

Figure 5.68: Wear (micron) with time profile at room temperature and sliding velocity 0.2 m/s at 5 N for Ni-P-TiO_2 composite coating (with 1.2 g/l TiO_2)

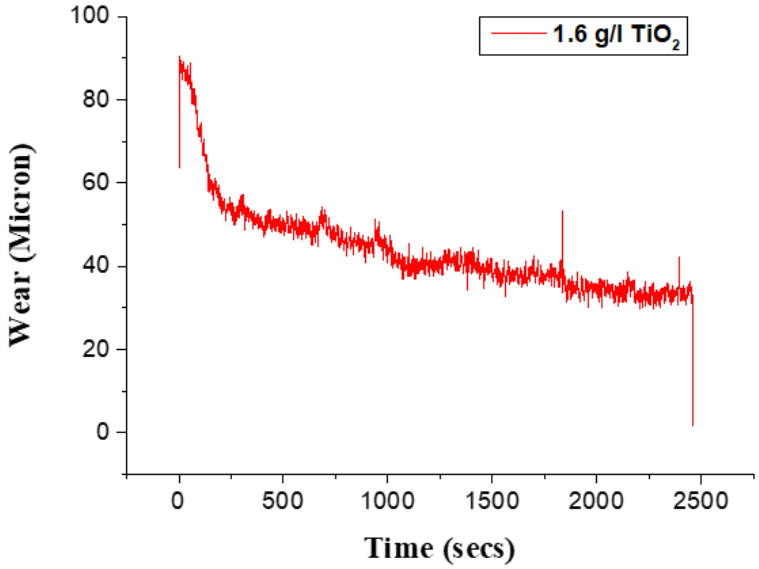

Figure 5.69: Wear (micron) with time profile at room temperature and sliding velocity 0.2 m/s at 5 N for Ni-P-TiO_2 composite coating (with 1.6 g/l TiO_2)

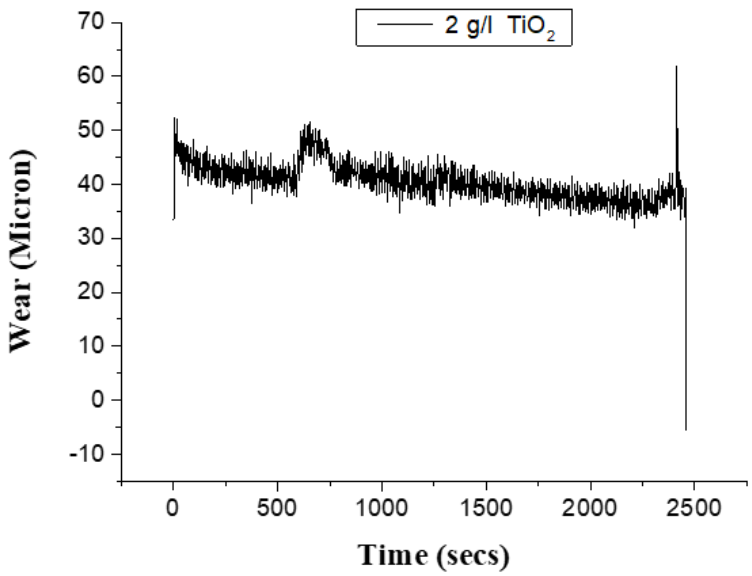

Figure 5.70: Wear (micron) with time profile at room temperature and sliding velocity 0.2 m/s at 5 N for Ni-P-TiO_2 composite coating (with 2 g/l TiO_2)

Table 5.11: Comparison of wear of Ni-P-TiO_2 nanocomposite coatings (0.4 g/l, 0.8 g/l, 1.2 g/l, 1.6 g/l and 2 g/l nano TiO_2 concentration) determine from the pin-on-disc tests

S. No.	Sample	Thickness of coating (µm)	Wear loss (gm)	Wear rate (mm^3/m)
1	Ni-P-TiO_2 nanocomposite coating with 0.4 g/l TiO_2	21	0.010	0.002857
2	Ni-P-TiO_2 nanocomposite coating with 0.8 g/l TiO_2	22	0.008	0.002285
3	Ni-P-TiO_2 nanocomposite coating with 1.2 g/l TiO_2	22	0.006	0.001714
4	Ni-P-TiO_2 nanocomposite coating with 1.6 g/l TiO_2	23	0.006	0.001714
5	Ni-P-TiO_2 nanocomposite coating with 2 g/l TiO_2	24	0.005	0.001429

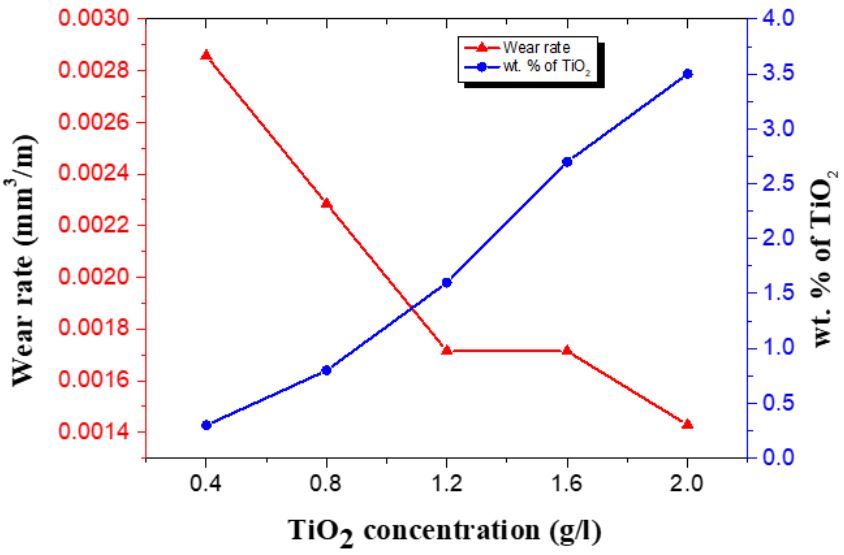

Figure 5.71: Comparison of the wear-rate along with TiO_2 content for electroless Ni-P-TiO_2 nanocomposite coatings deposited with the different TiO_2 concentration

Comparative study of the wear rate along with TiO_2 content for the Ni-P-TiO_2 nanocomposite coatings deposited with 0.4 g/l, 0.8 g/l, 1.2 g/l, 1.6 g/l, and 2 g/l nano TiO_2 particles are shown in Figure 5.71. Wear resistance property of the material is inversely propositional to the wear loss. Wear resistance of property nanocomposite coatings are increased when the concentration of hard TiO_2 particles is increased.

Ni-P-TiO_2 nanocomposite coatings were successfully developed on the mild steel substrate by same electroless plating technique using a hypophosphite reduced bath. FESEM and EDS analysis carried out on all Ni-P-TiO_2 composite coatings samples revealed the co-deposition of nano TiO_2 particles into Ni-P matrix and formation of a uniformly distributed homogeneous coating layer on mild steel substrate XRD results also revealed that co-deposited second phase particles (TiO_2) did not influence the phase transformation behavior and structure of deposits. Microhardness of the electroless Ni-P-TiO_2 nanocomposite coating is 343 VHN_{10} (for 0.4 g/l TiO_2 concentration) and 517 VHN_{10} (for 2.0 g/l TiO_2 concentration). Nanocomposite coating with high TiO_2 concentration shows decreased corrosion resistance compared to nanocomposite coating with low TiO_2 concentration. Wear during the pin-on-disc tests of coatings under 5 N load and 500 m sliding distance are calculated by weight loss methods. Wear loss is decreased with increased concentration of nano TiO_2 particles in the deposition

bath. Wear resistance of the material is inversely propositional to the wear loss. Wear resistance of the nanocomposite coatings are increased when the concentration of nano TiO_2 particles is increased.

In section 5.2, observations and their analysis related to electroless Ni-P-TiO_2 nanocomposite coatings on mild steel substrates deposited with various concentrations of nickel sulphate, sodium hypophosphite and nano TiO_2 particles in the deposition bath. As analyze the observations, the deposition rate is increased with increasing the concentration of constituents of deposition bath such as nickel sulphate, sodium hypophosphite, and nano TiO_2 particles. The content of nickel in the deposits is increased with increasing the concentration of nickel sulphate and decreasing the concentration of sodium hypophosphite in the bath. The content of phosphorus in the deposit is increased with increasing the concentration of sodium hypophosphite and decreasing the concertation of nickel sulphate in the bath. TiO_2 content in the Ni-P-TiO_2 nanocomposite coatings is increased by the increasing the concentration of nano TiO_2 particles in the deposition bath.

Study of the microhardness, corrosion and wear analysis of Ni-P-TiO_2 nanocomposite coatings on mild steel deposited with 25 g/l, 30 g/l and 35 g/l nickel sulphate in the deposition bath is discussed in section 5.2.1. and summarised observations are shown in Figure 5.72. Changes in the microhardness, corrosion-rate and wear-rate of electroless Ni-P-TiO_2 nanocomposite coatings on mild steel due to variation in the nickel sulphate concentration in the deposition bath are shown in Figure 5.72. As observations shown in Figure 5.72, microhardness and corrosion-rate of Ni-P-TiO_2 nanocomposite coatings are increased and wear-rate Ni-P-TiO_2 nanocomposite coatings are decreased with increasing the concentration of nickel sulphate in the deposition bath. It means Ni-P-TiO_2 nanocomposite coating deposited with 35 g/l nickel sulphate has higher microhardness, higher wear resistance, and lower corrosion resistance as compared to Ni-P-TiO_2 nanocomposite coatings deposited with 25 g/l and 30 g/l nickel sulphate. Reason for the high microhardness and wear resistance of the coating is high nickel content and low phosphorus content in the deposit. So, it can say that 35 g/l nickel sulphate concentration is suitable for developing the hard and wear resistance Ni-P-TiO_2 nanocomposite coating on mild steel.

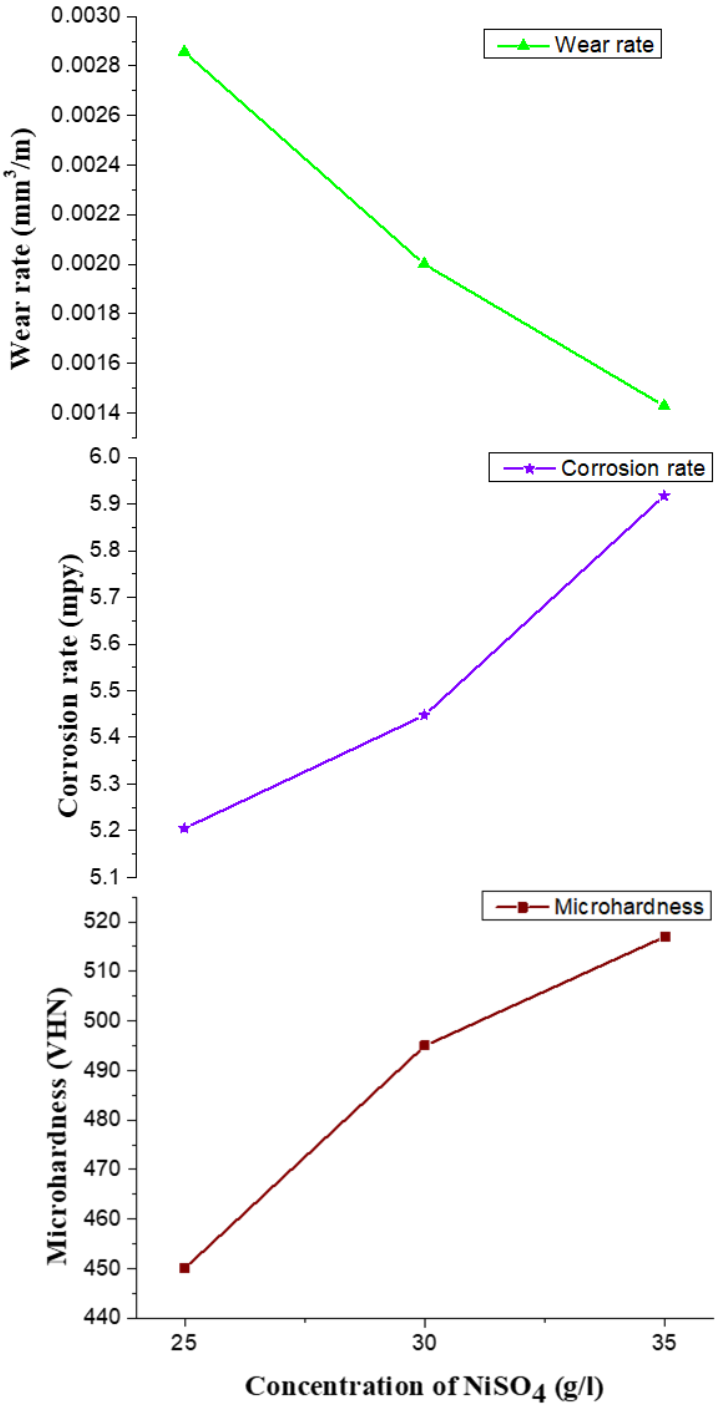

Figure 5.72: Comparison of the microhardness, corrosion-rate and wear-rate of electroless Ni-P-TiO_2 nanocomposite coatings deposited with the 25 g/l, 30 g/l and 35 g/l nickel sulphate concentration in the deposition bath

Study of the microhardness, corrosion and wear analysis of Ni-P-TiO_2 nanocomposite coatings on mild steel deposited with 20 g/l, 30 g/l and 40 g/l sodium hypophosphite in the deposition bath is discussed in section 5.2.2. and summarised observations are

shown in Figure 5.73. Changes in the microhardness, corrosion-rate and wear-rate of electroless Ni-P-TiO_2 nanocomposite coatings on mild steel due to variation in sodium hypophosphite concentration in the deposition bath are shown in Figure 5.73.

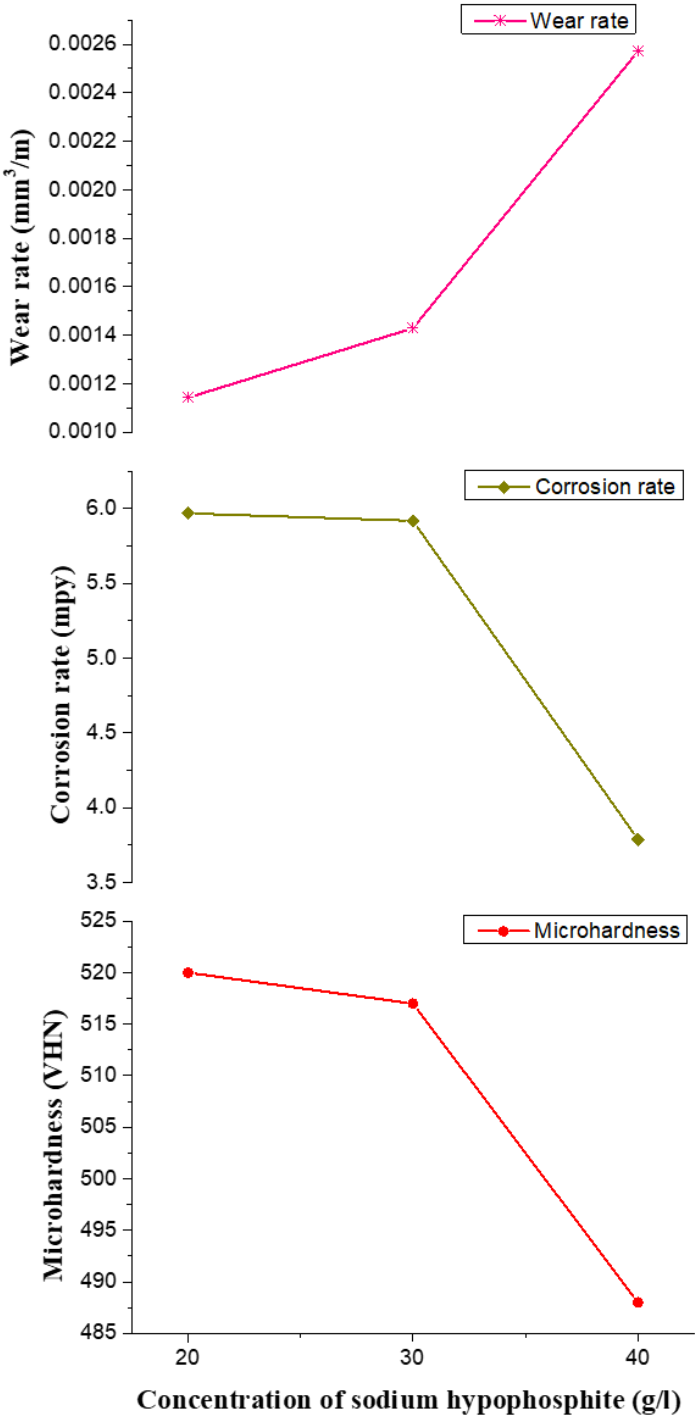

Figure 5.73: Comparison of the microhardness, corrosion-rate and wear-rate of electroless Ni-P-TiO_2 nanocomposite coatings deposited with the 20 g/l, 30 g/l, and 40 g/l sodium hypochlorite concentration in the deposition bath

As observations shown in Figure 5.73, microhardness and corrosion-rate of Ni-P-TiO_2 nanocomposite coatings are decreased and wear-rate Ni-P-TiO_2 nanocomposite coatings are increased with increasing the concentration of sodium hypophosphite in the deposition bath. It means Ni-P-TiO_2 nanocomposite coating deposited with 20 g/l sodium hypophosphite has higher microhardness, higher wear resistance, and lower corrosion resistance as compared to Ni-P-TiO_2 nanocomposite coatings deposited with 30 g/l and 40 g/l sodium hypophosphite. Corrosion resistance of the coating is increasing with increasing the concentration of sodium hypophosphite in the deposition bath due to the deposition of high phosphorus coating. High phosphorus coating has low crystallinity or amorous structure as compared to low phosphorus coating. The amorphous coating has a more homogeneous microstructure which makes coatings less prone to pitting. When corrosion resistance is the main aim of the coating while hardness and wear resistance is not much important then a high concentration of sodium hypophosphite can be used during the coating process.

Study of the microhardness, corrosion and wear analysis of Ni-P-TiO_2 nanocomposite coatings on mild steel deposited with 0.4 g/l, 0.8 g/l, 1.2 g/l, 1.6 g/l and 2.0 g/l nano TiO_2 particles in the deposition bath is discussed in section 5.2.3. and summarised observations are shown in Figure 5.74. Changes in the microhardness, corrosion-rate and wear-rate of electroless Ni-P-TiO_2 nanocomposite coatings on mild steel due to variation in the nano TiO_2 particles concentration in the deposition bath are shown in Figure 5.74. As observations shown in Figure 5.74, microhardness and surface roughness of Ni-P-TiO_2 nanocomposite coatings are increased while corrosion rate and wear-rate Ni-P-TiO_2 nanocomposite coatings are decreased with increasing the concentration of TiO_2 particles in the electroless bath. As it can see that in the analysis of corrosion rate of obtained Ni-P-TiO_2 nanocomposite coatings is initially decreased when concentrations of TiO_2 is increased during the deposition, further increased the concentration TiO_2 beyond 1.2 g/l, the corrosion rate is increased because of incorporation of high concentration of TiO_2 particles in the Ni-P matrix. When the high concentration of TiO_2 particles are co-deposited with the metal matrix then the formation of passive layer might be disturbed [215, 224]. Ni-P-TiO_2 nanocomposite coating on mild steel deposited with 2 g/l TiO_2 particles has the highest microhardness and wear- resistance because of dispersion strengthening the effect.

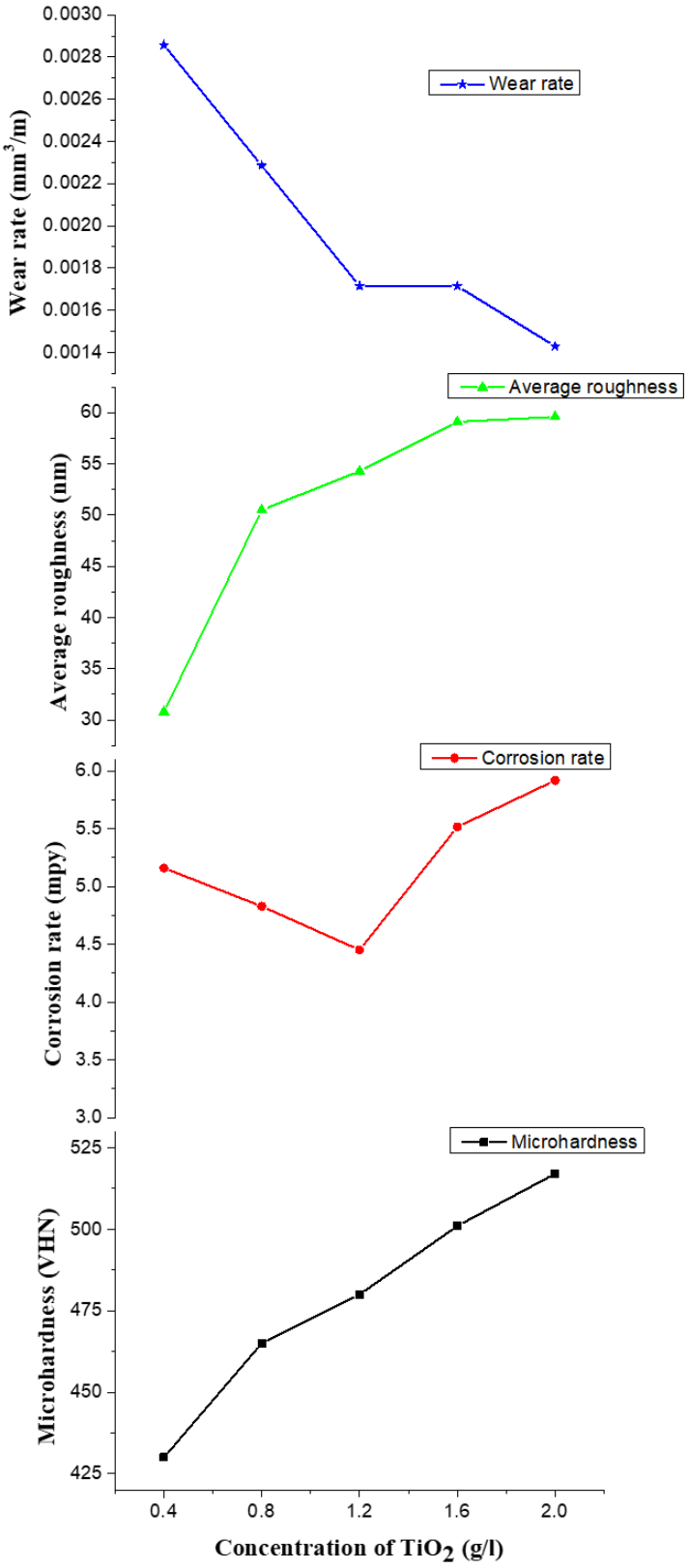

Figure 5.74: Comparison of the microhardness, corrosion-rate and wear-rate of electroless Ni-P-TiO_2 nanocomposite coatings deposited with the 0.4 g/l, 0.8 g/l, 1.2 g/l, 1.6 g/l and 2.0 g/l TiO_2 concentration in the deposition bath

5.3. Enhanced properties of mild steel by the Electroless Ni-P and Ni-P-TiO_2 nanocomposite coating

The aim of this research work is improvement of properties of mild steel by the coating on the surface by the electroless method. For enhancing the properties of mild steel, its surface was coated with two types of coatings. First deposited coating is Ni-P coating and second is Ni-P-TiO_2 nanocomposite coating with hard nano TiO_2 particles. Both types of coatings were successfully deposited on mild steel up to 24 µm thickness.

Comparison of the microhardness of the uncoated mild steel, Ni-P coated mild steel, and Ni-P-TiO_2 nanocomposite coated mild steel is given in Table 5.12.

Table 5.12: Comparison of microhardness of mild steel substrate, Ni-P, and Ni-P-TiO_2 nanocomposite coating

Sample	Coating Thickness (µm)	Microhardness (VHN_{10})
Mild steel	-------	~ 132
Ni-P coated mild steel	22	~ 400
Ni-P-TiO_2 nanocomposite coated mild steel	24	~ 517

As results are shown in Table 5.12, microhardness is mild steel is improved by the deposition of electroless Ni-P coating and Ni-P-TiO_2 nanocomposite coating on the surface of the mild steel. Higher microhardness is possessed by the Ni-P-TiO_2 nanocomposite coating as compared to the Ni-P coating because of inclusion of hard nano TiO_2 in Ni-P matrix. The inclusion of hard nano TiO_2 in Ni-P provides the resistance to deformation due to the dispersion strengthening effect.

Tafel graphs of mild steel, Ni-P coating, and Ni-P-TiO_2 nanocomposite coating are shown in Figure 5.75. By the comparative study of these Tafel curves, it is observed that the polarization potential of mild steel is more negative as compared to the coated mild steel. When corrosion potential moves in the positive direction, it offers high corrosion resistance property. In case of Ni-P-TiO_2 nanocomposite coating, corrosion potential is more positive as compared to Ni-P coating and uncoated mild steel.

Comparison of the electrochemical parameters of the uncoated mild steel, Ni-P coated mild steel, and Ni-P-TiO_2 nanocomposite coated mild steel is given in Table 5.13. The corrosion rate of mild steel in 3.5% NaCl solution highest as compare to Ni-P coated

mild steel and Ni-P-TiO_2 nanocomposite coated mild steel. These coatings act as a barrier of oxidation of mild steel.

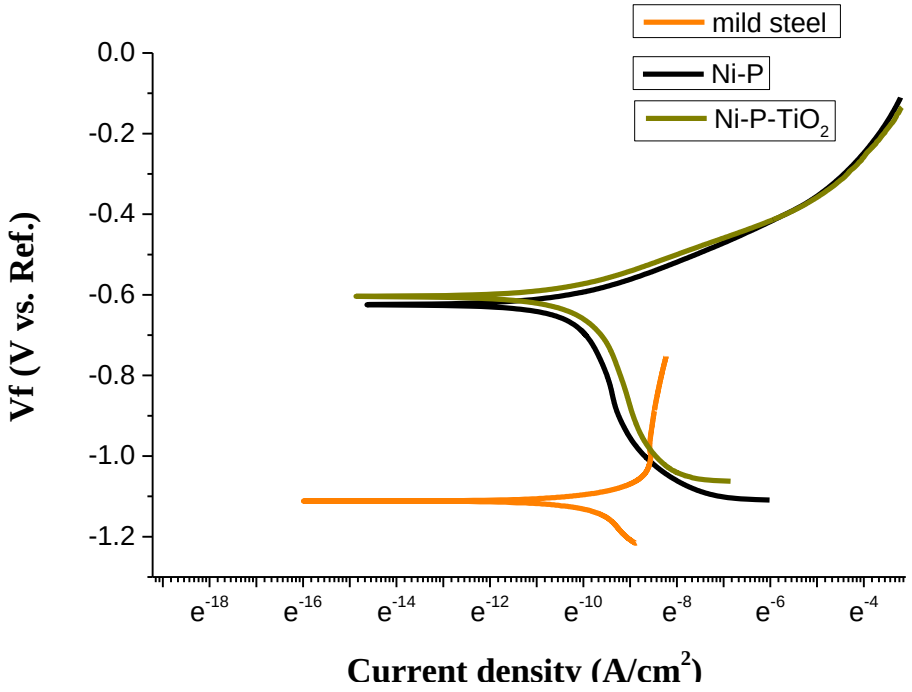

Figure 5.75: Comparative study of Tafel curves of uncoated mild steel, Ni-P coated mild steel & Ni-P-TiO_2 nanocomposite coated mild steel

Table 5.13: Comparison of electrochemical parameters of mild steel substrate, Ni-P and Ni-P-TiO_2 nanocomposite coating derived from the Tafel plots

Sample	**E_{corr} (mV)**	**I_{corr} (µA/cm^2)**	**Corrosion Rate (mpy)**
Mild steel	- 1105	97.01	9.14
Ni-P coated mild steel	- 701	70.23	6.61
Ni-P-TiO_2 nanocomposite coated mild steel	- 550.3	47.23	4.45

Comparison of the wear loss of the uncoated mild steel, Ni-P coated mild steel, and Ni-P-TiO_2 nanocomposite coated mild steel is given in Table 5.14. Wear loss of uncoated mild steel during the pin-on-disc test is higher as compared to coated mild steel with Ni-P coating and Ni-P-TiO_2 nanocomposite coating. Ni-P-TiO_2 nanocomposite coated

mild steel possess the enhanced wear-resistance property because of its smooth surface finish and high hardness.

Table 5.14: Comparison of wear loss during the pin-on-disc test of mild steel substrate, Ni-P, and Ni-P-TiO_2 nanocomposite coating

Sample	Coating Thickness (μm)	Weight loss (gm)
Mild steel	-------	~ 0.014
Ni-P coated mild steel	22	~ 0.009
Ni-P-TiO_2 nanocomposite coated mild steel	24	~ 0.005

Nano TiO_2 particles are not seen in electroless Ni-P-TiO_2 nanocomposite coatings because agglomeration of TiO_2 particles was avoided by inclusion of the proper amount of TiO_2 sol and proper suspension of TiO_2 particles in the solution. Proper dispersed nano TiO_2 particles can make the Ni-P-TiO_2 nanocomposite coating matrix more dense and fine grain size. The reason behind this, the combined effect of particle dispersion strengthening and grain refinement strengthening. By the strengthening effect and unique properties of hard nano TiO_2 particles, microhardness and wear resistance property of Ni-P-TiO_2 nanocomposite coating are highest as compare to Ni-P coating and uncoated mild steel.

Mild steel is an extensively used material by industries and constructer due to its economical, versatile, and easy to manufacture qualities. In spite of its wonderful properties mild steel has some working condition limitations such as corrosion is a major problem facing by industries and engineers. Wear is another problem in the industrial application of mild steel because mild steel is a structurally soft material. By the use of electroless Ni-P-TiO_2 nanocomposite coating on the surface of mild steel, corrosion resistance, hardness, wear resistance and surface finish can be improved and increase structural and industrial application of mild steel.

Chapter 6

CONCLUSIONS AND FUTURE WORK SUGGESTIONS

This research work is concluded in this chapter and suggestions for future work are also included here. Ni-P and Ni-P-TiO_2 nanocomposite coatings on mild steel were developed by the electroless deposition method. The conclusions drawn from this research work are discussed in the same order as presented in chapter five.

6.1. Conclusions

The important conclusions drawn from the present research work are as follows:

- The Ni-P and Ni-P-TiO_2 nanocomposite coating were successfully developed on the mild steel substrate by electroless plating technique using a sodium hypophosphite reduced bath.
- Both electroless Ni-P and Ni-P-TiO_2 nanocomposite coatings exhibit good adherence to the mild steel specimen and were deposited to thickness in range of 17-24 μm (both side).
- X-ray diffraction results obtained for Ni-P coating on mild revealed a peak corresponding to Ni (1 1 1) phase. The FESEM images of Ni-P coating clearly revealed globules of Ni-P on the mild steel substrate. The EDS analysis of Ni-P coating revealed the amorphous structure of electroless coating having 15.67 wt.% P content in the coating.
- X-ray diffraction analysis of electroless Ni-P-TiO_2 nanocomposite coatings revealed that co-deposited second phase particles (TiO_2) did not influence the structure and phase transformation behavior. Electroless deposited composite coatings exhibited the semi-crystalline structure of Ni-P matrix in which crystalline titanium oxide was incorporated. FESEM and EDS analysis carried out on Ni-P-TiO_2 composite coatings revealed that Ni-P globules were covered by TiO_2 film, so it can be inferred that mild steel substrate can be protected by Ni-P-TiO_2 nanocomposite coatings better than Ni-P coatings.

- Microhardness and wear resistance of Ni-P-TiO_2 nanocomposite coating deposited with 35 g/l $NiSO_4$ (highest concentration of $NiSO_4$) are increasing while corrosion resistance is decreasing in compare to Ni-P-TiO_2 nanocomposite coatings deposited with 25 g/l and 30 g/l $NiSO_4$.

- Corrosion resistance of Ni-P-TiO_2 nanocomposite coating deposited with 40 g/l sodium hypophosphite is increasing while microhardness and wear resistance are decreasing in compare to Ni-P-TiO_2 nanocomposite coating deposited with 20 g/l and 30 g/l sodium hypophosphite.

- An enhancement in microhardness was detected in both Ni-P coated mild steel and Ni-P-TiO_2 nanocomposite coated mild steel compared to without coated mild steel substrate. The order of improved microhardness was mild steel substrate <Ni-P<Ni-P-TiO_2 nanocomposite coating, also increased amount of TiO_2 particles concentration in bath increased the microhardness of coating.

- Microhardness of the mild steel is increased 203% and 291% by deposition of electroless Ni-P coating and Ni-P-TiO_2 nanocomposite coating on mild steel respectively.

- The results obtained from Tafel graphs confirmed that all coated sample showed improved corrosion resistance than the mild steel substrate in 3.5 wt.% NaCl solution. Deposition of the Ni-P coating and Ni-P-TiO_2 nanocomposite coating on mild steel provided corrosion protection efficiencies of 27.61% and 51.68% respectively.

- The results obtained from wear test revealed that all coated samples had significantly improved wear resistance than the mild steel substrate. The order of improved wear resistance was, substrate <Ni-P<Ni-P-TiO_2 nanocomposite coating, also increased amount of TiO_2 particles concentration in bath increased the wear resistance of the coating.

- Increased wear resistance of Ni-P-TiO_2 nanocomposite coatings may be due to the grain filling and dispersive strengthening effects offered by the hard-ceramic particles, which form a barrier to plastic deformation of Ni-P matrix under the load and hinder dislocation of Ni-P matrix.

- On the basis of this research work, it can be concluded that electroless Ni-P-TiO_2 nanocomposite coatings can be utilized to protect mild steel from corrosion and wear during structural and industrial applications of mild steel.

6.2. Suggestions for Future Work

- Post heat treatment of electroless Ni-P-TiO_2 nanocomposite coatings on mild steel should also be carry out to further improve the properties of these coatings.
- Transmission electron microscopic study may be attempted to know the internal structure of Ni-P-TiO_2 nanocomposite coatings on mild steel.
- To study the effect of other mechanical properties (tensile strength, stress, strain) of Ni-P-TiO_2 nanocomposite coated mild steel, dynamic mechanical analysis and one tester tests will be performed.
- To study the corrosion resistance of Ni-P-TiO_2 nanocomposite coating, electrochemical impedance spectroscopy (EIS) will be used.
- To study the tribological properties of electroless nanocomposite coating, the coefficient of friction with lubrication or without lubrication and various loads will be used.

References

1. Davis, Joseph R., ed. Surface engineering for corrosion and wear resistance. ASM international, (2001).
2. Burnell-Gray, J. S., and Prasanta Kumar Datta, eds. Surface Engineering Casebook: Solutions to Corrosion and Wear-related Failures. Elsevier, (1996).
3. Bockris, John O'M., and Shahad UM Khan. Surface electrochemistry: a molecular level approach. Springer Science & Business Media, (2013).
4. Hutchings, Ian, and Philip Shipway. Tribology: friction and wear of engineering materials. Butterworth-Heinemann, (2017).
5. Vazquez Aguilar, Reyna Areli. "Surface and wear analyses of cermet and ceramic coatings." (2012).
6. Halada, Gary P., and Clive R. Clayton. "The intersection of design, manufacturing, and surface engineering." Handbook of Environmental Degradation of Materials. (2005). 321-344.
7. Matthews, Allan, and David S. Rickerby, eds. Advanced surface coatings: a handbook of surface engineering. Glasgow: Blackie, (1991).
8. Lee, Daeyeon. Surface engineering using layer-by-layer assembly of pH-sensitive polymers and nanoparticles. Diss. Massachusetts Institute of Technology, (2007).
9. Paul, Swaraj. "Surface coatings. Science and technology." (1985).
10. Lambourne, Ronald, and T. A. Strivens, eds. Paint and surface coatings: theory and practice. Elsevier, (1999).
11. Paunovic, Milan, and Mordechay Schlesinger. "Fundamentals of electrochemical deposition." New York (1998).
12. Dini, Jack W. Electrodeposition. Noyes Publications, (1993).
13. Schlesinger, Mordechay, and Milan Paunovic, eds. Modern electroplating. Vol. 55. John Wiley & Sons, (2011).
14. Paunovic, Milan, and Mordechay Schlesinger. Fundamentals of electrochemical deposition. Vol. 45. john wiley & sons, (2006).
15. Bard, Allen J., et al. Electrochemical methods: fundamentals and applications. Vol. 2. New York: wiley, (1980).
16. Kanani, Nasser. Electroplating: basic principles, processes and practice. Elsevier, (2004)

17. Brenner, A., and G. E. Riddell. "J. Research NBS 37, 1-4 (1946)." Proc. Am. Electroplaters' Soc 33 (1946): 16.
18. Takalapally S., S. Kumar, S. H. Pusuluri and M. Palle, “A critical review on surface coatings for engineering materials, 7.5 (2016), 80-85.
19. Karlsson, Patrik. "Tribological characterization of selected hard coatings." (2009)
20. Munger, Charles G. "Corrosion prevention by protective coatings." (1985).
21. Gebretsadik, Daniel Woldegebriel, et al. "Tribological properties of composite multilayer coating." Tribology-Materials, Surfaces & Interfaces 5.3 (2011): 100-106.
22. Bonin, L., and V. Vitry. "Mechanical and wear characterization of electroless nickel mono and bilayers and high boron-mid phosphorus electroless nickel duplex coatings." Surface and Coatings Technology 307 (2016): 957-962.
23. Wurtz, Ann. "Formation of a cuprous hydride, by the action of hypophosphorus acid on a cupric salt solution." Ann. Chim. Phys 11 (1844): 250-252.
24. Brenner, Abner, and Grace E. Riddell. "Deposition of nickel and cobalt by chemical reduction." J. Res. Nat. Bur. Stand 39 (1947): 385-395.
25. Brenner, Abner. "Nickel plating on steel by chemical reduction." J. Res. NBS 37 (1946): 31-34.
26. Brenner, A., and AJ Riddell. "Electroless plating comes of age." Metal Finishing 37 (1954): 61-68.
27. Gutzeit, G., P. Talmey, and W. G. Lee. "Chemical nickel-plating processes and baths therefor." US Patent 2 (1958).
28. Gutzeit, G. "Catalytic nickel deposition from aqueous solution. I-IV." Plating surface finishing 46 (1959): 1158-1164.
29. Hanim, MA Azmah. "3.15 Electroless Plating as Surface Finishing in Electronic Packaging." (2017): 220-229.
30. Gillespie, P. "Electroless nickel coatings: case study." Surface Engineering Casebook. 1996. 49-72.
31. Ohno, Izumi. "Electrochemistry of electroless plating." Materials Science and Engineering: A 146.1-2 (1991): 33-49.
32. Taheri, Ray. "Evaluation of electroless nickel-phosphorus (EN) coatings." Saskatoon: University of Saskatchewan Saskatoon (2002).

33. Balaraju, J. N., and S. K. Seshadri. "Synthesis and corrosion behavior of electroless Ni-P-Si_3N_4 composite coatings." Journal of materials science letters 17.15 (1998): 1297-1299.
34. Sudagar, Jothi, Jianshe Lian, and Wei Sha. "Electroless nickel, alloy, composite and nano coatings–A critical review." Journal of Alloys and Compounds 571 (2013): 183-204.
35. Makkar, Preeti, R. C. Agarwala, and Vijaya Agarwala. "Development of Electroless Ni-P-ZrO_2 Nanocomposite Coatings by Codeposition of Mechanically Reduced ZrO_2 Nanoparticles." Advanced Materials Research. Vol. 740. Trans Tech Publications, (2013).
36. Makkar, Preeti, R. C. Agarwala, and Vijaya Agarwala. "Chemical synthesis of TiO_2 nanoparticles and their inclusion in Ni-P electroless coatings." Ceramics International 39.8 (2013): 9003-9008.
37. Makkar, Preeti, R. C. Agarwala, and Vijaya Agarwala. "Wear characteristics of mechanically milled TiO_2 nanoparticles incorporated in electroless Ni-P coatings." Advanced Powder Technology 25.5 (2014): 1653-1660.
38. Makkar, Preeti, et al. "A novel electroless plating of Ni-P-Al-ZrO_2 nanocomposite coatings and their properties." Ceramics International 40.8 (2014): 12013-12021.
39. Mallory, G. O. “Composition and kinetics of electroless nickel plating.” Electroless plating: fundamentals and application (1991): 57-98.
40. Riedel, Wolfgang. Electroless nickel plating. ASM International, (1991).
41. Gavrilov, Georgi G. Chemical (electroless) nickel-plating. Portcullis Press, (1979).
42. Djokic, S., ed. "Electroless Deposition Principles, Activation, and Applications." The Electrochemical Society, (2011).
43. Metzger, W., and Th Florian. "The deposition of dispersion hardened coatings by means of electroless nickel." Transactions of the IMF 54.1 (1976): 174-177.
44. Mallory, G. O., and J. B. Hajdu. "Electroless Plating Fundamentals and Applications, Reprint Edition, American, Electroplaters and Surface Finishers Society." (1990)
45. Colaruotolo, Joseph, and Diane Tramontana. "Engineering applications of electroless nickel." Electroless plating: fundamentals and applications 8 (1990): 208.

46. Bolger, Paul T., and David C. Szlag. "Investigation into the rejuvenation of spent electroless nickel baths by electrodialysis." Environmental science & technology 36.10 (2002): 2273-2278.
47. Scholder, R., and H. Heckel. "About Heavy Metal Phosphides, I. Communication: Effect of Hypophosphite on Nickel and Cobalt Salts." Journal of Inorganic and General Chemistry 198.1 (1931): 329-351.
48. Gabe, D. R. "Dr. Abner Brenner." (2009).
49. Wang, W. C., et al. "Electroless plating of copper on fluorinated polyimide films modified by surface graft copolymerization with 1-vinylimidazole and 4-vinylpyridine." Polymer Engineering & Science 44.2 (2004): 362-375.
50. Huang, Ting-Chia, Ming-Chi Wei, and Huey-Ing Chen. "Preparation of hydrogen-permselective palladium–silver alloy composite membranes by electroless co-deposition." Separation and Purification Technology 32.1-3 (2003): 239-245.
51. Krishnan, K. Hari, et al. "An overall aspect of electroless Ni-P depositions-A review article." Metallurgical and Materials Transactions A 37.6 (2006): 1917-1926.
52. Odekerken, Jules Marie. "Process for coating an object with a bright nickel/chromium coating." U.S. Patent No. 3,644,183. (1972).
53. Steinmetz, P., et al. "Electroless deposition of pure nickel, palladium and platinum." Surface and Coatings Technology 43 (1990): 500-510.
54. Mallory, G. O. "Influence of the electroless plating bath on the corrosion resistance of the deposits." Plating 61 (1974): 1005-1014.
55. Vitkavage, D., and M. Paunovic. "Maximum rate of the cathodic reaction in electroless copper deposition." Plating and surface finishing 70.4 (1983): 48-50.
56. Lukes, Robert M. "The mechanism for the autocatalytic reduction of nickel by hypophosphite ion." Plating 51 (1964): 969-971.
57. Mc Caskie, Jack, and Suzanne Redding. "Successful Automotive Applications for Electroless Nickel." Metal Finishing 4.106 (2008): 25-27.
58. Gawne, D. T., and U. Ma. "Friction and wear of chromium and nickel coatings." Wear 129.1 (1989): 123-142.
59. Liu, Hai-Ping, et al. "Effect of organic additives on the corrosion resistance properties of electroless nickel deposits." Thin solid films 516.8 (2008): 1883-1889.

60. Gad, M. Reda, and A. El-Magd. "Additives for electroless nickel alloy coating processes." Metal Finishing 99.2 (2001): 77-83.
61. Yin, X., Liang Hong, and B. H. Chen. "Role of a Pb^{2+} stabilizer in the electroless nickel plating system: A theoretical exploration." The Journal of Physical Chemistry B 108.30 (2004): 10919-10929.
62. Xiao, Zongyuan, et al. "Effect of Cd^{2+} as a stabilizer in the electroless nickel plating system." Surface and Coatings Technology 202.20 (2008): 5008-5011.
63. Cheong, Woo-Jae, Ben L. Luan, and David W. Shoesmith. "The effects of stabilizers on the bath stability of electroless Ni deposition and the deposit." Applied Surface Science 229.1-4 (2004): 282-300.
64. Bindra, Perminder, and Judith Roldan. "Mechanisms of electroless metal plating. III. Mixed potential theory and the interdependence of partial reactions." Journal of applied electrochemistry 17.6 (1987): 1254-1266.
65. Abrantes, L. M., and J. P. Correia. "On the Mechanism of Electroless Ni-P Plating." Journal of the electrochemical society 141.9 (1994): 2356-2360.
66. Agarwala, R. C., and Vijaya Agarwala. "Electroless alloy/composite coatings: A review." Sadhana 28.3-4 (2003): 475-493.
67. Rani, R. Uma, et al. "Studies on black electroless nickel coatings on titanium alloys for spacecraft thermal control applications." Journal of applied electrochemistry 40.2 (2010): 333-339.
68. Johnson, C. E. "Black electroless nickel surface morphologies with extremely high light absorption capacity." Metal Finishing 78.7 (1980): 21-24.
69. Kumar, S. N., L. K. Malhotra, and K. L. Chopra. "Low cost electroless nickel black coatings for photothermal conversion." Solar Energy Materials 3.4 (1980): 519-532.
70. Dini, J. W., and P. R. Coronado. Thick nickel deposits of high purity by electroless methods. No. SCL-DC--66-22; CONF-661202--1. Sandia Corp., Livermore, Calif., (1966)
71. Narayanan, TSN Sankara, K. Krishnaveni, and S. K. Seshadri. "Electroless Ni-P/Ni-B duplex coatings: preparation and evaluation of microhardness, wear and corrosion resistance." Materials Chemistry and Physics 82.3 (2003): 771-779.
72. Narayanan, TSN Sankara, and S. K. Seshadri. "Formation and characterization of borohydride reduced electroless nickel deposits." Journal of alloys and compounds 365.1-2 (2004): 197-205.

73. Bedingfield, Paul Bryron, et al. "Studies of electroless nickel-boron alloy coatings." Transactions of the IMF 70.1 (1992): 19-23.
74. Dervos, C. T., J. Novakovic, and P. Vassiliou. "Vacuum heat treatment of electroless Ni–B coatings." Materials Letters 58.5 (2004): 619-623.
75. Vitry, Véronique, Abdoul-Fatah Kanta, and Fabienne Delaunois. "Mechanical and wear characterization of electroless nickel-boron coatings." Surface and Coatings Technology 206.7 (2011): 1879-1885.
76. Wang, Lingling, et al. "Crystallization study of electroless Fe-Sn-B amorphous alloy deposits." Journal of alloys and compounds 287.1-2 (1999): 234-238.
77. Anik, Mustafa, Erhan Körpe, and Esin Şen. "Effect of coating bath composition on the properties of electroless nickel–boron films." Surface and Coatings Technology 202.9 (2008): 1718-1727
78. Das, Suman Kalyan, and Prasanta Sahoo. "Tribological characteristics of electroless Ni–B coating and optimization of coating parameters using Taguchi based grey relational analysis." Materials & Design 32.4 (2011): 2228-2238.
79. Duhin, A., et al. "Electroless deposition of Ni-W-B alloy on p-type Si (1 0 0) for NiSi contact metallization." Electrochimica Acta 54.25 (2009): 6036-6041.
80. Delaunois, Fabienne, and P. Lienard. "Heat treatments for electroless nickel–boron plating on aluminium alloys." Surface and Coatings Technology 160.2-3 (2002): 239-248.
81. Krishnaveni, K., TSN Sankara Narayanan, and S. K. Seshadri. "Electroless Ni–B coatings: preparation and evaluation of hardness and wear resistance." Surface and Coatings Technology 190.1 (2005): 115-121.
82. Delaunois, Fabienne, et al. "Autocatalytic electroless nickel-boron plating on light alloys." Surface and Coatings Technology 124.2-3 (2000): 201-209.
83. Agarwala, R. C., Vijaya Agarwala, and Rahul Sharma. "Electroless Ni-P Based Nanocoating Technology-A Review." Synthesis and Reactivity in Inorganic, Metal-Organic and Nano-Metal Chemistry 36.6 (2006): 493-515.
84. Sade, Wagner, et al. "Electroless Ni-P coatings: preparation and evaluation of fracture toughness and scratch hardness." ISRN Materials Science 2011 (2011).
85. Taheri, R., I. N. A. Oguocha, and S. Yannacopoulos. "Effect of heat treatment on age hardening behaviour of electroless nickel–phosphorus coatings." Materials science and technology 17.3 (2001): 278-284.

86. Taheri, R. I. N. A., I. N. A. Oguocha, and S. Yannacopoulos. "The tribological characteristics of electroless NiP coatings." Wear 249.5-6 (2001): 389-396.
87. Moniruzzaman, M., and Subrata Roy. "Effect of pH on electroless Ni-P coating of conductive and nonconductive materials." International Journal of Automotive and Mechanical Engineering 4 (2011): 481-489.
88. Ashassi-Sorkhabi, H., and S. Hl Rafizadeh. "Effect of coating time and heat treatment on structures and corrosion characteristics of electroless Ni–P alloy deposits." Surface and coatings Technology 176.3 (2004): 318-326.
89. Rabizadeh, Taher, Saeed Reza Allahkaram, and Arman Zarebidaki. "An investigation on effects of heat treatment on corrosion properties of Ni–P electroless nano-coatings." Materials & Design 31.7 (2010): 3174-3179.
90. Duchaniya[1], Rajendra Kumar, et al. "Morphology and Corrosion Study of Electroless Ni-P Coatings on Commercial Aluminium Alloy." (2011).
91. Domenech, S. C., et al. "Electroless plating of nickel–phosphorous on surface-modified poly (ethylene terephthalate) films." Applied Surface Science 220.1-4 (2003): 238-250.
92. Gould, A. J., P. J. Boden, and S. J. Harris. "Phosphorus distribution in electroless nickel deposits." Surface Technology12.1 (1981): 93-102.
93. Marshall, James H. "The nickel metal catalyzed decomposition of aqueous hypophosphite solutions." Journal of The Electrochemical Society 130.2 (1983): 369-372.
94. Guo, Z., K. G. Keong, and W. Sha. "Crystallisation and phase transformation behaviour of electroless nickel phosphorus platings during continuous heating." Journal of Alloys and Compounds 358.1-2 (2003): 112-119.
95. Higgs, C. E. "The effect of heat treatment on the structure and hardness of an electrolessly deposited nickel-phosphorus alloy." Electrodeposition and Surface Treatment 2.4 (1974): 315-326.
96. Brown, Richard JC, Paul J. Brewer, and Martin JT Milton. "The physical and chemical properties of electroless nickel–phosphorus alloys and low reflectance nickel–phosphorus black surfaces." Journal of Materials Chemistry 12.9 (2002): 2749-2754.
97. Papini, Marie. "Chemical, structural and optical characterization of Ni-P chemical conversion coatings for photothermal absorption of solar energy." Solar energy materials 13.4 (1986): 233-265.

98. Cheong, Woo-Jae, Ben L. Luan, and David W. Shoesmith. "Protective coating on Mg AZ91D alloy–The effect of electroless nickel (EN) bath stabilizers on corrosion behaviour of Ni–P deposit." Corrosion Science 49.4 (2007): 1777-1798.
99. Chen, B-H., et al. "Effects of surfactants in an electroless nickel-plating bath on the properties of Ni−P alloy deposits." Industrial & engineering chemistry research 41.11 (2002): 2668-2678.
100. Ashassi-Sorkhabi, H., M. Moradi-Haghighi, and M. G. Hosseini. "Effect of rare earth (Ce, La) compounds in the electroless bath on the plating rate, bath stability and microstructure of the nickel–phosphorus deposits." Surface and Coatings Technology 202.9 (2008): 1615-1620.
101. Ger, Ming-Der, Yuh Sung, and Jinn-Luh Ou. "A novel process of electroless Ni–P plating by nonisothermal method." Materials chemistry and physics 89.2-3 (2005): 383-389.
102. Vaghefi, Sayed Yousef Monir, and Sayed Mahmoud Monir Vaghefi. "Prediction of phosphorus content of electroless nickel–phosphorous coatings using artificial neural network modeling." Neural Computing and Applications 20.7 (2011): 1055-1060.
103. Keong, K. G., W. Sha, and S. Malinov. "Computer modelling of the non-isothermal crystallization kinetics of electroless nickel–phosphorus deposits." Journal of non-crystalline solids 324.3 (2003): 230-241
104. Keong, K. G., and W. Sha. "Crystallisation and phase transformation behaviour of electroless nickel-phosphorus deposits and their engineering properties." Surface Engineering 18.5 (2002): 329-343.
105. Keong, K. G., W. Sha, and S. Malinov. "Hardness evolution of electroless nickel–phosphorus deposits with thermal processing." Surface and Coatings Technology 168.2-3 (2003): 263-274.
106. Yan, M., H. G. Ying, and T. Y. Ma. "Improved microhardness and wear resistance of the as-deposited electroless Ni–P coating." Surface and Coatings Technology 202.24 (2008): 5909-5913.
107. Sahoo, Prasanta. "Friction performance optimization of electroless Ni–P coatings using the Taguchi method." Journal of Physics D: Applied Physics 41.9 (2008): 095305.

108. Randin, Jean-Paul, and H. E. Hintermann. "Electroless nickel deposited at controlled pH--mechanical properties as a function of phosphorus content." Plating 54.5 (1967): 523-532.
109. Kumar, M. Ananth, Ramesh Chandra Agarwala, and Vijaya Agarwala. "Synthesis and characterization of electroless Ni-P coated graphite particles." Bulletin of Materials Science 31.5 (2008): 819-824.
110. Palaniappa, M., and S. K. Seshadri. "Friction and wear behavior of electroless Ni–P and Ni–W–P alloy coatings." Wear 265.5-6 (2008): 735-740.
111. Zhou, Qing-Jun, et al. "The effect of hydrogen on friction and wear of Ni–P electroless coating." Wear 266.7-8 (2009): 810-813.
112. Crobu, Maura, et al. "The corrosion resistance of electroless deposited nano-crystalline Ni–P alloys." Electrochimica Acta 53.8 (2008): 3364-3370.
113. Lu, Guojin, and Giovanni Zangari. "Corrosion resistance of ternary Ni-P based alloys in sulfuric acid solutions." Electrochimica Acta 47.18 (2002): 2969-2979.
114. Peeters, P., et al. "Properties of electroless and electroplated Ni-P and its application in microgalvanics." Electrochimica Acta 47.1-2 (2001): 161-169.
115. Takács, D., et al. "Effects of pre-treatments on the corrosion properties of electroless Ni–P layers deposited on AlMg2 alloy." Surface and Coatings Technology 201.8 (2007): 4526-4535
116. Fundo, A. M., and L. M. Abrantes. "The electrocatalytic behaviour of electroless Ni–P alloys." Journal of Electroanalytical Chemistry 600.1 (2007): 63-79.
117. Liu, Zhenmin, and Wei Gao. "The effect of substrate on the electroless nickel plating of Mg and Mg alloys." Surface and Coatings Technology 200.11 (2006): 3553-3560.
118. Anık, Mustafa, and Erhan Körpe. "Effect of alloy microstructure on electroless NiP deposition behavior on Alloy AZ91." Surface and Coatings Technology 201.8 (2007): 4702-4710.
119. Huang, Y. S., and F. Z. Cui. "Effect of complexing agent on the morphology and microstructure of electroless deposited Ni-P alloy." Surface and Coatings Technology 201.9-11 (2007): 5416-5418.
120. Ashtiani, Amir Ahmadi, et al. "The study of electroless Ni-P alloys with different complexing agents on Ck45 steel substrate." Arabian Journal of Chemistry 10 (2017): S1541-S1545.

121. Arulvel, S., A. Elayaperumal, and M. S. Jagatheeshwaran. "Electroless nickel–phosphorus coating on crab shell particles and its characterization." Journal of Solid State Chemistry 248 (2017): 87-95.
122. Wang, Yanwen, Changgeng Xiao, and Zhonggang Deng. "Structure and corrosion resistance of electroless Ni-Cu-P." Plating and surface finishing 79.3 (1992): 57-59.
123. Georgieva, J., and S. Armyanov. "Electroless deposition and some properties of Ni-Cu-P and Ni-Sn-P coatings." Journal of Solid State Electrochemistry 11.7 (2007): 869-876.
124. Liu, Y., and Q. Zhao. "Study of electroless Ni-CuP coatings and their anti-corrosion properties." Applied Surface Science228.1-4 (2004): 57-62.
125. Liu, Guichang, et al. "Corrosion behavior of electroless deposited Ni-Cu-P coating in flue gas condensate." Surface and Coatings Technology 204.21-22 (2010): 3382-3386.
126. Valova, Eugenia, et al. "Corrosion behavior of hybrid coatings: Electroless Ni-Cu-P and sputtered TiN." Surface and Coatings Technology 204.16-17 (2010): 2775-2781.
127. Yuan, X. Y., et al. "Fabrication of Ni-W-P nanowire arrays by electroless deposition and magnetic studies." Physica E: Low-dimensional Systems and Nanostructures 23.1-2 (2004): 75-80.
128. Tien, Shih-Kang, Jenq-Gong Duh, and Yung-I. Chen. "Structure, thermal stability and mechanical properties of electroless Ni-P-W alloy coatings during cycle test." Surface and Coatings Technology 177 (2004): 532-536.
129. Balaraju, J. N., and K. S. Rajam. "Electroless deposition of Ni-Cu-P, Ni-W-P and Ni-W-Cu-P alloys." Surface and Coatings Technology 195.2-3 (2005): 154-161.
130. Liu, H., et al. "Microstructure and corrosion performance of laser-annealed electroless Ni-W-P coatings." Surface and Coatings Technology 204.9-10 (2010): 1549-1555.
131. Wang, Sen-Lin. "Studies of electroless plating of Ni-Fe-P alloys and the influences of some deposition parameters on the properties of the deposits." Surface and Coatings Technology 186.3 (2004): 372-376.

132. Tai, F. C., K. J. Wang, and J. G. Duh. "Application of electroless Ni-Zn-P film for under-bump metallization on solder joint." Scripta Materialia 61.7 (2009): 748-751.
133. Pang, Jianfeng, et al. "Preparation and characterization of electroless Ni-Co-P ternary alloy on fly ash cenospheres." Surface and Coatings Technology 205.17-18 (2011): 4237-4242.
134. Balaraju, J. N., TSN Sankara Narayanan, and S. K. Seshadri. "Electroless Ni-P composite coatings." Journal of applied electrochemistry 33.9 (2003): 807-816.
135. Li, Zhen, et al. "Tribological characteristics of electroless Ni-P-MoS_2 composite coatings at elevated temperatures." Applied Surface Science 264 (2013): 516-521.
136. Ramalho, A., and Jose Carlos Miranda. "Friction and wear of electroless NiP and NiP+ PTFE coatings." Wear 259.7-12 (2005): 828-834.
137. Sahoo, Prasanta, and Suman Kalyan Das. "Tribology of electroless nickel coatings–a review." Materials & Design 32.4 (2011): 1760-1775.
138. Rabizadeh, Taher, and Saeed Reza Allahkaram. "Corrosion resistance enhancement of Ni-P electroless coatings by incorporation of nano-SiO_2 particles." Materials & Design 32.1 (2011): 133-138.
139. Grosjean, A., et al. "Hardness, friction and wear characteristics of nickel-SiC electroless composite deposits." Surface and Coatings Technology 137.1 (2001): 92-96.
140. Balaraju, J. N., and K. S. Rajam. "Influence of particle size on the microstructure, hardness and corrosion resistance of electroless Ni-P-Al_2O_3 composite coatings." Surface and Coatings Technology 200.12-13 (2006): 3933-3941.
141. Chen, X. H., et al. "Dry friction and wear characteristics of nickel/carbon nanotube electroless composite deposits." Tribology international 39.1 (2006): 22-28.
142. Chen, W. X., et al. "Electroless preparation and tribological properties of Ni-P-Carbon nanotube composite coatings under lubricated condition." Surface and Coatings Technology 160.1 (2002): 68-73.
143. Song, Y. W., D. Y. Shan, and E. H. Han. "High corrosion resistance of electroless composite plating coatings on AZ91D magnesium alloys." Electrochimica Acta 53.5 (2008): 2135-2143.

144. Chen, W. X., et al. "Tribological properties of Ni-P-multi-walled carbon nanotubes electroless composite coating." Materials Letters 57.7 (2003): 1256-1260.
145. Zhang, Shusheng, Kejiang Han, and Lin Cheng. "The effect of SiC particles added in electroless Ni-P plating solution on the properties of composite coatings." Surface and Coatings Technology 202.12 (2008): 2807-2812.
146. Alirezaei, Sh, et al. "Effect of alumina content on surface morphology and hardness of Ni-P-Al_2O_3 (α) electroless composite coatings." Surface and Coatings Technology 184.2-3 (2004): 170-175.
147. Jiaqiang, Gao, et al. "Electroless Ni-P-SiC composite coatings with superfine particles." Surface and Coatings Technology 200.20-21 (2006): 5836-5842.
148. Xu, Hui, et al. "Synthesis and properties of electroless Ni-P-Nanometer Diamond composite coatings." Surface and coatings technology 191.2-3 (2005): 161-165.
149. Sharma, S. B., et al. "Dry sliding wear and friction behavior of Ni-P-ZrO_2-Al_2O_3 composite electroless coatings on aluminum." Materials and Manufacturing Processes 17.5 (2002): 637-649.
150. Li, Changjin, Yanmin Wang, and Zhidong Pan. "Wear resistance enhancement of electroless nanocomposite coatings via incorporation of alumina nanoparticles prepared by milling." Materials & Design 47 (2013): 443-448.
151. Liu, Y. Y., et al. "Synthesis and tribological behavior of electroless Ni-P-WC nanocomposite coatings." Surface and Coatings Technology 201.16-17 (2007): 7246-7251.
152. Farzaneh, Amir, et al. "Electrochemical and structural properties of electroless Ni-P-SiC nanocomposite coatings." Applied Surface Science 276 (2013): 697-704.
153. de Hazan, Yoram, et al. "Homogeneous Ni-P/Al_2O_3 nanocomposite coatings from stable dispersions in electroless nickel baths." Journal of colloid and interface science 328.1 (2008): 103-109.
154. Ma, Chunyang, et al. "Effect of heat treatment on structures and corrosion characteristics of electroless Ni-P-SiC nanocomposite coatings." Ceramics International 40.7 (2014): 9279-9284.

155. Sharma, Ankita, and A. K. Singh. "Electroless Ni-P and Ni-P-Al_2O_3 nanocomposite coatings and their corrosion and wear resistance." Journal of Materials Engineering and Performance 22.1 (2013): 176-183.
156. de Hazan, Yoram, et al. "Homogeneous electroless Ni–P/SiO_2 nanocomposite coatings with improved wear resistance and modified wear behavior." Surface and Coatings Technology 204.21-22 (2010): 3464-3470.
157. Daoush, Walid M., et al. "Electrical and mechanical properties of carbon nanotube reinforced copper nanocomposites fabricated by electroless deposition process." Materials Science and Engineering: A 513 (2009): 247-253.
158. Afroukhteh, S., C. Dehghanian, and M. Emamy. "Preparation of electroless Ni-P composite coatings containing nano-scattered alumina in presence of polymeric surfactant." Progress in Natural Science: Materials International 22.4 (2012): 318-325.
159. Mazaheri, Hamed, and Saeed Reza Allahkaram. "Deposition, characterization and electrochemical evaluation of Ni-P-ano diamond composite coatings." Applied Surface Science 258.10 (2012): 4574-4580.
160. Alirezaei, S., et al. "Novel investigation on tribological properties of Ni-P-Ag-Al_2O_3 hybrid nanocomposite coatings." Tribology International 62 (2013): 110-116.
161. Allahkaram, S. R., et al. "Characterization and corrosion behavior of electroless Ni-P/nano-SiC coating inside the CO_2 containing media in the presence of acetic acid." Materials & Design 32.2 (2011): 750-755.
162. Amell, A., C. Muller, and M. Sarret. "Influence of fluorosurfactants on the codeposition of ceramic nanoparticles and the morphology of electroless NiP coatings." Surface and Coatings Technology 205.2 (2010): 356-362.
163. Wu, Huihui, et al. "Preparation of Ni-P-GO composite coatings and its mechanical properties." Surface and Coatings Technology 272 (2015): 25-32.
164. Rattanawaleedirojn, Pranee, et al. "TiO_2 sol-embedded in electroless Ni-P coating: a novel approach for an ultra-sensitive sorbitol sensor." RSC Advances 6.73 (2016): 69261-69269.
165. Xiong, Liang, Guo Qing Zhang, and Hua Geng Pan. "Study on the preparation of Ni-P-TiO_2 coatings by electroless plating and its photocatalytic properties." Advanced Materials Research. Vol. 311. Trans Tech Publications, (2011).

166. Chen, Weiwei, Wei Gao, and Yedong He. "A novel electroless plating of Ni-P-TiO_2 nano-composite coatings." Surface and Coatings Technology 204.15 (2010): 2493-2498.
167. Lee, Cheng-Kuo. "Comparative corrosion resistance of electroless Ni-P/nano-TiO_2 and Ni-P/nano-CNT composite coatings on 5083 aluminum alloy." Int. J. Electrochem. Sci 7 (2012): 12941-12954.
168. Momenzadeh, M., and S. Sanjabi. "The effect of TiO_2 nanoparticle codeposition on microstructure and corrosion resistance of electroless Ni-P coating." Materials and Corrosion 63.7 (2012): 614-619.
169. Aal, A. Abdel, Hanaa B. Hassan, and MA Abdel Rahim. "Nanostructured Ni-P-TiO_2 composite coatings for electrocatalytic oxidation of small organic molecules." Journal of Electroanalytical Chemistry 619 (2008): 17-25.
170. Agarwala, Ramesh Chandra, Vijaya Agarwala, and Rahul Sharma. "Mechanical preparation of TiO_2 nanoparticles and their incorporation in electroless Ni-P coatings. Met." Org. Nano-Met. Chem 36 (2006): 493-515
171. Tamilarasan, T. R., et al. "Effect of surfactants on the coating properties and corrosion behaviour of Ni-P-nano-TiO_2 coatings." Surface and Coatings Technology 276 (2015): 320-326.
172. Wu, Xiaoyan, et al. "Improving the properties of 211Z Al alloy by enhanced electroless Ni-P-TiO_2 nanocomposite coatings with TiO_2 sol." Surface and Coatings Technology 270 (2015): 170-174.
173. Tamilarasan, T. R., et al. "Wear and scratch behaviour of electroless Ni-P-nano-TiO_2: Effect of surfactants." Wear 346 (2016): 148-157.
174. Parker, Konrad. "Effects of heat treatment on the properties of electroless nickel deposits." Plating and Surface Finishing 68.12 (1981): 71-77.
175. Parkinson, Ron. "Properties and applications of electroless nickel." Nickel Development Institute 33 (1997).
176. Kanta, A-F., Véronique Vitry, and Fabienne Delaunois. "Wear and corrosion resistance behaviours of autocatalytic electroless plating." Journal of Alloys and Compounds 486.1-2 (2009): L21-L23.
177. Chen, C. K., et al. "The effect of heat treatment on the microstructure of electroless Ni–P coatings containing SiC particles." Thin Solid Films 416.1-2 (2002): 31-37.

178. Huang, Y. S., et al. "Corrosion resistance properties of electroless nickel composite coatings." Electrochimica Acta 49.25 (2004): 4313-4319.
179. Balaraju, J. N., TSN Sankara Narayanan, and S. K. Seshadri. "Structure and phase transformation behaviour of electroless Ni-P composite coatings." Materials Research Bulletin 41.4 (2006): 847-860.
180. Matik, Ulaş. "Structural and wear properties of heat-treated electroless Ni-P alloy and Ni-P-Si_3N_4 composite coatings on iron based PM compacts." Surface and Coatings Technology 302 (2016): 528-534.
181. Promphet, Nadtinan, Pranee Rattanawaleedirojn, and Nadnudda Rodthongkum. "Electroless NiP-TiO2 sol-RGO: A smart coating for enhanced corrosion resistance and conductivity of steel." Surface and Coatings Technology 325 (2017): 604-610.
182. Gadhari, Prasanna, and Prasanta Sahoo. "Effect of process parameters on microhardness of Ni-P-Al_2O_3 composite coatings." Procedia materials science 6 (2014): 623-632.
183. Manjunath, G. L., and S. Surendran. "Effect of mono and composite coating on dynamic fracture toughness of metals at different temperatures." Composites Part B: Engineering 51 (2013): 359-367.
184. Balaraju, J., T. Sankara Narayanan, and S. Seshadri. "Evaluation of the corrosion resistance of electroless Ni-P and Ni-P composite coatings by electrochemical impedance spectroscopy." Journal of solid state electrochemistry 5.5 (2001): 334-338.
185. Gawad, SA Abdel, et. al. "Development of Electroless Ni-P-Al_2O_3 and Ni-P-TiO_2 Composite Coatings from Alkaline Hypophosphite Gluconate Baths and their Properties." International Journal of Electrochemical Science 8 (2013): 1722-1734.
186. Feldstein, N., et. al. "Electroless composite plating." Met. Finish. 81.8 (1983): 35-41.
187. Li, Libo, Maozhong An, and Gaohui Wu. "A new electroless nickel deposition technique to metallise SiC/Al composites." Surface and Coatings Technology 200.16-17 (2006): 5102-5112.
188. Grosjean, A., M. Rezrazi, and P. Bercot. "Some morphological characteristics of the incorporation of silicon carbide (SiC) particles into electroless nickel deposits." Surface and Coatings Technology 130.2-3 (2000): 252-256.

189. Reddy, V. V. N., B. Ramamoorthy, and P. Kesavan Nair. "A study on the wear resistance of electroless Ni-P/Diamond composite coatings." Wear 239.1 (2000): 111-116.
190. Apachitei, I., et. al. "Electroless Ni-P Composite Coatings: The Effect of Heat Treatment on the Microhardness of Substrate and Coating-Structure and Properties." Scripta Materialia 38.9 (1998): 1347-1353.
191. Li, Yongjun. "Investigation of electroless Ni-P-SiC composite coatings." Plating and surface finishing 84.11 (1997): 77-81.
192. Zhang, Y. Z., et. al. "Characterization of electroless Ni-P-PTFE composite deposits." Journal of Materials Science Letters 17.2 (1998): 119-122.
193. Kalantary, M. R., K. A. Holbrook, and P. B. Wells. "Optimisation of a bath for electroless plating and its use for the production of nickel-phosphorus-silicon carbide coatings." Transactions of the IMF 71.2 (1993): 55-61.
194. Pushpavanam, M. A. L. A. T. H. Y. "Electroless Ni-P-Al_2O_3 composites." Bulletin of Electrochemistry 8.08 (1992): 399-401.
195. Balaraju, J. N., and S. K. Seshadri. "Preparation and characterization of electroless Ni-P and Ni-P-Si_3N_4 composite coatings." Transactions of the IMF 77.2 (1999): 84-86.
196. Moonir-Vaghefi, S. M., A. Saatchi, and J. Hedjazi. "Tribological behaviour of electroless Ni-P-MoS_2 composite coatings." Zeitschrift für Metallkunde 88.6 (1997): 498-501.
197. Straffelini, G., D. Colombo, and A. Molinari. "Surface durability of electroless Ni–P composite deposits." Wear 236.1-2 (1999): 179-188.
198. Ajayan, Pulickel M., Linda S. Schadler, and Paul V. Braun. Nanocomposite science and technology. John Wiley & Sons, (2006).
199. Ajayan, Pulickel M., and Linda S. Schadler. "Nanocomposite science and technology/PM Ajayan, LS Schadler, PV Braun." (2003).
200. Sahu, N., and R. K. Duchaniya. "Synthesis of ZnO-CdO Nanocomposites." Journal of Materials Science & Surface Engineering 1.1 (2013): 11-14.
201. Xiang, Yingwei, Jinyuan Zhang, and Chenghai Jin. "Study of electroless Ni-P-Nanometer diamond composite coatings." Plating and surface finishing 88.2 (2001): 64-67.

202. Bigdeli, Faryad, and Saeed Reza Allahkaram. "An investigation on corrosion resistance of as-applied and heat treated Ni-P/nanoSiC coatings." Materials & Design 30.10 (2009): 4450-4453.
203. De Hazan, Yoram, et. al. "Homogeneous functional Ni-P/ceramic nanocomposite coatings via stable dispersions in electroless nickel electrolytes." Journal of colloid and interface science 365.1 (2012): 163-171.
204. Zielińska, Katarzyna, Alicja Stankiewicz, and Irena Szczygieł. "Electroless deposition of Ni-P-nano-ZrO_2 composite coatings in the presence of various types of surfactants." Journal of colloid and interface science 377.1 (2012): 362-367.
205. Hosseini, M. G., et. al. "Deposition and corrosion resistance of electroless Ni-PCTFE-P nanocomposite coatings." Surface and Coatings Technology 206.22 (2012): 4546-4552.
206. Karthikeyan, S., and B. Ramamoorthy. "Effect of reducing agent and nano Al_2O_3 particles on the properties of electroless Ni-P coating." Applied Surface Science 307 (2014): 654-660.
207. Luo, Hong, et. al. "Development of electroless Ni-P/nano-WC composite coatings and investigation on its properties." Surface and Coatings Technology 277 (2015): 99-106.
208. Sadeghzadeh-Attar, A., G. AyubiKia, and M. Ehteshamzadeh. "Improvement in tribological behavior of novel sol-enhanced electroless Ni-P-SiO_2 nanocomposite coatings." Surface and Coatings Technology 307 (2016): 837-848.
209. Calderón, J. A., J. P. Jiménez, and A. A. Zuleta. "Improvement of the erosion-corrosion resistance of magnesium by electroless Ni-P/Ni $(OH)_2$-ceramic nanoparticle composite coatings." Surface and Coatings Technology 304 (2016): 167-178.
210. Novakovic, J., et. al. "Electroless NiP-TiO_2 composite coatings: their production and properties." Surface and Coatings Technology 201.3-4 (2006): 895-901.
211. Novakovic, J., and P. Vassiliou. "Vacuum thermal treated electroless NiP-TiO_2 composite coatings." Electrochimica Acta 54.9 (2009): 2499-2503.
212. Gadhari, Prasanna, and Prasanta Sahoo. "Study of wear behavior of Ni-P-TiO_2 composite coatings by optimizing coating parameters." Materials Today: Proceedings 4.2 (2017): 1883-1892.

213. Cotolan, Nicoleta. Smart Corrosion Resistant Coatings: PhD Thesis. Diss. N. Cotolan, (2015).
214. Munger, Charles G. "Corrosion prevention by protective coatings." (1985).
215. Song, Laizhou, et. al. "Primary investigation of corrosion resistance of Ni-P/TiO_2 composite film on sintered NdFeB permanent magnet." Surface and Coatings Technology 202.21 (2008): 5146-5150.
216. Soboyejo, Wole. Mechanical properties of engineered materials. Vol. 152. CRC press, (2002).
217. Johansson, Staffan. A surface engineering approach to reduction of frictional losses of heavy duty diesel engines. Chalmers University of Technology, 2012.
218. Shibli, S. M. A., and V. S. Dilimon. "Effect of phosphorous content and TiO_2-reinforcement on Ni–P electroless plates for hydrogen evolution reaction." International Journal of Hydrogen Energy 32.12 (2007): 1694-1700.
219. Zhao, Qi, et. al. "Antibacterial characteristics of electroless plating Ni-P-TiO_2 coatings." Applied Surface Science 274 (2013): 101-104.
220. Hajdu, Juan. "Surface preparation for electroless nickel plating." Electroless plating: fundamentals and applications (1990): 193-206.
221. Bushroa, A. R., et al. "Approximation of crystallite size and microstrain via XRD line broadening analysis in TiSiN thin films." Vacuum 86.8 (2012): 1107-1112.
222. Mote, V. D., Y. Purushotham, and B. N. Dole. "Williamson-Hall analysis in estimation of lattice strain in nanometer-sized ZnO particles." Journal of Theoretical and Applied Physics 6.1 (2012): 6.
223. Lawal, S. A., et al. "Rubber Scrap as Reinforced Material in the Production of Environmentally Friendly Brake Lining." (2014).
224. Weil, Rolf, and Konrad Parker. "The properties of electroless nickel." Electroless plating: fundamentals and applications (1990): 111-137.
225. Feldstein, Nathan. "Composite electroless plating." Electroless Plating: Fundamentals and Applications (1990): 269-287.

Publications

- Vibha Uttam and R. K. Duchaniya "Potentiodynamic studies of Ni-P-TiO_2 nano-composited coating on the mild steel deposited by electroless plating method", AIP Conference Proceedings 1728, 020270 (2016).

View online: http://dx.doi.org/10.1063/1.4946321 by the AIP Publishing

- Komal Yadav, Vibha Uttam, R. K. Duchaniya "Study of Corrosion Behavior of Ni-P-TiO_2 Nanocomposite Coating on Mild Steel Deposited by Electroless Deposition Process", Journal of Materials Science & Surface Engineering Vol. 4 (4), pp 410-414 (2016).
- Vibha Uttam, Parul Yadav, R. K. Duchaniya "Characterization Study of Ni-P-TiO_2 Nanocomposite Coating on Mild Steel by Electroless Plating Method", Journal of Materials Science & Surface Engineering Vol. 4 (5), 2016, pp 432-435.

International Conference Proceeding

- Vibha Uttam[a*], R.K. Duchaniya[a] "Effect of pH on electroless bath for Ni-P coating on mild steel", Intonational Conference on Recent Trends in Science, Engineering and Management (ICRTSEM-2018, Jaipur).
- Vibha Uttam[a*], R.K. Duchaniya[a] "Effect of temperature & pH on Ni-P deposits on mild steel deposition by electroless coating process", (ICETMM 2018 Poornima university Jaipur, Jan 29-30, 2018).
- Vibha Uttam[1*], R.K. Duchaniya[1] "Ni-P-TiO_2 Nanocomposite by Electroless Coating Process - A Review", International Conference on Advance Materials and Technology (ICAMT-2017- Thailand).
- Vibha Uttam[1a], R.K. Duchaniya[1b] "Tribological studies of the electroless Ni-P-TiO_2 composite coating on mild steel", 8th National Conference Thermophysical Properties (NCTP-2015 MNIT, Jaipur).
- Parul Yadav, Vibha Uttam, R.K.Duchaniya "Characterization Study of Ni-P-TiO_2 Nanocomposite Coating on Mild Steel by Electroless Plating Method", Conference on Advanced Materials and Processing (CAMP- 2015, Jaipur).
- Vibha Uttam and R. K. Duchaniya "Potentiodynamic studies of Ni-P-TiO_2 nanocomposite coating on the mild steel deposited by electroless plating method", International Conference on Condensed Matter & Applied Physics (ICC-2015).